

ÉCOLE DOCTORALE DES SCIENCES DE LA VIE ET DE LA SANTE

Institut de Génétique et de Biologie Moléculaire et Cellulaire

THÈSE présentée par :

Jordi Del POZO RODRIGUEZ

soutenue le : **22 septembre 2020**

Pour obtenir le grade de : **Docteur de l'université de Strasbourg**

Discipline/ Spécialité : Neurosciences-Biologie Cellulaire et Moléculaire

**Understanding the role of the tRNA modifiers
ADAT3-ADAT2 and WDR4-METTL1 in the
development of the cerebral cortex**

THÈSE dirigée par :

Dr. Juliette GODIN

CR, INSERM, IGBMC, Illkirch

RAPPORTEURS :

Dr. Emilie PACARY

CR, INSERM, NeuroCentre Magendie , Bordeaux

Pr. Sebastian LEIDEL

PR, University of Bern, Bern

EXAMINATEUR INTERNE

Pr. Laurence MARÉCHAL-DROUARD PR, IBMP, Strasbourg

To my parents, Ana and Javi, I owe you many achievements, including this work. Thank you for always encouraging me to achieve my goals and your unconditional support.

A mis padres, Ana y Javi, muchos de los logros de mi vida os los debo a vosotros, entre ellos este trabajo. Gracias por haberme incentivado siempre a alcanzar mis objetivos y vuestro apoyo incondicional.

Acknowledgements

These 4 years have been an intense period with many challenges and beautiful moments both professionally and personally during which I encountered many people who helped me and supported me.

First of all, I would like to thank my thesis committee jury members as well as Dr. Laurent Nguyen (MEMBRE INVITÉ) for evaluating my work. I thank also the workers from the facilities from the IGBMC (Cell culture, Mouse house, Imaging facility, ICS...) and the funding agencies that founded this project (INSERM, ARC & FMR).

In our team, I thank each and every member, thanks for creating a welcoming, supportive and fun environment. I thank my supervisor, Juliette Godin, for coaching and mentoring me in any possible way. Despite we faced many difficulties during the project, you always believed in it and helped me keeping the right track.

Thanks Efil for being so supportive during all the PhD, both professionally and personally. Your supervision, patience and orientation really helped me during these years. Thanks, Peggy for helping me with all the mouse work, for coming to the lab every day with a smile despite a huge amount of work and for helping me to improve my French. Thank you Hakima, for the nice discussions we had and for your help, I look forward to meet your baby soon!. Thanks Laure, José and Charlotte for creating such a good environment and being always ready to provide some help when needed. We also shared all many beautiful not-lab related moments: lunches, cakes, dinners, room escapes. Most of you became friends with whom I enjoyed working, discussing and sharing many personal things. I am sure that our friendship will last beyond this chapter of our lives.

I would like to thank also many people for their friendship and support during this time. We shared many beautiful moments during these 4 years. I thank everyone involved in my lunch breaks in the lunch breaks for their nice discussions as well as many friends that were sharing different types of activities with me such as padel, climbing, football or even learning French. Particularly, I would like to give a big thank you to Arantxa, Bea, Roberto, Raquel, Pau, Laia and Rafa. Muchas gracias a todos por todo lo que hemos compartido juntos estos 4 años, ha sido genial compartir multitud de momentos a vuestro lado y conocerlos a lo largo de esta aventura. Muchas gracias a todos por mantener siempre el buen ambiente y ser la “familia” que uno necesita cuando está lejos de casa.

I would like to thank my family. Doy las gracias a todos por animarme y cuidarme en todo momento y por llenarme de buen humor y cariño en general y por las visitas que han hecho a Estrasburgo a lo largo de estos años. Agradezco especialmente a mis padres y mi hermana, los cuales siempre me han apoyado y motivado a lo largo de mi vida a la vez que siempre han creído en mí. Me habéis dado fuerza en todo momento para llevar a cabo todo lo que me he propuesto siempre. Os quiero mucho, por favor, no cambiéis nunca <3.

Last, but most importantly, I want to thank Xènia. Vam arribar aquí junts i els dos ens hem donat suport pràcticament incondicional en molts moments, sobretot personal però també inclús en algunes vegades professional. Gràcies per escoltar-me sempre i per tots els moments que hem compartit junts aquests 4 anys. Em caldrien infinitat de pàgines per agrair-te tot. Vull que sàpigues que t'estimo molt i que estic desitjant seguir vivint experiències al teu costat.

Table of contents

List of main abbreviations	1
Preamble	3
INTRODUCTION	
General introduction	5
CHAPTER 1: CORTICAL DEVELOPMENT	
1.1. Cerebral cortex – Overview	5
1.2. Cellular composition and cell types	6
1.2.1. Cortical neurons	6
1.2.2. Glial cells	8
1.3. Embryonic origin of the cerebral cortex	8
1.4. Neurogenesis	11
1.4.1. Generation of cortical interneurons	11
1.4.2. Generation of cortical projection neurons	12
1.4.2.1. Cortical lamination	13
Cajal-retzius neurons	14
Subplate neurons	14
1.4.2.2. Progenitor cell types	15
Neuroepithelial cells	15
Apical radial glial cells	16
Apical intermediate progenitors	17
Basal intermediate progenitors	17
Basal radial glial cells	17
1.4.2.3. Mechanisms regulating neurogenesis	18
1.4.2.3.1 Cytoskeleton	18

1.4.2.3.2 Cell cycle length	20
1.4.2.3.3 Cellular signalisation	20
1.4.2.3.4 Transcriptional regulation	23
1.4.2.3.5 Epigenetic modifications.....	24
1.4.2.3.5 Post-transcriptional regulation of gene expression	24
1.4.2.4. Neuronal diversity origins	25
1.5. Neuronal migration.....	28
1.5.1. Tangential migration	29
1.5.2. Radial migration.....	30
1.5.2.2. Somal translocation.....	30
1.5.2.3. Radial-glia guided locomotion	31
1.5.2.3.1 Generation of bipolar neurons and bipolar to multipolar transition	32
1.5.2.3.2 Multipolar to bipolar transition.....	33
1.5.2.3.3 Locomotion	33
1.5.2.3.4 Locomotion termination and Terminal translocation.....	35
1.5.2.4. Main molecular pathways implicated.....	35
1.5.2.4.1 Transcriptional regulation	37
1.5.2.4.2 Adhesion-molecules	38
1.5.2.4.3 Cytoskeleton	39
1.5.2.4.4 Cellular signalisation	40
1.6. Maturation and connectivity	42
1.7 In Utero electroporation: a tool to study cortical development	46
CHAPTER 2: TRANSFER RNAs & TRANSLATION.....	48
2.1 Translation.....	48
2.1.1 The genetic code	48

2.1.1.1 Wobble hypothesis.....	49
2.1.2 Cytoplasmic translation.....	49
2.1.2.1 Phase 1: Initiation	50
2.1.2.2 Phase 2: Elongation.....	51
2.1.2.3 Phase 3: Termination	51
2.2 Transfer RNAs.....	53
2.2.1 Transfer RNA architecture	53
2.2.2 Issoacceptors and isodecoders	54
2.2.3 Transfer RNA biogenesis.....	56
2.2.4 tRNA fragments	59
2.2.5 tRNAs as regulators of biological processes	60
2.3 Transfer RNA modifications	61
2.3.1 Overview.....	61
2.3.2 Function.....	62
2.3.3 tRNA modifications and positions.....	64
2.3.3.1 Modifications at or near the anticodon loop	66
2.3.3.2 Modifications at the tRNA body or arms	67
2.4 Transfer RNAs and the brain	68
2.4.1 Sensitivity of the brain to translation defects	68
2.4.1.1 Elongation factors	69
2.4.1.2 Ribosomal proteins	70
2.4.2 Sensitivity of the brain to tRNA defects	71
2.4.2.1 Transfer-RNA associated neurodevelopmental disorders	75
2.4.2.2 tRNA synthesis and splicing.....	76
2.4.2.3 tRNA aminoacylation.....	77

2.4.2.4 tRNA modifications.....	77
2.5 The ADAT3-ADAT2 complex	79
2.5.1 Domains and structural insights	80
2.5.2 Inosine 34 transfer RNA modification.....	82
2.5.3 Biological relevance	83
2.5.4 Patients.....	85
2.6 The WDR4-METTL1 complex.....	87
2.6.1 Domains	87
2.6.2 m ⁷ G ₄₆ transfer RNA modification.....	89
2.6.3 Biological relevance	90
2.6.4 Patients.....	92
RESULTS	
Article 1: Disruption of the catalytical activity of the tRNA modification complexes, Adat2/Adat3 and Mettl1/Wdr4, impairs neuronal migration and leads to Human neurodevelopmental disorders.....	98
Preliminary results: Characterization of an <i>ADAT3</i> p.V128M homozygous Knock-in mice line	155
DISCUSSION & FUTURE PERSPECTIVES	
1. Functions of Adat2/3 and Wdr4/Mettl1 in the cerebral cortex	188
1.1 Radial neuronal migration.....	188
1.1.1 How to determine which phases of radial migration are impaired?.....	189
1.1.2 Is the function of Adat3 and WDR4 in migrating neurons dependent on their catalytic partners Adat2 and Mettl1?.....	189
1.1.3 Are their deaminase and methylation activities involved?	190
1.2 Cellular proliferation/fate.....	190
2 Does dosage of the Adat2/3 and Wdr4/Mettl1 complex matter?	194

2.1 Use of conditional knock-out animals as models?	196
3. Which are the functions and downstream pathways behind the phenotypes?	197
3.1 tRNA modification: I ₃₄ and m ⁷ G ₄₆	197
3.1.2 Effect I ₃₄ and m ⁷ G ₄₆ tRNA modifications in protein translation.....	198
3.1.3 Possible downstream mechanisms of ADAT2/ADAT3 and WDR4/METTL1 dependent-tRNA defects?.....	200
3.2 Other functions than catalyzing I ₃₄ and m ⁷ G ₄₆ tRNA modifications?	201
3.3 How to determine if the functions of the complexes are linked to their tRNA modifying activity?	204
4. Other brain related functions?	205
5. Effect of ADAT3 and WDR4 variants in cortical development.....	207
5.1 Variants in ADAT3, WDR4 and METTL1 and human disease.....	207
5.1.1 Structural consequences	207
5.1.2 Molecular consequences	209
5.1.3 Cellular consequences.....	212
5.1.4 No variants for ADAT2 in patients: Impossibility or lack of screening?	213
5.2 The Adat3 V128M Knock-in model	213
5.2.1 A good model for disease?	214
5.2.2 Which could be the alternatives to this model?	214
5.2.3 Different sensitivity to ADAT3 or I ₃₄ impairment in human and mice?.....	216
5.2.4 Which compensatory effects?	216
6. Sensitivity of the cortex to ADAT2/3-WDR4/METTL1 and tRNA impairment.....	217

Table of figures

Fig. 1 Representations of the cerebral cortex	6
Fig. 2 Neocortex cortical layers	7
Fig. 3 Origin and overview of CNS glial cells	8
Fig. 4 Initial steps of nervous system formation	9
Fig. 5 overview of CNS formation during human embryonic development	10
Fig. 6 Cortical development chronologic representation	10
Fig. 7 Developmental origins and diversity of cortical interneurons.....	11
Fig. 8 Neurogenesis overview during mice cerebral cortex development.....	13
Fig. 9 Scheme depicting the formation of the cortical plate	14
Fig. 10 Interkinetic nuclear migration	16
Fig. 11 Direct and indirect neurogenesis selected examples in rodents and primates	18
Fig. 12 Regulation of the mitotic spindle during neurogenesis	20
Fig. 13 Molecular pathways regulating the onset, progression, and termination of neurogenesis in the rodent cerebral cortex.	21
Fig. 14 UPR signalling controls neurogenesis during cortical development	23
Fig. 15 Temporal molecular patterning in the mouse neocortex.....	27
Fig. 16 Stochastic scenario of neuronal diversity generation	28
Fig. 17 Neuronal migration in the developing cerebral cortex	29
Fig. 18 Phases for interneurons integration in the cortical plate	30
Fig. 19 Somal translocation	31
Fig. 20 Radial-glia guided migration	32
Fig. 21 Subplate neurons promote multipolar to bipolar transition	33
Fig. 22 Locomotion insights in migrating neurons	34
Fig. 23 Molecular pathways involved in the MP to BP transition, locomotion and termination phases of radial migration.....	36

Fig. 24 Reelin signalling pathway in the developing cortex	42
Fig. 25 Neuronal maturation and connectivity continues after birth	43
Fig. 26 Axon guidance	44
Fig. 27 Cortical projection neuron diversity	45
Fig. 28 In utero electroporation	46
Fig. 29 Overview of translation	48
Fig. 30 The universal genetic code and the wobble hypothesis	49
Fig. 31 Eukaryotic CAP-dependent translation overview	52
Fig. 32 tRNA architecture	54
Fig. 33 tRNA complexity is expanded by isoacceptors and isodecoders	55
FIG. 34 NUMBER OF TRNA SPECIES	55
Fig. 35 tRNA biogenesis overview	56
Fig. 36 Overview of tRNA degradation pathways in <i>S.cerevisiae</i>	59
Fig. 37 tRNA fragments	60
Fig. 38 Various roles of charged and uncharged tRNAs in the cell	61
Fig. 39 Phylogenetic distribution tRNA modifications in three domains of life	62
Fig. 40 Molecular and cellular effects of tRNA modifications	64
Fig. 41 Post-transcriptional tRNA modifications	65
Fig. 42 modifications in the tRNA anticodon stem loop in eukaryotes	67
Fig. 43 Local translation in neurons	69
Fig. 44 Example of an important tRNA in the CNS	72
Fig. 45 Neurological disorders and tRNA-associated genes grouped by category	75
Fig. 46 Bibliographic analysis of disease-associated variants within tRNA related genes ..	75
Fig. 47 tRNA modifications and neurodevelopmental disorders	78
Fig. 48 Domains for human and mice ADAT2/3	81

Fig. 49 Inosine 34 tRNA modification.....	82
Fig. 50 Reported mutations in ADAT3 and clinical features associated	87
Fig. 51 Structure of the yeast Trm8-Trm82 complex.....	88
Fig. 52 Domains for human and mice WDR4-METTL1	89
Fig. 53 m ⁷ G ₄₆ tRNA modification	90
Fig. 54 Reported mutations in WDR4 and clinical features associated	94

List of main abbreviations

aa: amino acid	ID: Intellectual disability
aaRS: aminoacyl-tRNA synthetases	IF: Immunofluorescence
ADAT2: tRNA-specific adenosine deaminase 2	IHC: Immunohistochemistry
ADAT3: tRNA-specific adenosine deaminase 3	INM: Interkinetic nuclear migration
aIPs: Apical intermediate progenitors	IUE: In utero electroporation
aRGCs: Apical radial glia cells	IZ: Intermediate zone
bIPs: Basal intermediate progenitors	KD: Knock-down
BP: Bipolar	KI: Knock-in
bRGCs: Basal radial glia cells	KO: Knock-out
cDNA: Complementary deoxyribonucleic acid	LCLs: Lymphoblastoid cell lines
CDS: Coding sequence	LGE: Lateral Ganglionic Eminence
CGE: Caudal Ganglionic Eminences	m^7G_{46} : N7-methylguanine at position 46
cKO: conditional Knock-out	MAP: Microtubule associated protein
CNS: Central nervous system	MCD: Malformations cortical development
CP: Cortical plate	METTL1: tRNA (guanine-N(7)-)methyltransferase
CR: Cajal-Retzius	MGE: Medial Ganglionic Eminence
CSF: Cerebrospinal fluid	miRNA: micro RNA
DNA: Deoxyribonucleic acid	miRNAs: micro RNAs
E: Embryonic day	MP: Multipolar
EMSA: Electrophoretic Mobility shift assay	MT: Microtubules
ER: Endoplasmic reticulum	mt: Mitochondrial
ESC: Embryonic stem cell	MZ: Marginal zone
GE: Ganglionic eminences	N2a: Neuro2a cells
GW: Gestational week	nbIPs: Neurogenic basal intermediate progenitors
HEK293T: Human embryonic kidney 293T cells	NEC: Neuroepithelial cells
I ₃₄ : Inosine at position 34	pblIPs: Proliferative basal intermediate progenitors
	PoA: Preoptic area

PTM: Post-transcriptional modification

qPCR: Quantitative Polymerase Chain reaction

RG: Radial glia

RNA: Ribonucleic acid

shRNAs: Small hairpin RNAs

siRNAs: Small interfering RNAs

SP: Subplate

SVZ: Sub-ventricular zone

tfRNA: fragmented transfer RNAs

tiRNA: tRNA halves

tRNA: transfer RNA

UPR: Unfolded protein response

UTR: Untranslated region

VZ: Ventricular zone

WB: Western Blot

WDR4: tRNA (guanine-N(7))-methyltransferase non-catalytic subunit

WT: Wild-type

Preamble

A growing body of data supports the idea that many neurological and psychiatric illnesses - ranging from epilepsy to mental retardation - originate from impaired processes of development of the cerebral cortex. Understanding the mechanisms that govern the development and functioning of the cortex is therefore essential to better understand the bases of these neurological disorders. The efficiency and accuracy of protein translation, a mechanism primarily controlled by transfer RNA (tRNA), is an important determinant of cell homeostasis. Interestingly, the brain shows high levels of tRNA compared to many other tissues and great variability in the tRNA pool between the embryonic and adult stages. In order to be fully functional, the tRNAs are subject to post-transcriptional maturation stages. In particular, certain nucleotides undergo chemical modifications catalyzed by so-called modification enzymes. These chemical modifications are crucial for their structure, function and stability. Mutations in genes encoding these tRNA modification enzymes have recently been associated with neurodevelopmental diseases, such as intellectual disability or epilepsy. How do such mutations lead to neurological disorders? What are the major stages of cortical development requiring strict regulation of modifications of tRNAs? These questions remain unanswered to date.

The main goal of my thesis is to identify and better understand the role of modifications of tRNAs during cortical development in physiological and pathological conditions. My main objective is to define the cellular processes which depend on the strict regulation of modifications of tRNAs. For this, I studied two candidate genes, for which variants have been identified in patients with microcephaly: *ADAT3* and *WDR4*. *ADAT3* and *WDR4* are respectively the non-catalytic subunits of two heterodimers: *ADAT2* / *ADAT3*, which modifies adenosine to inosine at position 34 (I₃₄), and *WDR4* / *METTL1* which catalyzes the formation of N (7) -methylguanosine position 46 (m⁷G₄₆).

Along the introduction I make an overview on cortical development, focusing in neurogenesis and neuronal radial migration as well as giving an overview of the main technique I used to study cortical development (In Utero Electroporation). Subsequently, I concentrate on translation and tRNAs, their association to neurological diseases and provide a review about the *ADAT2/ADAT3* and *WDR4/METTL1* complexes.

PART1

INTRODUCTION

General introduction

CHAPTER 1: CORTICAL DEVELOPMENT

1.1. Cerebral cortex – Overview

The cortex is the gray matter that covers the surface of the two cerebral hemispheres (left and right), which are connected by a large bundle of fibers, the corpus callosum. In Human, the cerebral cortex is highly evolved; it contains approximately 20% of all the neurons in the brain and represents almost 80% of the total brain mass (Azevedo et al., 2009). From a functional point of view the cortex can be divided functionally into different areas (See Fig.1), which control different cognitive, motor or sensory functions. From a structural point of view, the cerebral cortex can be classified into two types, the neocortex, which is a large area with six cell layers, and the allocortex, a much smaller area of three or four layers. The brain is the most complex organ in our body. Regarding the diversity of cell types, cytoarchitecture, and neural connections and circuits, this complexity becomes even greater in the neocortex, the basis of higher cognitive functions. Some fundamental aspects of the structure of the neocortex are conserved among various mammalian species, however, there are important differences in terms of size and morphology: For example, in mouse and rat (the two most widely used models for studying the brain) the neocortex is lissencephalic (smooth) while in most primates (including humans) the neocortex is gyrencephalic (folded) and exhibits gyri (fold or ridge) and sulci (grooves) (Namba et al., 2017). The major sulci and gyri mark the divisions of the cerebrum into the lobes of the brain (See Fig.1).

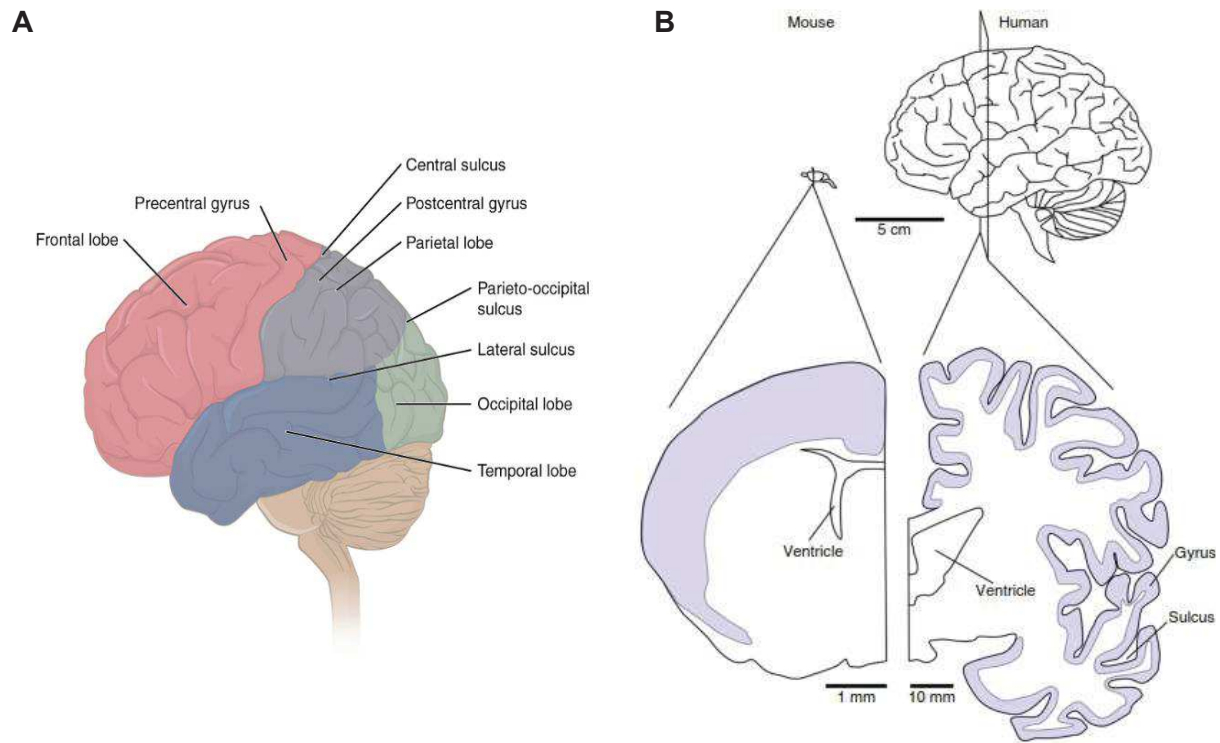


FIG. 1 REPRESENTATIONS OF THE CEREBRAL CORTEX

(A) *The cerebral cortex is divided in four lobes (frontal, parietal, temporal and occipital). Sulci and gyri increase the surface area available for cerebral functions (William, 2020).*

(B) *Schematic representation of a coronal section from an adult brain in mice and human. Blue areas indicate the gray matter. (Namba et al., 2017)*

1.2. Cellular composition and cell types

In the mammalian neocortex there are hundreds of different neuronal types and a wide range of glial cells.

1.2.1. Cortical neurons

There are two main classes of cortical neurons: 1) Projection neurons and 2) Interneurons. Projection neurons are essentially glutamatergic and excitatory and represent 70-80% of the total number of cortical neurons. These neurons have a typical pyramidal morphology and extend their axons to reach distant intracortical, subcortical, and subcerebral targets. During development, they are generated from progenitors from ventricular (VZ) and subventricular (SVZ) zones located in the dorsolateral wall of the telencephalon. In the mature neocortex, there exist 6 different cortical layers (I-VI), different types of projection neurons are located in different cortical layers and areas (See Fig. 2). The different cellular types are classified based

on unique morphological aspects, different functions, or the expression of different genes, such as transcription factors. On the other hand, interneurons are essentially GABAergic and inhibitory and represent the remaining 20%. These neurons establish local connections and are generated from progenitors in the ganglionic eminences (GE) and the preoptic area (PoA) (Molyneaux et al., 2007).

The different origin of these two classes of cortical neurons influences the migration paths that these they use to reach their final location. Whereas projection neurons follow a radial migration (See section 1.5.2), interneurons follow a tangential migration (See section 1.5.2) and migrate long distances to reach their final location in the neocortex.

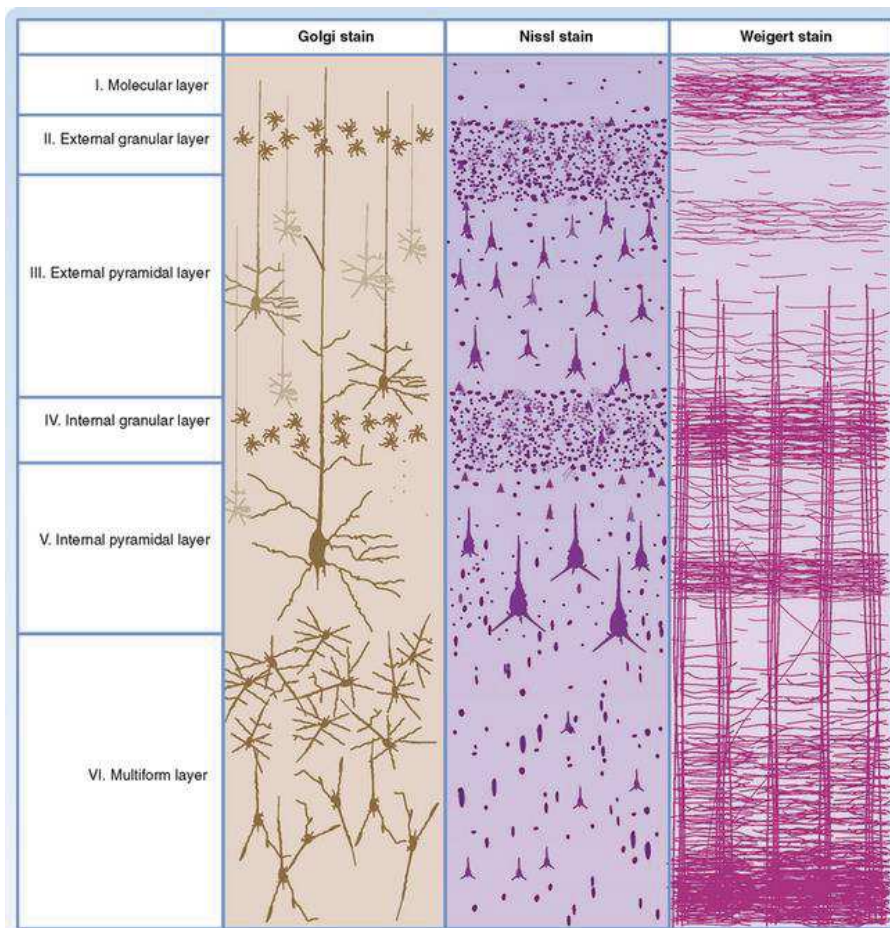


FIG. 2 NEOCORTEX CORTICAL LAYERS

The diagram shows the six cortical layers of the neocortex and their appearance when stained by three different methods: Golgi, Nissl and Weigert. Golgi staining allows to see dendritic details, Nissl stains neuronal bodies and shows how different neuronal populations are distributed by the different layers and Weigert stains myelin and allows the observation of axons extended either vertically (entering and leaving the cortex) or horizontally (connecting neurons within a layer). From ("Higher Functions of the Nervous System," 2016)

1.2.2. Glial cells

Glial cells are part of approximately 50% of the cells of the central nervous system (CNS). There are different types of glial cells (See Fig. 3): Astrocytes, oligodendrocyte progenitor cells, oligodendrocytes, and microglia. The most well-known functions of glia are the supply of nutrients (astrocytes), the formation of myelin (oligodendrocytes) and the immune defense (microglia). However, glia influence nervous system development, including the neocortex, in other aspects such as neuronal migration, axon specification, and growth through circuit assembly and synaptogenesis (Allen et al., 2018).

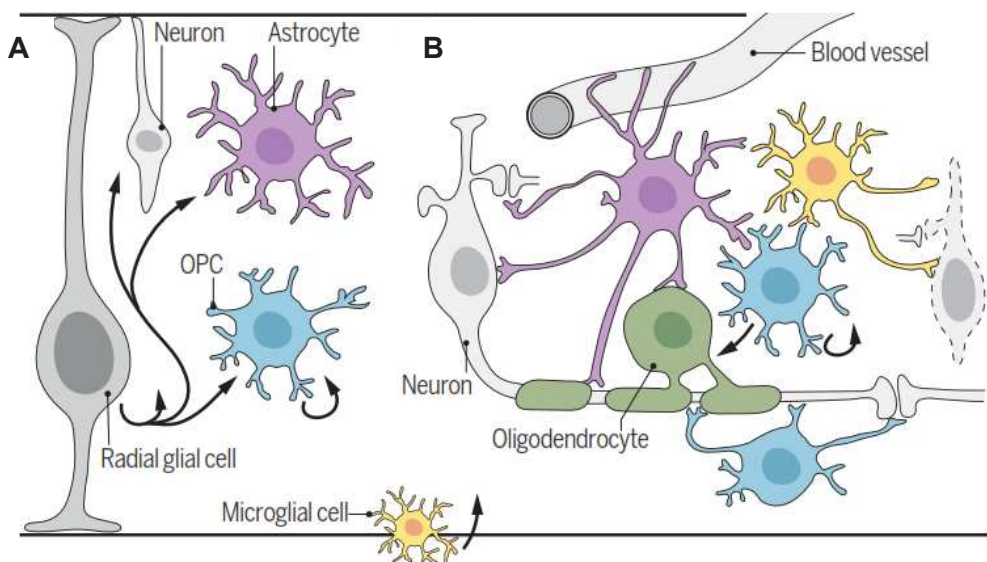


FIG. 3 ORIGIN AND OVERVIEW OF CNS GLIAL CELLS

(A) *Radial glial cells generate directly or indirectly most of CNS cells (neurons and) glia. For generating glial cells, RGCs can directly differentiate into astrocytes or differentiate into oligodendrocyte precursor cells (OPCs).* (B) *Neurons and glia interact in many different ways. Microglial cells enter the CNS during embryonic development.* (Allen et al., 2018)

1.3. Embryonic origin of the cerebral cortex

Throughout embryonic development, during the neurulation process, the neural plate transforms into the neural tube (Fig. 4), which will give rise to the CNS, including the brain and the spinal cord (Eom et al., 2013). The initial steps of nervous system formation are conserved between human and mice.

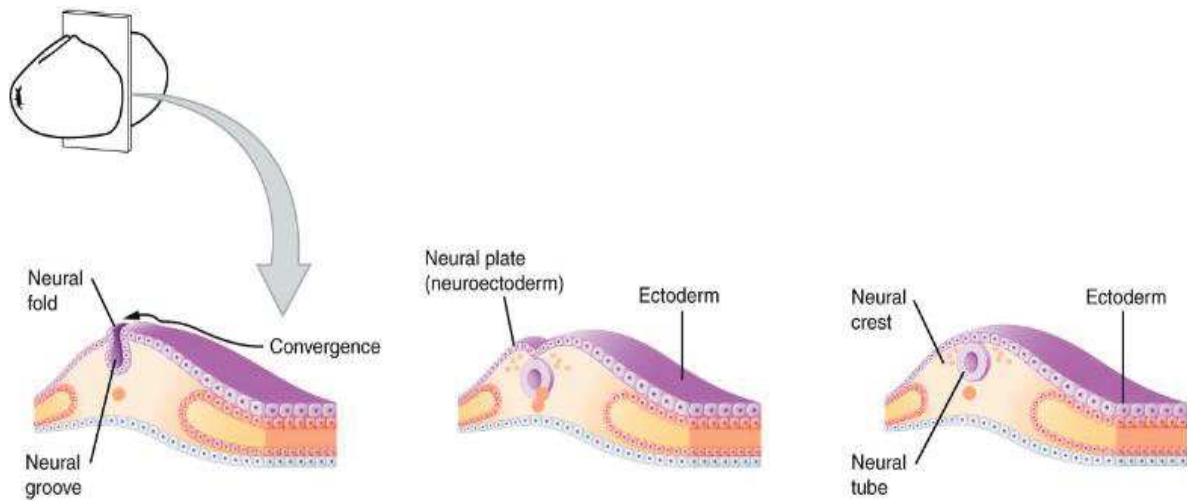


FIG. 4 INITIAL STEPS OF NERVOUS SYSTEM FORMATION

Neuroectoderm folds to form the neural groove, when the two sides of this structure converge the neural tube is formed. The anterior end of the neural tube will develop into the brain and the posterior one into the spinal cord. (William, 2020)

In Human, the neural tube increases its size, giving rise to three primary vesicles in a 3-4 week stage embryo. These three primary vesicles are the prosencephalon (forebrain), the mesencephalon (midbrain) and the rhombencephalon (hindbrain), which are named based on their location along the length of the developing nervous system. The prosencephalon is the most anterior one, whereas, the rhombencephalon is the one located more posteriorly. The brain will continue to develop and the vesicles will differentiate further, by the 5th week of development, the three primary vesicles give rise to the five secondary vesicles: The prosencephalon enlarges into two vesicles, the telencephalon, which will give rise to the cerebrum, and the diencephalon, which will give rise to several structures such as the thalamus and the hypothalamus. The mesencephalon (or midbrain) does not differentiate into other structures. The rhombencephalon develops into the metencephalon, which will develop further into the pons and the cerebellum, and the myelencephalon, which corresponds to the medulla oblongata in the adult stage (William, 2020). A scheme of the process is depicted in Fig. 5.

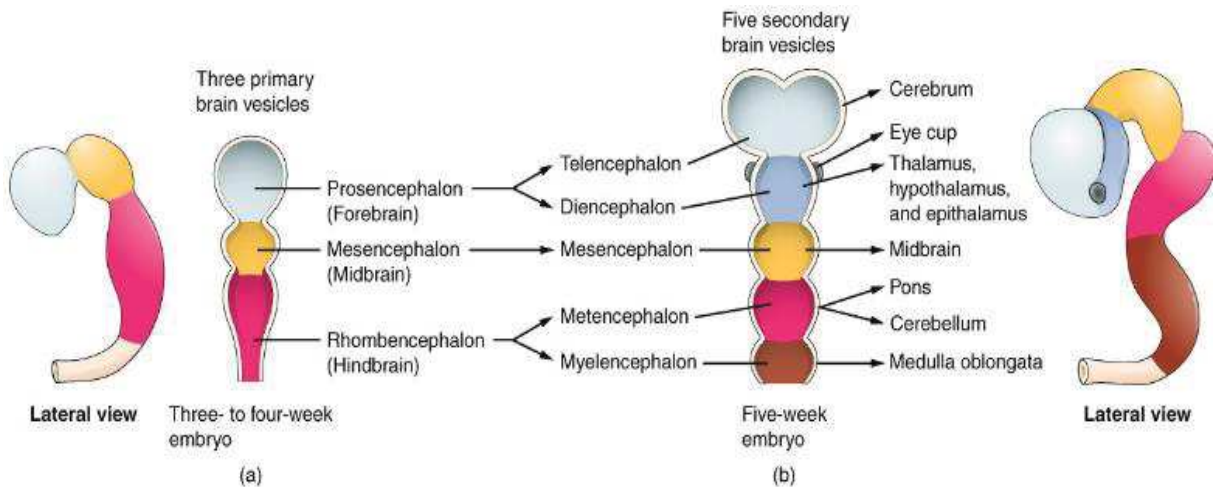


FIG. 5 OVERVIEW OF CNS FORMATION DURING HUMAN EMBRYONIC DEVELOPMENT

Enlargements of the neural tube are called vesicles. (A) The primary vesicle stage consists of three regions, which throughout development will give rise to (B) the secondary vesicle stage, which consists of five regions. CNS structures that develop from each of the regions are detailed. From (William, 2020)

As I mentioned above, the cerebral cortex has its embryonic origin in the forebrain. Its formation requires multiple stages including, the proliferation of progenitor cells, the migration of post-mitotic neurons and their differentiation and maturation (Molyneaux et al. (2007)). Each one of these steps, is explained in detail in the following sections. Fig.6 shows a chronologic overview of cortical development for human, monkey and mice.

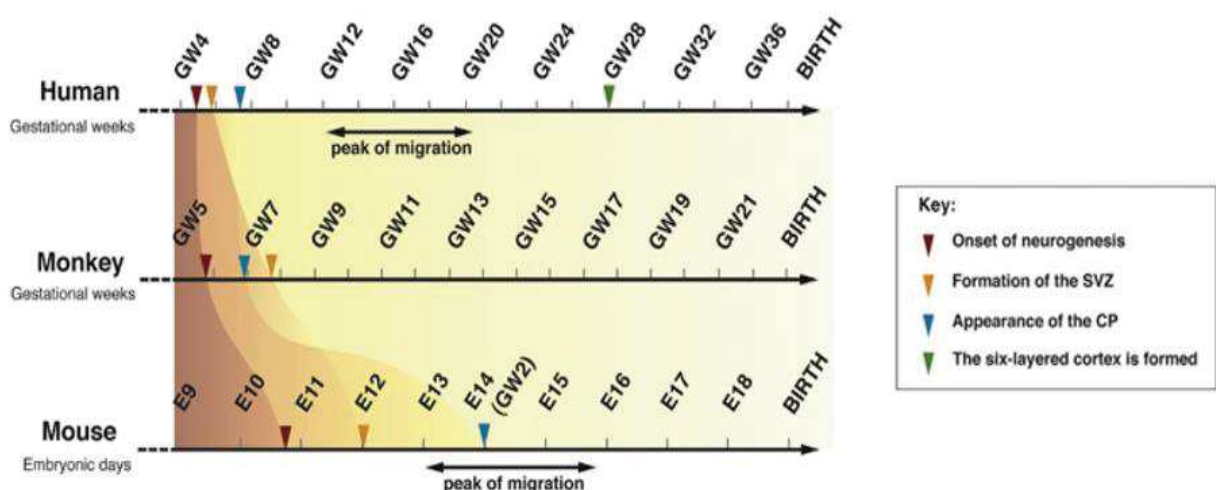


FIG. 6 CORTICAL DEVELOPMENT CHRONOLOGIC REPRESENTATION

The main events for the formation of the cerebral cortex are shown as a chronologic representation for human, monkey and mouse. The neural tube closes at Gestational week (GW) 4, GW5, and E9 in humans, monkey, and mouse respectively. Neurogenesis begins around GW5-6 in human and primate and E10-11 in mice. Neural migration peaks occur between GW12 to GW20 and E13 to E16 in human and mouse, respectively. From (Jaglin et al., 2009)

1.4. Neurogenesis

Neurogenesis is the process by which new neurons are generated from stem cells and progenitor cells. Lineage tracing experiments have shown that projection neurons and interneurons are generated separately during development and do not share a common origin (S. A. Anderson et al., 2002). Whereas projection neurons are born in the dorsal telencephalon, most if not all interneurons are originated in the ventral telencephalon. The generation of interneurons and projection neurons is explained below. There is more information about projection neurons neurogenesis as my PhD work has been mainly focused on this cell population.

1.4.1. Generation of cortical interneurons

In mice, cortical interneurons are born during embryonic stages in the ventral telencephalon (See Fig. 7), specifically, in the ganglionic eminences (GE) and the preoptic area (PoA). The GE is a transitory structure during embryonic development, which anatomically divided into three zones, lateral, medial and caudal (LGE, MGE and CGE, respectively). Interneurons are generated from E11 to E17 in the MGE (peak at E13.5) and a bit later ~E12.5 in the CGE (peak at E15.5)(Butt et al., 2005; K. T. Sultan et al., 2018).

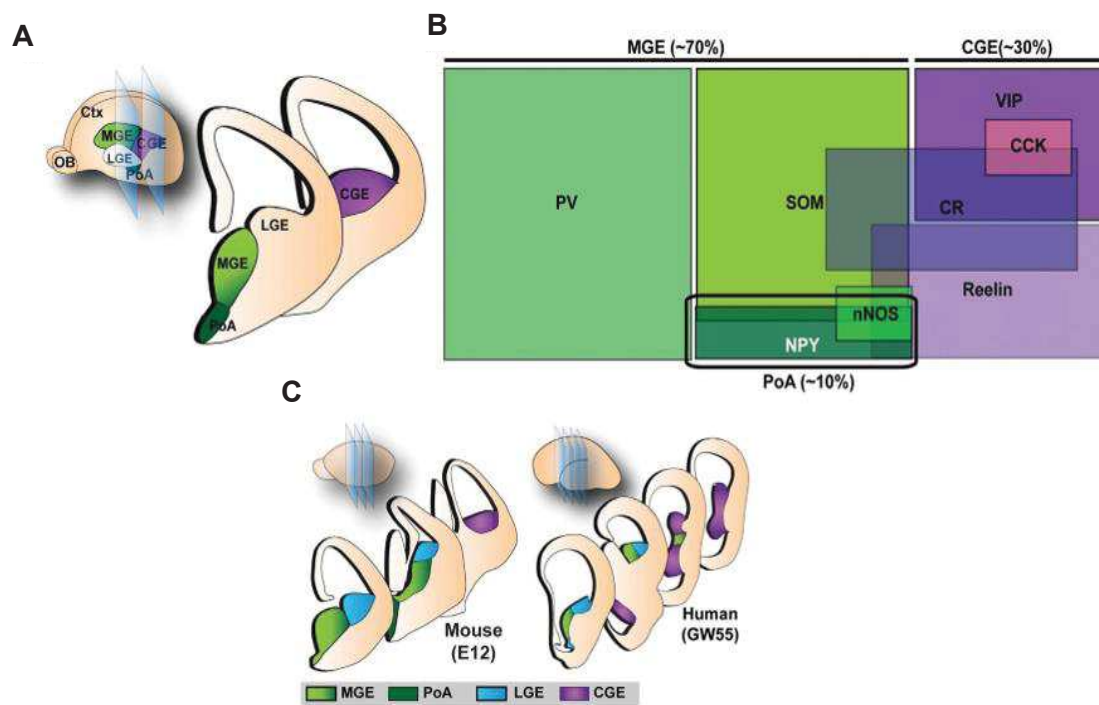


FIG. 7 DEVELOPMENTAL ORIGINS AND DIVERSITY OF CORTICAL INTERNEURONS

(A) *Cortical interneurons in mouse are generated from progenitor cells located in the MGE (light green), CGE (purple) and PoA (dark green).* (B) *MGE is the main source of interneurons, giving rise to ~ 70%*

of the total, which will be divided into two subgroups, depending on whether they express PV (parvalbumin) or SOM (somatostatin). Approximately the 30% is generated in the CGE, this represents a much more heterogeneous group and is classified in subgroups based on the expression of 5HTR (serotonin receptor), VIP (vasointestinal peptide) or reelin. In addition, the CGE is the main source of CR (calretinin) and CCK (cholecystokinin) -expressing cells. The PoA generates ~ 10% of interneurons, and gives rise to interneurons that express NPY (neuropeptide Y), nNOS (neuronal nitric oxide synthase), or SOM. (C) Developmental origin of interneurons in mouse and human. Abbreviations: E, embryonic day; GW, gestation week, LGE, lateral ganglionic eminence; Ctx, cortex; OB, olfactory bulb. Adapted from (K. T. Sultan et al., 2018)

1.4.2. Generation of cortical projection neurons

The neurogenesis of cortical projection neurons begins after the closure of the neural tube at the 4th gestational week in humans and Embryonic day 9 (E9) in mice. During early stages of cerebral cortical development (E10.5-E11.5 in mice) there is an expansion phase in which neuroepithelial cells expand their cellular pool. In later stages (E12.5-E16.5 in mice, peak at E14.5), the neurogenic phase takes place and neurons are generated this sequentially and populate the cortex in an-inside-out fashion (later born neurons migrate past earlier born neurons) (See Fig.8). The gliogenic phase occurs from E17.5 to postnatal stages (mice), during this phase the other CNS cell types (astrocytes, oligodendrocytes, and ependymal cells) are generated (Mukhtar et al., 2018). An overview of the process is shown in Fig.8.

The cell types involved, as well as their main characteristics and regulatory mechanisms are detailed below.

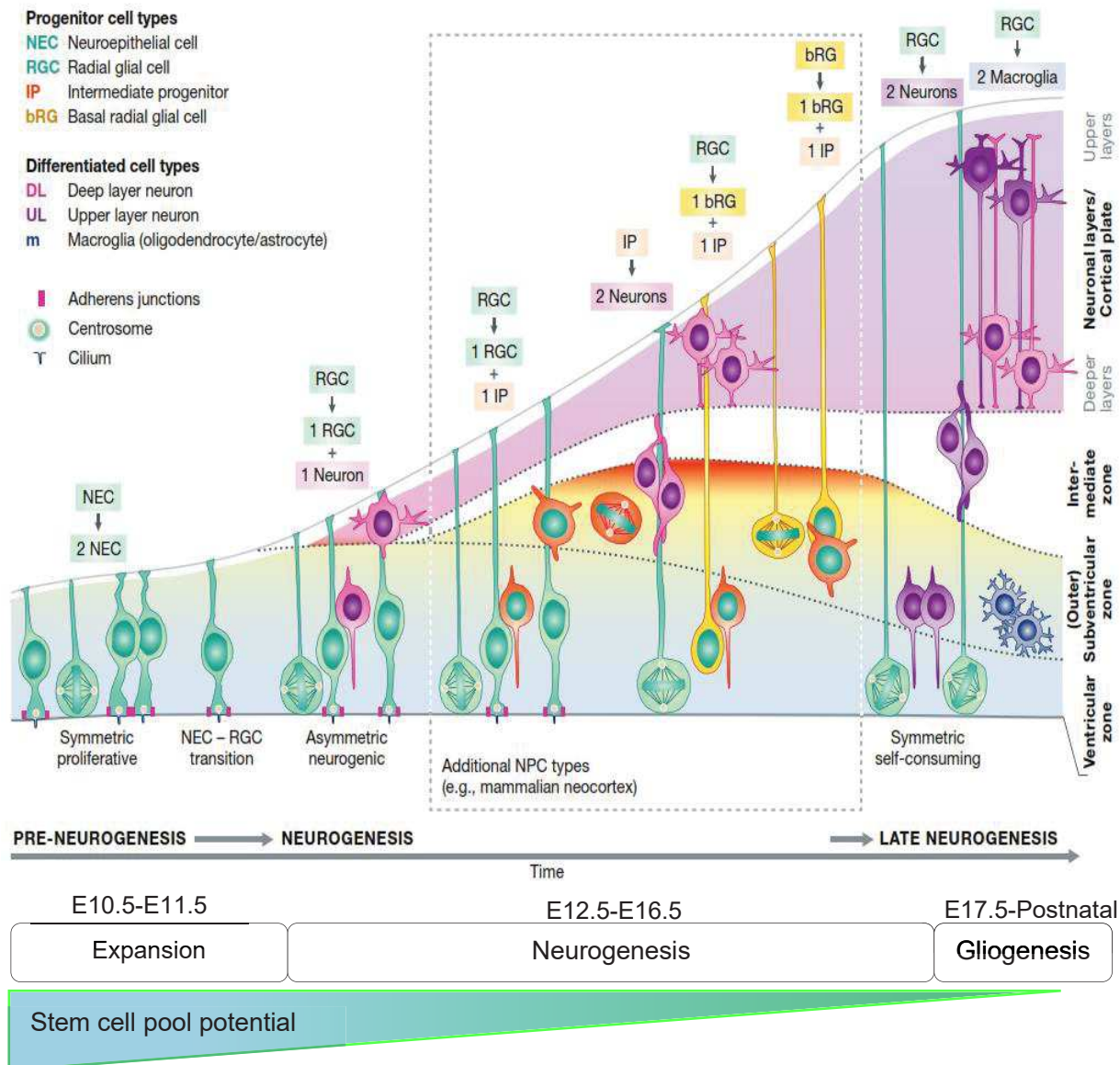


FIG. 8 NEUROGENESIS OVERVIEW DURING MICE CEREBRAL CORTEX DEVELOPMENT

The principal types of progenitor cells as well as the progeny that they produce are indicated by different colors, for simplification only some of the possible daughter cells are shown. The stem cell pool potential decreases as cortical development progresses. The timing of the expansion, neurogenesis and gliogenesis phases is indicated. Adapted from (Paridaen et al., 2014)

1.4.2.1. Cortical lamination

The first projection neurons generated during neurogenesis (~ E11 in mice) are Cajal-Retzius (CR) and subplate (SP) neurons colonize the Marginal zone (MZ, future layer I) and the subplate (SP) respectively (Martinez-Cerdeno et al., 2014). Subsequently, different

overlapping temporal waves will take place producing different subtypes of projection neurons which will populate the CP completing the layers VI to II in an inside-out-manner (neurons born later migrate through the deeper layers to settle on the most superficial ones) until the complete formation of the CP (See Fig. 9) (Nadarajah et al., 2002) (Molyneaux et al., 2007).

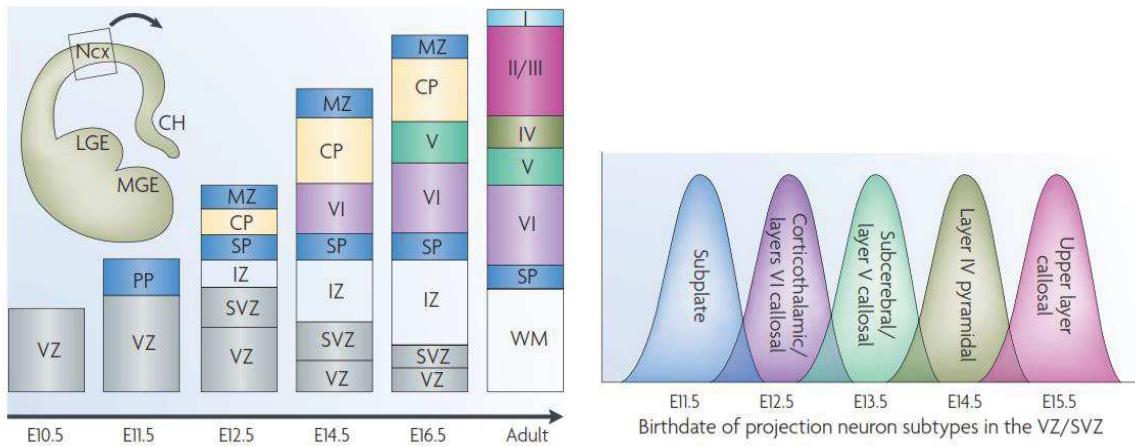


FIG. 9 SCHEME DEPICTING THE FORMATION OF THE CORTICAL PLATE

The first neurons to be generated will form the preplate (PP), which will later be divided into the marginal zone (MZ) and the subplate (SP). The cortical plate (CP), where the 6 layers of the neocortex are located, is formed between the MZ and the SP. Different types of projection neurons form in overlapping temporal waves. From (Molyneaux et al., 2007)

CR and SP neurons have critical functions for cortical lamination and radial migration, an overview of these two cell populations is included below:

Cajal-retzius neurons

CR neurons are located in the MZ, whereas in rodents they disappear from the cerebral cortex once radial migration has ended (Derer et al., 1990). In higher mammals some CR cells could persist until adulthood (Abraham et al., 2005). They are a heterogeneous population in terms of transcription factors expression and their origins (which can be the pallium VZ, the medial GE, the cortical hem or the retrobulbar VZ) suggests that the CR population comprises different neural subpopulations (Bielle et al., 2005). Nevertheless, all CR cells are characterized by the expression of the extracellular matrix protein reelin (CR cells being its main production source (Rice et al., 2001)), which is essential for correct cortex lamination and radial migration (D'Arcangelo et al., 1995) (details in 1.5.2.4.4).

Subplate neurons

The subplate represents a transitory layer that is found during the development of the cerebral cortex, it is located between the IZ and the CP. SP neurons are a heterogeneous population that are formed before the first CP neurons, between E11 and E12 and that disappears

completely by P8 in mice (Price et al., 1997; Valverde et al., 1995). Some of them are derived from apical or basal progenitors located in the VZ and SVZ, others however, are originated from progenitors in the MGE and migrate tangentially (Lavdas et al., 1999) to reach the SP. SP neurons represent the first cortical neurons that receive synaptic input from axons from the thalamus, thus establishing a temporal connection between the thalamic axons and the layer IV, which will be their final destination (McConnell et al., 1989). These cells have relatively mature structures such as the extensive presence of axons or arborization (Hanganu et al., 2002). They are also important for cortical wiring (Judas et al., 2010) and functional maturation (Kanold et al., 2003) as well as during radial migration in which they serve as a physical border between the CP and IZ and accommodate neurons during and after their migration.

1.4.2.2. Progenitor cell types

The progenitor cell types nomenclature is sometimes controversial, in the following sections the nomenclature from a recent review will be used (Namba et al., 2017).

Neuroepithelial cells

Neuroepithelial cells (NECs) constitute a monolayer that forms a pseudostratified epithelium, they will give rise directly or indirectly to all neuronal and glial cells that compose the adult cerebral cortex (Gotz et al., 2005). They exhibit Pax6 and Nestin expression, tight and adherent junctions, apico-basal polarity, with an apical surface, apical junctions and contact with the basal lamina. Throughout the cell cycle, NECs carry out a very characteristic movement of their nuclei, known as interkinetic nuclear migration (INM) (detailed in Fig.10) (Taverna et al., 2010). INM is responsible for the pseudostratified appearance of the neuroepithelium and allows the neuroepithelium to pack more cells into a limited surface area (Laguesse et al., 2015). During the initial phases of neurogenesis, embryonic days 10.5 and 11.5 (E10.5-11.5) in mice), NECs undergo symmetric cell divisions (each NEC gives rise to two NECs) to expand the NEC pool. As neurogenesis proceeds, NECs will switch to an asymmetric division (generating a NEC and a radial glial cell (RGC)) and change their identity to RGCs (in mice between E10 and E12) (Noctor et al., 2004). In the NEC to RGC transition NECs will undergo some changes, including the loss of tight functions and the acquisition of astroglial hallmarks (Laguesse et al., 2015).

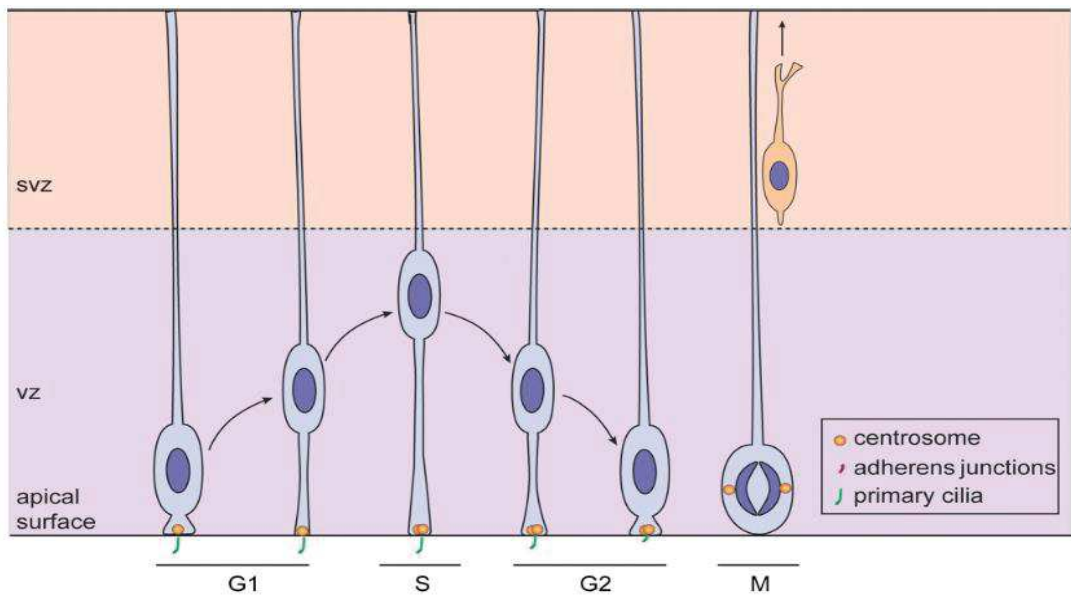


FIG. 10 INTERKINETIC NUCLEAR MIGRATION

NECs nuclei occupy different positions along the apical-basal axis depending on the cell cycle phase: During G1, the nucleus exhibits an apical position, and initiates an apical-to-basal movement to be located basally in the S phase. During G2, a basal-to-apical movement takes place. Finally, by M phase, the nucleus returns to the apical surface and cell division takes place, which can be symmetric or asymmetric. From (Laguesse et al., 2015)

Apical radial glial cells

Apical radial glial cells (aRGCs) share important characteristics with NECs, such as apical-basal polarity, INM, and the expression of markers such as Pax6 and Nestin. Although, some of the mechanisms in the transition from NEC to aRGC are not yet fully understood, it is known that in this transition aRGCs begin to express astroglial markers, such as GLAST and BLBP (Paridaen et al., 2014). An important difference between NECs and aRGCs is the presence, in the latter aRGCs, of a basal process that starts from the ventricular zone (VZ) and reaches the cortical plate (CP), which will serve as a scaffold during neuronal migration (Namba et al., 2017). aRGCs have been shown to be more restricted in their differentiation potential than NECs by fate mapping experiments (Noctor et al., 2004). Whereas during early neurogenesis they divide mostly symmetrically to amplify their cellular pool, in later phases they mostly divide asymmetrically to self-renew and generate a neuron either directly (direct neurogenesis) or indirectly through the generation of a basal intermediate progenitor (indirect neurogenesis). By E17.5 in mice, 5/6 of aRGCs will undergo a last terminal symmetric division giving rise to two neurons whereas the 1/6 will become gliogenic (Beattie et al., 2017).

Apical intermediate progenitors

Apical intermediate progenitors (aIPs) are part of the progeny of aRGCs. aIPs show several similarities with aRGCs, such as INM, however, aIPs basal processes do not reach the basal lamina, and they do not express astroglial markers (Although they express Pax6) (Gal et al., 2006). Regarding their cell division, most carry out symmetrical divisions, giving rise to two neuronal daughter cells (Noctor et al., 2004).

Basal intermediate progenitors

Basal intermediate progenitors (bIPs) have delaminated from the ventricular surface, do not present apical-basal polarity and are usually located in the sub-ventricular zone (SVZ) where they carry out mitosis (Miyata et al., 2004). bIPs can carry out symmetric cell divisions to amplify their own cellular pool (10-20%, known as proliferative bIP, pbIP), or generate two neurons (known as neurogenic bIP, nbIP). nbIPs are thought to contribute to most cortical neurons in rodents (Noctor et al., 2004). TBR2 and NEUROG2 are characteristic markers bIPs (PAX6 is no expressed in rodents bIPs, whereas in humans and other gyroencephalic species the expression of this marker could be sustained) (Turrero Garcia et al., 2016).

Basal radial glial cells

Basal radial glial cells (bRGCs) share certain features with aRGCs, such as, the presence of a basal process towards the basal lamina, having cellular polarity or the expression of astroglial and PAX6 markers. Nevertheless, they are not in contact with the surface of the ventricle and do not have apical cell polarity (Hansen et al., 2010). These cells are numerous in species with gyrencephalic brains like primates and ferret, however, in lissencephalic species, like rodents their presence is very low (Penisson et al., 2019).

Indirect neurogenesis has evolved in gyrencephalic species to reach a higher demand in terms of neuronal generation. The differences among gyrencephalic and lissencephalic species on the different cell types, particularly bIPs and bRGCs, as well as in the neurogenic pathways are depicted in Fig.11.

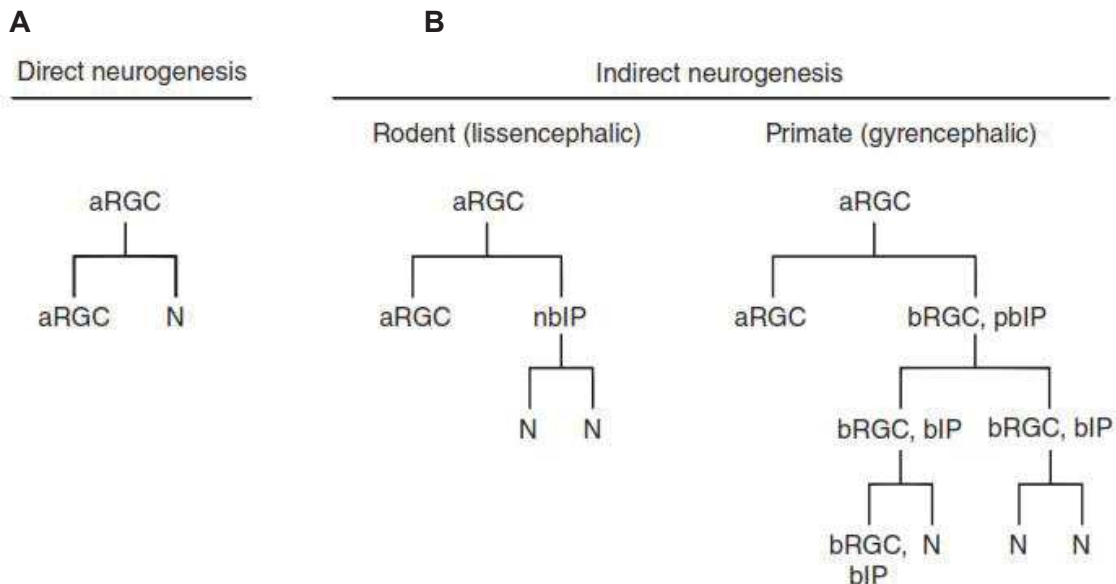


FIG. 11 DIRECT AND INDIRECT NEUROGENESIS SELECTED EXAMPLES IN RODENTS AND PRIMATES

(A) *Direct neurogenesis by asymmetric division of an aRGC (common mechanisms in rodents and primates).* B) *Indirect neurogenesis selected differences between 1) rodents, and 2) primates. In 1) an aRGC undergoes asymmetric cell division yielding another aRGC and a nbIP, which divides symmetrically to yield two neurons. In 2) an aRGC undergoes asymmetric cell division yielding another aRGC and a bRGC or a pbIP, which both can carry out a symmetric cell division to yield more bRGC or bIP. These then undergo either asymmetric or symmetric division to yield neurons.* From (Namba et al., 2017)

1.4.2.3. Mechanisms regulating neurogenesis

There are several intrinsic and extrinsic factors known to be involved in cortical neurogenesis. In the next sections the main mechanisms regulating neurogenesis will be summarized.

1.4.2.3.1 Cytoskeleton

Cytoskeleton components play an essential role during cortical development influencing both neurogenesis and neuronal migration (discussed in section 1.5). The organization of the mitotic spindle can determine if a symmetrical or asymmetric segregation of various cellular components and cell fate determinants occurs, therefore influencing cells generated from the cell division.

The organization of the mitotic spindle is regulated by various mechanisms, including the centrosome, astral microtubule (MT) positioning, and the interaction with cell cortex proteins (Lancaster et al., 2012). The mitotic spindle stays anchored to the cell cortex through the combined action of astral MT, together with dynein and the LGN / Gai / NuMa complex (Konno et al., 2008; Peyre et al., 2011). The Lis1 / Nde1 complex together with dynein allow astral MT

to stay anchored to the cell cortex. Insc is important for the orientation of the mitotic spindle in asymmetric divisions (Postiglione et al., 2011).

Interestingly, several centrosomal proteins, such as Aspm, Cdk5rap2 or MCPH1 have been associated to microcephaly when mutated (Gilmore et al., 2013). When cell division occurs there will be a newer and an older centriole, in NECs and RGCs, the oldest centriole is normally received by the cell that will maintain the stem cell status, this is because the oldest centriole is the one mediates the nucleation of the primary cilium (X. Wang et al., 2009), a structure formed from the centrosome and present in the apical membrane of aRGCs and NECs, where it acts as a sensor for extracellular signals from the CSF (cerebrospinal fluid) (C. T. Anderson et al., 2009). Interestingly, Paridaen and colleagues showed that there is an asymmetric inheritance of the centrosome-associated primary cilium membrane which acts as a determinant for controlling ciliogenesis after cell division (Paridaen et al., 2013). Inheritance of basal and / or apical domains is important for the maintenance of RGC cell typology, the presence of an earlier primary cilium is thought to contribute to the maintenance of RGC status (Konno et al., 2008; Shitamukai et al., 2011). The symmetric divisions that NECs and RGCs perform to expand their own cellular pool are perpendicular to the VZ (vertical cleavage), whereas in the mammalian neocortex, oblique (majority) or horizontal (minority) cuts occur to allow asymmetric divisions that give rise to basal progenitors (ex: IPs and bRGCs) (Kosodo et al., 2004; Postiglione et al., 2011). In the case of the RGCs that carry out asymmetric divisions, an unequal distribution of cellular polarity proteins, such as Par3, and signalling pathways, such as Notch (involved in the regulation of neurogenesis, see following sections), takes place and promotes the generation of two different cell types (Bultje et al., 2009; Kosodo et al., 2004). An overview of the regulation of mitotic spindle during neurogenesis is shown in Fig. 12.

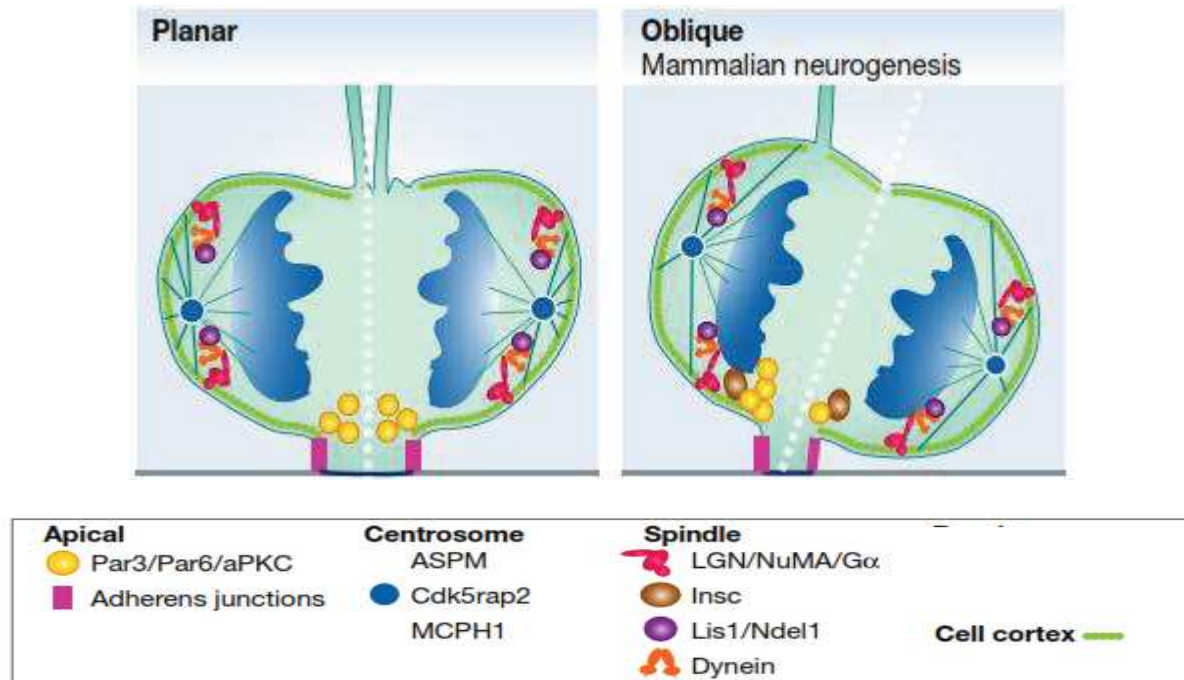


FIG. 12 REGULATION OF THE MITOTIC SPINDLE DURING NEUROGENESIS

Mitotic spindle orientation, which is regulated by centrosomal proteins and spindle orientation complexes, determines the direction of the cell division cut (planar or oblique). Inheritance of several fate determinants plays a key role during symmetric/asymmetric cell divisions. From (Paridaen et al., 2014)

1.4.2.3.2 Cell cycle length

Cell cycle length and kinetics are an important cell fate determinant during neurogenesis (Dehay et al., 2007). Takahashi and colleagues reported that as neurogenesis progresses the cell cycle length of NECs increases (Takahashi et al., 1995). It was later observed, that the cell cycle length of other cortical progenitors, such as RGC, also changes throughout the development of the cortex. For example, while proliferative RGC have a longer S phase, neurogenic RGCs have a longer G1 phase (24-26). In particular, the duration of the G1 phase has been proven to be a determining factor on cell fate, whereas, a forced lengthening of this phase in progenitors leads to early neurogenesis, its forced shortening causes delayed neurogenesis (Calegari et al., 2003; Lange et al., 2009).

1.4.2.3.3 Cellular signalisation

Several signaling pathways regulate neurogenesis in different ways, nevertheless there is a significant crosstalk between them. An overview of the main molecular pathways implicated in regulating the onset, maintenance and the end of neurogenesis and the switch to gliogenesis are depicted in Fig. 13.

Onset and progression of neurogenesis

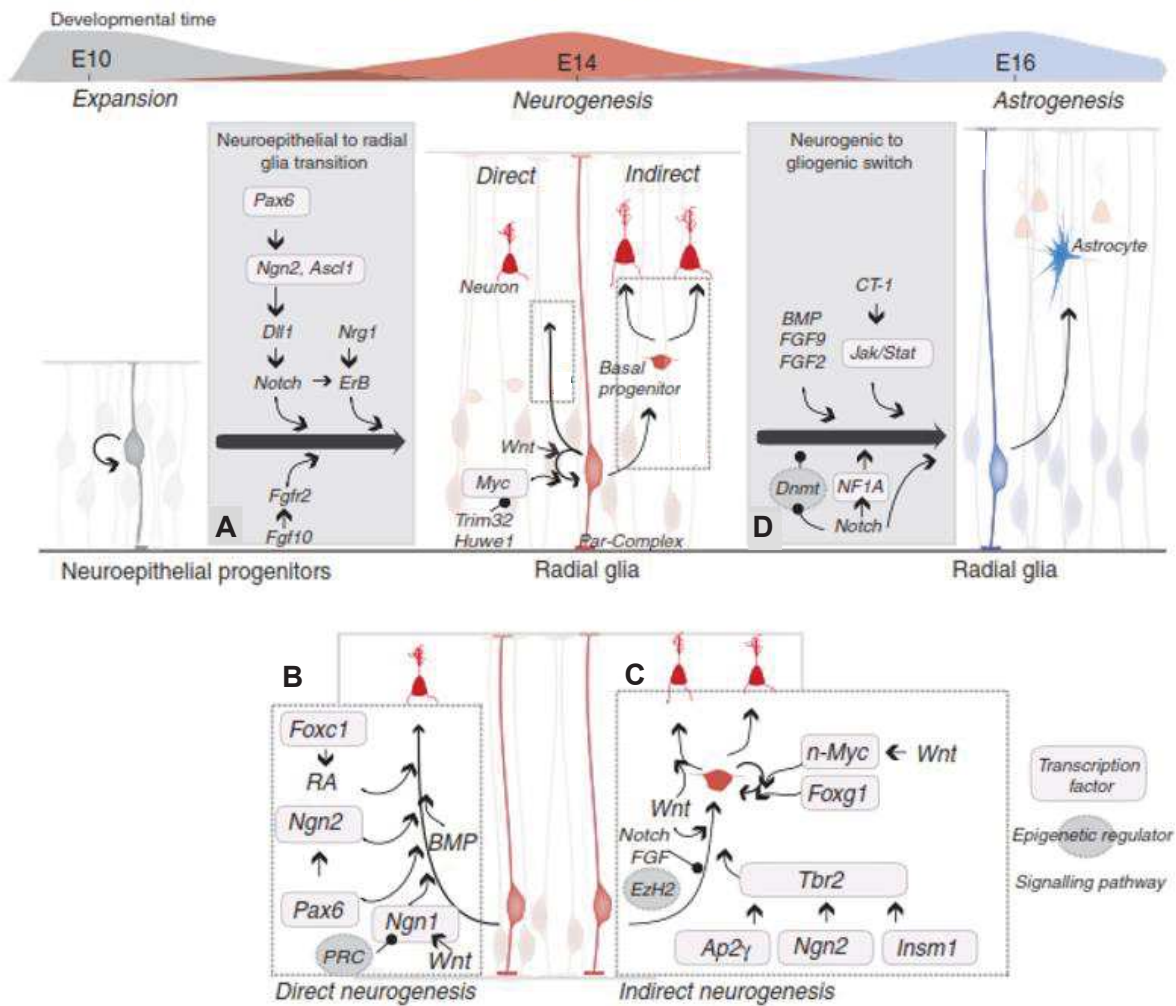


FIG. 13 MOLECULAR PATHWAYS REGULATING THE ONSET, PROGRESSION, AND TERMINATION OF NEUROGENESIS IN THE RODENT CEREBRAL CORTEX.

The main molecular pathways are detailed for the following stages: (A) NEC to RGC transition; (B) Direct neurogenesis; (C) Indirect neurogenesis; (D) Neurogenic to gliogenic switch. The main details of each of the paths are explained in the text. Transcription factors are labelled with a rectangle, epigenetic regulators with a circle and signaling pathways as italic text. From (Martynoga et al., 2012).

In the transition from NEC to RGC it is known that there is an increase in signaling by Notch (Hatakeyama et al., 2004), and a signaling of Neuregulin 1 (Nrg1) through its receptors (ErB2 and ErB4), which promote RG identity and suppress astrocyte lineage differentiation (Schmid et al., 2003). Fibroblast-growth-factor (FGF) ligands have been shown to inhibit neurogenesis and promote the proliferation of cortical progenitors, by regulating the duration of their cell cycle.

In a similar way to FGF ligands, Insuline-like growth factor-1 (IGF-1) also acts on the cell cycle and promotes cortical progenitors division. Retinoic acid has also been shown important during

neurogenesis, since in the absence of retinoic acid signaling there is not neuronal progeny (Martynoga et al., 2012).

In addition to their role in proper dorsoventral patterning of the telencephalon Wnt, bone morphogenetic protein (BMP) and sonic hedgehog (Shh) signalling pathways play important roles during neurogenesis. Wnt signaling promotes proliferation and the self-renewal of RG progenitors (Chenn et al., 2002), however, its role is regulated by time, since in later stages other studies have linked this pathway to the maturation of RG to Basal progenitors (Hirabayashi et al., 2004). Similarly to Wnt signaling, BMP signaling also has an important and changing role depending on the development stage, while in earlier stages it favors neurogenesis, in later stages, it blocks neurogenesis and favors the differentiation to astrocytes (Nakashima et al., 2001). Shh signaling regulates neurogenesis at different levels, it affects RGCs cell cycle kinetics and promotes that they undergo symmetric proliferative divisions promoting the expression of the Notch transcription factor Hes1 (Dave et al., 2011; Saade et al., 2013). Moreover, as neurogenesis progresses, Shh signaling decreases, promoting IP production and neuronal differentiation (H. Wang et al., 2011).

Around E17.5 in mice, the RG progenitors stop producing neurons and the first astrocytes begin to appear. During this process, the RGCs move from the VZ upwards, losing their radial processes and gradually acquire a multipolar and astrocytic form (Martynoga et al., 2012). The regulation of this transition is very important since once the transition from neurogenic to astrogenic has occurred, very few neurons will be produced, both in the cortex of rodents and primates (Kriegstein et al., 2009). There are three main events that are really important for this transition to occur: 1) The Jak/Stat pathway activity increases greatly; 2) There is a decrease in the expression of the pro-neural factors Ngn1 and Ngn2; 3) Differentiated neurons begin to express cytokine cadiotrophin-1 (CT-1), which is one of the main ligands of the Jak/Stat pathway. Once neurogenesis is reaching its end, the levels of CT-1, Fgf9, BMP, and Notch ligand are much higher, this quantitative effect together with a collaboration between pathways is what will ultimately result in the switch from neurogenesis to gliogenesis (Martynoga et al., 2012).

During neurogenesis, there is a high protein synthesis demand in order to satisfy the extensive cell proliferation and the correct maturation of neurons. To cope with this increase in protein synthesis, the action of cellular control mechanisms, such as the Unfolded protein response (UPR) pathway, might be necessary (Godin et al., 2016). UPR signaling pathway detects misfolded or unfolded proteins in the endoplasmic reticulum (ER) (generally caused by different types of cellular stress) and comprises different signaling mechanisms, including the

inositol-required enzyme 1 (Ire-1), the protein kinase like ER kinase (Perk) and the activating transcription factor 6 (Atf6) to restore cellular homeostasis or to trigger apoptosis (M. Wang et al., 2014). UPR signaling plays a crucial role in the synthesis of approximately one third of the proteins produced in a cell, most of them being secreted or integrated in the plasma membrane (Anelli et al., 2008). The dynamic regulation of the Perk branch of UPR signaling has an important role in the transition between direct and indirect neurogenesis. As the development of the cortex progresses, there is a progressive downregulation of UPR signaling in progenitors promoting the amplification of IPs and indirect neurogenesis. Interestingly, UPR signaling can be triggered by several mechanisms including defective tRNA modification (See Fig. 14 and section 2.4.2.2 for further details) (Laguesse et al., 2015), if UPR signaling levels are maintained high the rate of indirect neurogenesis decreases, which can lead to microcephaly (Laguesse et al., 2015)

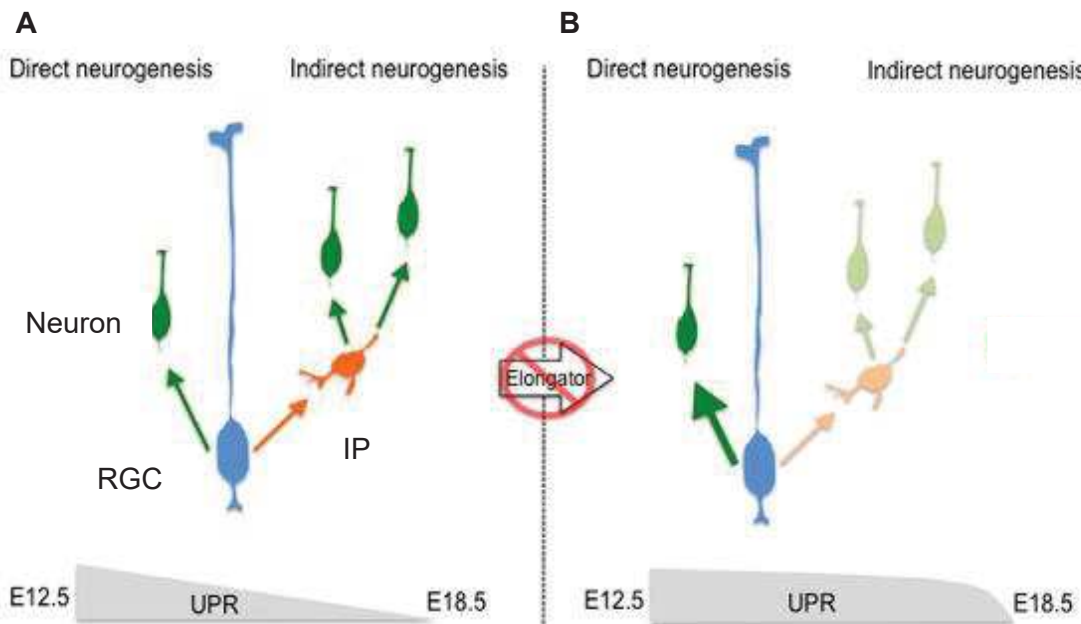


FIG. 14 UPR SIGNALLING CONTROLS NEUROGENESIS DURING CORTICAL DEVELOPMENT

(A) In physiological conditions there is a progressive decrease in UPR signaling and a balance between direct and indirect neurogenesis. (B) Upon UPR stress (in this case incorrect transfer RNA modification by lack of Elongator) progenitors maintain high levels of the Perk branch of UPR signaling throughout cortical development and a lower rate of indirect neurogenesis. From (Laguesse et al., 2015)

1.4.2.3.4 Transcriptional regulation

There are several transcription factors that are considered crucial for the regulation of embryonic neurogenesis, this is the case of Pax6, Lhx2, Arx, Foxg1 and the nuclear receptor

Tlx, for which defects in progenitors division and brain growth have been reported in mice bearing mutations in these genes (Martynoga et al., 2012).

Pax6 is one of the most studied, it induces the expression of several genes to promote proliferation during early cortical development. Furthermore, it can promote neurogenesis in cortical progenitors and astrocytes (Heins et al., 2002) and promote indirect neurogenesis by inducing Ngn2 expression both in the cortex and in the spinal cord (Scardigli et al., 2003). Ngn2, along with Ngn1 and Ascl1 (also known as Mash1), are part of the basic-helix-loop-helix (bHLH) transcription factors, which are also essential in the regulation of neurogenesis (Ross et al., 2003). These three factors, are expressed in RGCs, and can re-specify cells (even from other lineages) into cortical projection neurons. Tbr2 is a primary transcription factor for indirect neurogenesis, since it is necessary for the generation of basal progenitors (Miyata et al., 2004). Tbr2 expression is induced by various transcription factors, such as Ngn2 (previously mentioned), Insm1 and AP2γ.

Transcription factors levels in the cells can also be influenced to favor or suppress neurogenesis, for example, by ubiquitin ligases or epigenetic mechanisms. Some examples of ubiquitin ligases acting on neurogenesis are Huwe1 and TRIM32, which promote the degradation of n-Myc (X. Zhao et al., 2009), or TRIM11 which promotes Pax6 degradation (Tuoc et al., 2008).

1.4.2.3.5 Epigenetic modifications

DNA methylation or histone modifications regulate neurogenesis and the switch to glial production through the control of gene expression (MuhChyi et al., 2013), one of the clearest evidences is that chromatin shows a less condensed state in early-stage progenitors than in late-stage ones (Kishi et al., 2012).

From several works in which the enzymes that catalyze different epigenetic modifications have been mutated, it has been reported that epigenetic mechanisms can influence the expression of transcription factors regulating neurogenesis, for example, the methylation of histones by members of the Polycomb complex has been shown to suppresses the expression of the pro-neuronal factor Ngn1 (Hirabayashi et al., 2004). One of the ways through which epigenetic modifications regulate transition to gliogenesis is regulating glial gene expression, for example the methylation of Gfap (glial gene) DNA prevents a premature transition to gliogenesis (Fan et al., 2005).

1.4.2.3.5 Post-transcriptional regulation of gene expression

There are several mechanisms that allow post-transcriptional regulation of gene expression, for example alternative splicing, miRNAs or long-non-coding RNAs (lncRNAs), which have all

been shown to be involved in the regulation of neurogenesis (Calarco et al., 2011) (Bian et al., 2013) (Fatica et al., 2014). Regarding miRNAs, there are groups of these highly conserved non-coding RNAs that regulate RGC proliferation or neuronal differentiation, for example, miR-92 prevents the transition of RGC into IPs by silencing the expression of the transcription factor Tbr2 (Bian et al., 2013). The previously mentioned ubiquitin-ligase TRIM32, has also been reported to influence neurogenesis by binding to the Argonaute complex and promoting the activity of microRNAs (ex. Let-7) which induce neuronal differentiation (Schwamborn et al., 2009). An example of lncRNAs regulating neurogenesis is Rmst lncRNA which activates the Ascl and Ngn1 proneuronal genes (Ng et al., 2013).

1.4.2.4. Neuronal diversity origins

Cortical Projection neurons can be classified into different subclasses, which have different transcriptional signatures (Tasic et al., 2018), based on their projections, cortical layer and electrophysiological properties (Greig et al., 2013; Jabaudon, 2017).

Neuronal diversity is generated from an interaction between progenitors-derived genetic information and environment-derived signals, however the exact mechanisms contributing to neuronal diversity are still not fully understood. Despite the different types of projection neurons are better characterized, to this day, it has not been possible to identify a set of molecularly diverse neocortical progenitors that could explain this neuronal diversity (Telley et al., 2019). In the neocortex, temporal molecular patterning of progenitors (successive emergence of progenitors with distinct molecular properties) is thought to be the main origin of neuronal diversity (Gaspard et al., 2008; Jabaudon, 2017; M. Okamoto et al., 2016).

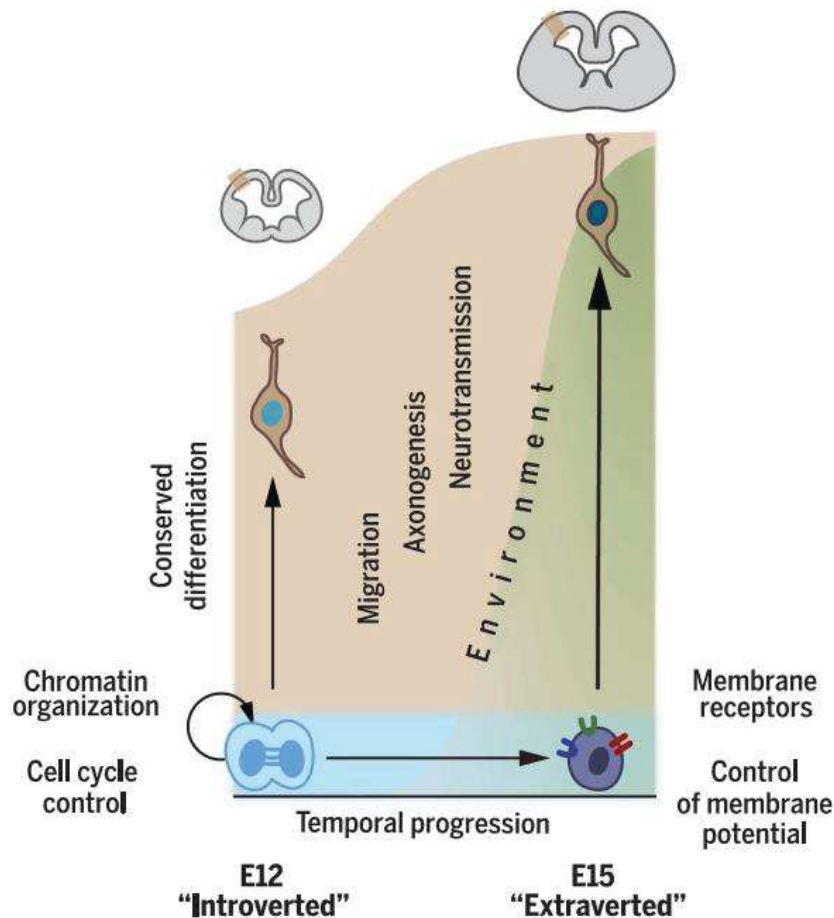
In experiments carried out in ferret, early stage cortical progenitors, which generate deep-layer neurons, have been shown to be able to produce superficial layers neurons when being transplanted to a cortex at a later stage. However, when late stage cortical progenitors were transplanted in an earlier cortex, they could only generate superficial layer neurons (Frantz et al., 1996; McConnell et al., 1991). Studies carried out with cortical progenitors in vitro have shown that they generate deep layer neurons during initial divisions and in later divisions they generate superficial layers neurons. The culture of late progenitors in vitro showed a reduced ability to generate neuronal subtypes generated during the early development of the cerebral cortex (Shen et al., 2006) Taken together, these results suggest that the generation of neuronal subtypes is controlled by cell intrinsic mechanisms.

Recently several studies have expanded our knowledge on this field. In 2016 Telley and colleagues carried out single cell RNA-seq combined with “Flash-tag” to analyse the transcriptome of mice cortical progenitors at different time-points after birth (E14.5) and

showed that deep layer neurons (early generated neurons) undergo a sequence of transcriptional waves in a specific order which is critical for their correct differentiation. The authors propose that these transient transcriptional combinations can act as checkpoints throughout neuronal differentiation (Telley et al., 2016). Subsequently, in 2019, again using single cell RNA-seq combined with “Flash-tag” Telley and colleagues showed that there are dynamic transcriptional states in apical progenitors and neurons, epigenetically controlled by Prc2 (polycomb repressor complex 2) and transferred from apical progenitors to their neuronal offspring. They also showed that as the development of the cortex progresses, apical progenitors transit from an introverted state (not very receptive to the environment) to an extroverted state (more receptive to the environment) (See Fig. 15) (Telley et al., 2019).

Experiments similar to those performed in ferret by Franz & McConnell in 1996 have recently been performed in mice but with different results, Oberst and colleagues (Oberst et al., 2019) combined the use of “Flash-Tag” (technique that allows labelling and tracing of progenitor cohorts born at the same time of development) together with Flow cytometry to isolate apical progenitors and carried out transplantation experiments of apical progenitors from E12 to E15 and vice versa. When transplanting E12 progenitors into E15 cortices, they observed that they could not generate superficial layer neurons. However, when transplanting E15 progenitors into E12 cortices, E15 progenitors could be re-specified and give rise to deep layer neurons. Importantly, WNT signaling pathway promoted this re-specification. The authors think that the differences in the results obtained with those of Franz & McConnell in 1996 are due to the use of different species and the methodology used, they think that in the ferret cortex Franz & McConnell in 1996 probably isolated IPs, since the VZ and SVZ are bigger in ferret than in mouse, which are much more restricted in terms of cell fate and competence than the RGCs and that would explain the differences in the results.

FIG. 15 TEMPORAL MOLECULAR PATTERNING IN THE MOUSE NEOCORTEX



As corticogenesis progresses apical progenitors change their transcriptional profile and become more responsive to environmental factors. From (Talley et al., 2019)

In a recent publication, Llorca and colleagues, they used different techniques to genetically tag cortical progenitors and perform lineage tracing experiments. They found that 80% of the progenitors analysed gave rise to neurons both in deep and superficial layers, while the remaining 20% gave rise to neurons from either deep layers or superficial layers (Llorca et al., 2019) In addition, they looked for the best mathematical model that fit their observations, their simulations suggest that there is a limited number of progenitors, capable of stochastically (randomly) generating a diverse range of neuron types, from which the neuronal diversity in the neocortex arises (See Fig. 16) (Llorca et al., 2019).

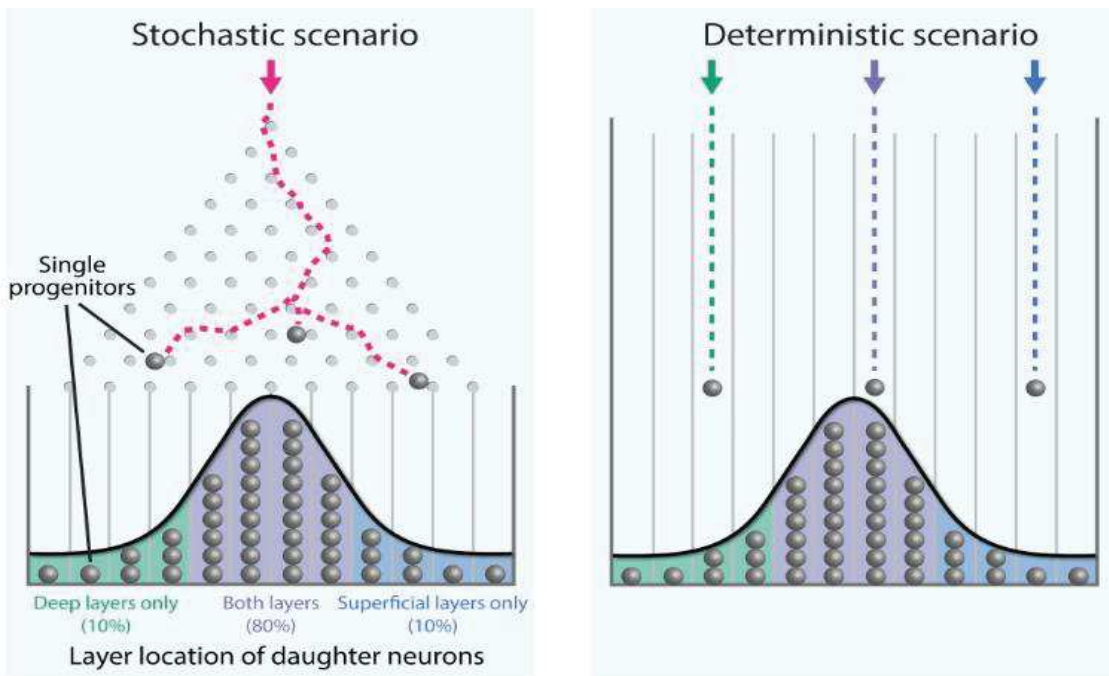


FIG. 16 STOCHASTIC SCENARIO OF NEURONAL DIVERSITY GENERATION

Llorca and colleagues propose that neuronal diversity is best explained by cortical progenitors undergoing stochastic fate choices (stochastic scenario) instead of a fate-restricted model (deterministic scenario). From (Klingler et al., 2020)

1.5. Neuronal migration

Neuronal migration is an essential process for the development of the nervous system in mammals. As it was previously mentioned (Fig.6), neural migration peaks occur at different timepoints, in human and mice, (between GW12 to GW20 in human and between E13 to E16 in mice). The correct formation of the cerebral cortex, both in mice and humans, requires that neurons migrate in a coordinated and regulated manner, otherwise, several disease conditions may arise, including schizophrenia, epilepsy, intellectual disability (ID) or malformations of cortical development (MCDs). MCDs are known to lead to developmental delay, intellectual disability and dysmorphic features in humans (Guerrini et al., 2014) (Jamuar et al., 2015) (Romero et al., 2018). The different embryonic origin of interneurons and cortical projection neurons has a repercussion in the migration modes of this two populations (See Fig.17), whereas interneurons follow a tangential migration, projection neurons follow a radial migration. Both migration routes are explained in the following sections emphasizing mainly on radial migration as my PhD work has been mainly focused on this projection neurons.

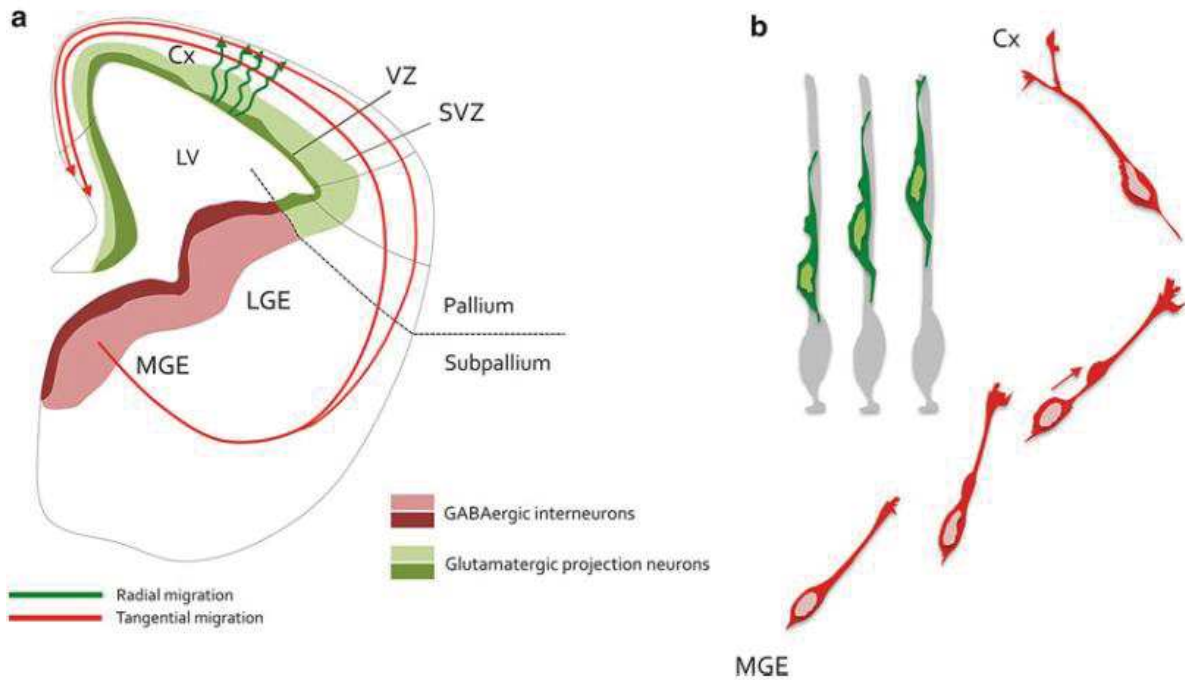


FIG. 17 NEURONAL MIGRATION IN THE DEVELOPING CEREBRAL CORTEX

(A) Mice brain section at E14.5 scheme showing the different migratory routes of cortical neurons. Cortical projection neurons and interneurons follow different migration routes to integrate the cortex (Cx). Cortical projection neurons migrate radially (green arrows) to integrate the cortical plate. Cortical interneurons undergo a tangential migration (red arrows), to integrate the cortex. (B) Differences in the migration modes of cortical projection neurons and interneurons. Projection neurons (green cells) perform locomotion on radial glial fibers (gray) to perform radial migration. Interneurons (red cells) tangential migration process is characterized by extensive nucleokinesis (red arrow) and a dynamic growth leading process. From (Godin et al., 2014).

1.5.1. Tangential migration

During tangential migration, interneurons adopt a characteristic morphology (Shown in Fig. 17B): They exhibit saltatory nuclear movements (nucleokinesis) and project forward a dynamic and branched anterior prolongation, known as the “leading process” (Bellion et al., 2005). Interneurons use a specific group of migration routes to integrate the cerebral cortex. There are three routes, from which two of them are used by most of the interneurons. The two main routes cross the marginal zone (MZ) and the SVZ respectively. A small fraction of the interneurons follows a third route to migrate through the subplate (Marin et al., 2001). The enrolment of interneurons in these routes is generally done by chemokine signaling. The integration of interneurons in the cortical plate occurs through 3 main steps (See Fig.18). Once the cells reach the cortex, a tangential dispersion of the interneurons occurs, subsequently,

they switch from a tangential migration mode to a radial one, finally, they separate into different cortical layers of the cerebral cortex depending on their lineage (Marin, 2013).

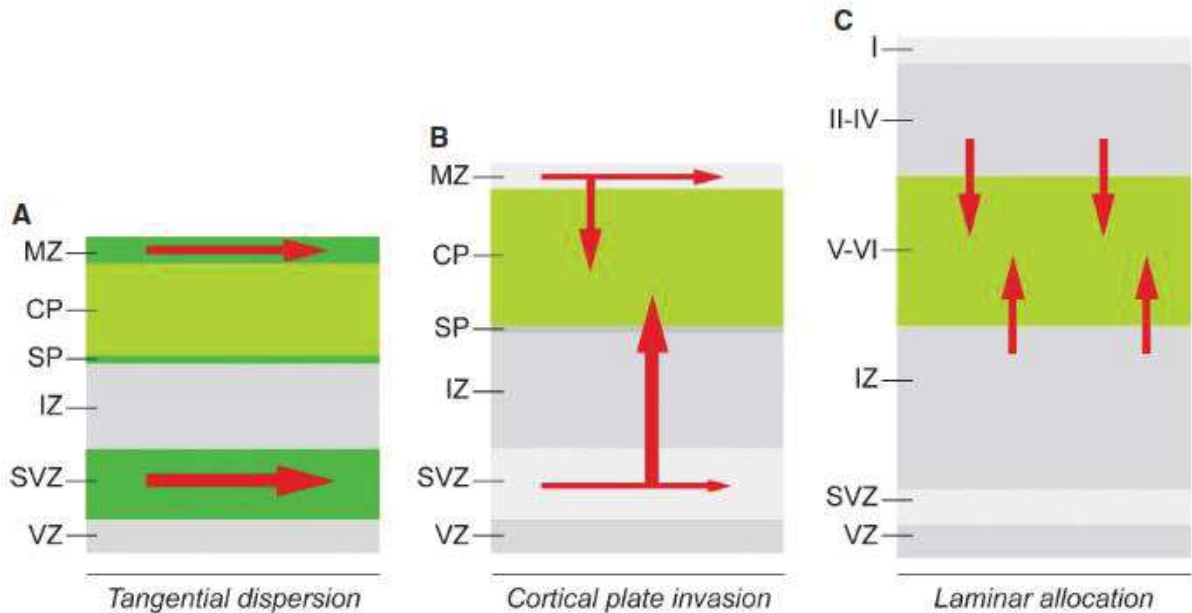


FIG. 18 PHASES FOR INTERNEURONS INTEGRATION IN THE CORTICAL PLATE

Representations of the cerebral cortex at different stages of development are shown along with the main steps for the integration of interneurons in the cortical plate. (A) Tangential dispersion: After reaching the cortex through one of the 3 routes (MZ, SP or SVZ, in dark green) interneurons migrate tangentially and disperse. (B) Cortical plate invasion: Interneurons change their migration mode from tangential to radial to invade the cortical plate. (C) Laminar allocation: Interneurons sort out into different cortical layers. From (Marin, 2013).

1.5.2. Radial migration

Projection neurons adopt two different modes of movement during radial migration: During early corticogenesis stages (E12-E13 in mice) they will adopt somal translocation and later on they will switch into a glia-guided mode of movement (Nadarajah et al., 2002). The following sections detail both modes of movement as well as the main cellular processes and molecular mechanisms involved.

1.5.2.2. Somal translocation

Somal translocation is a radial glia independent process that allows neurons to reach the preplate (PP) in early phases of cortical development. Early-born cortical neurons (E12-E13 in mice) are generated from aRGCs and inherit the bipolar morphology from the aRGCs, which makes them indistinguishable from their progenitors. Somal translocation begins once the newly generated neurons detach from the VZ (Miyata et al., 2001). During this process (See

Fig. 19), cells present a long radially oriented process that reaches the pial surface and transient trailing processes. As the soma of translocating cells is constantly advancing forward the basal process becomes thicker and progressively shorter, these two movements together allow cells to reach the PP (Nadarajah, 2003). As the cerebral cortex becomes thicker, the distance between the neuronal soma and the pial surface increases and neurons are unable to attach their processes to the pia. At this point, neurons start a radial glial-guided locomotion.

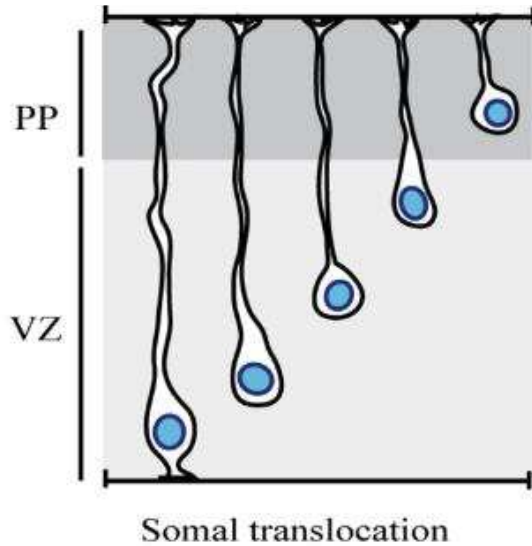


FIG. 19 SOMAL TRANSLOCATION

Translocating cells lose their apical attachment and show a basal process that reaches the pial surface, in order to reach the preplate their basal process will progressively shorten. (Azzarelli et al., 2015)

1.5.2.3. Radial-glia guided locomotion

In contrast to somal translocation, during radial-glia guided migration, cells change their morphology and migration mode on multiple occasions throughout the different zones of the cerebral cortex (See Fig.20). The different steps in this process as well as the main mechanisms involved in its regulation are explained in the following sections.

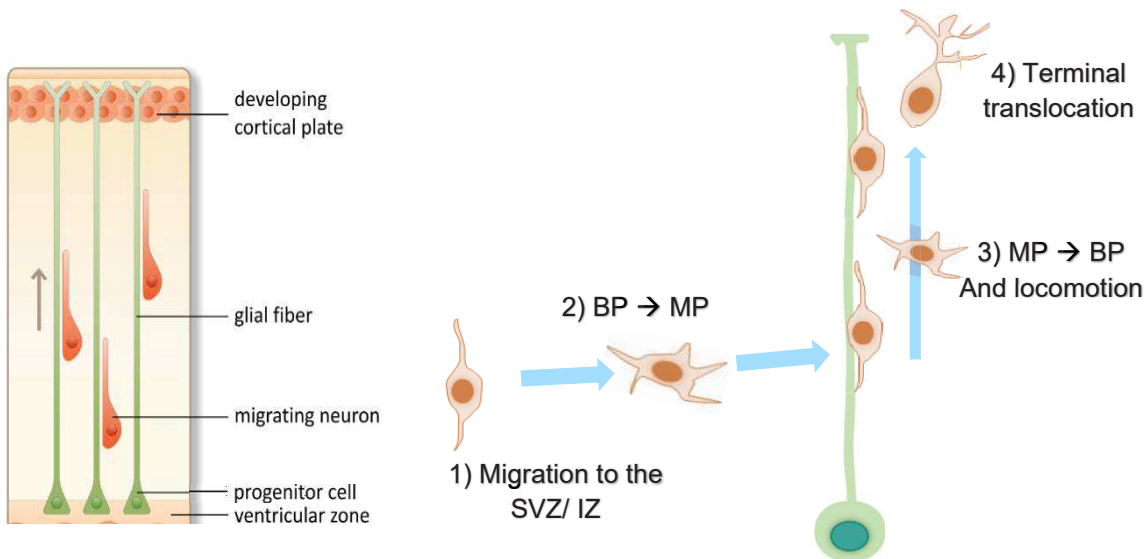


FIG. 20 RADIAL-GLIA GUIDED MIGRATION

There are four different phases during radial-guided migration. (1) New-born neurons migrate towards the SVZ/IZ, (2) Once in the SVZ/IZ they switch from a bipolar (BP) to a multipolar (MP) state and carry out multipolar migration, (3) The cells undergo a multipolar to bipolar transition and use the RG fibers as scaffolds to pursue their migration towards the CP (lomocotion), (4) Cells detach from the RG fiber and carry out terminal translocation. Adapted from (Amy Rosenfeld, 2017).

1.5.2.3.1 Generation of bipolar neurons and bipolar to multipolar transition

After being generated by aRGCS, neurons, like their progenitor cells, adopt a bipolar shape (BP) and they are attached to the VZ, where they will remain for ~ 10 hours. Subsequently, they detach from the VZ and move to the apical area of the SVZ/IZ where they will switch to a multipolar morphology (MP) (Itoh et al., 2013). MP neurons present multiple neurites and migrate in random directions (Tabata and Nakajima 2003). During this random migration phase, MP cells extend their axons (Hatanaka et al., 2004) (Barnes et al., 2009). MP cells have thin processes which extend and retract dynamically as well as a dynamic movement of the centrosome, which suggests that they do not have a fixed polarity (de Anda et al., 2010). The biological sense of the MP phase of the cells is not clear, however there are different hypotheses: 1) The cells adjust the timing at which they enter the CP; 2) To allow lateral dispersion of the sibling cells generated from a radial parental glial; 3) The cells carry out a microenvironment exploration in order to determine in which direction the axon and the leading process will extend (Tabata et al., 2016).

1.5.2.3.2 Multipolar to bipolar transition

After being in the SVZ / IZ for ~ 24h, the MP cells return to a BP morphology. The MP to BP transition is a critical period of radial migration in which many genes are involved (J. J. LoTurco et al., 2006). Once in the BP state cells reorient Golgi and the centrosome towards the pia and establish a dominant process directed towards the pia as well (de Anda et al., 2010; Hatanaka et al., 2004). Subsequently, the leading process establishes adhesive interactions with the basal process of RGCs for guidance in their locomotion and neurons.

There exist many genes shown to modulate the MP to BP transition, most of them identified from knock-down (KD) or knock-out (KO) studies. They can be classified into 5 different categories: 1) Transcriptional regulators; 2) Small GTP-binding proteins; 3) Proteins related to microtubule dynamics; 4) Receptors and other membrane proteins and 5) Protein Kinases. Despite the presence of these 5 categories, most downstream effectors converge in the same function: the regulation of the cytoskeleton (See next sections for details) (Ohtaka-Maruyama et al., 2015).

Recently, Ohtaka-Maruyama and colleagues (Ohtaka-Maruyama et al., 2018), have shown that SP neurons favor the transition from MP to BP by projecting axons towards the IZ and establishing glutamatergic synapses with MP neurons (See Fig.21).

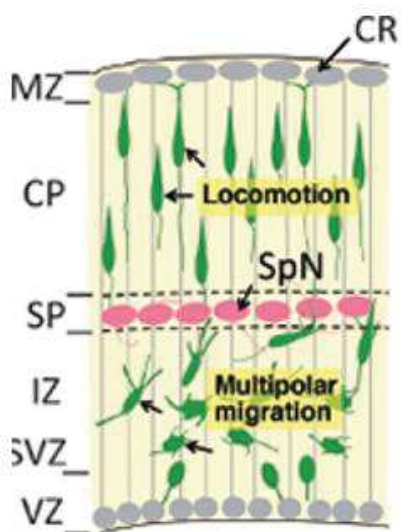


FIG. 21 SUBPLATE NEURONS PROMOTE MULTIPOLAR TO BIPOLEAR TRANSITION

The SP has a strategic position for radial migration. During the MP to BP switch, SP neurons establish glutamatergic synapses with MP neurons to induce their MP to BP switch and their migration mode change from MP migration to locomotion. From (Ohtaka-Maruyama et al., 2018)

1.5.2.3.3 Locomotion

The locomotion phase is the period during which neurons cover most the displacement required to reach the CP. Once BP neurons have established adhesive interactions with the basal processes of RGCs they begin a rapid locomotion process in which they use RGCs basal processes as scaffolds. During the locomotion mode radially migrating neurons repeat several steps in order to perform their progressive displacement (Ayala et al., 2007): 1) Neurons extend

a leading process (Yee et al., 1999), 2) Formation of a dilation in the plasma membrane proximal to the leading process; 3) Movement of the centrosome towards the swelling; 4) The neuronal nuclei undergo a saltatory movement known as nucleokinesis (a displacement of the nucleus and soma towards the leading process) (Nadarajah et al., 2001; Schaar et al., 2005); 4) Neurons eliminate their trailing process which results in a net displacement of the cell. Fig.22 shows insights into the formation of the dilation and nucleokinesis. The locomotion cycle starts again with the remodeling of the leading process and continues until the neurons reach their final destination.

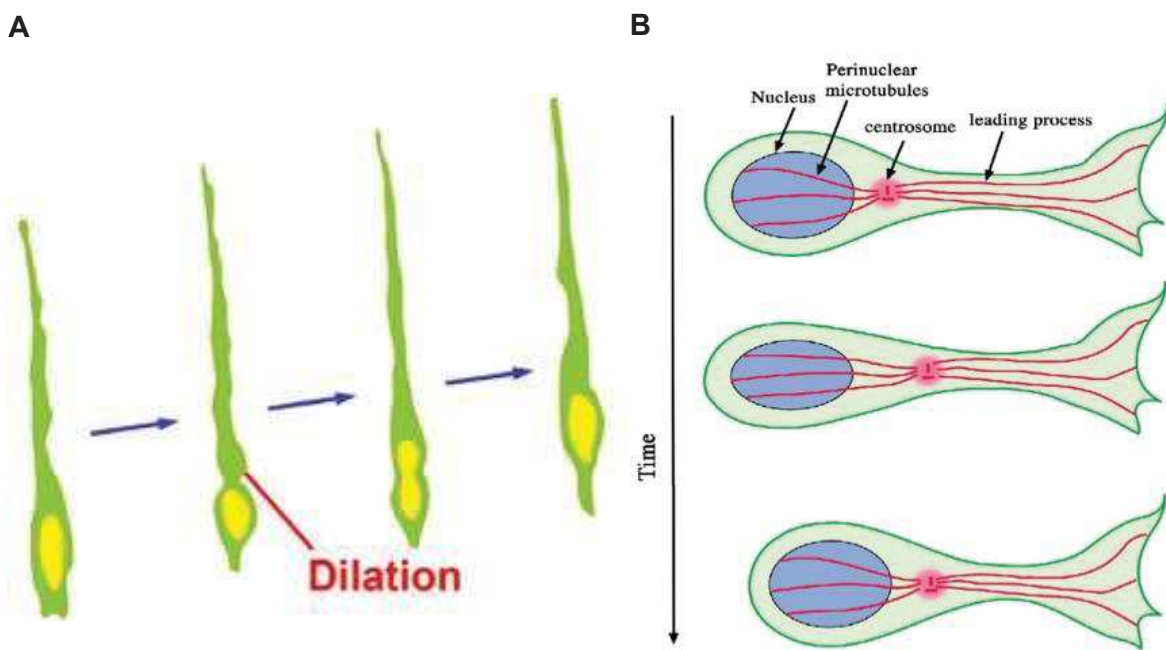


FIG. 22 LOCOMOTION INSIGHTS IN MIGRATING NEURONS

(A) *Morphological changes during projection neuron locomotion: Projection neurons extend a leading process and form a cytoplasmic dilation at the proximal area of the leading process which allows nucleokinesis to occur. From (Y. V. Nishimura et al., 2017)* (B) *Nucleokinesis: Movement of the centrosome precedes movement of the nucleus. A cell with the nucleus, microtubules, centrosome and leading process is shown. Time-lapse experiments indicate that first the leading process advances in the direction of migration, subsequently, the centrosome advances towards the leading process and finally the nucleus translocates forward. Neuronal migration results from the repetition of these series of events. From (L. H. Tsai et al., 2005)*

The leading process establishes adhesive interactions with RGCs fibers and will guide the direction of migrating neurons. Until recently, it was thought that radial migrating neurons had a single leading process without ramification, nevertheless, in a recent study, Martínez-Martínez and co-workers demonstrated that branching occurs in the leading process of many radial migrating neurons and that this event is more frequent in ferret than in mouse. The

authors show that the branching process is related to tangential displacement and that it could be a mechanism to allow radial migrating neurons to spread laterally (Martinez-Martinez et al., 2019).

1.5.2.3.4 Locomotion termination and Terminal translocation

Radial migration ends in many cases by stopping signals, such as reelin (See section 1.5.2.4.4). Once neurons arrive to the pial surface of the CP they end their migration by a terminal somal translocation. This process is carried out in three stages: 1) End of locomotion; 2) RG fiber separation; 3) Terminal translocation. Afterwards, a process of maturation and extension of axon and dendrites begins, which precedes synaptogenesis and their establishment in microcircuits (Ohtaka-Maruyama et al., 2015). Time-lapse analyzes experiments have revealed that locomoting neurons pause transiently before entering the uppermost part of the CP (termed primitive cortical zone, PCZ), which has some distinct features from the lower CP, and during this pause they switch into the terminal translocation mode (Sekine et al., 2011). Terminal translocation process is critical to establishing correct cortex lamination, as it allows neurons to locate above the pre-existing ones.

1.5.2.4. Main molecular pathways implicated

There is a huge number of molecules reported to influence many of the stages of radial migration, in the following lines some of the most well-known paths controlling each of the cell states and switches in radial migration steps are summarized. Figure 23 includes the main molecular pathways involved in the regulation of the MP to BP transition, locomotion and the termination of radial migration.

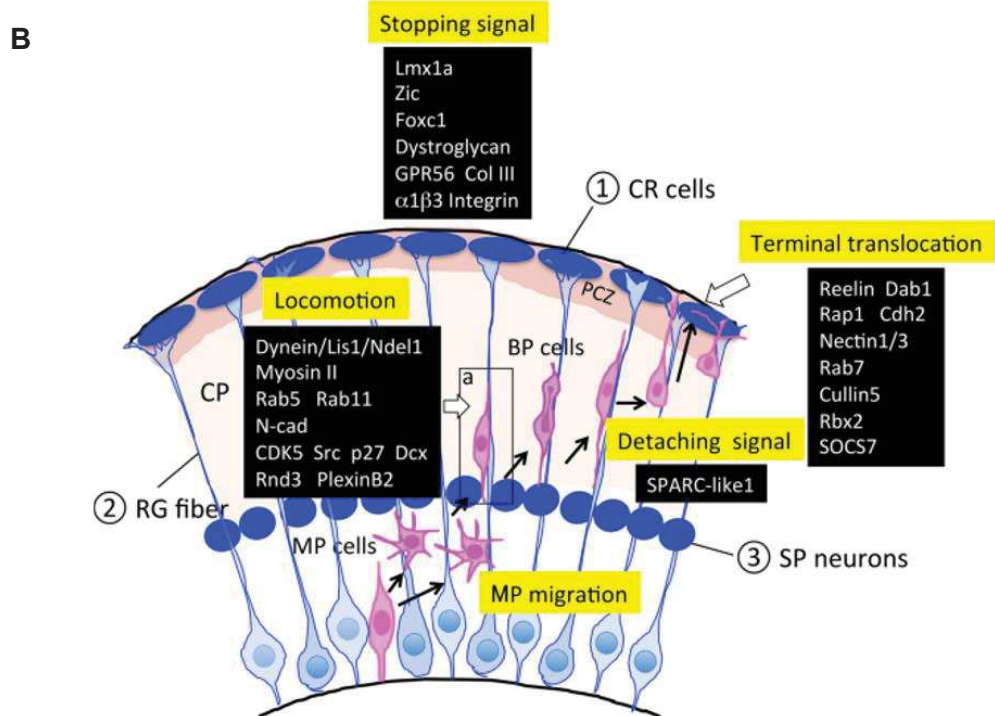
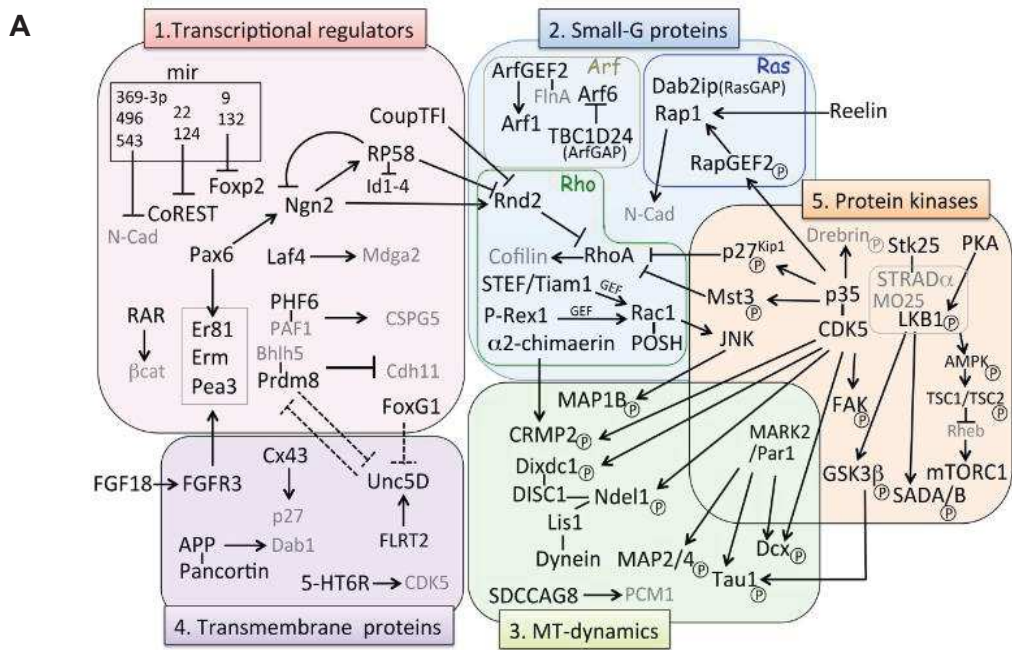


FIG. 23 MOLECULAR PATHWAYS INVOLVED IN THE MP TO BP TRANSITION, LOCOMOTION AND TERMINATION PHASES OF RADIAL MIGRATION

(A) Main molecular pathways involved in regulation of the MP to BP transition. Factors involved can be classified in 5 classes based on their molecular function: 1) Transcriptional regulators, 2) Small-G proteins, 3) MT-dynamics, 4) Transmembrane proteins, 5) Protein kinases. “→” indicate positive regulations and “→” negative regulation. *From (Ohtaka-Maruyama et al., 2015)*

(B) Structures and molecular pathways involved in the locomotion and termination of radial migration. *CR cells, RG fibers and SP neurons are transient structures that disappear after birth. The main molecular factors regulating the final phases of radial migration (locomotion, stop signals, detachment from the RG fiber and terminal translocation) are shown. PCZ, primitive cortical zone. (See text for details). From (Ohtaka-Maruyama et al., 2015)*

1.5.2.4.1 Transcriptional regulation

Both the beginning and the end of the MP phase are controlled by various transcription factors. Foxg1 expression changes dynamically at different stages of radial migration (M. Inoue et al., 2014; Miyoshi et al., 2012). This transcription factor is downregulated at the beginning of the MP phase, when the cells are still in the lower IZ, at this time, the neurons begin to express NeuroD1 and Unc5D (receptor involved in axon guidance). Subsequently, already in the most superficial part of the IZ, the expression of FoxG1 increases and the expression of Unc5D decreases, leading the cells to the transition from MP to BP (Miyoshi et al., 2012). During the MP to BP transition NeuroD1 acts by repressing Prdm16, a chromatin modifying enzyme that regulates mitochondrial reactive oxygen species (M. Inoue et al., 2017). Changes in Prdm8 expression levels have also been documented to affect the MP to BP transition (M. Inoue et al., 2014).

Many transcription factors involved in radial migration termination have been identified from over-migration defects, this is the case of the LIM homeobox gene Lmx1a (Costa et al., 2001), the zinc finger transcription factor Zic (T. Inoue et al., 2008) and the transcription factor Foxc1 (Hecht et al., 2010).

Different publications have demonstrated the importance of miRNA-dependent gene regulation during neuronal migration. This regulation appears to occur in a specific time-window: While an overall reduction of mouse miRNA levels in early postnatal stages does not affect neuronal migration (Davis et al., 2008), similar experiments in late-born embryonic neurons causes an impairment of neuronal migration (Kawase-Koga et al., 2009). Several miRNA have been reported to affect neuronal migration. miR-9 and miR132 for example regulate radial migration through suppression of expression of FoxP2, a transcription factor involved in migration (Clovis et al., 2012). The expression of Dcx, a gene regulating MT dynamics during neuronal migration, is also regulated by miRNAs either directly for example by miR-134 (Gaughwin et al., 2011) or indirectly in the case of miR-22 and miR-124, which target components of the CoREST / REST transcriptional repressor complex decreasing Dcx levels in migrating neurons and promoting neuronal polarization (Volvert et al., 2014). miR-140 was also recently reported to regulate axon-dendrite polarity through repression of Fyn Kinase

mRNA (Ambrozkiewicz et al., 2018). miR369-3p, miR-496 and miR-543 also act on neuronal migration by reducing N-Cadherin expression (Rago et al., 2014).

1.5.2.4.2 Adhesion-molecules

There exist various mechanisms controlling neuronal delamination from the apical surface of the ventricle. Among the most important ones, we find Scratch1 and 2, members of the snail super-family of transcription factors, which promote delamination by suppressing E-cadherin expression (Itoh et al., 2013). The microtubule associated protein Lzts1 has also been reported to promote delamination by altering apical junction organization (Kawaue et al., 2019).

TAG-1 (also known as Contactin 2) modulates cell polarity acting as an adhesion molecule between newly formed and pre-existing axons, the knock-down of TAG-1 prevents the formation of new axons and prevents the MP to BP transition (Suter et al., 2020).

Fibroblast-growth-factor receptors (FGFRs) have also been shown to regulate cell polarity by Erk1/2 as downstream effectors, in particular they regulate multipolar neuron orientation and their MP to BP transition. FGFRs function is regulated by N-Cadherin (also known as Cdh2), which stabilizes the FGFRs and stimulates neuron migration. Interestingly, on this molecular pathway, reelin (described in 1.5.2.4.4) acts as an upstream regulator preventing FGFR degradation through N-cadherin (Kon et al., 2019).

The attachment of the migrating neuron to the RG fiber is a key event for locomotion. The proteins with the greatest relevance in this adhesion are N-Cadherin ((Kawauchi et al., 2010) and Connexins 26 (Cx26) and 43 (Cx43) (L. A. Elias et al., 2007). Regarding the detachment of the locomoting neurons of the RG fibers, SPARC-like 1 protein (SC1), a member of the extracellular matrix protein family SPARC, plays an important role. SC1 is expressed at the top and bottom of the RG fibers and acts through an antiadhesive activity allowing the separation of locomoting neurons (Gongidi et al., 2004).

During terminal translocation Nectin1 and 3 adhesion molecules are critical. CR cells, which were previously described in section 1.4.2.1 have an essential role during radial migration through diffusive cues (such as Reelin, described below), but also via cell contact-mediated signaling. CR cells express nectin1- and mediate heterophilic cell adhesions with nectin3-migrating neurons stabilizing their leading processes in the process of anchoring to the MZ (Gil-Sanz et al., 2013). The regulation of the degradation of these adhesion molecules is carried out by the E3 ubiquitin ligase complex (which includes Cullin5, Rbx2 and the scaffold protein SOCS7) (Simo et al., 2013; Simo et al., 2010).

Interestingly, molecules that regulate neuronal migration can also influence cortical folding. Genetic ablation of FLRT1 and FLRT3 adhesion molecules has been shown to promote the development of macroscopic cortical sulci in mice during embryogenesis. Upon their ablation, cortical neurons show a wider dynamic migratory profile and a lateral distribution (Del Toro et al., 2017), which are considered characteristic features of the onset of cortical folding in gyrencephalic species such as ferret or human (Gertz et al., 2015).

1.5.2.4.3 Cytoskeleton

Microtubules (MTs) and actin networks are crucial during neuronal migration, particularly regulating cell polarity and locomotion. In the next paragraphs there is an overview about the role of MTs and actin networks in radial migration.

Several neurological disorders characterized by abnormal neuronal migration, differentiation and axon guidance have been attributed to mutations in alpha- and beta- tubulin isotypes as well as Microtubule-associated proteins (MAPs) (Ivanova et al., 2019; Keays et al., 2007; Poirier et al., 2010; Saillour et al., 2014). Throughout the locomotion phase, neurons adopt a very characteristic morphology that relies on the MT organization. After the transition from MP to BP, the centrosome changes its position and locates at the base of the leading process, and the locomotion phase begins. The dynein complex, which is composed of cytoplasmic dynein and Lis1, Ndel1, Nde1 and NudC as associated proteins (Shu et al., 2004; Tanaka et al., 2004; J. W. Tsai et al., 2005) participates in the nucleokinesis phase of locomotion by bringing the nucleus closer to the centrosome (Tanaka et al., 2004) (Aillaud et al., 2017; Creppe et al., 2009; Salmi et al., 2013). Dysregulation of various components of the dynein complex result in neuronal migration defects and MCDs (Sasaki et al., 2005; Shu et al., 2004; Toyo-Oka et al., 2005). Several pathways can modulate the MT network. The acetylation or deacetylation of Alpha-tubulin by MEC-17 or HDAC6 respectively (among other proteins) have a fundamental role in the regulation of MT dynamics as well as the JNK kinase pathway (L. Li et al., 2012) . JNK acts among other substrates, negatively regulating the activity of SCG10, a stathmin family protein that induces the depolymerization of MT (Taranuk et al., 2006). MAPs also regulate MTs networks at many levels, including their dynamics, stability, and organization. Within MAPs there is a family that has been studied extensively, the Dcx protein family, which includes Dcx, Dclk1 and Dclk2. Dcx is thought to help maintain the structure of the leading process by promoting the stability of the MTs (Horesh et al., 1999). Mutations in Dcx family members has been associated to lissencephaly type 1 (Reiner, 2013).

The actin cytoskeleton is also essential during locomotion, actin filaments promote the formation of cytoplasmic dilation (T. Yang et al., 2012) and the movement of the soma and the

centrosome (Norden et al., 2009; Solecki et al., 2009). Several proteins acting on the actin cytoskeleton have been reported to modulate the MP state. This is the case of Lamellipodin, whose KD was shown to interfere negatively in neuronal radial migration (Pinheiro et al., 2011). Lamellipodin acts on the regulation of MP cells processes by modulating actin fiber-remodeling recruiting ENA/VASP to the cell membrane locally (Drees et al., 2008). Dbnl, a protein that interacts with F-actin, has also been shown to be essential for regulating MP cell morphology, polarity and migration by regulating N-Cadherin levels (S. Inoue et al., 2019). Recently, Nicole and colleagues (Nicole et al., 2018) have shown that CamKII β regulates the actin cytoskeleton through both kinase-dependent and kinase-independent activities having a fundamental impact during the MP to BP transition and the saltatory movement of locomoting neurons. The authors also showed that it regulates actin remodeling through its action on cofilin, an actin depolymerizing protein also involved in the migration of cortical neurons (Chai et al., 2016; Kawauchi et al., 2006).

1.5.2.4.4 Cellular signalisation

Wnt signaling also plays an important role in neuronal polarization, there are two Wnt signaling pathways, the canonical (stabilizes beta-catenin) and the non-canonical (beta-catenin independent) (G. Y. Yang et al., 2011). Both have been shown to be key in regulating the duration and progression of the MP phase. However, they act differently, while the canonical pathway promotes the MP state, the non-canonical promotes the BP transition (Boitard et al., 2015).

Other important proteins that affect cell polarity are Par3 and Par4. Par3 is a protein that forms an important complex in cell polarization of various types of epithelial cells, which is formed by Par3, Par6 and aPKC. Par3 accumulates at the tip of what will become the future axon together with KIF3A (Kinesin) (T. Nishimura et al., 2004), it is thought to act in the same way for establishing the leading process during the MP to BP transition. Par4 (a serine / threonine kinase also known as LKB1) forms a complex with two more proteins, Stk25 (Reeling-Dab1 signaling modifier) and GM130 (Golgi matrix protein) and they act by modulating the polarity of neurons by compacting the Golgi apparatus (Matsuki et al., 2010).

Cdk5 is a cyclin-dependent kinase (CDK) that has key regulatory roles on several stages of radial migration. RhoA is a member of the family of small GTPases, that influences cellular morphology and motility regulating actin cytoskeleton dynamics, during the MP to BP transition Cdk5 decreases RhoA activity in two different ways: 1) By phosphorylation of p27 serine 10, which leads to the stabilization of p27 and favors the formation of the p27-RhoA complex, interfering in the interaction of RhoA with RhoGEFs (Kawauchi et al., 2006) (Besson et al.,

2004); 2) Phosphorylation of Mst3, a serine / threonine kinase that phosphorylates RhoA resulting in decreased activity (Tang et al., 2014). P27 plays a key role in the regulation of the cytoskeleton during radial migration. P27 has been shown to promote neuronal migration of both projection neurons and interneurons by blocking RhoA signaling. p27 also regulates the actin cytoskeleton by inducing activation of cofilin (Godin et al., 2012). Furthermore, it is thought that p27 can promotes the transcription of other genes that regulate radial migration through the regulation of the transcription factor Ngn2 (Nguyen et al., 2006)

During the locomotion phase CDK5 and Src-family kinases have shown to be important. Their activity decrease by the use of inhibitors results in lower locomotion speed (Y. V. Nishimura et al., 2010). CDK5 regulates key processes during locomotion, such as cytoplasmic dilatation and nuclear translocation through the modulation of Dcx, p27 (thus RhoA) (Y. V. Nishimura et al., 2014). RhoA activity is tightly regulated during locomotion, while Rnd3 regulates locomotion by repressing F-actin polymerization and inhibiting RhoA (Pacary et al 2011), PlexinB2 (semaphorin receptor) promotes RhoA activity by Rho-GEFs recruitment and avoiding RhoA Rnd3-dependent RhoA inactivation (Azzarelli et al., 2014).

N-cadherin trafficking by Rab-5, which is also regulated by Cdk5 (Y. V. Nishimura et al., 2014), and Rab-11 dependent endocytosis pathways has been shown to be important for locomotion and terminal translocation. Rab7 KD has also been documented to interfere in terminal translocation (Kawauchi et al., 2010). Protein receptors such as Dystroglycan (Myshrrall et al., 2012) and CPR56 (a G-Protein Coupled Receptor) (Singer 2013) have also been reported to participate in radial migration stop. GPR56 receptor was found to bind collagen III (collIII) and produce a stop signal together with $\alpha 3 \beta 1$ integrin (Jeong et al., 2013).

Reelin, an extracellular glycoprotein mainly secreted by CR cells, plays a major role in neuronal migration and cortical lamination, majorly through its action on the actin cytoskeleton organization. Most of the work about Reelin function in the CNS comes from the Reeler mice, which are deficient for Reelin. Reeler mice were shown to present failure of neuronal positioning throughout the CNS, with a cortical plate aligned in a practically inverted fashion (“outside-in”) (Falconer, 1951). Reelin is recognized by the very low-density lipoprotein receptor (VLDLR) and the Apolipoprotein E receptor (ApoER), both expressed by migrating cortical neurons. Its binding to these receptors leads to a phosphorylation of Dab1 by Src family of tyrosine kinases (SFKs) (Hiesberger et al., 1999) triggering several signaling pathways that regulate radial migration (Bock et al., 2016). Among the molecules that are downstream of phosphorylated Dab-1 we find Crk / Crkl, phosphatidylinositol-3kinase (PI3K) and Nck β . Crkl ends up triggering the formation of Rap1-GTP, which will activate key cell adhesion molecules

during terminal translocation, such as $\alpha 5\beta 1$ integrin and N-cadherin (Dulabon et al., 2000; Franco et al., 2011). PI3K branch leads to the activation of mTOR and cofilin, which together with Nck β regulate the actin cytoskeleton during dendritogenesis and neuronal migration (Ishii et al., 2016).

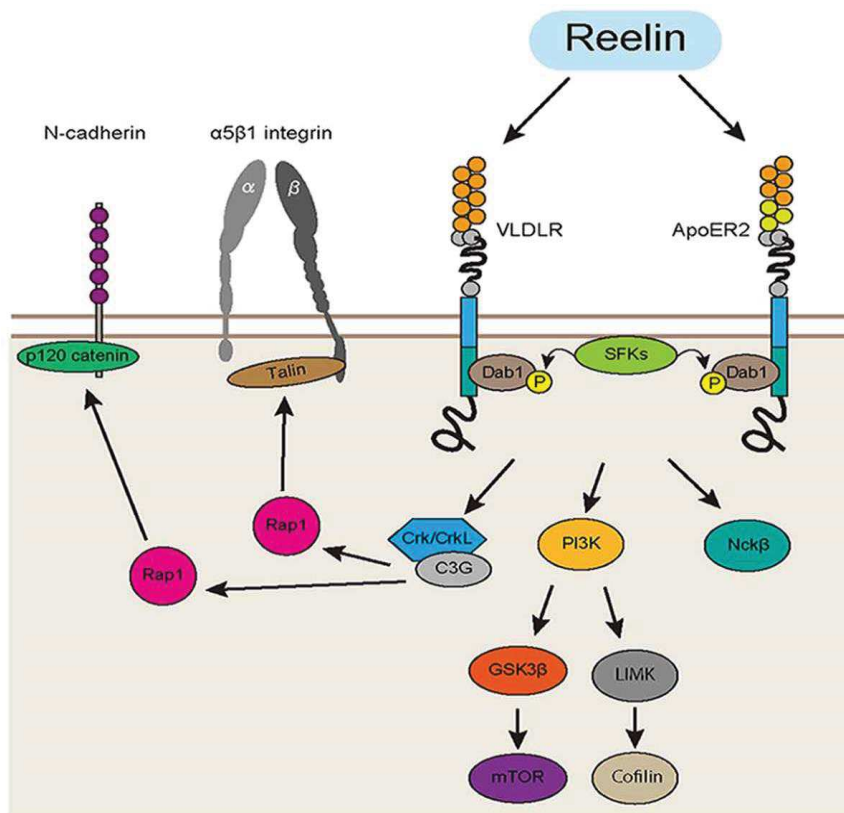


FIG. 24 REELIN SIGNALLING PATHWAY IN THE DEVELOPING CORTEX

Reelin is recognized in migration neurons by the VLDLR and ApoER2 receptors and acts through several signalling pathways to regulate radial migration. Details in the text. From (Ishii et al., 2016)

1.6. Maturation and connectivity

Neuronal Maturation and connectivity pursue after birth (See Fig. 25A). During and after migration, neurons mature and establish neural connections between them. One of the first steps for establishing cortical connections is the formation of axons and dendrites, which increase in number and complexity (branching and length) as development progresses (See Fig. 25B).

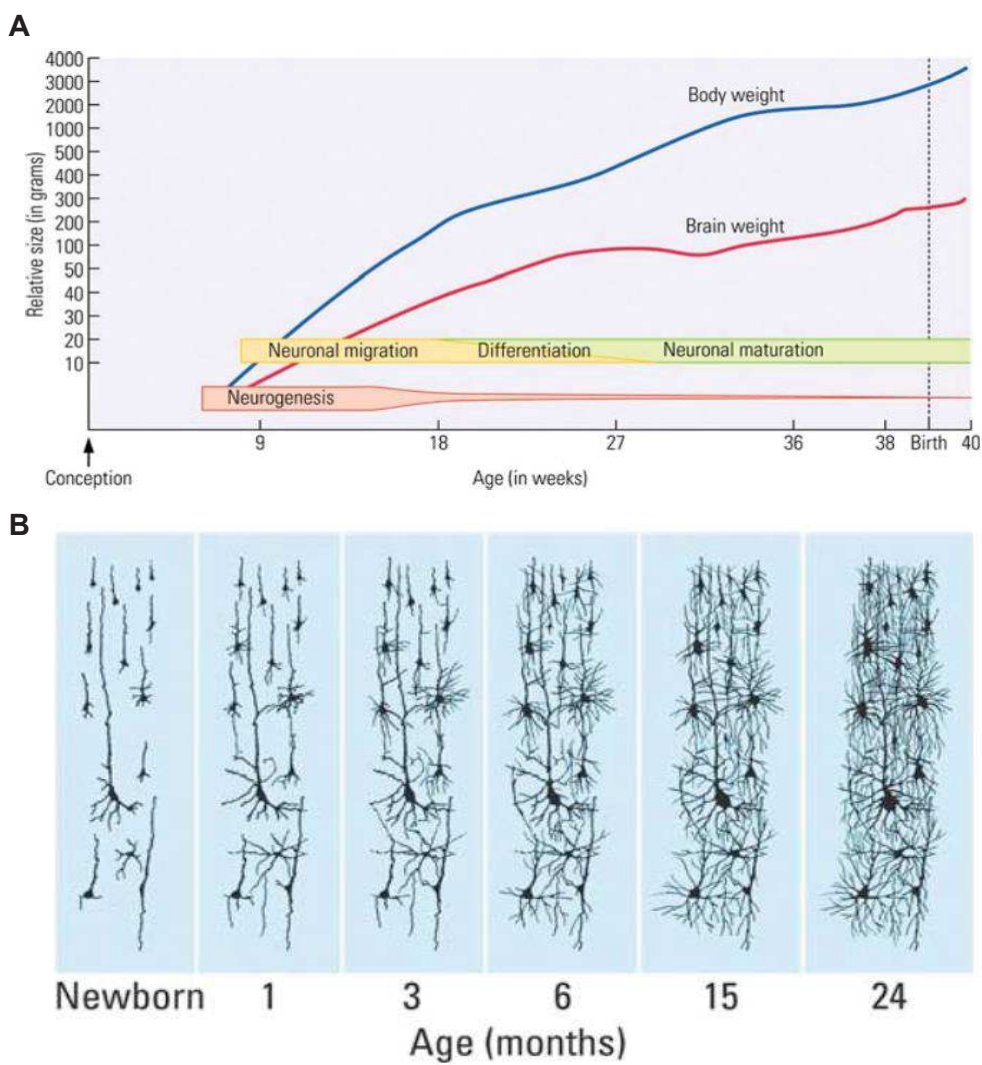


FIG. 25 NEURONAL MATURATION AND CONNECTIVITY CONTINUES AFTER BIRTH

(A) *Progression of the main stages of brain development as well and body and brain weight throughout time in humans. (B) Axon and dendrite number and complexity increase throughout post-natal development (Drawings from human cerebral cortex Golgi-Cox preparations). From (Bryan Kolb, 2009)*

For neurons to establish adequate connectivity, they require proper growth of their axons and dendrites, as well as molecules that guide them to cortical or subcortical targets (including thalamus, brain stem or spinal cord) (Price et al., 2006). The extension and guidance of both axons and dendrites depends on the growth cone, a conical expansion structure located at the distal end of axons and dendrites, composed of lamellipodia and filopodia that is essential for neurons to achieve adequate synaptic connections (Tessier-Lavigne et al., 1996), which is composed of lamellipodia and filopodia (See Fig. 26). Branches can be formed by bifurcation of the growth cone and enable neurons to connect to multiple targets.

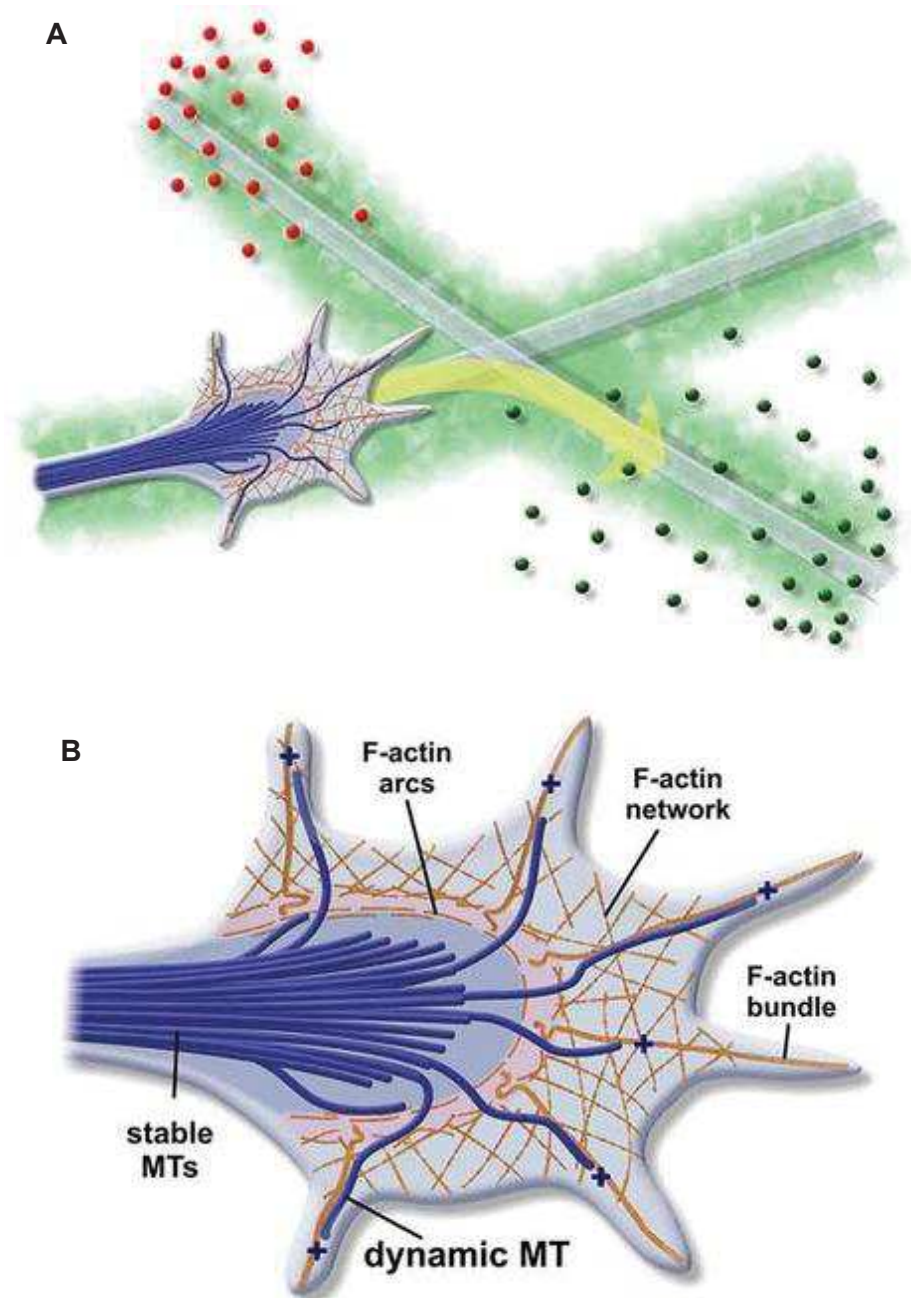


FIG. 26 AXON GUIDANCE

(A) Axons rely on guidance molecules (red and green) which will be sensed by the growth cone to make adequate connections. (B) Structural organization of the growth cone cytoskeleton (Actin and microtubules networks). Growth cone ‘fingers’ (filopodia) sense the environment, between the filopodia actin networks create lamellipodia veils. From (Bryan Kolb, 2009)

Projection neurons will be progressively specified into different neuronal subtypes, depending on where their axons project, they can be classified into three different groups (associate, commissural or cortico-fugal) (Greig et al., 2013), see Fig. 27 for details.

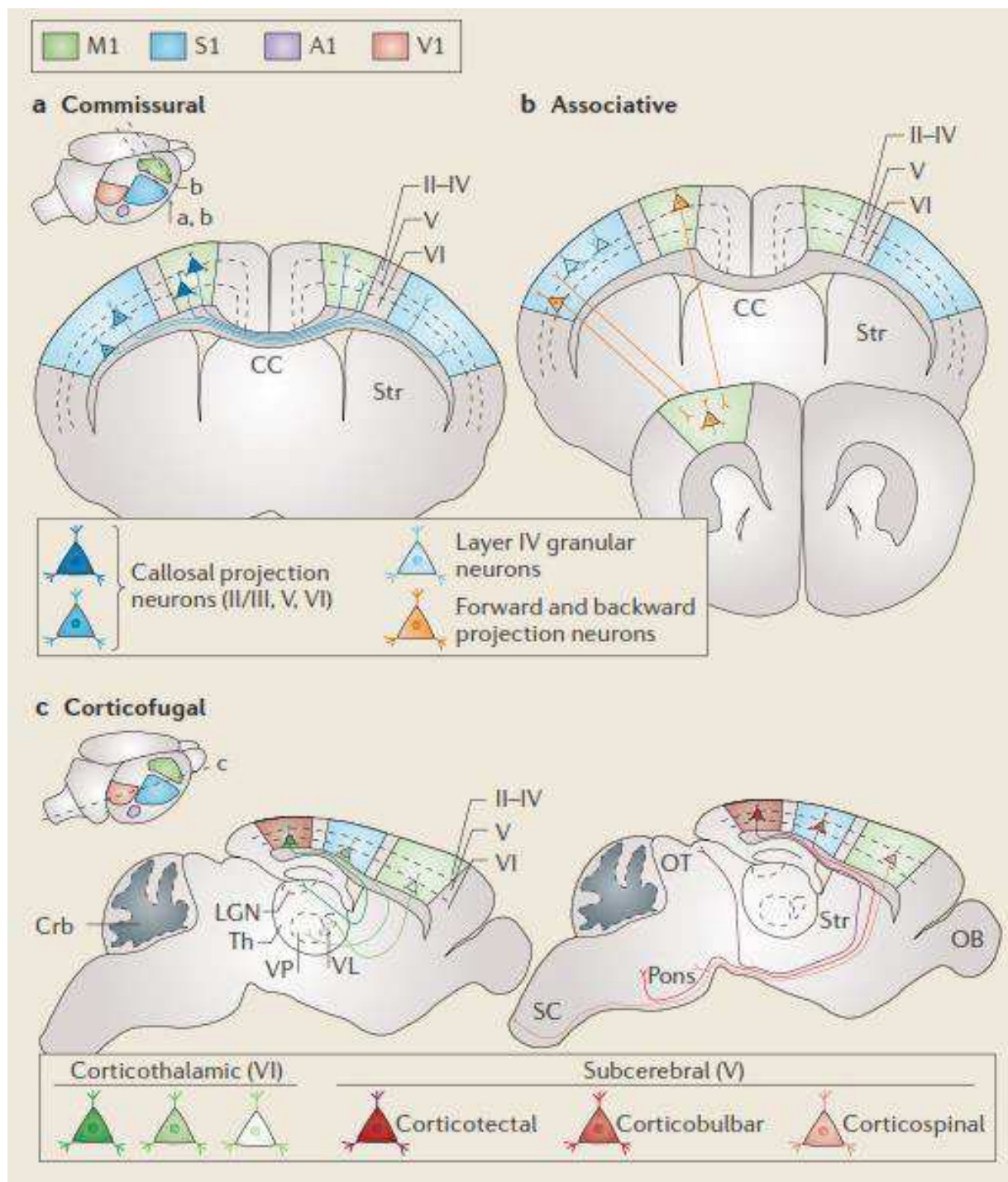


FIG. 27 CORTICAL PROJECTION NEURON DIVERSITY

Projection neurons can be classified based on where their axons project, to note, neurons within one class residing on different cortical areas project to anatomically different targets. (A) Commissural neurons project their axons across the midline to the contralateral hemisphere; (B) Associative neurons project their axons within the same cortical hemisphere; (C) Corticofugal neurons project their axons away from the cortex. From (Greig et al., 2013)

1.7 In Utero electroporation: a tool to study cortical development

In utero electroporation (IUE) is a widely used technique in the field neurobiology, particularly, for the study of a small population of interest in the context of wild type (WT) brains (J. LoTurco et al., 2009). It is based on causing an increase in the electrical conductivity and permeability of the cellular plasmatic membrane by applying an electric field that will allow electroporated cells to acquire a genetic construct of interest. A solution containing the genetic material is injected into one of the lateral ventricles of the mice embryos through the uterine wall prior to electroporation. The application of electric current (using paddle electrodes) after the injection of the genetic material results in an area- and time-specific transfection (Tabata et al., 2001) (See Fig. 28). To allow visualization of the electroporated cells, co-transfection with fluorescent reporter genes is usually performed.

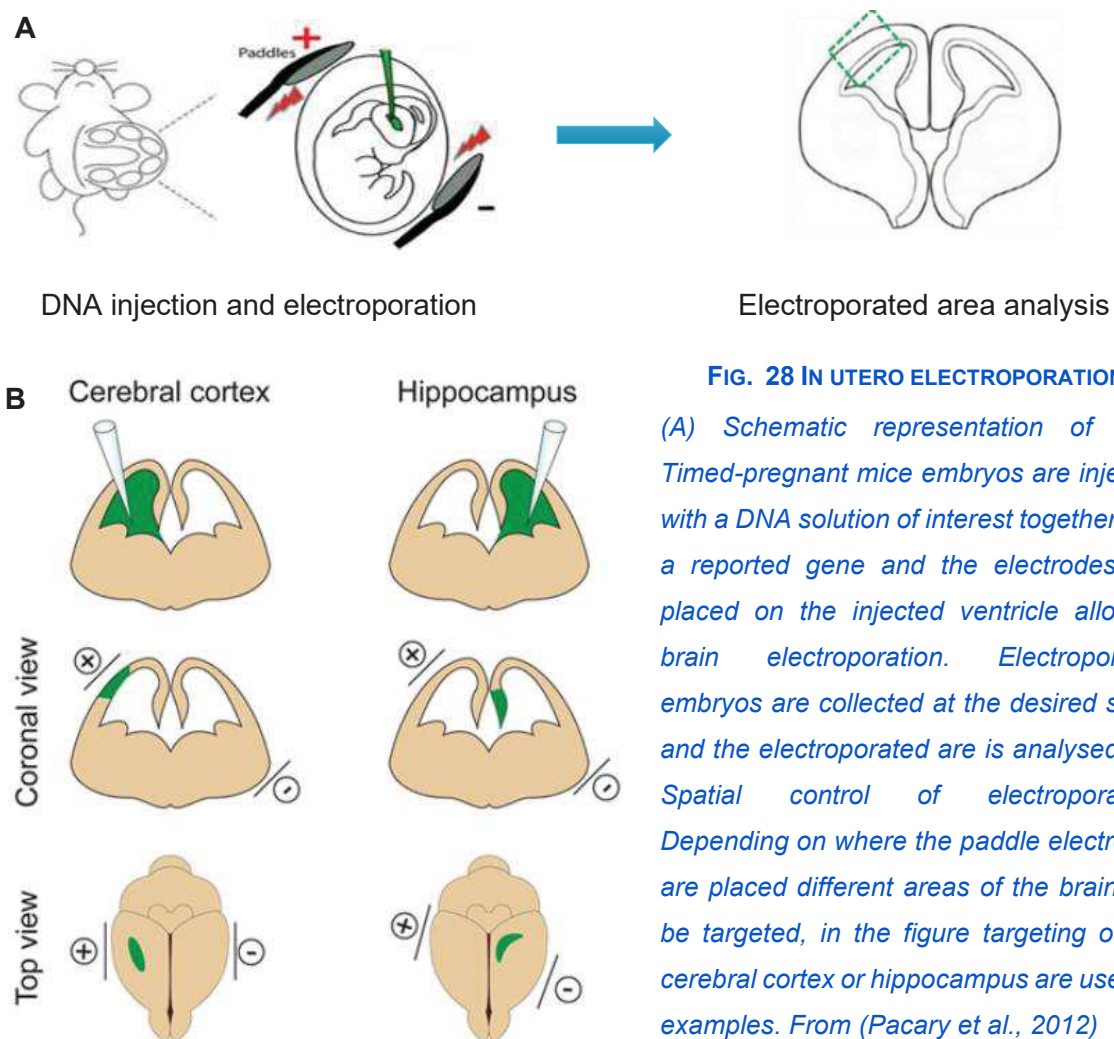


FIG. 28 IN UTERO ELECTROPORATION

(A) *Schematic representation of IUE. Timed-pregnant mice embryos are injected with a DNA solution of interest together with a reported gene and the electrodes are placed on the injected ventricle allowing brain electroporation. Electroporated embryos are collected at the desired stage and the electroporated area is analysed.* (B) *Spatial control of electroporation. Depending on where the paddle electrodes are placed different areas of the brain can be targeted, in the figure targeting of the cerebral cortex or hippocampus are used as examples. From (Pacary et al., 2012)*

IUE is a powerful tool to perform gain and loss of function studies, since it allows injecting cDNA, siRNAs (small interfering RNA), shRNA (small hairpin RNA), morpholinos or miRNAs (Shimogori et al., 2008).

Several developmental events can be studied using IUE, including regional patterning, proliferation, neuronal differentiation/fate, neuronal migration, dendrite and spine development, axon formation and guidance, synaptogenesis and synapse maturation and astrogliogenesis (Pacary et al., 2020). One of the main disadvantages of IUE is that it differs from physiological conditions, however, in comparison to the generation of transgenic animal models, it is faster and less expensive.

CHAPTER 2: TRANSFER RNAs & TRANSLATION

2.1 Translation

Translation is an essential process for cellular homeostasis and function, in which ribosomes synthesize proteins from messenger RNA (mRNA). The orchestrated action of ribosomes, transfer RNAs (tRNAs) and other factors allow the decoding of the mRNA in a unique direction (5'-3') (See Fig.29) and the synthesis of chain of amino acids (aa) or polypeptide, which will fold, giving rise to an active protein. mRNA decoding is performed in codons according to the genetic code (see next section). mRNA codons are sequences of nucleotide triplets in the mRNA which bind to the anticodon, sequence of nucleotide triplets complementary to the mRNA codon, of tRNA molecules (Explained in detail in the section “2.2”).

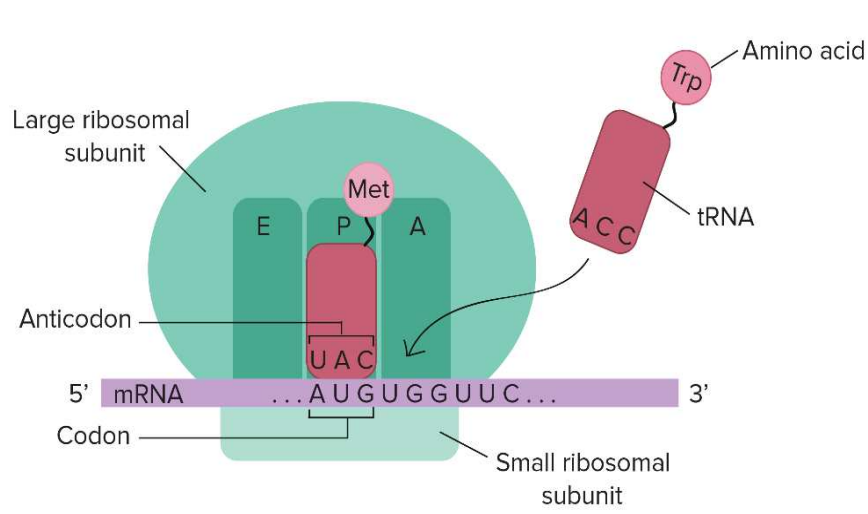


FIG. 29 OVERVIEW OF TRANSLATION

Ribosomes, mRNA, tRNAs orchestrate protein translation. tRNA allow decoding of the mRNA by pairing of their anticodons to the mRNA and supplying the encoded amino acids to the ribosome. From ("Overview of translation," 2016)

2.1.1 The genetic code

The genetic code defines the relation between every codon in the mRNA and each aa. It consists of a common set of rules to all living organisms (with small variations) that determines how a mRNA sequence is translated into a protein (See Fig. 30A). It defines the relationship between each codon and each aa, in a way that a codon codes for only one aa, however, the genetic code is degenerate, there are several codons that code for the same aa. There exist 64 possible codons, 61 which encode aa and 3 encoding translation stop codons. Among the codons that code for the same aa, the differences occur in the third position, which generally has a greater tolerance to changes than the first and second codon positions (Spencer et al., 2012).

2.1.1.1 Wobble hypothesis

There are 64 different codons, however, living organisms do not have tRNAs with 64 different anticodons, on average, they have about 45 (51 anticodon families in human) (Chan et al., 2016). This assumes that some tRNAs have to pair with more than one codon. The Watson-Crick base pairing rules establish that adenine (A) binds to thymine (T) or uracil (U) whilst, guanine (G) binds to cytosine (C). In 1966 Francis Crick proposed the wobble hypothesis, according to which position 34 of the anticodon was not as restricted in terms of pairing as the other two positions and could carry out non-standard base pairing. A wobble ("movement") base pair is a pairing between two bases that does not follow the Watson-Crick rules of base pairing (See Fig.30B).

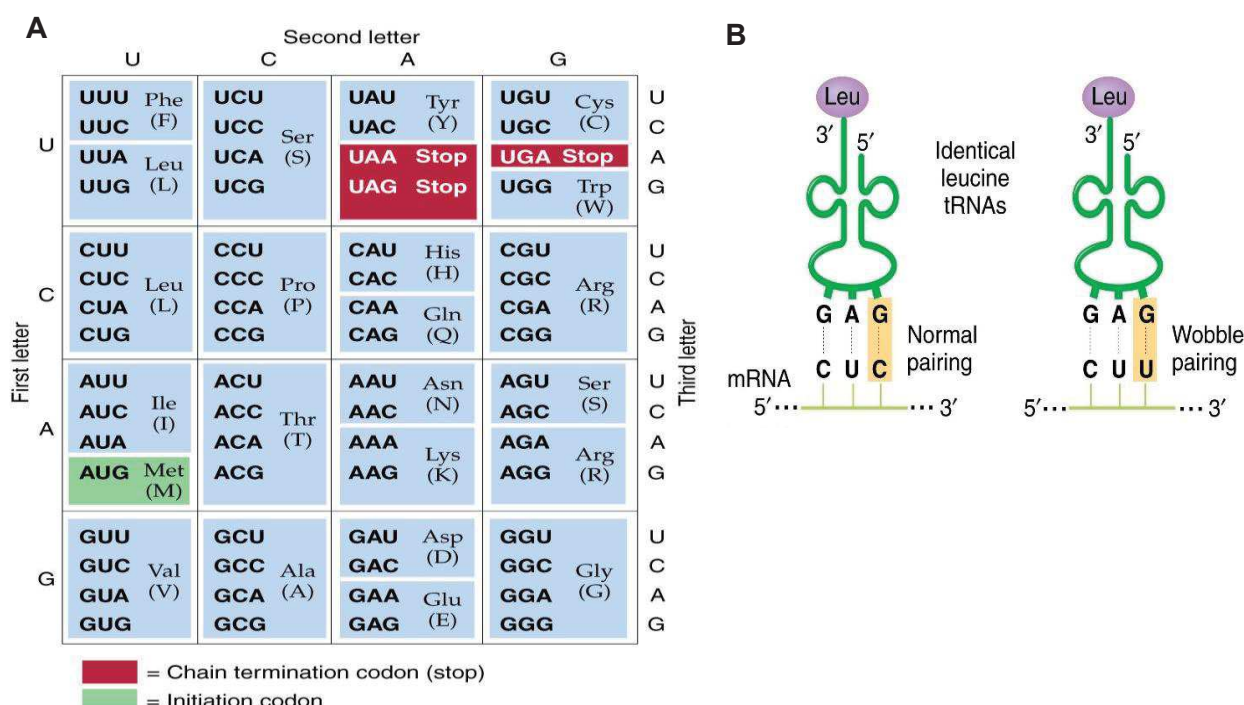


FIG. 30 THE UNIVERSAL GENETIC CODE AND THE WOBBLE HYPOTHESIS

(A) *The Universal genetic code: Note that this is an RNA code: the three-letter codons include U. There are 64 different codons, 61 sense codons and 3 stop codons (red). AUG codon codes for methionine and serves as an initiation code (green). From (Russell, 2010)*

(B) *Wobble pairing: In contrast to standard Watson-Crick base pairing in wobble pairing bases can establish non-Watson-Crick interactions. Note how the same Leucine-tRNA can decode two different codons depending on the pairing established by position 34 (yellow). From (Russell, 2010)*

2.1.2 Cytoplasmic translation

In eukaryotes, most of the genes are encoded by the nuclear genome and are translated in the cytoplasm, nevertheless, there exists also a group of protein-coding genes encoded by the

mitochondrial genome (14 in humans and 8 in yeast) which are translated in the mitochondria. Mitochondrial translation is more similar to the prokaryotic translation system and presents unique features, such as different tRNAs, and a different genetic code (Smits et al., 2010). In this thesis only cytoplasmic translation will be introduced. Cytoplasmic translation is a cyclical process consisting in initiation, elongation and termination phases that ends with the recycling of the ribosome (Hershey et al., 2019). The initiation phase is in most conditions the limiting phase of the process (Livingstone et al., 2010) and is regulated by several pathways including the mammalian mechanistic target of rapamycin (mTOR), the mitogen activated protein kinases (MAPKs) or the integrated stress response (ISR) (Tahmasebi et al., 2018). Under homeostatic conditions, most protein synthesis is performed through an initial binding of the translation machinery to the 5'cap of the untranslated region (UTR) of the mRNA (cap-dependent translation), nevertheless, in a small subset of mRNAs, 5' UTR scanning is not performed (cap-independent translation) (Lacerda et al., 2017).

2.1.2.1 Phase 1: Initiation

During the initiation phase of the eukaryotic cap-dependent translation (See Fig. 31A), the cytoplasmic ribosome is recruited to mRNA through several translation initiation factors. The 40S ribosomal subunit binds to a ternary complex, composed of the initiator methionyl-tRNA (Met-tRNA), the eukaryotic initiation factor (eIF) 2 and GTP, and gives rise to the 43S pre-initiation complex (PIC). The 43S PIC is recruited to the 5'cap of the mRNA by the eIF4F heterodimeric complex, which is composed of eIF3E, eIF4A, eIF4G and eIF4G. eIF4G interacts with PABP (poly (A)-binding protein), which binds the polyA tail of mRNA thus promoting mRNA circularization around the complex. Subsequently, eIF4A unwinds the 5'UTR of the mRNA and the PIC scans the 5'UTR until a translation start codon is found. The recognition of a start codon triggers the dissociation of various factors and conformational changes leading to the formation of the 48S complex. Finally, in a process catalyzed by eIF5B the 60S subunit of the ribosome joins the PIC leading to the dissociation of other factors and the formation of the 80S complex. The final ribosome is composed of two subunits, one small (40S) and one big (60S) and contains one binding site for the mRNA and three tRNA binding sites. The three tRNA binding sites are the acceptor (A) (binds the tRNA complementary to the codon), peptidyl (P) (holds the tRNA with the growing polypeptide chain) and exit (E) (serves as a transitory step before the tRNA is let go by the ribosome) (Hinnebusch, 2014). In the 80S ribosome initiator met-tRNA pairs with the initiation codon in the P site and translation starts. Regulation of translation initiation is mainly carried out by activation or inactivation of eIFs, for example, under starvation or stress conditions translation initiation can be reduced by inactivation of eIFs (Sonenberg et al., 2009).

2.1.2.2 Phase 2: Elongation

The 80S complex begins the synthesis of the encoded protein during elongation (See Fig. 31B). The next codon of the transcript is located in the A site, a complementary aminoacyl-tRNA to the following codon is delivered there by the eukaryotic elongation factor (eEF) 1A. Cognate codon recognition leads to the release of eEF1A. Subsequently, the polypeptide chain of the tRNA is transferred to the aminoacyl tRNA of the A site, thereby extending the peptide chain. At this point, the ribosome undergoes many conformational changes and a translocation along the mRNA which resets its state (eEF2 participates in the translocation process).

Several factors influence elongation rates, among them, those influencing decoding speed are particularly important. Decoding speed is mainly related to tRNAs, their relative abundance, the cognate:near cognate tRNA ratios, and their aminoacylation and modification extent can highly influence decoding speed and the elongation phase. Other factors that determine elongation rates are epigenetic modifications in the mRNA and levels of expression and activity of proteins that participate in the elongation phase, such as eEF2 (important in the translocation process) or eIF5A (which favors the formation of peptide bonds between proline residues) (Knight et al., 2020).

2.1.2.3 Phase 3: Termination

The cycle continues so that the encoded aa are added until a STOP codon is found in the mRNA. This event leads to the end of translation with the help of eRF1, eRF3, ABCE1 and other factors which promote ribosome separation in the 60S and 40S subunits and the separation of the mRNA and the deacetylated tRNA (Dever et al., 2012).

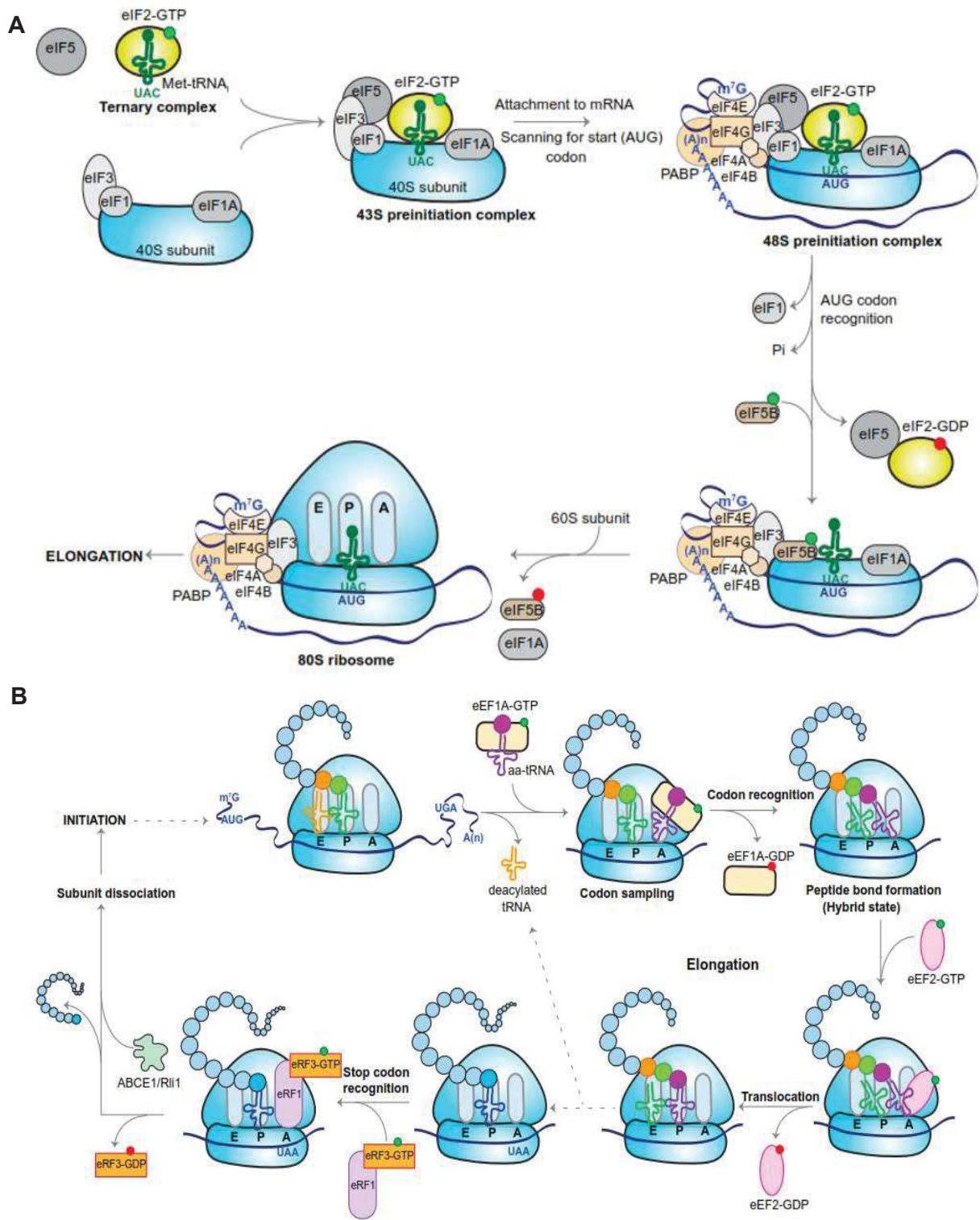


FIG. 31 EUKARYOTIC CAP-DEPENDENT TRANSLATION OVERVIEW

Eukaryotic CAP-dependent translation is a cyclic process which comprises (A) Initiation (B) Elongation, termination and ribosome recycling phases. Details in the text. From (Kapur et al., 2017)

2.2 Transfer RNAs

tRNA molecules are conserved in the three kingdoms of life. As described before, tRNAs are fundamental molecules for translation, acting as adaptors and carrying aa to the ribosome to allow mRNA decoding. tRNAs represent 4-10% of the total cellular RNA, being the most abundant class of small non-coding RNA molecules, there are roughly 60 million tRNA molecules per mammalian cells (Schimmel, 2018).

There are 20 different aa and for each of them there is at least a tRNA specie. In humans there is ~500 nuclear-encoded tRNA genes, for which there exist copy number variations between individuals (Iben et al., 2014). Eukaryotic cells contain in addition to cytoplasmic tRNAs a pool of mitochondria-encoded tRNAs (mt-tRNAs), in human there is 22 mt-tRNAs (Chan et al., 2009). mt-tRNAs dysregulation has been associated to several human diseases. In terms of structure, mt-tRNAs are more similar to bacterial tRNAs, they are enriched in adenine and uracil which makes them more unstable. They are shorter than their cytoplasmic counterparts and can have smaller stem and loop regions or lack entire domains (Suzuki et al., 2011). Since mt-tRNAs are outside the scope of this PhD thesis, I will concentrate on cytoplasmic tRNAs.

2.2.1 Transfer RNA architecture

They are characterized by a cloverleaf-life secondary structure (See Fig. 32A) with 76 nucleotides being the canonical and most common form (Zheng et al., 2015). By convention, tRNA nucleotides are numbered from the 5'-Phosphorylated terminus. At the 3' end of the molecule there is the CCA trinucleotide, where the aminoacylation will be performed. tRNAs contain 4 arms which are designated as acceptor stem, dehydrouridine (D) stem-loop (4-12 nucleotides), anticodon stem-loop (7 nucleotides), and T ψ C stem – loop (7 nucleotides), where ψ represents pseudouridine (See Fig.32A). t-RNA molecules also contain a variable-loop ranging between 4 and 23 nucleotides. When the molecule is folded into its ternary structure (See Fig.32B), the triplet anticodon (which recognizes the codon in the mRNA) and the aa attachment site are the most distant points of the molecule. The architecture of all cytoplasmic tRNA molecules follows a series of identity rules (Giege, 2008) and structural features (Ramakrishnan, 2002) to fit in the ribosomal site. tRNAs are among the most stable RNA molecules in cells due to their structure, which is stabilized by extensive secondary and tertiary structural contacts and chemical modifications (Gebetsberger et al., 2013)

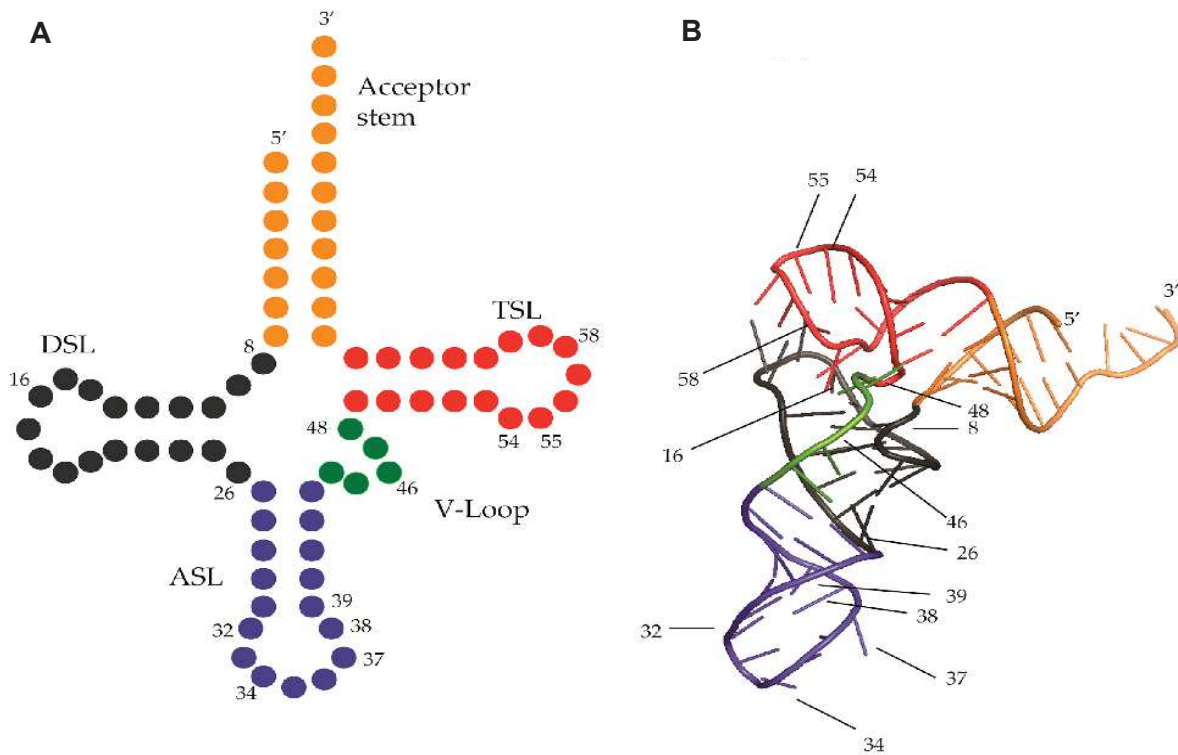


FIG. 32 tRNA ARCHITECTURE

tRNA domains are shown in a secondary (A) and tertiary (B) tRNA structure. The Anticodon stem loop (ASL), D-stem loop (DSL), T-Stem loop (TSL), Variable-loop (V-loop) and acceptor stem are with different colours. From (Vare et al., 2017)

2.2.2 Isoacceptors and isodecoders

The fact that the genetic code is degenerate has given rise to what are known as tRNA isoacceptors, molecules of tRNAs with different sequences, including the anticodon, but which carry the same aa. In higher eukaryotes, in addition to isoacceptors, there are also isodecoders, which are tRNAs that share the same anticodon but differ elsewhere in the sequence. There are approximately 270 isodecoders associated with 51 different isoacceptors for cytoplasmic tRNAs in humans (Chan et al., 2009, 2016; Dittmar et al., 2006; Geslain et al., 2010; Parisien et al., 2013). The number of gene copies for each isodecoder varies widely across living organisms (Marck et al., 2002). Interestingly, in human, more than half of the isodecoders are encoded by a unique gene and only 24 isodecoder genes are present in more than 3 copies (Chan et al., 2016). Although tRNAs isodecoders are highly conserved in mammalian genomes their function is still not completely clear. It is thought that they could enhance cell type-specific translation in a codon or mRNA-dependent manner. In accordance with that hypothesis, not all isodecoders are expressed in all cells, the expression of isodecoders is thought to vary between different human tissues (ex: brain (See section 2.4.2) or in some pathologies (ex: cancer) (Schmitt et al., 2014). Interestingly, tRNA content has been

shown to be a mechanism through which cells alter the expression of some transcripts and proteins, for example, in some cancers (Goodarzi et al., 2016).

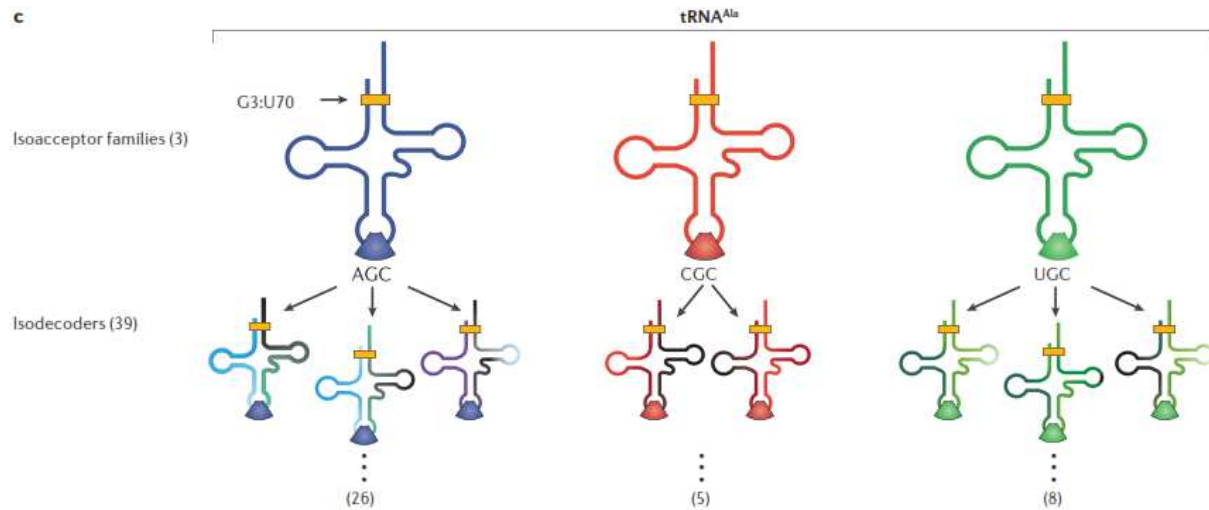


FIG. 33 tRNA COMPLEXITY IS EXPANDED BY ISOACCEPTORS AND ISODECODERS

Isoacceptors and isodecoders are shown for alanine-tRNA. There are three families of isoacceptors with several isodecoders for alanine-tRNA. Different colourings for isodecoders indicate differences within the same isoacceptor family while the anticodon triplet remains the same. Whereas there is 3 different isoacceptor families for alanine-tRNA there is respectively 26, 5 and 8 isodecoders within each of the isoacceptor families. From (Schimmel, 2018).

tRNA genes, isoacceptors and isodecoders contribute to increase tRNA complexity (See Fig. 33). This complexity can be further expanded by tRNA base modifications. tRNA modifications (explained in detail in the next section) expand the number of microspecies of tRNAs that exist adding even more complexity to the system (See Fig. 34).

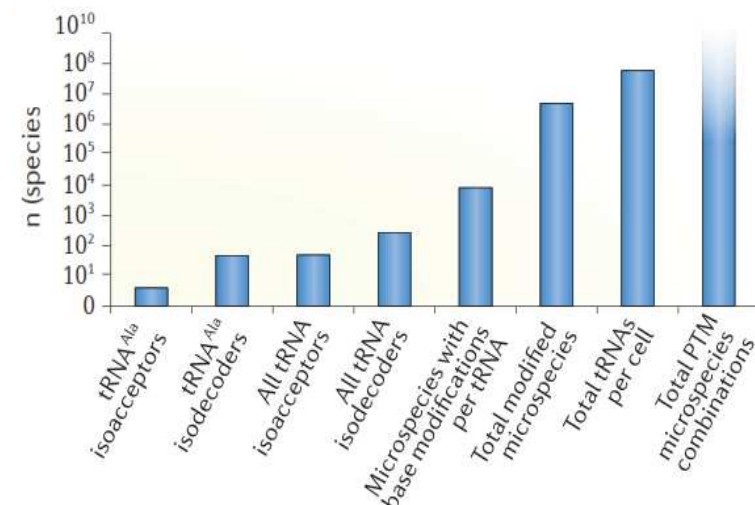


FIG. 34 NUMBER OF TRNA SPECIES

tRNAs species arise as a result of tRNA genes, isoacceptors, isodecoders and post-transcriptional modifications (PTMs). From (Schimmel, 2018).

2.2.3 Transfer RNA biogenesis

Studies of the three-dimensional nuclear organization of tRNA genes in eukaryotic cells have revealed that they cluster in the nucleolus (Thompson et al., 2003), which suggests that the regulation of their transcription could be coordinated. tRNA biosynthesis encompasses their transcription and maturation, an overview of the process is depicted in Fig.35.

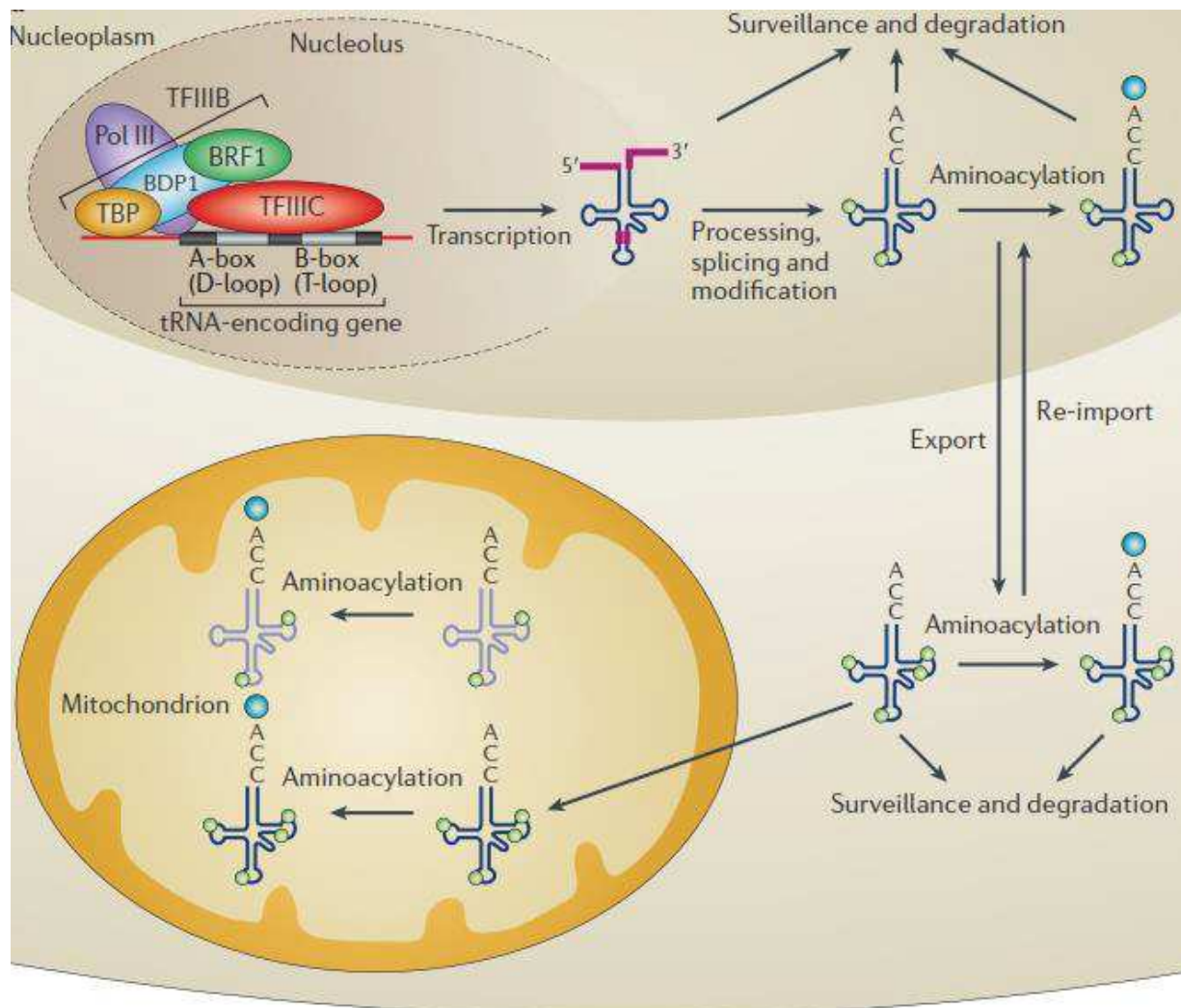


FIG. 35 tRNA BIOGENESIS OVERVIEW

tRNA biogenesis comprises their transcription, processing, splicing and post-transcriptional modifications (green circles), aminoacylation (blue circles) and transport (nuclear export/re-import and mitochondrial import in some cases). Cytoplasmic tRNAs and Mitochondrial tRNAs are respectively shown dark blue and light blue. The biogenesis pathway may differ in some organisms (ex: plants and yeast). See text for further details. From (Kirchner et al., 2015).

During tRNA genes transcription TFIIC and TFIIB transcription factors bind to various areas of the tRNA gene, the transcription factor TFIIC binds to the intragenic regions A-box and B-

box, which encode the D-and T-stems loops respectively. On the other hand, TFIIIB, which is composed of by BDP1, BRF1 and TATA-binding protein, binds to upstream regions of the gene. The binding of these two factors triggers the recruitment of RNA polymerase III (Pol III) allowing transcription to begin. The sequences located in the 5' upstream of the tRNA genes have been shown to modulate the binding force of PolIII (Kutter et al., 2011). Recently, Gerber and colleagues (A. Gerber et al., 2020) identified a direct role of RNA polymerase II (Pol II) in the transcription of tRNAs through the repression of PolIII activity via transcriptional interference, the authors showed that this repression of PolII occurs in some cellular contexts such as serum starvation.

tRNAs are synthesized as precursor molecules (pre-tRNAs), which are bigger in size than mature tRNAs due to the presence of 5'leader and 3'trailer sequences and introns. Only 6% of all tRNA genes in humans contain introns (In humans, there are 24 intron-containing tRNA genes isodecoders classified into 4 isoacceptor families) (Chan et al., 2016; Lowe et al., 1997). Pre-tRNAs undergo several processing steps before becoming a mature tRNA molecule. Processing steps include: 1) splicing of introns (for intron-containing tRNAs(Lowe et al., 1997)) is carried out firstly by a complex formed by CLP1 and TSEN (cleavage and polyadenylation factor I subunit 1/ tRNA splicing endonuclease) and secondly by the tRNA-ligase complex (Greer, 1986; Popow et al., 2011; Trotta et al., 1997); 2) Removal of the 5' leader by La protein and RNase P; 3) trimming of the 3' trailer by ELAC; 4) addition of the CCA trinucleotide to the 3' terminal end of the molecule by TRNT1, the CCA is a not-genome encoded in eukaryotic genomes; 5) Modification of multiple residues (described in more detail in section 2.3). Aminoacylation occurs mainly in the cytoplasm, although it can also occur in the nucleus to a much lower extent than in the cytoplasm. Nuclear aminoacylation is proposed to be a proofreading step for structural integrity of the tRNAs since only correctly processed tRNAs are substrates of Aminoacyl tRNA synthetases (aaRS) (Lund et al., 1998).

tRNA aminoacylation is carried out in a two-step reaction in which first aaRS activate the aa with ATP and second the activated aa is transferred to its cognate tRNA. This reaction is catalyzed by 20 different aaRs, each of which is specific for one of the 20 aa (Ibba et al., 2000). Once aminoacylated, tRNAs are transported by translation elongation factor to the ribosome for protein synthesis (Fredrick et al., 2010). aaRS recognize tRNAs by both positive and negative determinants. The majority of identity determinants are located in distal clusters in the distal extremities of tRNA molecules, nevertheless, in some cases, some determinants can be found in the core region of tRNAs. All 20 tRNA families contain aminoacylation determinants located in the acceptor stem, which highlights the importance of this stem as an aminoacylation determinant. In addition, 18 of them have determinants in the anticodon loop, highlighting the

importance of this structure for aminoacylation. In many cases tRNA modifications can also act as aminoacylation determinants (Pang et al., 2014).

Only the tRNAs that have matured correctly leave the nucleus through a nuclear receptor. Some nuclear-encoded tRNAs can also be imported into the mitochondria (Schneider, 2011). pre-tRNAs that have not been correctly processed are eliminated in the nucleus through degradation of their 3' ends, tRNAs that are exported but not properly modified are degraded from their 5' ends in the cytosol (Phizicky et al., 2010). There exist two tRNA degradation pathways: The tRNA nuclear surveillance pathway and the Rapid tRNA decay pathway (See Fig. 3 for an overview of these two paths). Most of the knowledge about these pathways is derived from work in *S. cerevisiae*. The tRNA nuclear surveillance pathway acts primarily on pre-tRNAs. In *S. cerevisiae*, nuclear hypo-modified pre-tRNAs are detected by the TRAMP complex and degraded by the exosome (Megel et al., 2015). The rapid tRNA decay pathway (RTD) acts as a quality control for mature tRNAs, and is thought to act on a wide range of unstable or non-functional tRNAs. RTD safeguards mostly the structural integrity of tRNAs as it has been shown to act on tRNA bearing deleterious mutations for their stability (Whipple et al., 2011). The RTD pathway is mainly mediated by Rat1 and Xrn1, respectively in the nucleus and cytoplasm. Interestingly, the CCA-adding enzyme is also involved in this pathway by selectively labeling unstable tRNAs (Wilusz et al., 2011).

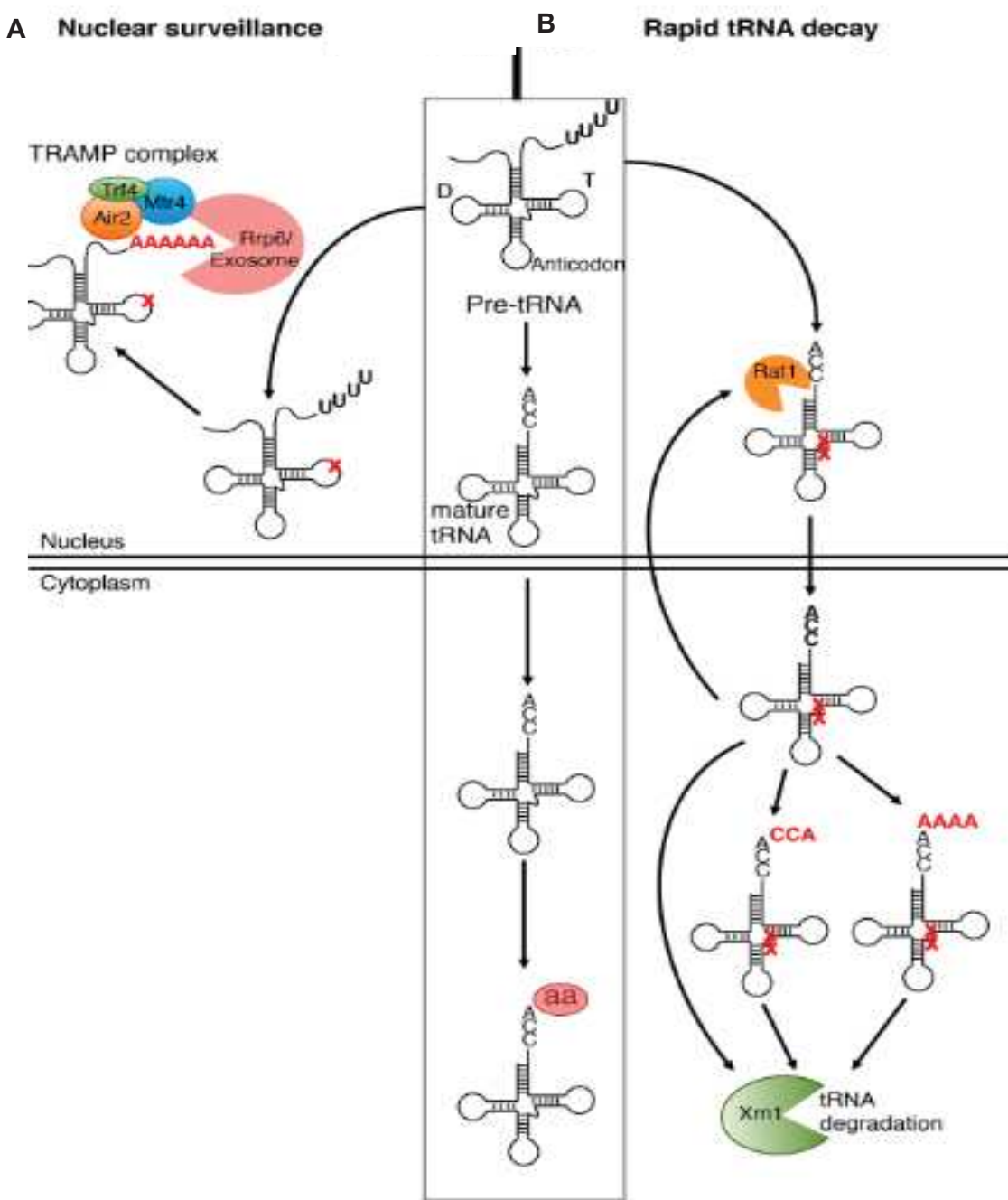


FIG. 36 OVERVIEW OF tRNA DEGRADATION PATHWAYS IN *S.CEREVIAE*

(A) Nuclear surveillance pathway. (B) Rapid tRNA decay pathway. See text for details. From (Megel et al., 2015)

2.2.4 tRNA fragments

tRNAs can be fragmented by angiogenin or other nucleases generating fragments (See Fig. 37) that in many cases participate in other cellular functions, including translation regulation and gene silencing among others (Schimmel, 2018). tRNA fragmentation usually occurs due to various cellular stresses. The levels of the tRNA fragments can vary in various conditions

such as inflammation, aging, calorie restriction and tissue damage (Dhahbi et al., 2013; Mishima et al., 2014; Y. Zhang et al., 2014). Nucleolytic cuts in the anticodon of tRNAs generate 5' and 3' halves, which are called translation interfering (tiRNAs), since they have been shown to inhibit translation. Depending on the position of the nucleolytic cut, other types of fragments can be generated, called fragmented tRNAs (tfRNAs), which can be much smaller than tiRNAs. tRNA fragments have been found to be abundant in vertebrates from fish to humans and some to be more abundant than others and conserved between species (Y. Zhang et al., 2014). In the same way that tRNAs, fragments of tRNAs can contain many different modifications, which expand their complexity (Cozen et al., 2015).

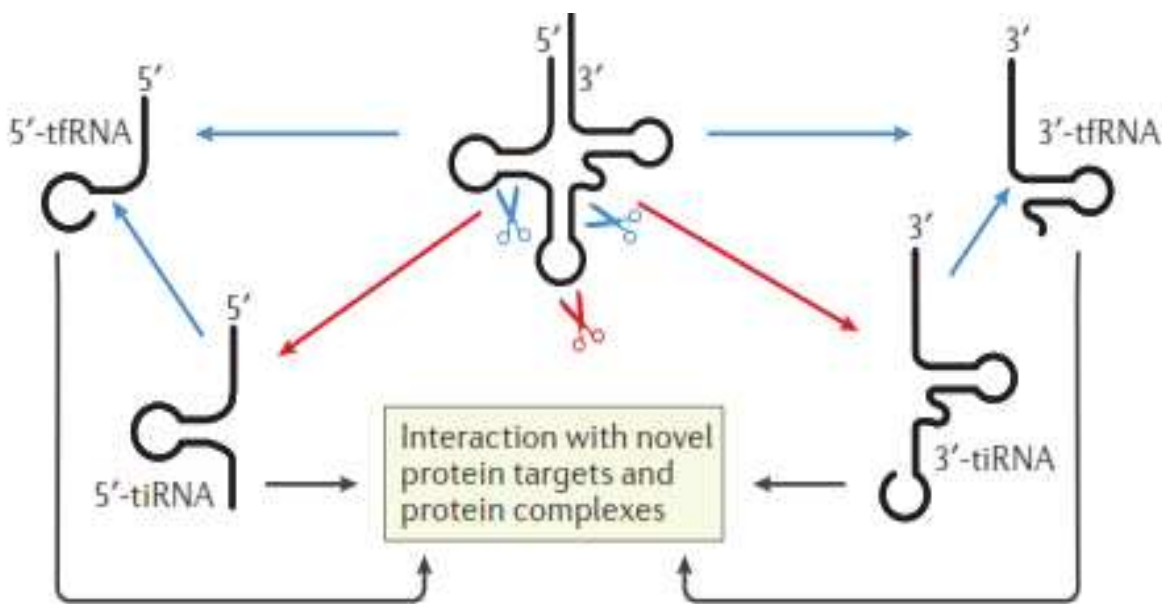


FIG. 37 tRNA FRAGMENTS

tRNAs fragmentation generates different types of fragments, which expose previously unexposed sequences that allow their interaction with other cellular factors and their participation in other functions.
From (Schimmel, 2018)

2.2.5 tRNAs as regulators of biological processes

In addition to their role as adaptor molecules during translation, tRNAs have been seen to act as signaling molecules participating in the regulation of various cellular and metabolic processes, both in prokaryotes and eukaryotes (Raina et al., 2014) (See Fig.38).

tRNAs have a huge effect on cell metabolism, not only affecting protein translation but also participating in several biosynthetic pathways, for example they have been implicated as substrates for non-ribosomal peptide bond formation, post-translational protein labeling, antibiotic biosynthesis and modification of phospholipids in the cell membrane (Raina et al., 2014). In addition, they have been directly involved in several signaling pathways. Uncharged

tRNAs lead to activation of Gcn2p kinase, which has a preference for binding of uncharged tRNAs (Dong et al., 2000), and can phosphorylate eIF2, causing a reduction in its activity reducing overall protein synthesis. tRNAs have also been shown to interact with cytochrome c and inhibit apoptosisome formation (Mei et al., 2010), demonstrating a role for these molecules in regulating cellular apoptosis.

Their functions in the cells apart from translation can also be carried out indirectly, for example through aaRs or tRNA fragments (explained in previous section). In addition to their role in aminoacylation several human aaRS have been reported to act in other processes such as the regulation of transcription, extracellular signaling, or the regulation of mRNA accessibility through the recruitment of binding partners (Pang et al., 2014)

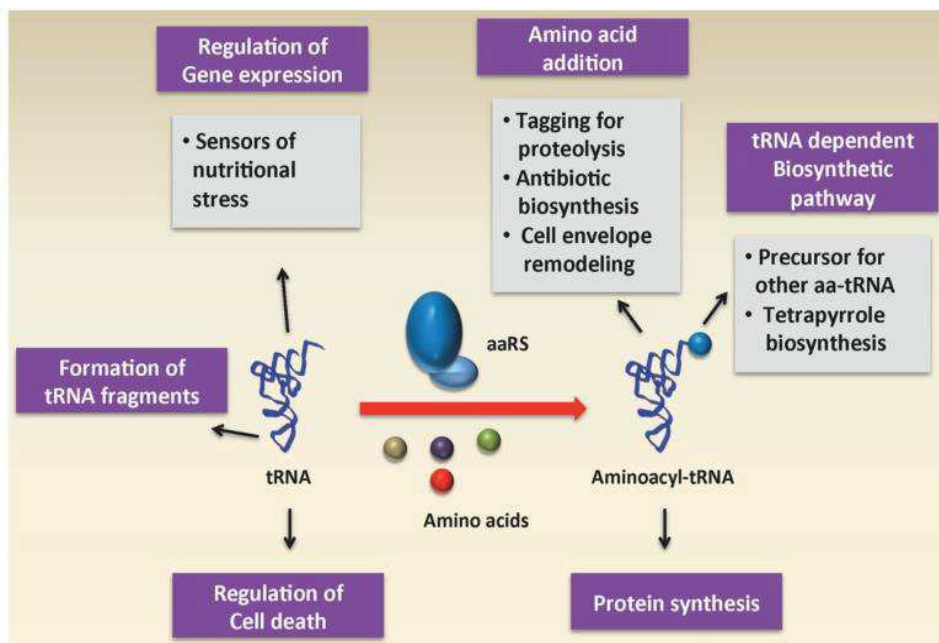


FIG. 38 VARIOUS ROLES OF CHARGED AND UNCHARGED tRNAs IN THE CELL

tRNAs can directly act on different cellular functions based on their aminoacylations status. See main text for details. From (Raina et al., 2014)

2.3 Transfer RNA modifications

2.3.1 Overview

There are over 90 possible nucleoside modifications in humans (Cantara et al., 2011), some of them are common to all three domains of life whereas other are specific to some of the domains (See Fig.39)(Y. Motorin, & Grosjean, H, 2005). tRNAs are the RNA class with most post-transcriptional modifications. On average a human tRNA has between 11 and 13 (PTMs) (Saikia et al., 2010), some of which are common to the vast majority of tRNAs, while others are found only in one group or a specific tRNA. In most cases, the modifications are not found in all the molecules of a specific tRNA. Usually, a percentage of the molecules present a modification on a specific base while others do not. Levels of tRNA modifications have been

found to vary between 10 and 80% for a specific base depending on the type of modification and its location in the tRNA molecule (Clark et al., 2016).

FIG. 39 PHYLOGENETIC DISTRIBUTION tRNA MODIFICATIONS IN THREE DOMAINS OF LIFE

Modified nucleosides exclusively present in eukaryotic mitochondrial tRNAs are depicted in yellow background. From (Y. Motorin, & Grosjean, H, 2005)

Simple modifications such as methylation or pseudouridylation are mostly associated to a single enzyme or complex, whereas, more complex modifications depend on multiple enzymes. The enzymes catalysing many tRNA modifications are already identified, however, the enzymes behind many other modifications remain still unknown (de Crecy-Lagard et al., 2019) (See Fig.47). Approximately a total of 135 genes are estimated to be required for catalysis of cytosolic and mitochondrial tRNAs. Among them, 22% require further validations and 23% have not been identified yet.

2.3.2 Function

tRNA modifications influence several aspects of tRNA molecules and their function (See Fig.40 and 41). Some can have a global influence on tRNA molecules by: 1) Stabilization of the 2D/3D structure of whole RNA molecule or its domain (for example 2'-O-methylation, m^5U and m^5s^2U , m^5C) (Y. Motorin et al., 2010), 2) Contributing to tRNA proper folding (for example m^2G_{26} (Sonawane et al., 2016)) or flexibility (for example dihydrouridines increase the flexibility of the D-loop (Dyubankova et al., 2015)), 3) Affecting further maturation of the molecule by affecting posterior modifications, tRNA processing and/or aminoacylation. Some can act as identity elements to promote or prevent molecular recognition by other molecules (mainly aaRS). For example, I_{34} was shown to be a positive identity element in yeast tRNA Alle for aminoacylation by Ile-RS (Bruno Senger et al., 1997). On the other hand, m^1G_{37} in yeast tRNA Asp prevents misaminoacylation by Arg-RS (Pütz et al., 1994). The absence of modifications on tRNAs can have a diverse range of implications, including tRNA misfolding, inhibition of further modifications and their impaired aminoacylation, which altogether can lead to their decay or cleavage (in general hypomodified tRNAs are targeted for degradation) (Phizicky et al., 2010).

In addition, certain tRNA modifications affect translational efficiency and fidelity by playing crucial roles during different phases of translation, for example by promoting initiation at canonical start sites (example: t^6A) (Daugeron et al., 2011), by regulating the entry of tRNAs in the ribosome (examples: s^2U_{34} and mcm^5U_{34}) (Rezgui et al., 2013) or in proper translation termination at stop codons (example: m^1C) (Torabi et al., 2011). Their functions during protein synthesis ensure proteins with proper sequences, a balance in the protein synthesis output

and a proper translation rate contributing to their correct folding. In terms of translation, the absence of tRNA modification can lead to inappropriate start site recognition (example: t⁶A) (Daugeron et al., 2011), ribosome pausing or frameshifting during elongation (U₃₄ modifications (Nedialkova et al., 2015)) or stop codon readthrough (example: m¹C) (Torabi et al., 2011). These impairments during translation can lead to frameshifts, extended polypeptides, and improper protein folding and aggregation. Some modifications in tRNAs are thought to affect specific cellular pathways by modulating the translation of groups of specific transcripts enriched in some codons (Novoa et al., 2012).

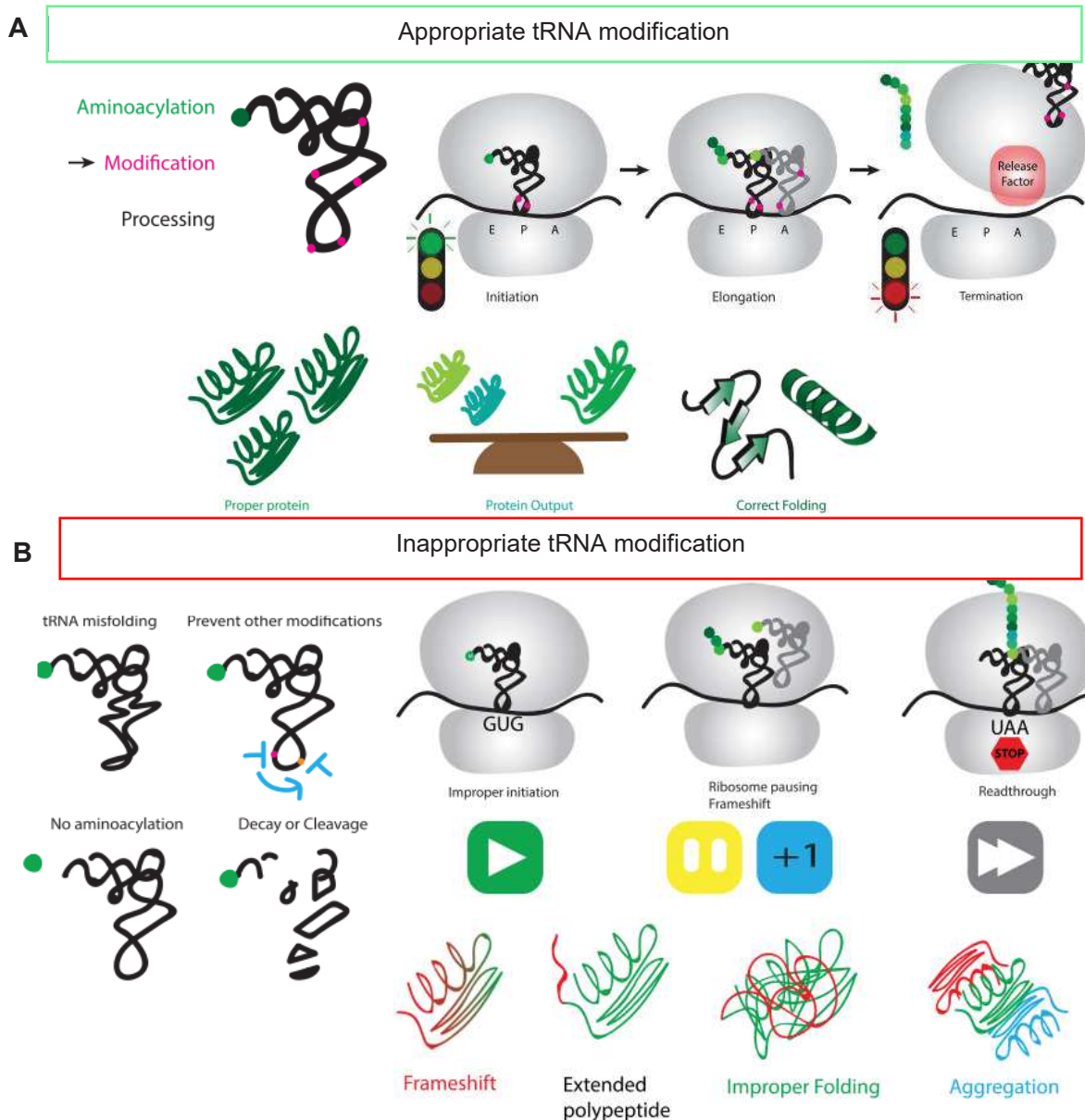


FIG. 40 MOLECULAR AND CELLULAR EFFECTS OF tRNA MODIFICATIONS

Appropriate tRNA modifications (A) influences posterior maturation steps of tRNA molecules and participate in the proper function of tRNAs during translation affecting the proteome. On the other hand, inappropriate tRNA modification (B) can disturb tRNA molecules, translation and negatively impact the proteome. See text for further details. Adapted from (J. Ramos et al., 2019)

2.3.3 tRNA modifications and positions

Both cytosolic and mt-tRNAs are modified by different classes of tRNA modifying enzymes. tRNA modifications take place all over tRNA molecules (See Fig.41). Depending on their location within the molecule, their effect can vary (See next paragraphs about modifications at

the anticodon stem loop or at the tRNA arms). The function of many tRNA modifications is still nowadays unknown.

Positions	tRNA modification		Function
	Nuclear-encoded tRNA	Mitochondrial-encoded	
1, 29, 30, 35, 36 and 65	Ψ	Unknown	Unknown
4	Cm and Am	Unknown	Unknown
9	m^1G	m^1G and m^1A	tRNA folding
10	Unknown	m^2G	Unknown
12	ac^4C	Unknown	Unknown
16, 17 and 47	D	Unknown	Unknown
18	m^2G	Unknown	Unknown
20 and 20a-b	D	D	Unknown
26	m^2_2G	m^2_2G and m^2G	Unknown
27 and 31	Unknown	Ψ	Unknown
28, 39, 55 and 67	Ψ	Ψ	Unknown
32	Ψ , 2'-O-methylribose and Cm	Ψ and m^3C	Unknown
34	I, Ψ , m^5C , Cm, Gm, 2'-O-methylribose, Q, mcm^5U , ncm^5U , ncm^5Um and mcm^5s^2U	tm^5U , tm^5s^2U , f^5C , s^2U and Q	Wobble base-pairing (codon–anticodon interaction)
37	ms^2t^6A , yW, m^1I , I^6A and m^1G	m^1G , t^6A , i^6A , ms^2A and ms^2i^6A	Stabilization of codon–anticodon interaction and prevention of frameshifting
38	Ψ and m^5C	Unknown	Unknown
40 and 50	m^5C	Ψ	Unknown
41	m^5U	Unknown	Unknown
44	Um	Unknown	Unknown
46	m^7G	Unknown	Unknown
48	m^5C	Unknown	Unknown
49	m^5C	m^5C	Unknown
54	m^5U and rT	m^5U	tRNA stability
58	m^1A	m^1A	Unknown
64	Ar(p)	Unknown	Discrimination between initiator and elongator tRNA ^{Met}

FIG. 41 POST-TRANSCRIPTIONAL tRNA MODIFICATIONS

Overview of tRNA modifications in both nuclear and mitochondrial encoded tRNAs and their known functions. Abbreviations: tm^5s^2U , 5-taurinomethyl-2-thiouridine; tm^5U , 5-taurinomethyluridine; Ψ , pseudouridine; ac^4C , N^4 -acetylcytidine; Am, 2'-O-methyladenosine; Ar(p), 2'-O-ribosyladenosine (phosphate); Cm, 2'-O-methylcytidine; D, dihydrouridine; f^5C , 5-formylcytidine; Gm, 2'-O-methylguanosine; I, inosine; I^6A , N^6 -isopentenyladenosine; m^1A , 1-methyladenosine; m^1G , 1-methylguanosine; m^1I , 1-methylinosine; m^2G , N^2 -methylguanosine; m^2G , N^2,N^2 -dimethylguanosine; m^3C , 3-methylcytidine; m^5C , 5-methylcytidine; m^5U , 5-methyluridine; m^7G , 7-methylguanosine; mcm^5s^2U , 5-methoxycarbonylmethyl-2-thiouridine; mcm^5U , 5-methoxycarbonylmethyluridine; ms^2A , 2-methylthioadenosine; ms^2i^6A , 2-methylthio- N^6 -isopentenyladenosine; ms^6t^2A , 2-methylthio- N^6 -threonyl carbamoyladenosine; ncm^5U , 5-carbamoylmethyluridine; ncm^5Um , 5-carbamoylmethyl-2'-O-methyluridine; Q, queuosine; rT, ribothymidine; s^2U , 2-thiouridine; t^6A , N^6 -threonylcarbamoyladenosine; Um, 2'-O-methyluridine; yW, wybutosine. From (Kirchner et al., 2015)

2.3.3.1 Modifications at or near the anticodon loop

Modifications at or near the anticodon loop are the most common. Most tRNA modifications occur at position 34 to ensure correct codon-anticodon pairing, reading frame maintenance and translation frameshifting prevention (Ranjan et al., 2016). Modifications at position 34 generally extend the recognition ability of various codons by wobbling pairing. Some typical modifications of this position include: U₃₄ modifications with hydroxyl, methyl or thiol groups, A₃₄ modifications such as Inosine34 (I₃₄), C₃₄ modifications such as 5-methylcytosine (m⁵C) and G₃₄ modifications, such as queuosine (Q) (See Fig.42) (Novoa et al., 2012; Phizicky et al., 2010). Subsequently, there is a brief description of some of the mentioned examples.

I₃₄ modification is reviewed in detail in section 2.5.2. U₃₄ modifications are ubiquitous in all organisms and play critical roles in mRNA decoding (Grosjean et al., 2010). It is often modified to xnm⁵U in bacteria and xcm⁵U in eukaryotes but it can be additionally modified for increased specificity by thio, seleno or methyl groups allowing decoding of A- or U-ending codons (El Yacoubi et al., 2012). U₃₄ modifications have been correlated with translational fidelity and proteostasis (W. Deng et al., 2015; Nedialkova et al., 2015; Rezgui et al., 2013). G₃₄ is often modified to Gm or Q which enables decoding of C- or U-ending codons (Morris et al., 1999). Interestingly, Eukaryotes are non-autotrophic for queuosine (Q) biosynthesis, in order to synthesize it animals need to obtain Q or its analogs from dietary sources of the gut microbiota. Q availability has been shown to correlate with translation fidelity and genome recoding (Zaborske et al., 2014). C₃₄ modifications are thought to strengthen G:C pairing therefore preventing misreading of AUG Met codons (El Yacoubi et al., 2012).

Modifications at position 37 and position 38 also influence anticodon stem loop dynamics. At position 37 modifications such as m²t⁶A (N2-methyl-N6-thereonylcarbamoyladenosine) or yW (wybutosine) generally improve intra-strand stacking interactions within the anticodon loop and improve codon-anticodon interactions (Tuorto et al., 2016). Regarding position 38, m⁵C₃₈ for example has been shown to contribute to tRNA stability and enable discrimination of near-cognate codons therefore affecting translational accuracy (Tuorto et al., 2015). Selected modifications occurring in the anticodon stem loop are depicted in Fig. 42.

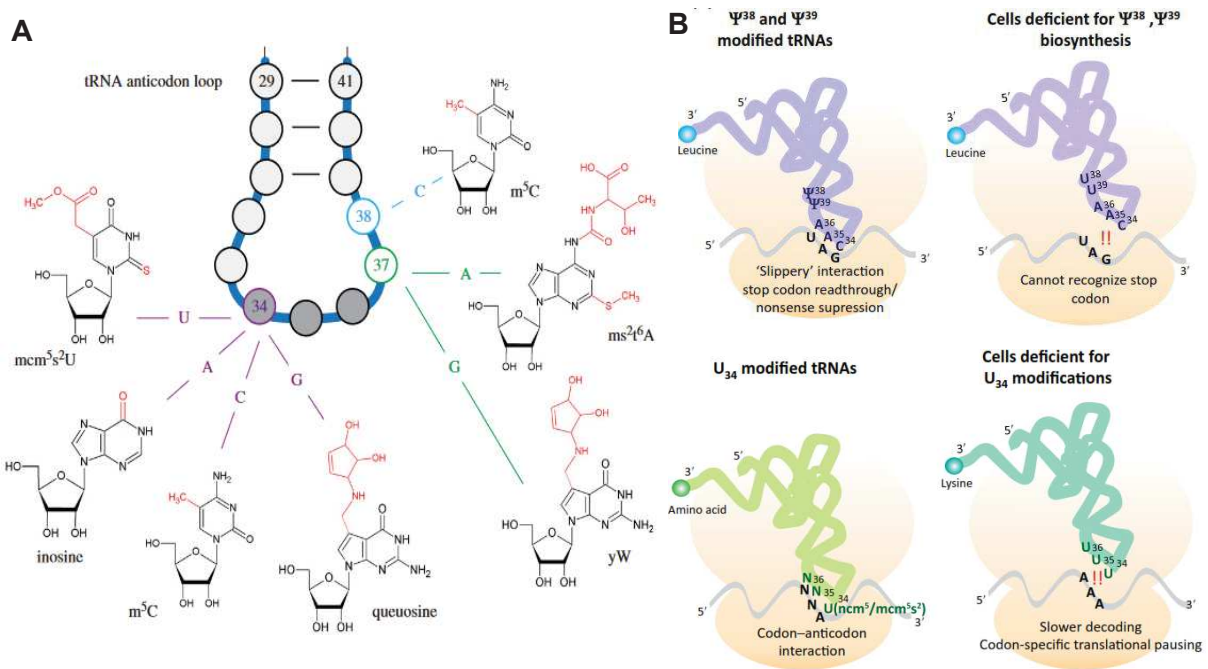


FIG. 42 MODIFICATIONS IN THE tRNA ANTICODON STEM LOOP IN EUKARYOTES

(A) Several modifications are shown for positions 34 (wobble), 37 & 38. Highlighted modifications in position 34 ensure correct decoding, modifications in positions 37 and 38 are mainly involved in translation fidelity and maintenance of the reading frame. From (Tuorto et al., 2016)

(B) Selected examples of tRNA modifications in positions of the anticodon 34, 38 and 39 of the anticodon stem loop and their physiological roles and effect upon deficiency. From (Kapur et al., 2018)

Abbreviations: $Mcm5s2U$: 5-methoxycarbonylmethyl-2-thiouridine, $m2t6A$ (N2-methyl-N6-thereonylcarbamoyladenosine), yW (wybutosine), m^5C (5-methylcytosine), 5-methoxycarbonylmethyl-2-thiouridine ($mcm5s^2U$), 5-carbamoylmethyluridine ($ncm5U$), pseudouridine (Ψ).

2.3.3.2 Modifications at the tRNA body or arms

Modifications occurring at the tRNA body or at multiple arms usually contribute to a functional folding of the molecule and its stability although they can also affect translation at different levels. Their absence can lead to the degradation of the tRNA molecule and deregulation tRNA pools. Moreover, modifications at the tRNA body or arms tend to influence other steps of tRNA maturation, including the formation of other modifications or the aminoacylation of the tRNA molecule (Lorenz et al., 2017). They can have an effect on the tRNA structure by affecting base-pairing interactions, hydrogen bonds and conformational rigidity (Vare et al., 2017). While some modifications can provide an increase in binding affinity and rigidity of the tRNA structure (ex: pseudouridines), others contribute to provide flexibility to the molecule (ex: dihydrouridines) (El Yacoubi et al., 2012).

Subsequently, some selected examples of modifications occurring in the tRNA body or arms are described: N²N²-dimethylguanosine (m₂²G) modification at G26 participates in preventing alternative structures of the tRNA anticodon stem loop (Sonawane et al., 2016)) and promotes translation efficiency being particularly important for oxidative stress resistance (Dewe et al., 2017) , 5-methylcytosine (m5C) promotes tRNA stability and protein synthesis. When absent m5C deficient cells show reduced protein synthesis which is proposed to occur by ribosome stalling and inhibition of translation by tRNA cleavage products (Tuorto et al., 2012). Another example of such modifications is 7-methylguanosine (m₇G) which is described in detail in section 2.6.2.

2.4 Transfer RNAs and the brain

The nervous system and particularly the brain seem to be particularly dependent on the correct functioning of different components involved in translation. Dysregulations of several translation components including ribosomal proteins (and proteins implicated in their synthesis and maturation), elongation factors or translation related processes such as aminoacylation by aaRs and tRNA processing have all been proven to lead to neurological diseases (Kapur et al., 2018; Kapur et al., 2017).

2.4.1 Sensitivity of the brain to translation defects

The fact that the brain is such a complex and functionally specialized organ is related with its need for a very high protein demand. However, there are two phases of its development that are particularly demanding in terms of protein content. The first one, comprises the processes of neurogenesis and differentiation that occur up to 3 years of age in humans. The second one, consists of the remodeling and refinement that take place in the human brain during adolescence (M.Lowe, 2017).

Neurons have different cellular compartments, which have different sets of proteins, this implies an extensive regulation of mRNA positioning in these compartments to supply them with the proteins they need (Turriano, 2011). Protein synthesis is critical for neuronal development, survival, and proper function. Neuronal proteins have a half-life of ~ 5.5 days *in vitro* (Cohen et al., 2013) and ~10 days *in vivo* (Fornasiero et al., 2018). When proteins in synapses and axonal growth cones are considered, the half-life of these group of proteins is lower than the average half-life of cellular proteins (Cohen et al., 2013; Deglincerti et al., 2015; Fornasiero et al., 2018), which suggests that these specialized structures require extensive protein renewal. Neuronal synaptic plasticity requires a very high level of protein synthesis as well. The establishment of synapses that participate for example in long-term memory has

been shown to require the synthesis of new RNAs and proteins (Sutton et al., 2006). Everything mentioned above implies that it is very important to maintain and modify the proteome in the axonal and dendritic synaptic compartments. The regulation of protein synthesis in these neuronal compartments has been seen to be carried out by localized translation, which is a ubiquitous component of both the pre- and post-synaptic compartments allowing a correct functioning of synaptic plasticity *in vivo* (See Fig.43) (Hafner et al., 2019). Local translation in neurons is thought to supply synaptic compartments the proteins they need without having to wait for their transport from the soma.

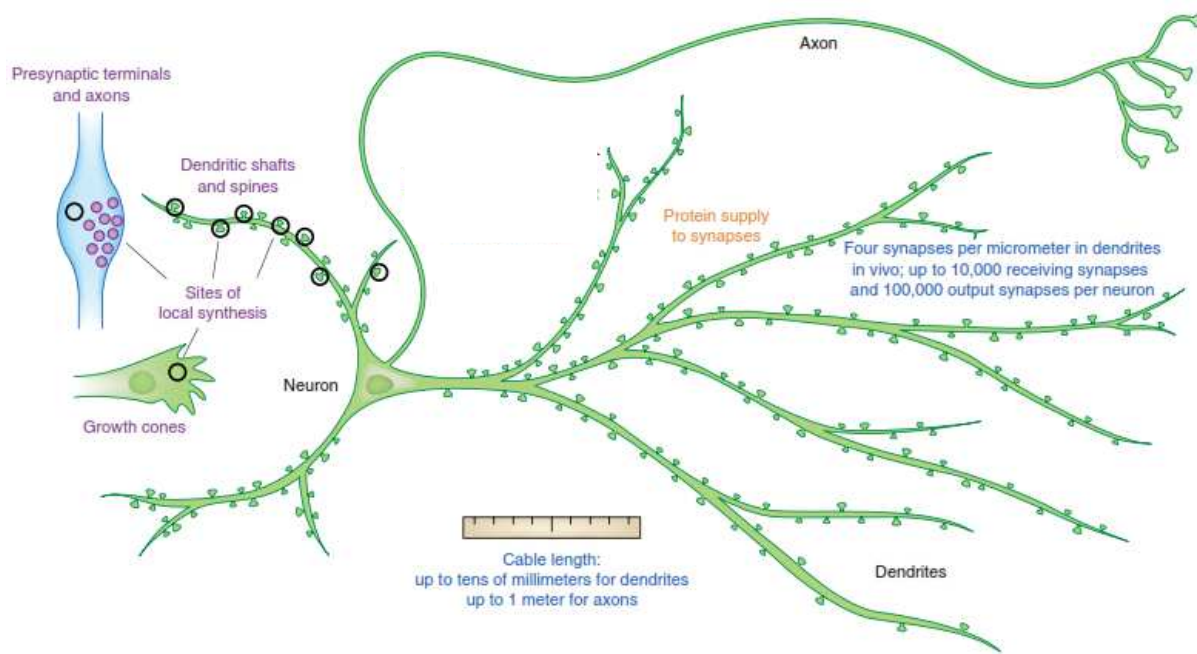


FIG. 43 LOCAL TRANSLATION IN NEURONS

Anatomy of a neuron, sites of local protein translation and neuronal functions dependent on local translation are shown. From (Holt et al., 2019)

As it has just been described, both the brain and neurons require an extensive protein synthesis. During the next lines I will describe briefly how translation machinery defects have shown to affect the brain.

2.4.1.1 Elongation factors

Elongation factors play a crucial role in translation primarily through their participation in ribosome decoding and frame maintenance. Some examples of elongation factors involved in neurological diseases are eEF1A and eEF2. Through exome sequencing, mutations in EEF1A2 associated with different neurodevelopmental syndromes characterized by epilepsy, ID and autism have been identified (de Ligt et al., 2012; Inui et al., 2016; Lam et al., 2016; Nakajima et al., 2015). EEF1A2 is a gene that codes for eEF1A, and whose expression is

restricted to muscle and neurons (S. Lee et al., 1993). Interestingly, the mutation in one of these patients was shown to interfere with translation fidelity: When introduced into yeast eEF1A it led to an increase in frameshift and nonsense suppression (Sandbaken et al., 1988). However, the implication of other mutations in translational fidelity remains still to be elucidated. eEF1A has also been implicated in different cell pathways, including the organization of the cytoskeleton and nuclear export (Mateyak et al., 2010), however, to this day, it is not yet known if these functions could also be affected in this type of disease. Another example of elongation factor which has also been linked to neurological diseases is eEF2. A mutation in the coding gene eEF2 was shown to cause autosomal dominant spinocerebellar ataxia (SCA26), a neurodegenerative disease (Hekman et al., 2012). This mutation is believed to interfere with ribosome translocation. Moreover, experiments in yeast with an eEF2 mutation recapitulating the one in human patients resulted in increased frameshifting. These studies highlight the essential roles of elongation factors for translation in general and how sensitive the brain is to its alterations.

2.4.1.2 Ribosomal proteins

Various genes encoding ribosomal proteins have been implicated in the pathogenesis of some neurodevelopmental disorders. Some examples are uS12 and uL16. uS12 is a small ribosomal protein, which stabilizes the conformation of the ribosome induced by codon recognition (Shao et al., 2016). In the case of uS12, *de novo* mutations have been described in *RPS23*, its coding gene. These mutations are associated to a syndrome characterized by microcephaly, hearing loss and ID (Paolini et al., 2017). In yeast it has been shown that the substitution of one of the patient mutations caused a reduction in translation fidelity and an increase in frameshifting (Paolini et al., 2017). Interestingly, an analysis of the polysomes in patients revealed an under-representation of mutated uS12 (R. S. Singleton et al., 2014; Loenarz et al., 2014). On the other hand, uL16 is a ribosomal protein located in the core of the large ribosomal subunit, encoded by the *RPL10* gene. Mutations in *RPL10* have been related to autism, ID and cerebellar hypoplasia (Brooks et al., 2014; Klauck et al., 2006; Thevenon et al., 2015; Zanni et al., 2015), some of the mutations have been shown to alter the fidelity of translation in yeast (Sulima et al., 2014). It is thought that the phenotype observed in patients may be due to translation problems, since some of the mutations described in patients have been shown to alter cellular polysomes, causing translation fidelity impairment in yeast (Sulima et al., 2014). These examples reveal how mutations in ribosomal proteins can lead to neurological diseases and affect translation and how even low levels of faulty ribosomes can cause pathological conditions.

2.4.2 Sensitivity of the brain to tRNA defects

As my PhD is focused on the study of tRNA modification enzymes during corticogenesis in the following paragraphs I will concentrate on relevant findings highlighting the role of tRNAs and tRNA modifications in the brain and the cerebral cortex.

Several evidences suggest a crucial biological relevance of tRNAs in the brain and suggest a high sensitivity of the human brain and the cerebral cortex to impairment in tRNAs and tRNA modifications. The human brain expresses high levels of tRNAs, compared to many other tissues. Dittmar and colleagues analysed tRNA levels in brain, liver, vulva, testis, ovary, thymus, lymph node, and spleen and showed that overall levels of nuclear tRNAs are higher in the brain compared to all tissues except spleen. Although levels of nuclear-encoded tRNAs were higher in spleen levels were quite similar to those in the brain. Compared for example to liver and vulva or testis and ovary the brain expresses one third and two thirds more tRNAs respectively. On the other hand, mitochondrial encoded tRNAs levels are higher in the brain than in any of the other tissues examined (Dittmar et al., 2006).

Interestingly, in the brain, changes in tRNA levels have been observed between different developmental stages, both embryonic and post-natal (Schmitt et al., 2014). Interestingly, in this study, Schmitt and colleagues showed that although the triplet codons within mRNA transcripts and thus aminoacid demand remain invariant across mouse development, up to 20% of tRNA genes are differentially expressed between developmental stages mainly due to changes in tRNA isodecoder expression (Schmitt et al., 2014). In accordance with these results, in a recent publication, Torres and colleagues showed tRNA expression differences at the isodecoder but not the isoacceptor level between HEK293T and human brain tissue (Torres et al., 2019).

No mutations in genes encoding cytoplasmic tRNAs have been reported to lead to any disease yet in humans. This might be explained by the fact that most of the variants have been detected in the exome (Protein coding region of the genome)(Choi et al., 2009) or by the fact that tRNAs are present in multiple copies in the genome. However, in mice a mutation in a CNS-specific isodecoder for tRNA Arg has been associated with neurodegeneration showing how hazardous the lack of a unique tRNA isodecoder can be in the brain. Interestingly, neurodegeneration only occurs in the context of mutated GTPBP2, a binding partner of the ribosome recycling protein Pelota (See Fig. 44) (Ishimura et al., 2014).

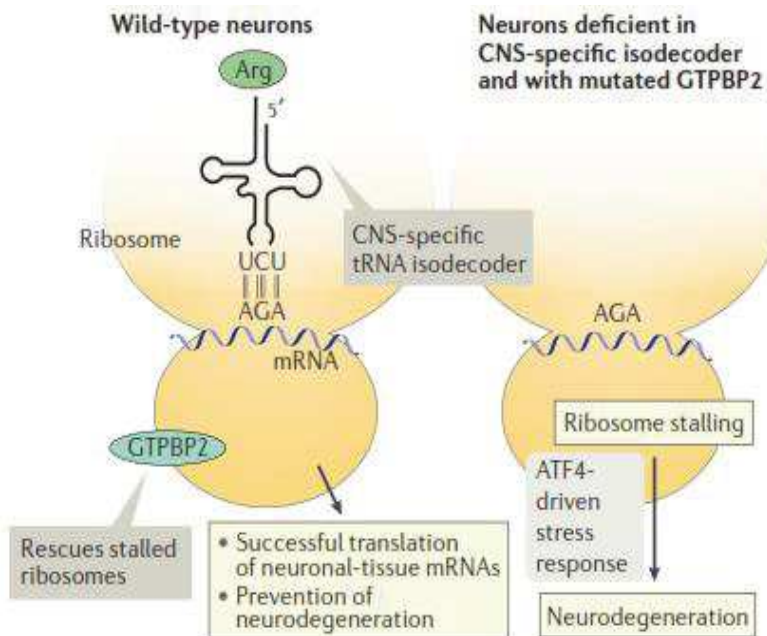


FIG. 44 EXAMPLE OF AN IMPORTANT tRNA IN THE CNS

tRNA Arg/UCU is specifically expressed in the CNS where it regulates neuronal homeostasis. When absent, ribosomes stall at AGA codons and the integrated stress response is activated through ATF4, leading to neuronal death and neurodegeneration. Ribosome stalling can be rescued by GTPBP2 (GTP-binding protein 2), which rescues translational pauses. From (Schimmel, 2017)

Mutations in genes involved in tRNA biogenesis, maturation, and function, have increasingly been associated to neurological disorders (Fig. 46), which are congenital in most of the cases (Schaffer et al., 2019). Among these diseases there is both neurodevelopmental and neurodegenerative conditions. Altogether, these evidences highlight the importance of translation fidelity in the nervous system (See Fig. 45).

Disorder	OMIM	Inheritance pattern	Gene(s)	Reference(s)
Mitochondrial tRNA gene mutations or deletions				
Kerns–Sayre síndrome	530000	Mi	Deletion of <i>MT-TL2</i> , <i>MT-TS2</i> , <i>MT-TH</i> , <i>MT-TR</i> , and/or <i>MT-TG</i>	PMID: 2895391
Leigh síndrome	256000	Mi	<i>MT-TV</i> , <i>MT-TK</i> , <i>MT-TW</i> , <i>MT-TL1</i> , <i>MT-TI</i> , <i>MT-TL2</i>	PMID: 15121771; 9266739; 27574709; 9222976
Mitochondrial complex I deficiency	252010	Mi	<i>MT-TL1</i> , <i>MT-TW</i> , <i>MT-TN</i>	PMID: 16908752; 21364701
Mitochondrial complex IV deficiency	220110	Mi	<i>MT-TS1</i> , <i>MT-TL1</i>	PMID: 16326995; 9832034
Mitochondrial DNA depletion syndrome 1 (MNGIE type)	603041	AR	<i>TYMP</i>	PMID: 12177387
Mitochondrial myopathy with diabetes	500002	Mi	<i>MT-TE</i>	PMID: 7726154
Mitochondrial myopathy, encephalopathy, lactic acidosis, and stroke-like episodes (MELAS)	540000	Mi	<i>MT-TL1</i> , <i>MT-TQ</i> , <i>MT-TH</i> , <i>MT-TK</i> , <i>MT-TC</i> , <i>MT-TS1</i> , <i>MT-TS2</i>	PMID: 11171912; 1549215; 14967777; 7669057; 8069654
Mitochondrial myopathy, infantile, transient (MMIT)	500009	Mi	<i>MT-TE</i>	PMID: 19720722
Mitochondrial myopathy, lethal, infantile (LIMM)	551000	Mi	<i>MT-TT</i>	PMID: 1645537
Myoclonic epilepsy with ragged red fibers (MERRF)	545000	Mi	<i>MT-TL1</i> , <i>MT-TK</i> , <i>MT-TH</i> , <i>MT-TS1</i> , <i>MT-TS2</i> , <i>MT-TF</i>	PMID: 19273760; 15184630; 14967777; 7669057; 2112427

Wolfram syndrome, mitochondrial form	598500	Mi	Deletion of <i>MT-L2</i> , <i>MT-TS2</i> , <i>MT-TH</i> , <i>MT-TR</i> , <i>MT-TG</i> , <i>MT-TK</i> , <i>MT-TD</i> , and/or <i>MT-TS1</i>	PMID: 8383698
tRNA biogenesis				
Cerebellofaciodental síndrome	616202	AR	<i>BRF1</i>	PMID: 25561519
Combined oxidative phosphorylation deficiency 17	615440	AR	<i>ELAC2</i>	PMID: 23849775
HSD10 mitochondrial disease	300438	XLD	<i>HSD17B10</i>	PMID: 11102558
Leukodystrophy, hypomyelinating, 7, with or without oligodontia and/or hypogonadotropic hypogonadism	607694	AR	<i>POLR3A</i>	PMID: 23355746; 21855841; 22036171
Leukodystrophy, hypomyelinating, 8, with or without oligodontia and/or hypogonadotropic hypogonadism	614381	AR	<i>POLR3B</i>	PMID: 23355746; 22036171; 22036172)
Leukodystrophy, Hypomyelinating, 11	616494	AR	<i>POLR1C</i>	PMID: 26151409
Pontocerebellar hypoplasia, type 10	615803	AR	<i>CLP1</i>	PMID: 26281201
Pontocerebellar hypoplasia, type 2B	612389	AR	<i>TSEN2</i>	PMID: 18711368
Pontocerebellar hypoplasia, type 2C	612390	AR	<i>TSEN34</i>	PMID: 18711368
Pontocerebellar hypoplasia, type 2F	617026	AR	<i>TSEN15</i>	PMID: 25558065 ; PMID: 27392077
Pontocerebellar hypoplasia, type 4 or 5	225753	AR	<i>TSEN54</i>	PMID: 21824568 ;
Brain Malformations With Or Without Urinary Tract Defects; Chromosome 1P32-P31 Deletion Syndrome	613735; 613735	AD	<i>NF1A</i>	PMID: 24462883; 27081522; 22030051
Spinocerebellar Ataxia 17 and Parkinson Disease, Late-Onset.	168600; 607136	AD	<i>TBP</i>	PMID: 10484774
Sideroblastic anemia with B cell immunodeficiency, periodic fevers, and developmental delay	616084	AR	<i>TRNT1</i>	PMID: 25193871
Autosomal Recessive Non-Syndromic Sensorineural Deafness Type Dfnb.	618257	AR	<i>BDP1</i>	PMID: 24312468
tRNA charging				
Cataracts, growth hormone deficiency, sensory neuropathy, sensorineural hearing loss, and skeletal dysplasia	616007	AR	<i>IARS2</i>	PMID: 25130867
Charcot–Marie–Tooth disease, axonal, type 2N	613287	AD	<i>AARS</i>	PMID: 22009580
Charcot–Marie–Tooth disease, axonal, type 2U	616280	AD	<i>MARS</i>	PMID: 23729695
Charcot–Marie–Tooth disease, axonal, type 2W	616625	AD	<i>HARS</i>	PMID: 22930593
Charcot–Marie–Tooth disease, dominant intermediate C	608323	AD	<i>YARS</i>	PMID: 16429158
Charcot–Marie–Tooth disease, recessive intermediate, B	613641	AR	<i>KARS</i>	PMID: 20920668
Charcot–Marie–Tooth disease, type 2D	601472	AD	<i>GARS</i>	PMID: 8872480
Combined oxidative phosphorylation deficiency 12	614924	AR	<i>EARS2</i>	PMID: 22492562
Combined oxidative phosphorylation deficiency 14	614946	AR	<i>FARS2</i>	PMID: 22499341
Combined oxidative phosphorylation deficiency 15	614947	AR	<i>MTFMT</i>	PMID: 21907147
Combined oxidative phosphorylation deficiency 20	615917	AR	<i>VARS2</i>	PMID: 25058219
Combined oxidative phosphorylation deficiency 21	615918	AR	<i>TARS2</i>	PMID: 24827421
Combined oxidative phosphorylation deficiency 24	616239	AR	<i>NARS2</i>	PMID: 25629079
Combined oxidative phosphorylation deficiency 25	616430	AR	<i>MARS2</i>	PMID: 25754315
Combined oxidative phosphorylation deficiency 8	614096	AR	<i>AARS2</i>	PMID: 21549344
Epileptic encephalopathy, early infantile, 29	616339	AR	<i>AARS</i>	PMID: 25817015

Growth retardation, intellectual developmental disorder, hypotonia, and hepatopathy	617093	AR	<i>IARS</i>	PMID: 27426735
Hydrops, lactic acidosis, and sideroblastic anemia	617021	AR	<i>LARS2</i>	PMID: 26537577
Hyperuricemia, pulmonary hypertension, renal failure, and alkalosis	613845	AR	<i>SARS2</i>	PMID: 21255763
Hypomyelination with brain stem and spinal cord involvement and leg spasticity	615281	AR	<i>DARS</i>	PMID: 23643384
Infantile-onset multisystem neurologic, endocrine, and pancreatic disease	616263	AR	<i>PTRH2</i>	PMID: 25574476
Leukodystrophy, hypomyelinating, 17	618006	AR	<i>AIMP2</i>	PMID: 21092922; PMID: 24958424
Leukodystrophy, hypomyelinating, 3	260600	AR	<i>AIMP1</i>	PMID: 29215095
Leukodystrophy, hypomyelinating, 9	616140	AR	<i>RARS</i>	PMID: 24777941; PMID: 28905880
Leukoencephalopathy with brain stem and spinal cord involvement and lactate elevation	611105	AR	<i>DARS2</i>	PMID: 17384640
Leukoencephalopathy, progressive, with ovarian failure	615889	AR	<i>AARS2</i>	PMID: 24808023
Microcephaly, progressive, seizures, and cerebral and cerebellar atrophy	615760	AR	<i>QARS</i>	PMID: 20169446; PMID: 26000875
Neurodevelopmental disorder with brain, liver, and lung abnormalities	618007	AR	<i>FARSB</i>	PMID: 29573043
Neurodevelopmental disorder with microcephaly, ataxia, and seizures	617709	AR	<i>SARS</i>	PMID: 28236339
Leukodystrophy, Hypomyelinating, 15	617951	AR	<i>EPRS</i>	PMID: 29576217
Neurodevelopmental disorder with microcephaly, seizures, and cortical atrophy	617802	AR	<i>VARS</i>	PMID: 26539891
Neurodevelopmental disorder, mitochondrial, with abnormal movements and lactic acidosis, with or without seizures	617710	AR	<i>WARS2</i>	PMID: 28236339
Neuropathy, distal hereditary motor, type VA	600794	AD	<i>GARS</i>	PMID: 12690580
Pontocerebellar hypoplasia, type 6	611523	AR	<i>RARS2</i>	PMID: 17847012
Spastic ataxia 3	611390	AR	<i>MARS2</i>	PMID: 22448145
Spastic paraplegia 77	617046	AR	<i>FARS2</i>	PMID: 25851414
Autosomal-recessive intellectual disability and parkinsonism	None	AR	<i>PTRHD1 E</i>	PMID: 27753167; 27134041
Usher syndrome type 3B	614504	AR	<i>HARS</i>	PMID: 22279524
Pontocerebellar Hypoplasia, Type 2D and Pontocerebellar Hypoplasia, Type 2E.	613811	AR	<i>SEPSECs</i>	PMID: 20920667
tRNA modification				
Mental retardation, autosomal recessive 5	611091	AR	<i>NSUN2</i>	PMID: 15162322; 29631977
Myopathy, lactic acidosis, and sideroblastic anemia 1	600462	AR	<i>PUS1</i>	PMID: 28832011; 17056637
Combined oxidative phosphorylation deficiency 26	616539	AR	<i>TRMT5</i>	PMID: 27055666
Combined oxidative phosphorylation deficiency 35	617873	AR	<i>TRIT1</i>	PMID: 24901367
Combined oxidative phosphorylation deficiency 23	616198	AR	<i>GTPBP3</i>	PMID: 27426735
Mental retardation, autosomal recessive 55	617051	AR	<i>PUS3</i>	PMID: 27055666 +
Galloway–Mowat syndrome 3	617729	AR	<i>OSGEP</i>	PMID: 28805828; 28272532
Combined oxidative phosphorylation deficiency 10	614702	AR	<i>MTO1</i>	PMID: 22608499
Mental retardation, autosomal recessive 36	615286	AR	<i>ADAT3</i>	PMID: 23620220; 26842963
Galloway-Mowat syndrome 4 (GAMOS4)	617730	AR	<i>TP53RK</i>	PMID: 28805828
Galloway-Mowat Syndrome 5 and Galloway-Mowat Syndrome.	617731	AR	<i>TPRKB</i>	PMID: 28805828

Galloway-Mowat Syndrome 5 and Galloway-Mowat Syndrome.	617731	AR	LAGE3	PMID:28805828
Mental retardation, X-linked 44 (MRX44)	309549	XLR	FTSJ1	PMID:26310293; PMID: 32558197
Microcephaly, Growth deficiency, Seizures and brain malformations	618346	AR	WDR4	PMID:29983320 ; 26416026
Microcephaly, Short Stature, And Impaired Glucose Metabolism 1 /	616033	AR	TRMT10A	PMID:24204302 ; 25053765 ; 26526202; 26535115
Galloway-Mowat syndrome	None	AR	YRDC	PMID: 31481669
Galloway-Mowat syndrome	None	AR	GON7	PMID: 31481669
Intellectual developmental disorder with abnormal behavior, microcephaly, and short stature	618342	AR	PUS7	PMID: 30526862
Neuropathy, hereditary sensory and autonomic, Type III; HSAN3	223900	AR	ELP1	PMID: 29290691
Galloway-Mowat syndrome 3	617729	AR	KAE1	PMID: 28272532

FIG. 45 NEUROLOGICAL DISORDERS AND tRNA-ASSOCIATED GENES GROUPED BY CATEGORY

tRNA associated to neurological disorders can be separated into 4 main groups: mt-tRNA gene deletion or mutations, tRNA biogenesis, tRNA charging and tRNA modification. The disorder or phenotypes, OMIM number, type of inheritance, gene name and reference. Abbreviations: AD (autosomal dominant); AR (autosomal recessive); Mi (mitochondrial); XLR (X-linked recessive); XLD (X-linked dominant). Adapted from (Schaffer et al., 2019).

2.4.2.1 Transfer-RNA associated neurodevelopmental disorders

As seen above (Fig. 45), there is a clear enrichment in neurologic (79%) and especially neurodevelopmental disorders (90%) when variants in genes involved in tRNA biogenesis, maturation or function are considered (See Fig. 46).

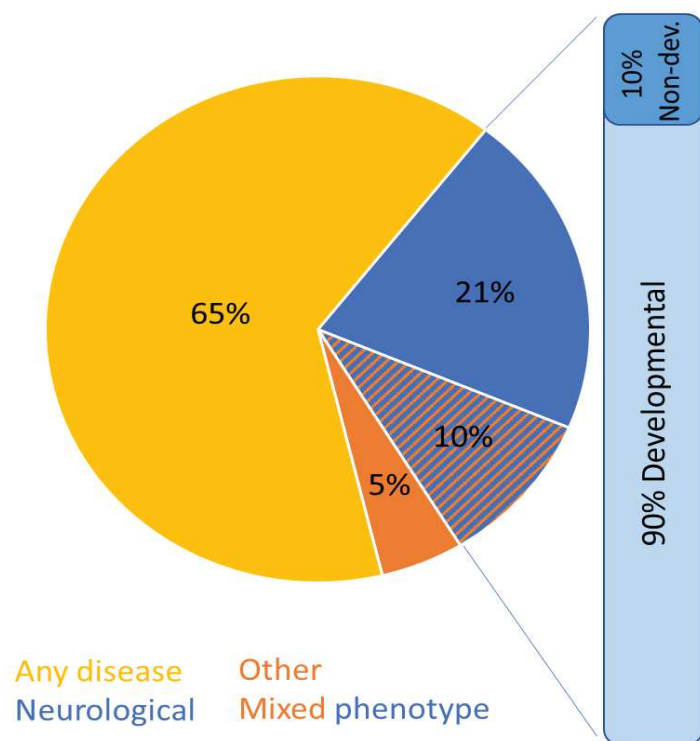


FIG. 46 BIBLIOGRAPHIC ANALYSIS OF DISEASE-ASSOCIATED VARIANTS WITHIN tRNA RELATED GENES

A bibliographic analysis carried out in our lab of variants in 179 genes involved in tRNAs biogenesis, maturation or function reveals a statistical enrichment in neurologic (blue) and in particular in neurodevelopmental disorders (light blue) over other disorders (orange).

Neurodevelopmental disorders, such as intellectual disabilities (IDs), autism and epilepsy, are diseases associated primarily with defects in the functioning of the brain, which affect between 3-8% of children in Europe (Weiss et al., 2000). Affected children undergo difficulties with many neurological functions such as memory, learning and behaviour. In the past years a tremendous progress has been achieved in unraveling the genetics of this common group of diseases. Among the neurodevelopmental disorders/phenotypes most enriched in our analysis (Fig. 46) we found: ID (44%), malformation of cortical development (MCD) (26%), and pontocerebellar hypoplasia (PCH) (18%) (a heterogenous group of disorders with prenatal onset and characterized by microcephaly, seizures, cerebellar hypoplasia and developmental impairment).

Altogether, these findings raise the hypothesis about the existence of tRNA regulatory pathways in the developing brain, including the cerebral cortex. The following sections summarize the role of tRNAs, their biogenesis and processing, as well as their modifications in several neurodevelopmental disorders.

2.4.2.2 tRNA synthesis and splicing

RNA editing and alternative splicing is overall higher in the brain than in other organs and tissues (Norris et al., 2012). As it was previously described, tRNA introns are removed by two independent machineries: First, the CLP1/TSEN complex and second, the tRNA-ligase complex. The CLP1/TSEN complex is composed of five subunits in metazoans, TSEN2, TSEN15, TSEN34 and TSEN54, and the RNA kinase CLP1 (Ramirez et al., 2008; Weitzer et al., 2007). In the last years, numerous point mutations have been identified both in the TSEN subunits and in CLP1 in patient suffering of neurological diseases such as Pontocerebellar Hypoplasia (Battini et al., 2014; Karaca et al., 2014; Schaffer et al., 2014). The efficiency of tRNA splicing due to the CLP1/TSEN complex was shown to be clearly decreased in these patients. Microcephaly in patients with CLP1 or TSEN mutations arises prenatally and worsens over time, which suggests a developmental origin of the phenotype.

Interestingly, defects in the tRNA splicing machinery have been exclusively linked to neurological disorders, however, it remains still to be elucidated why the brain and the nervous system are particularly sensitive to tRNA splicing machinery alterations. Although a lot of progress has been done in understanding the mechanisms of tRNA splicing, still nowadays, there are some topics that remain controversial. Among them we find the cellular physiology of tRNA splicing defects. On one hand, several publications report no alteration of mature tRNA or pre-tRNA pools upon alteration of TSEN or CLIP function: For example, in a cellular context loss of CLP1 function in patient fibroblasts, Karaca and colleagues showed that mature tRNA

levels remain unaltered and pre-tRNAs do not accumulate (Karaca et al., 2014). On the other hand, other studies have shown an alteration of tRNA levels or pre-tRNA pools upon alteration of TSEN or CLP1 function: For example, Schaffer and colleagues reported a decrease in mature tRNA and an accumulation of pre-tRNAs in CLP1 deficient neurons (Schaffer et al., 2014). However, it remains still unclear whether these discrepancies are due to the cell type.

2.4.2.3 tRNA aminoacylation

Human aaRS are particularly involved in diseases of the nervous system. In particular, they have been reported to be implicated Charcot-Marie Tooth disease (neuropathy in which there is a progressive deterioration of distal sensory and motor neurons), leukoencephalopathies (heterogeneous group of disorders characterized by white matter loss), severe early-onset brain disorders and fatal infantile syndromes (Ognjenovic et al., 2018).

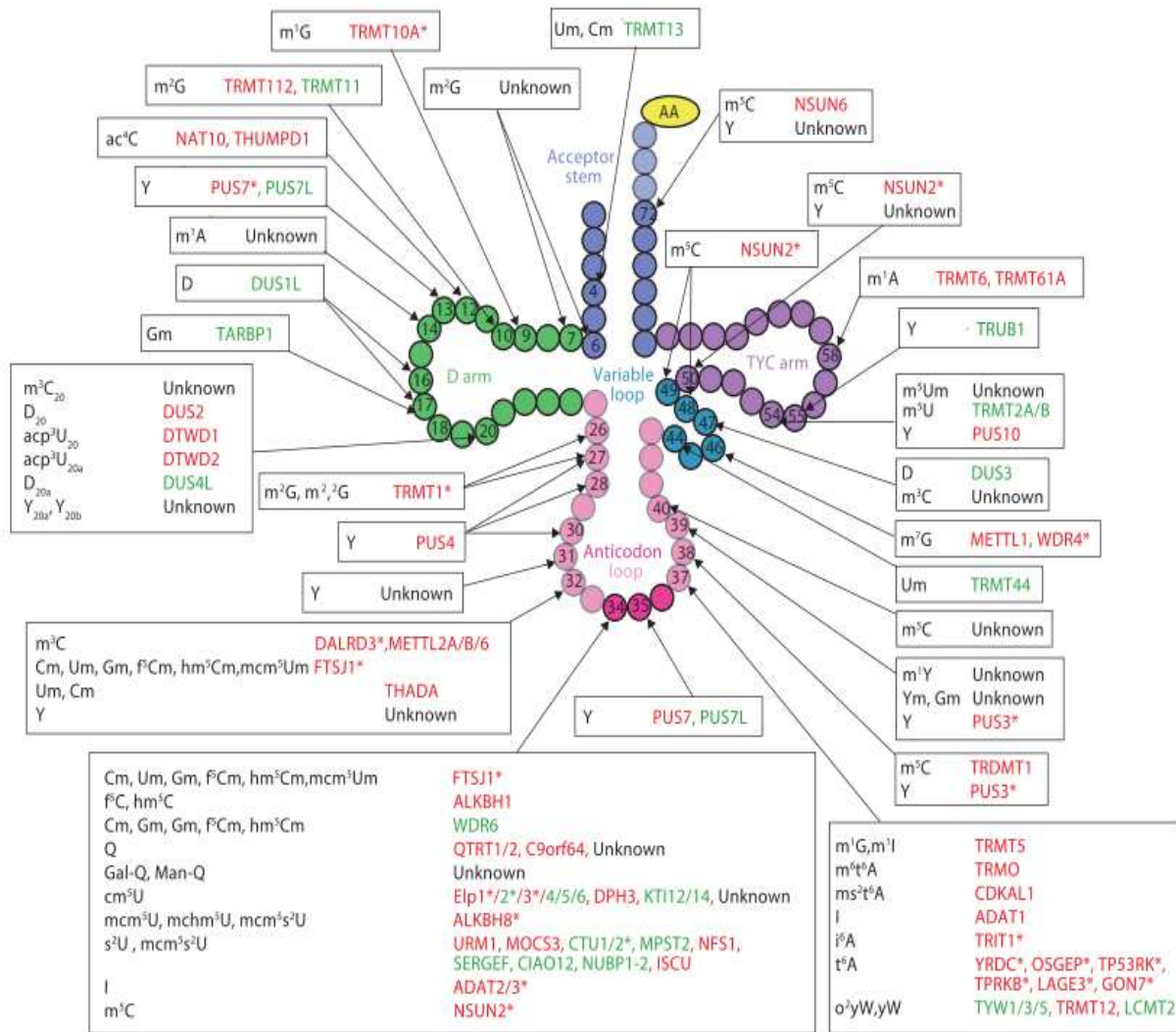
Some examples of human aaRS implicated in neurological diseases are QARS and RARS, glutamine and arginine aaRS respectively. Mutations in either QARS or RARS were shown to lead to early-onset epileptic encephalopathy in patients (Kodera et al., 2015; Nishri et al., 2016), a group of diseases characterized by seizures and developmental delay. In both cases patients exhibited seizures, microcephaly, cerebral atrophy and developmental delay as the major phenotypes.

2.4.2.4 tRNA modifications

Dysregulations of tRNA modifications and tRNA modifying enzymes all over tRNA molecules as well as other proteins involved in their processing and maturation have been increasingly linked to several diseases, mainly neurological disorders, cancer and mitochondrial-linked disorders (Pereira et al., 2018).

Genetic analyses of various neurodevelopmental disorders have identified mutations in genes coding for tRNA modifying enzymes, including ADAT3 (Alazami et al., 2013), (El-Hattab et al., 2016), WDR4 (Shaheen et al., 2015), DALRD3 (Lentini et al., 2020), PUS1 (Bykhovskaya et al., 2004), TRMT5 (Powell et al., 2015), TRIT1 (Yarham et al., 2014), GTBP3 (Kopajtich et al., 2016), OSGEP (Braun et al., 2017; Edvardson et al., 2017), YRDC (Arrondel et al., 2019), GON7 (Arrondel et al., 2019), TP53RK (Braun et al., 2017; Hyun et al., 2018), TPRKB (Braun et al., 2017), MTO1 (Ghezzi et al., 2012), PUS3 (Shaheen et al., 2016), NSUN2 (Fahiminiya et al., 2014), TRMT10A (Igoillo-Esteve et al., 2013), FTSJ1 (Freude et al., 2004; Takano et al., 2008; J. Li et al., 2020), TRMT1 (K. Zhang et al., 2020), PUS7 (de Brouwer et al., 2018), ELP1 (Rubin et al., 2017), and KAE1 (Edvardson et al., 2017). The respective tRNA modifications catalyzed by each of these enzymes is shown in Fig 47. Besides ID, patients with those mutations show further symptoms of neurological abnormalities such as microcephaly (a small

brain volume), suggesting that these highly evolutionary conserved enzymes play an important role in regulating neurodevelopment. In terms of their location within tRNA molecules, most of the tRNA modifications associated to neurological and neurodevelopmental disorders are located within the anticodon stem loop or at junctions affecting the tRNA structure. Interestingly, as shown in Fig.45, all the variants in tRNA modifying enzymes associated to neurodevelopmental disorders are recessive which suggests that reduction of their protein levels or function might be critical for the brain.



To date, the mechanisms by which lack of tRNA modifications leads to human disease and particularly neurodevelopmental disorders is not understood. In addition to the publications reporting variants in tRNA modification enzymes and their association to neurodevelopmental diseases, several publications have provided a causal link between tRNA modification alteration and malformation of brain development (Arrondel et al., 2019; Blanco et al., 2014; Braun et al., 2017; de Brouwer et al., 2018; Flores et al., 2017; Laguesse et al., 2015; J. Ramos et al., 2019). In the following lines details will be provided for two of them. The first one was previously mentioned in the neurogenesis section, where the authors showed that the loss of the anticodon wobble uridine (U_{34}) modification (cm^5U) in a subset of tRNAs leads to elevated UPR signaling levels, which are responsible for a decrease of indirect neurogenesis rate. Specifically, authors showed that elevated UPR signaling favors direct neurogenesis at the expense of indirect neurogenesis and leads, in mice, to premature neuron generation and microcephaly (Laguesse et al., 2015). Regarding U_{34} modification, Laguesse and coworkers and Nedialkova and Leidel showed that loss of U_{34} modifications results in increased ribosome pausing in mouse forebrain tissue and *C. Elegans* and *S. Cerevisiae* respectively (Laguesse et al., 2015; Nedialkova et al., 2015). Furthermore, U_{34} deficient cells show proteotoxic stress and protein aggregates. Interestingly, overexpression of hypomodified tRNAs was able to alleviate ribosome pausing and restore protein homeostasis (Nedialkova et al., 2015). Another publication on this topic is from Flores and colleagues, who showed that loss of cytosine-5 tRNA methylation mediated by NSUN2 in mice resulted in an impairment of neural differentiation (increase of IPs and a decrease of upper layer neurons) and microcephaly in mouse cortices. Moreover, the authors showed that loss of NSUN2-mediated methylation increased the cleavage of tRNAs by angiogenin leading to an accumulation of 5' tRNA fragments in the brain and induction of stress pathways (Flores et al., 2017).

Among all of the tRNA modifiers linked to neurodevelopmental conditions, two particularly interesting genes are *ADAT3* and *WDR4*, which are part of two heterodimers that I studied during my thesis, the ADAT3-ADAT2 and WDR4-METTL1 heterodimers respectively.

2.5 The ADAT3-ADAT2 complex

ADAT3 and ADAT2 stand for Adenosine Deaminase tRNA-specific 3 and Adenosine Deaminase tRNA-specific 2 respectively and are the homologs of tadA in bacteria and tad3 and tad2 in yeast. ADAT3 and ADAT2 form a heterodimeric complex (ADAT) that catalyzes the formation of Inosine 34 (I_{34}) of all mature tRNAs with the anticodon starting with A (tRNA ANN) at the wobble position of tRNAs (A. P. Gerber et al., 1999). TadA underwent a gene duplication process and divergence process in eukaryotes giving rise to eukaryotic ADAT

which has a broader substrate range (Grosjean et al., 2010). Torres and colleagues showed that ADAT3 and ADAT2 colocalize in the nucleus of human cells in an ADAT2 dependent manner and incorporate I₃₄ to human tRNAs at the precursor tRNA level as well as during maturation, however, ADAT3 and ADAT2 have also been found in the cytoplasm (Torres et al., 2015).

2.5.1 Domains and structural insights

Both human ADAT3 and ADAT2 bear CMP/dCMP-type deaminase domains and are highly conserved to mouse proteins (See Fig.48). Interestingly, eukaryotic ADAT2 and ADAT3 bear homology regions to tadA (prokaryotic enzyme) located in the N-terminal two-thirds in the case of ADAT2 and the C-terminal half in the case of ADAT3 (Spears et al., 2011). Although both members of the heterodimer bear deaminase domains and ADAT3 is needed for the deamination reaction to occur, ADAT3 was for long considered the non-catalytic subunit of the complex, since a critical glutamate in the active site of ADAT3 was mutated during evolution but kept in the deaminase domain of ADAT2 (See Fig.48) (Rubio et al., 2007). Spears and colleagues however reported that the ADAT2/3 complex in *Trypanosoma Brucei* (TbADAT2/3) bears two Zn²⁺ per heterodimer and that a mutation in one of the key cysteines coordinating Zn²⁺ yielded a heterodimer with a single-bound Zn²⁺ which was functional suggesting a role of ADAT3 in catalysis via the coordination of the catalytic Zn²⁺ (Spears et al., 2011). Due to their similarities with other members of the cytidine deaminase superfamily, it was suggested that ADAT2 and ADAT3 use similar metal coordinating motifs, HXE and PCXXC in ADAT2 and HXV and PCXXC in ADAT3 (where X represents any aminoacid)(A. P. Gerber et al., 1999). Histidine and cysteine residues are conserved across evolution in both subunits and are thought to coordinate the zinc ion, an activated water molecule is also required for the reaction to occur. On the other hand, the glutamate residue in ADAT2 (which is not conserved in ADAT3) is proposed to act as a proton shuttle between the activated water molecule and the exocyclic nitrogen atom at C-6 of the purine ring. (Spears et al., 2011).

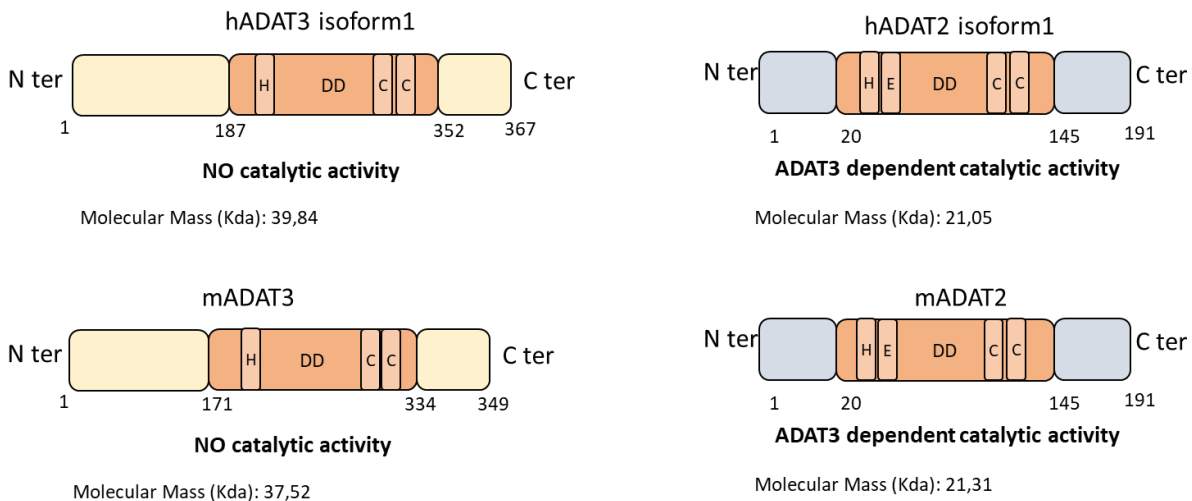


FIG. 48 DOMAINS FOR HUMAN AND MICE ADAT2/3

Both members of the heterodimer bear CMP/dCMP-type deaminase domains (depicted with DD), but ADAT3 is bigger in size, particularly due to its N-terminal domain. Both subunits are highly conserved between human and mice. The deaminase domain contains several putative Zn²⁺ chelating residues: one histidine (H), two cysteines (C) and one glutamate (E) which are predicted to participate in proton shuttling and catalysis. Although the other chelating residues (histidine and cysteines) are present in ADAT3, the glutamate residue is not present in ADAT3.

Interestingly, mutations in the active domain of ADAT2 do not impair its binding to ADAT3, since catalytically inactive ADAT2 still interacts with ADAT3 (Rubio et al., 2007). ADAT3 has been reported to be insoluble and to become soluble when in complex with ADAT2 (Rubio et al., 2007). In lines with these results, Ramos and colleagues, showed that ADAT2 is able to prevent self-association of ADAT3 suggesting that stoichiometric levels of ADAT2 and ADAT3 are important to promote proper ADAT3 folding. In particular, the authors showed that ADAT2 co-expression prevents association of ADAT3 to HSP60 the TCP1 and CCT7 subunits of the TriC complex (all members of the chaperonin protein family), which suggests that ADAT2 association is required for prevent misfolding of ADAT3 and subsequent targeting by chaperonin complexes (J. Ramos et al., 2019).

Despite I₃₄ biosynthesis is not affected by the presence of other modifications such as pseudouridine 32 or 1-methyl-guanosine 37 in the anticodon loop, the efficacy of the reaction depends on the sequence of the anticodon loop and its proximal stem, being tRNAs with a purine at position 35 the best substrates (Auxilien et al., 1996). A conserved FFxxxR motif, which is unique to tadA, is critical for tRNA recognition in prokaryotes (Y. Elias et al., 2005). Nevertheless, tadA and eukaryotic ADAT2/3 have been shown to have different tRNA substrate requirements: whereas for tadA the stem-loop RNA corresponding to the anticodon

region of tRNA is a substrate, biochemical studies suggest that for eukaryotic ADAT2/3 global features of tRNA molecules must be the factors determining substrate recognition since for the reaction to occur the full length tRNA is required (Y. Elias et al., 2005; A. P. Gerber et al., 1999). The regions of ADAT2/3 that are not homologous to tadA are hypothesized to participate in further interactions with tRNAs. Important insights into the binding of ADAT to tRNAs comes from the work in *Trypanosoma Brucei*, Ragone and colleagues showed that a "KRKRK" string at the C-terminus of TbADAT2 was crucial for tRNA binding (Ragone et al., 2011). Recently, Roura-Frigole and coworkers showed that tRNA recognition by human ADAT2/ADAT3 varies between substrates and does not rely on conserved identity elements, but on overall structural features of tRNA molecules. They checked for example binding to tRNA-Arg-ACG and tRNA-Ala-AGC and showed that recognition of the tRNA-Arg was dependent on interactions with the anticodon loop while recognition of tRNA-Ala was dependent on additional regions in the molecule. Importantly, they also reported that the complex can be inhibited by tRNA fragments *in vitro*. In particular, they proved that deamination of tRNA-Arg-ACG and tRNA-Ala-AGC could be inhibited by natural occurring tRNA fragments derived from tRNAs tRNA-Ala-AGC and tRNA-Cys-GCA (Roura Frigole et al., 2019).

2.5.2 Inosine 34 transfer RNA modification

I_{34} was the first modification to be identified in the anticodon tRNAs, it is formed by hydrolytic deamination of the C6 in A_{34} base (See Fig. 49A).

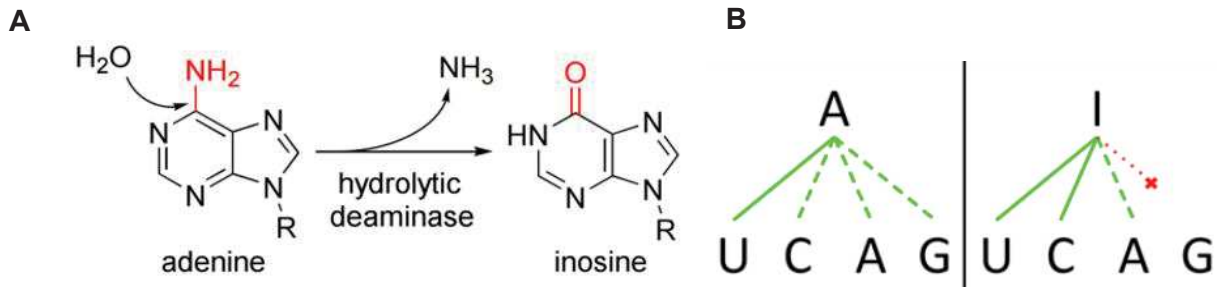


FIG. 49 INOSINE 34 tRNA MODIFICATION

(A) I_{34} is formed by a hydrolytic deamination catalysed by ADAT2/3. (B) Schematic representation adenosine and inosine pairing with other bases. Green lines indicate preferred pairings, green dashed lines poor pairings and Dashed red lines no pairing. From (Rafels-Ybern et al., 2015)

The number of tRNAs presenting I_{34} is different between prokaryotes and eukaryotes, while in prokaryotes only tRNA ArgACG can be modified, in eukaryotes between 7 (yeast) to 8 (human) different tRNAs contain I_{34} . The following cytosolic tRNAs have been detected to have I_{34} in higher eukaryotes: AlaAGC, ArgACG, IleAAT, ProAGG, SerAGA, ThrAGT, Val AAC

(Boccaletto et al., 2018). TadA underwent a gene duplication process in eukaryotes giving rise to ADAT2/3, which has a broader substrate range recognition to include all A₃₄ tRNAs in 3, 4 and 6 box codon sets, with the unique exception of tRNA-Gly, which is absent in eukaryotic genomes (Grosjean et al., 2010). This event changed the tRNA gene content and codon usage bias of eukaryotic genomes towards an enrichment in A₃₄ containing tRNAs and the loss of their synonymous G₃₄ containing tRNA isoacceptors (Novoa et al., 2012). Interestingly, Saint Léger and colleagues revealed that tRNA-Gly-ACC is a poor substrate of the ADAT2/3 complex being this probably one of the main reasons why is absent in eukaryotic genomes (Saint-Leger et al., 2016).

Inosine is a molecular analog of guanosine which has a pairing ability with A, C and U (See Fig. 49B) (Murphy et al., 2004). This fact confers a single tRNA isoacceptor presenting I₃₄ the ability to recognize up to three synonymous codons with a different base in the third position. I₃₄ therefore confers to tRNAs a greater decoding capacity and allows the translation of synonymous C or A-ending codons in organisms otherwise would not be able to decode them (due to the lack of a cognate tRNA isoacceptor containing G₃₄ or U₃₄) (Grosjean et al., 2010). Among the base pairings that I₃₄ can establish, there exists differences in terms of their stability, being cytosine and adenosine the most and least favored respectively (I: C > I: U > I: A) (Devi et al., 2018; Lim et al., 2001). The lower affinity of I₃₄ for adenosine is proposed to be one of the triggers that has influenced the codon usage of living organisms towards a lower presence of codons ending in this base (Quax et al., 2015). I₃₄ is found in almost all adenosines in the wobble position in both bacterial and eukaryotic tRNAs (Andachi et al., 1987; Sibler et al., 1986), this could be due to the greater pairing capacity of I₃₄ with respect to A₃₄ or to a possible deleterious effect of A₃₄ on translation, since translocation of A₃₄ tRNAs in the ribosome can disturb tRNA binding to the ribosomal A-site and have a negative effect on translation efficiency (Lim, 1995).

Bioinformatic studies have shown that the codons that can be decoded by I₃₄ are favored over those that cannot match I₃₄ (G-ending codons) in eukaryotes (Rafels-Ybern et al., 2015) (Rafels-Ybern et al., 2018), and that codons that can be decoded by I₃₄ are very abundant in genes with high expression levels in eukaryotes. Taken together, the knowledge available up to date about I₃₄ suggests that alterations of its levels within tRNAs may have important negative consequences at the level of various cellular proteins in eukaryotes.

2.5.3 Biological relevance

Although I₃₄ is absent in archaea, both ADAT3 and ADAT2 are essential genes for prokaryotes and eukaryotes, which shows the importance of this modification for living organisms. The

reduction in I₃₄ levels can be tolerated to some extent by yeast, plant, and human cells (Torres et al., 2015; Tsutsumi et al., 2007; Zhou et al., 2014): 1) Deletion of Tad2 or Tad3, the yeast homologues of ADAT2 and ADAT3, leads to lethality (A. P. Gerber et al., 1999); 2) Knockdown of Tad2 or Tad3 in plant induces growth retardation (Zhou et al., 2014); 4) Both ADAT2 and ADAT3 are essential genes in human cell lines, although those cells can tolerate to some extend the reduction in I₃₄ levels (~80% reduction in ADAT2 levels) (Torres et al., 2014).

In addition to its action catalyzing the formation of I₃₄, other functions of ADAT2/3 have been reported in other organisms: In *trypanosoma brucei*, in addition to catalyzing the formation of I₃₄ in tRNAs, ADAT2/3 can catalyze C to U deamination in some tRNAs in addition to single-stranded DNA *in vivo* but not *in vitro*. Interestingly, single-stranded DNA deamination cannot be performed by ADAT2 alone (Rubio et al., 2007). In bacteria, TadA was reported to be able to edit the coding region of some mRNAs (Rubio et al., 2017). Nonetheless, these functions have not been reported yet in higher eukaryotes. Rubio and colleagues also showed that ADAT2/3 interacts with TRM140 in *trypanosome brucei*, a protein which is able to keep the mutagenic activity of the ADAT2/3 complex in check. In addition, the authors showed that C₃₂ of Thr tRNA is methylated to m³C₃₂ to allow C to U deamination in a reaction catalysed by ADAT2/3 and TRM140 (Rubio et al., 2017).

Although the cellular roles of I₃₄ modified tRNAs are poorly understood and ADAT2/3 role in the brain has not been described so far several findings illustrate the biological importance of I₃₄ modification: 1) Reduction of I₃₄ levels in yeast reduces the aminoacylation efficiency on tRNA-Ile (Aminoacylation rate was decreased by 410 folds when tRNA-Ile-AAU was used instead of tRNA-Ile-IAU) (B. Senger et al., 1997); 2) Mutation in the deaminase domain of Tad3 (which destabilizes the Tad2/3 complex) in yeast induces cell cycle arrest in G1/S and G2/M phases and increased sensitivity to cycloheximide (translation inhibitor) (Tsutsumi et al., 2007), suggesting an important role for I₃₄ tRNA modification in cell cycle progression; 3) Knock-down of *adat2* in *Neurospora crassa* was shown to severely impair I₃₄ modification levels in ADAT-related tRNAs resulting in major profile changes and reprogramming of translation kinetics on ADAT-codons as well as causing ribosome pausing on mRNAs and proteome landscape changes (Lyu et al., 2020). Interestingly, CPC-1, the homolog of yeast bZIP transcription factor GCN4 was shown to mediate the transcriptional response upon *adat2* silencing and aminoacid starvation; 4) Comparison of expression of ADAT2 mRNA transcript showed a higher expression in self-renewing ESCs compared to differentiating state. In accordance, I₃₄ modification levels were higher in self-renewing stem cells (83-86%) than in differentiating ones (60-79%) (Bornelov et al., 2019); 5) Mutations in ADAT3 gene in human have been linked to neurological disorders (See section 2.5.4).

2.5.4 Patients

Although there are no ADAT2 variants associated to human disease yet, several publications highlight an important role of ADAT3 in human disease, particularly in neurodevelopmental disorders: 1) Mutation in ADAT3 (p.V144M) is associated to ID, microcephaly and epilepsy in Human in a total of 43 patients (Alazami et al., 2013; El-Hattab et al., 2016; Hengel et al., 2020; Sharkia et al., 2018). This mutation is mainly associated to consanguineous Arab families and found to originate from a common founder (Mutation is estimated to have occurred between 65th to 111th generation ago). Alazami and colleagues showed that this residue is conserved from human to Amoeba and hypothesized that the mutation to Methionine could cause a kink leading to a conformational change of a small hook where the residue is located (Alazami et al., 2013). In addition, ADAT3 p.V144M has been recently shown to impair I₃₄ in certain tRNAs (tRNA-Val-AAC, tRNA-Ile-AAU and tRNA-Leu-AAG), display aberrant subcellular localization, association with cytoplasmic chaperonins (HSP60 and TriC) and propensity to aggregate but maintained interaction with ADAT2 (J. Ramos et al., 2019); 2) An 8-bp duplication in ADAT3 leads to microcephaly, ID, and hyperactivity in 1 patient from a consanguineous family (Salehi Chaleshtori et al., 2018); 3) A compound heterozygous variant of ADAT3 (p.A196V,p.A196L) leads to severe syndromic ID, hypotonia, esotropia, failure to thrive and microcephaly in 2 siblings (non-consanguineous family) (Thomas et al., 2019). All variants implicated in disease are either homozygous or compound heterozygous and are associated mainly to ID, microcephaly, strabismus and developmental delay as major phenotypes. See Fig. 50 for details. Apart from p.V144M mutation there is no information about how mutations in ADAT3 might impair the complex and lead to neurodevelopmental diseases.

	Alazami et al 2013	El Hattab et al 2016	Sharkia et al 2018	Hengel et al 2020	Salehi Chaleshtori et al 2018	Thomas et al 2019
	Hom	Hom	Hom	Hom	Hom	Comp.Het
	c.430G>A, p.Val144Met					c.587C>T, p.Ala196Val; c586_587delins TT,p.Ala196Leu
Patients	24, 12M, 12F	15, 8M, 7F	2, 1M, 1F	2, NA	1, 1F	2, 1M, 1F

Age at diagnosis (years)	2-24y	1-24y	14-15y	NA	6y	7-12y
Clinical features						
Brain function/Structure						
Intellectual disability	24/24	15/15	2/2	2/2	1/1	2/2
Spasticity	7/24	6/15	0/2	NA	ND	1/2
Epilepsy	3/24	3/15	0/2	NA	ND	0/2
Brain anomalies	9/15	9/13	2/2	NA	ND	0/1; ND
Attention deficit hyperactivity disorder/ hyperactivity	1/24	2/15	ND	NA	1/1	0/2
Aggressive	ND	4/15	ND	NA	ND	0/2
Hypotonia	10/24	6/15	2/2	2/2	ND	2/2
Eyes/vision						
Esotropia /Strabismus	22/24	10/15	2/2	2/2	0/1	2/2
Myopia	ND	1/15	ND	NA	ND	2/2
Hearing loss	ND	1/15	ND	NA	ND	0/2
Growth/ Gastrointestinal						
Intrauterine growth restriction	ND	1/15	0/2	NA	0/1	2/2
Failure to thrive/short stature	22/24	11/15	2/2	NA	ND	2/2
Microcephaly	11/24	11/15	2/2	NA	1/1	1/2
Gastroesophageal reflux disease	ND	2/15	ND	NA	ND	2/2
Skeletal/joints						
Joint contractures	ND	1/15	2/2	NA	ND	1/2
Talipes/vertical talus	2/24	2/15	0/2	NA	ND	0/2
Physical features						
Prominent forehead	ND	5/15	2/2	NA	ND	0/2
High forehead	ND	4/15	1/2	NA	ND	2/2
Slanted palpebral fissures	ND	4/15	2/2	NA	ND	1/2
Epicanthus	ND	4/15	2/2	NA	ND	1/2

Hypertrichosis/ Telecanthus	ND	4/15	2/2	NA	ND	2/2
--------------------------------	----	------	-----	----	----	-----

FIG. 50 REPORTED MUTATIONS IN ADAT3 AND CLINICAL FEATURES ASSOCIATED

ADAT3 mutations described in the literature in human patients are shown. Clinical features are divided into the following categories: Brain function/structure, Eyes/vision, Growth/Gastrointestinal, Skeletal/Joints, Physical features. Abbreviations: Homozygous (hom); Compound heterozygous (comp.het); male (M); female (F); year (y); Not determined (ND); Not available (NA).

2.6 The WDR4-METTL1 complex

WDR4 and METTL1 stand for WD Repeat-Containing Protein 4 and Methyltransferase Like 1 respectively and are respectively the mammalian homologues of Trm82 and Trm8 in yeast and TrmB in bacteria (Bahr et al., 1999) (Michaud et al., 2000). The WDR4-METTL1 heterodimer catalyzes the formation of 7-methylguanosine 46 (m^7G_{46}) in tRNAs (Alexandrov et al., 2005; Alexandrov et al., 2002).

2.6.1 Domains

Much of the initial insights in the complex comes from work by Alexandrov and colleagues which showed in yeast, that both Trm8 and Trm82 were shown to be necessary for the formation of m^7G_{46} both *in vivo* and *in vitro*. Additionally, they showed that basal activities of purified Trm8, or Trm82 alone increased respectively by 250 and 1000 fold if co-expressed with Trm82 or Trm8 respectively *in vitro*. Furthermore, they showed that human METTL1 and WDR4 (but not any of them alone) were able to restore m^7G_{46} defects in yeast lacking Trm8 or Trm82. Among the two subunits of the heterodimer METTL1's homologue Trm8 was shown to be the catalytically active partner in yeast. Alexandrov and colleagues identified several SAM binding domains (based on homology) in Trm8 and highlighted a key role for residues G103, G105 and G124 for reaction to occur. They identified Trm8 as the catalytic subunit of the complex, since it had residual catalytic activity when purified from *E.Coli* and showed cross-linking to pre-tRNA-phe *in vitro* whereas Trm82 did not. Nevertheless, WDR4's homologue, Trm82 was shown to be required for the tRNA modification function. Deletion of Trm82 in yeast resulted in a severe reduction of Trm8 protein levels and no active Trm8 was detected in the absence of Trm82 (Alexandrov et al., 2005).

Yeast Trm8 and Trm82, are unrelated and have no homology between them. Co-translational association of WDR4 and METTL1 seems to be essential for their activity, as mixing of separately expressed of Trm8 and Trm82 resulted in no m^7G_{46} activity whereas their co-translation resulted in m^7G_{46} activity (Matsumoto et al., 2007). Trm82 belongs to the WD protein family, a family of proteins rich in WD domains which are ~40 amino acids long and usually

fold into a propeller functioning as rigid scaffolds for protein interactions. Its mammalian homolog, WDR4 contains seven WD repeat domains which are thought to mediate interaction with other proteins regulating the WDR4-METTL1 complex (Leulliot et al., 2008). WD repeat domain-containing proteins can function in many cellular functions through interaction with other cellular proteins. Among them signal transduction, RNA processing, vesicular trafficking, cytoskeleton assembly, cell cycle regulation and transcription of the initiation complex stand out (Smith, 2008).

Leulliot and colleagues published the structure of the yeast Trm8/Trm82 complex and showed that there are particular residues both in Trm8 and Trm82 that are important for their interaction (See Fig.51). Among them, K223 and D219 of yeast Trm82 (corresponding to R170 and D164 respectively in human WDR4) have been reported to form salt bridges with residues E204 and K164 of Trm8 (E183 and K143 respectively in human METTL1) and are speculated to be important for maintaining Trm8 in an active conformation. Furthermore, they showed that the conformation of Trm8 changes when bound to Trm82. They also report that the tRNA binds to Trm8 in accordance with what the data from Alexandrov and colleagues reporting that METTL1 was the catalytic subunit of the complex (Alexandrov et al., 2005; Leulliot et al., 2008).

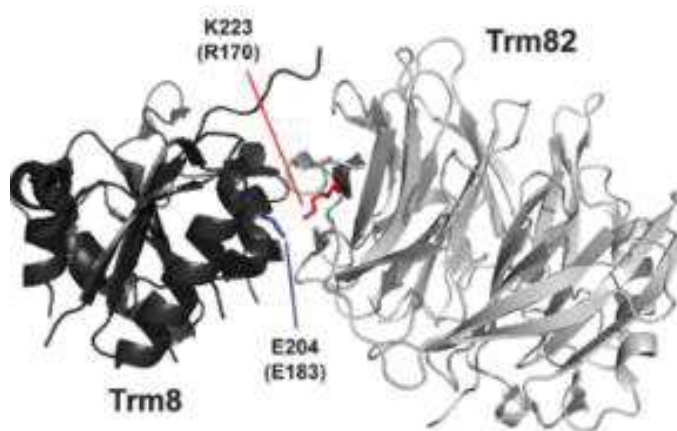


Fig. 51 Structure of the yeast Trm8-Trm82 complex

Structure of the yeast Trm82-Trm8 is shown highlighting the implication of residues K223 and E204 in salt bridge formation. Residue numbers in human are shown in parenthesis. From (Shaheen et al., 2015)

Interestingly, based on the structure they also revealed important information about the active site of Trm8. They showed that residues T219 and D220 which are absolutely conserved provide hydrogen bond recognition of the guanine base and that R128 and K264 which are charged could be involved in binding to tRNA through interaction with its 5' and 3' phosphate groups. In terms of tRNA recognition yeast Trm8/Trm82 is stricter than eubacterial TrmB. For catalysis to occur in bacteria, tertiary base-pairs in the tRNA molecule are not essential, the most important site for the reaction to occur was shown to be in the T-arm (H. Okamoto et al., 2004). In contrast, the yeast complex requires for reaction to take place tertiary base pairing between the D- and T-loops of the tRNA molecule and the absence of aminoacyl-stem contact

with either Trm8 or Trm82 subunits (Matsumoto et al., 2008; Matsumoto et al., 2007). Figure 52 shows the domains of WDR4 and METTL1 in humans and mice and highlights their similitude.

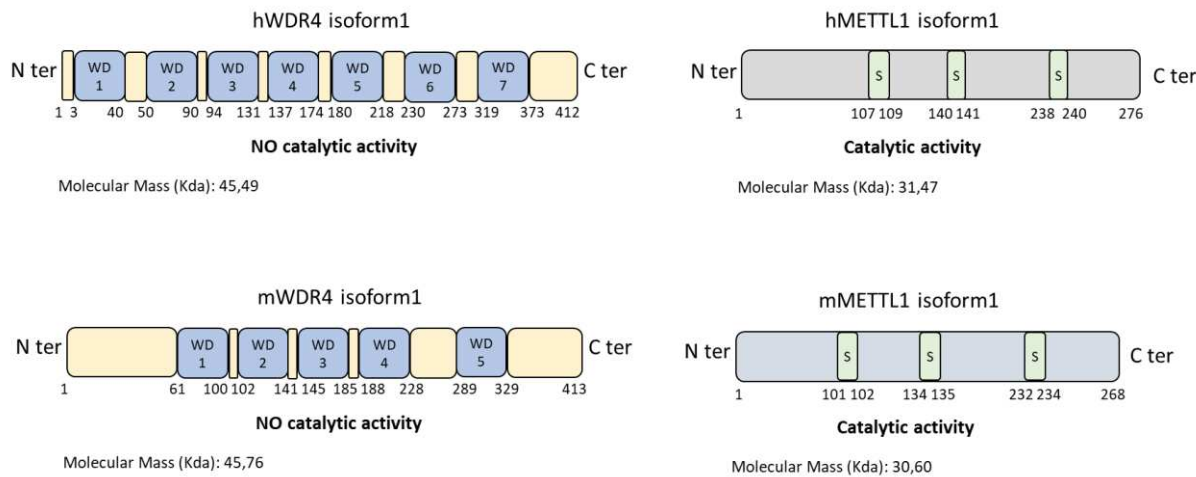


FIG. 52 DOMAINS FOR HUMAN AND MICE WDR4-METTL1

WDR4 bears 7 WD domains in humans and 5 in mice, METTL1 catalyses the reaction through its methyltransferase activity, it contains 3 S-adenosyl-L-methionine-binding (Depicted with S) identified regions. Both subunits are highly conserved between human and mice.

2.6.2 m^7G_{46} transfer RNA modification

N7 position of guanosine 46 (G_{46}) in various tRNAs from eukaryotes, bacteria and archaea is methylated to form m^7G_{46} which highlights the biological importance of this modification (See Fig.53). Lin and colleagues revealed the importance of the “RAGGU” motif for this tRNA modification to occur: whereas in yeast 11 tRNAs contain m^7G_{46} , in mice up to 22 tRNAs have recently been reported to bear m^7G_{46} modification (L. S. Zhang et al., 2019) (Lin et al., 2018). To date, no m^7G_{46} modification has been detected in mitochondrial tRNAs. The following cytosolic tRNAs have been detected to have m^7G_{46} in mice: AlaAGC, AlaCGC, AlaTGC, ArgTCT, AsnGTT, CysGCA, GlyACC, IleAAT, LysCTT, LysTTT, MetCAT, PheGAA, ThrTGT, TrpCCA, TyrGTA, ProAGG, ProCGG, ProTGG, ValACC, ValCAC, ValTAC (Lin et al., 2018). This modification has the peculiarity of being able to be protonated and confer a positive charge on G_{46} , which can favor and stabilize long-range hydrogen bonds with another guanosine residues at position 22 and a cytosine residue in position 13 of tRNAs (See Fig.46) (Agris et al., 1986). The establishment of these interactions is thought to contribute to correct folding of the tRNA molecule (Lorenz et al., 2017).

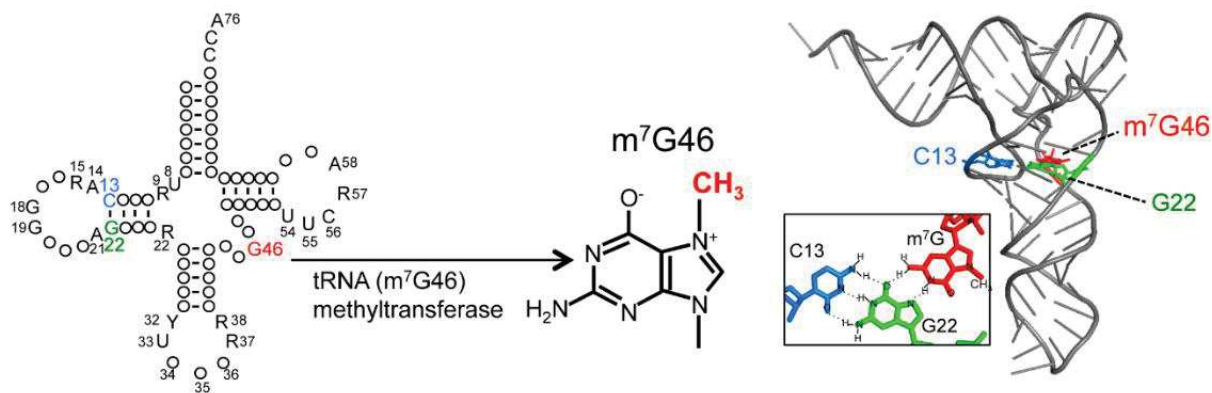


FIG. 53 m^7G_{46} tRNA MODIFICATION

G_{46} is methylated in several tRNAs. m^7G_{46} forms a tertiary base pair with the $\text{C}_{13}\text{-G}_{22}$ base pair in the L-shaped tRNA structure. Conserved nucleotides are depicted as follows: adenosine, A; guanosine, G; cytidine, C; uridine, U; purine, R; pyrimidine, Y. From (Tomikawa, 2018)

In accordance with this hypothesis, reduction of m^7G_{46} in combination with reduction of any of seven other tRNA modifications results in instability and degradation of tRNA molecules through the tRNA decay pathway (Alexandrov et al., 2006). Additionally, m^7G_{46} has little effect on aminoacylation (Lin et al., 2018) and appears to be a determinant for proper codon occupancy by ribosomes since Trm82-deficient yeast cells display significant changes in global ribosome occupancy (Chou et al., 2017). Furthermore, lack of m^7G_{46} tRNA modification was shown to lead to increased ribosome occupancy at the corresponding codons in METTL1 KO mouse embryonic stem cells (Lin et al., 2018).

2.6.3 Biological relevance

Regarding their tRNA activity, several findings illustrate the biological importance of the WDR4/METTL1 complex: 1) Although Trm8 and Trm82 are not essential for cell viability in yeast, *trm8* or *trm82* yeast mutants show growth defects under restrictive nutrient conditions and increased temperature-sensitivity, interestingly these phenotypes are mainly due to the de-aminoacylation and instability of a unique tRNA, tRNA-Val-AAC (Alexandrov et al., 2006); 2) WDR4 knockout mice shows lethality at early developmental stages (E9.5-E10.5) with some embryos showing different resorption degrees, some show severe resorption and are small, and some show only minor morphological defects but strong brain abnormalities and internal bleeding (Cheng et al., 2016); 3) *Wdr4* was shown to be a tightly regulated gene in the cortex (authors compared a Down syndrome mouse model to euploid mice reporting a differential variation coefficient) and has been proposed as a potential candidate gene contributing to the Down syndrome phenotype (WDR4 is located in human chromosome 21q22.3), suggesting that dosage of WDR4 is important for the brain (M. Sultan et al., 2007). In accordance with this

publication, Pereira and co-workers also revealed *Wdr4* as a candidate for cognitive phenotypes associated to Down syndrome; 4) WDR4 Drosophila homologue is critical for cellular differentiation and division during gametogenesis (Wu et al., 2006); 5) WDR4 deficiency leads to heterochromatin relaxation and induction of apoptosis via DNA damage through p53 activation and caspase-mediated apoptotic pathway as well as p21-mediated G2/M cell cycle arrest resulting in an inhibition of cell proliferation in mouse embryonic fibroblasts (C. C. Lee et al., 2018); 6) Mettl1 is activated transcriptionally by thyroid hormone 3 and regulates stem cell formation and/or proliferation during intestinal remodelling in *Xenopus tropicalis* metamorphosis (Na et al., 2020); 7) m⁷G₄₆ WDR4/METTL1 mediated modification is required for mouse embryonic stem cells mRNA translation, self-renewal and differentiation towards neural lineages, interestingly, METTL1 depleted cells show decreased translation of genes related to forebrain and cerebrum morphology and skull size (Lin et al., 2018).

In addition to their action catalyzing the formation of m⁷G₄₆ in tRNAs, other functions have been reported both for WDR4 and METTL1. WDR4 has been shown to play critical roles in growth, development and maintenance of genome stability in human cell lines through its interaction with FEN1, an endonuclease protecting the integrity of replication forks both in humans and mice. The authors showed that upon WDR4 depletion there is cellular DNA damage and loss of cell viability. To note, they could not conclude whether WDR4 function in maintaining genome stability was linked to its tRNA methylase activity. However, METTL1 silencing with miRNAs did not lead to cellular DNA damage or loss of cell viability. For this reason they focused on studying its interaction with FEN1 and PCNA which were already linked to genome stability (Cheng et al., 2016). In addition, WDR4 also controls germline homeostasis via TRIM-NHL tumour suppressor Mei-p26 in Drosophila (Rastegari et al., 2020). METTL1 in addition of being regulated by Thyroid hormone 3 has been shown to be regulated by insulin signalling. Upon insulin signaling, PKB (Protein Kinase B, also called Akt) and RSK (Ribosomal S6 Kinase) both catalyze the phosphorylation of METTL1 at ser27 leading to the inactivation of its tRNA modifying activity (Cartlidge et al., 2005) which hypothesizes that it would impact the synthesis of cellular proteins in response to insulin or other growth factors in human cells. Furthermore, METTL1 has been proven to limit differentiation and functioning of endothelial progenitor cells (derived from human-induced pluripotent stem cells through the MAP/ERK pathway) (Y. Deng et al., 2020). METTL1 has also been implicated in cancer, acting as tumor suppressor in colon cancer (Y. Liu et al., 2020) and promoting hepatocellular carcinoma progression (Tian et al., 2019). Interestingly, METTL1 and WDR4 were also recently proven to N7-methylate guanosines in mRNAs and miRNAs to increase translation efficiency and miRNA processing

respectively (Pandolfini et al., 2019; L. S. Zhang et al., 2019). Furthermore, Pandolfini and colleagues recently showed that METTL1 performs m⁷G methylation in a subset of miRNAs, including let-7 family of miRNAs, promoting their processing from primary transcript to precursor miRNA. Upon depletion of METTL1 levels the authors showed that m₇G modified tRNAs tend to form G-quadruplexes, which are known to be inhibitory for miRNA processing (Pandey et al., 2015). Among the miRNAs that were downregulated upon METTL1 Knock-down 50% of them (10/20) were linked to inhibiting cell migration. Zhang and colleagues showed that the WDR4-METTL1 complex does not catalyse m⁷G in RNA probes ranging from 12-mer to 17-er which suggests that it requires tRNA like structures with a stem loop with a certain minimum length to recognize the substrate and carry out the reaction (L. S. Zhang et al., 2019). These new functions of both members of the complex and the new insights into hormones regulating them open new scopes about the function of the complex in addition to their role in m⁷G₄₆tRNA modification and in other human diseases, such as cancer.

2.6.4 Patients

Regarding the WDR4/METTL1 complex, to date, there were only variants in *WDR4* associated to human disease, which highlight an important role of WDR4 in human disease and particularly in neurodevelopmental disorders: 1) A homozygous mutation in WDR4 (p.Arg170Leu) was shown to be causative for primordial dwarfism with microcephaly being a common feature of patients (2 patients) (Shaheen et al., 2015). Interestingly, this mutation resulted in reduced levels of m⁷G₄₆methylation in tRNA-Phe in patients (Shaheen et al., 2015); 2) WDR4 p.Arg170Gln;pGln310Glyfs*30 (2 patients) (Trimouille et al., 2018) and p.Asp164Ala;p.Leu314Profs*16 (1 patient) (X. Chen et al., 2018) biallelic variants also cause a distinct form of microcephalic primordial dwarfism characterized with growth retardation and ID. 3) A splice site mutation (c.454-2A>C) in *WDR4* patients causes growth deficiency, microcephaly, developmental delay and ID combined to renal-glomerular disease leading to Galloway-Morat syndrome, a disease characterized by neurological abnormalities and early onset progressive kidney disease (Braun et al., 2018).

Interestingly, the variants described in Shaheen et al 2005, Trimouille et al 2008 and Chen et al; 2008 in *WDR4* are located in the same residues that Leulliot and colleagues reported to participate in the formation of salt bridges described above. Shaheen and colleagues, used yeast as a model to analyze the effects of WDR4 p.R170L mutation and reported that in position 223 of yeast Trm82, lysine and arginine were interchangeable residues, however, this was not the case for leucine (Shaheen et al., 2015).

A summary of each of the mutations and the phenotypes associated to each of them is shown in Fig.54.

Primordial dwarfism/microcephaly			Galloway-Morat syndrome
Shaheen et al 2015	Trimouille et al 2018	Chen et al 2018	Braun et al 2018
Hom	Comp.Het	Comp.Het	Hom
c.509G >T; pR170L	c.509G > A; c911_927dup; p.R170Q; pQ310Gfs*30	c.491A > C; c940dupC; pD164A;pL314Pfs*16	c.454-2A>C, splice site
Patients	2, 2F	2, 2F	1, 1M
Age at diagnosis	4m	After birth	1y
Clinical features			
Neurologic			
Seizures	2/2	0/2	0/1
Hypertonia	2/2	ND	0/1
Agenesis of corpus callosum	2/2	0/2	0/1
Vermian atrophy of cerebellum	0/2	2/2	0/1
Bilateral optic nerve atrophy	2/2	ND	0/1
Peripheral nervous system impairments	2/2	ND	0/1
Motor development delay	2/2	2/2	1/1
Language delay	ND	2/2	1/1
Severe sleep disturbances	ND	2/2	0/1
Mental retardation	2/2	2/2	1/1
Head & physical features			
Microcephaly	2/2	2/2	1/1
Face abnormalities	2/2	2/2	0/1
Teeth perturbances	1/2	2/2	0/1
High arched palate	1/2	2/2	0/1
Skeletal			
Limbs perturbances	1/2	2/2	0/1
Growth			
Growth retardation	2/2	2/2	1/1
Laboratory			
Low IGF-1	0/2	2/2	0/1
Growth Hormone deficiency	0/2	1/2	0/1
Hypothyroidism	ND	ND	3/4

Hypalbuminemia	ND	ND	ND	1/4
Renal				
Nephrotic range proteinuria	ND	ND	ND	3/4

FIG. 54 REPORTED MUTATIONS IN WDR4 AND CLINICAL FEATURES ASSOCIATED

WDR4 mutations described in the literature in human patients are shown. Clinical features are divided into the following categories: Neurologic, Head & Physical features, Skeletal, Growth, Laboratory, Renal. Abbreviations: Homozygous (hom); Compound heterozygous (comp.het); male (M); female (F); year (y); month (m); Not determined (ND); Not available (NA).

Altogether there are several evidences supporting a role of the ADAT2/3 and WDR4-METTL1 complexes in corticogenesis. Towards this aim, I performed a characterization of the roles of these two complexes during mammalian cortical development in health and disease.

AIMS

As it has been explained along the introduction, the development of the cerebral cortex comprises several phases which are essential for the formation of a functional brain. Perturbation of one or more of these stages can lead to various neurological and cognitive disorders of varying severity. Identification of the molecular and cellular mechanisms that control cortical development is therefore crucial for a better understanding of these disorders. Post-transcriptional tRNA modifications and tRNA modification enzymes have increasingly been shown to be important in neurodevelopmental disorders, including ID, microcephaly and epilepsy, and appear to be important regulatory mechanisms during cortical development both in human and mice.

Although the molecular mechanisms of tRNA modifications are more understood, very little is known about the exact roles of post-transcriptional modifications during cortical development and how their dysregulation can lead to neurodevelopmental diseases. How do mutations in tRNA modifying enzymes lead to neurological disorders? What are the major stages of cortical development requiring strict tRNA modification regulation? These questions remain unanswered to date.

Towards these aims, in order to unravel new mechanisms governing cortical development and their implication in neurodevelopmental disorders during my PhD I performed a characterization of two tRNA modifying enzymes, ADAT3 and WDR4 as well as their respective interacting partners, ADAT2 and WDR4, and tRNA PTMs, I_{34} and m^7G_{46} , during cerebral cortex development both in health and disease.

Along my PhD, I have:

- 1) Characterized the expression profile of Adat2/3 and Wdr4/Mettl11 complexes throughout cortical development in mice showing that both complexes are expressed in a stable manner throughout cortical development.
- 2) Identified a role of the Adat2/3 and Wdr4/Mettl11 complexes in the regulation of projection neuronal radial migration by IUE experiments in WT cortices.
- 3) Identified in collaboration with clinicians new variants in ADAT3, WDR4 and METTL1 associated to neurodevelopmental diseases
- 4) Studied the role of both published and newly identified variants of ADAT3, WDR4 and METTL1 variants in projection neuron radial migration *in vivo* by IUE and showed that

human variants in mouse Adat3, Wdr4 or Mett1 genes lead to a loss of function of the Adat2/3 and Wdr4/Mettl11 complexes respectively during neuronal migration.

- 5) Studied how variants in ADAT3 and WDR4 alter the stability of the ADAT2/3 and WDR4/METTL1 complexes in vitro showing that p.Val144Met and WDR4 p.Arg170Leu destabilize their respective heterodimers and negatively affect the function of the complex.
- 6) Performed a neuroanatomical characterization of a newly generated Knock-in Adat3 p.V128M model showing an alteration of neurogenesis upon Adat3 p.V128M mutation.

Results for points 1-5 are all included in “Article 1”, currently in preparation. Results for points 6 are included in “Preliminary results: Characterization of an Adat3 p.V128M homozygous Knock-in mice line”.

My results clearly identified the ADAT2/3 and WDR4/METTL1 complexes as regulators of key processes for the development of the cerebral cortex and showed how mutations in these genes can lead to neurodevelopmental disorders.

PART 2

RESULTS

Article 1: Disruption of the catalytical activity of the tRNA modification complexes, Adat2/Adat3 and Mettl1/Wdr4, impairs neuronal migration and leads to Human neurodevelopmental disorders.

Disruption of the catalytical activity of the tRNA modification complexes, Adat2/Adat3 and Mettl1/Wdr4, impairs neuronal migration and leads to Human neurodevelopmental disorders.

Jordi Del Pozo Rodriguez^{1,2,3,4}, Peggy Tilly^{1,2,3,4,*}, Charlotte Hardion^{1,2,3,4,*}, Elizabeth R. Morales^{1,2,3,4}, , Martin Marek^{1,2,3,4}, Fowzan S. Alkuraya^{5,6}, Eleina M. England⁷, Dragana Josifova⁸, Katherine Lachlan⁹, Melanie O'Leary⁷, Michele Pinelli^{10,11}, Ken Saida¹², Karen L. Stals¹³, Grace VanNoy⁷, Christophe Romier^{1,2,3,4}, Efil Bayam^{1,2,3,4, #}, Juliette D. Godin^{1,2,3,4, #}

1. Institut de Génétique et de Biologie Moléculaire et Cellulaire, Illkirch, France.
2. Centre National de la Recherche Scientifique, UMR7104, Illkirch, France.
3. Institut National de la Santé et de la Recherche Médicale, INSERM, U1258, Illkirch, France.
4. Université de Strasbourg, Strasbourg, France.
5. Department of Genetics, King Faisal Specialist Hospital and Research Center, Riyadh, Saudi Arabia.
6. Department of Anatomy and Cell Biology, College of Medicine, Alfaisal University, Riyadh, Saudi Arabia.
7. Center for Mendelian Genomics, Broad Institute of MIT and Harvard, Cambridge, Massachusetts, USA.
8. Northern Genetics Service, Newcastle upon Tyne NHS Foundation Trust, Newcastle upon Tyne, UK.
9. Wessex Clinical Genetics Service, Princess Anne Hospital, Southampton, UK.
10. Department of Translational Medicine, Federico II University, Naples, Italy.
11. Telethon Institute of Genetics and Medicine, Pozzuoli, Naples, Italy.
12. Department of Human Genetics, Yokohama City University Graduate School of Medicine, Yokohama, Japan.
13. Department of Molecular Genetics, Royal Devon & Exeter NHS Foundation Trust, Exeter, UK.

* These authors contributed equally to this work.

Corresponding authors: godin@igbmc.fr, bayame@igbmc.fr.

Introduction

Cellular homeostasis and growth require protein synthesis to be both efficient to guarantee sufficient production, and accurate to prevent generation of defective or unstable proteins. Efficient and faithful protein translation rely on the activity of transfer RNAs (tRNAs), the adaptor molecules needed to decode genetic information into a peptide sequence. To be fully active, tRNAs molecules need to be heavily modified post-transcriptionally. About 30 chemical modifications have been identified at various position in human tRNAs (Cantara et al., 2011; Machnicka et al., 2013), for a total of 83 tRNAs modifications (de Crecy-Lagard et al., 2019). On average, a single tRNA carries 13 modifications (Phizicky and Alfonzo, 2010). These modifications are catalyzed by different classes of tRNA modification enzymes and influence tRNA structure, function and stability (Agris et al., 2007). Nucleotides in the anticodon loop are extensively modified (Agris et al., 2007). Those modifications are crucial as they regulate the tRNA-mRNA interaction to either stabilize cognate Watson-Crick base pairing (position 37) or to facilitate wobble pairing (position 34) to increase the decoding capacity and to prevent frameshift errors (Agris et al., 2007).

Thanks to the recent identification of human homologs for many tRNAs modification enzymes and to the wide use of whole exome sequencing, an increasing number of genes encoding for tRNA modification enzymes have been linked to human diseases (de Crecy-Lagard et al., 2019). Reflecting a key role of tRNAs modification in brain development, variants in several human tRNA modification enzymes-encoding genes (*ADAT3* (adenosine deaminase tRNA-specific 3) (Alazami et al., 2013; El-Hattab et al., 2016; Hengel et al., 2020; Salehi Chaleshtori et al., 2018; Sharkia et al., 2018; Thomas et al., 2019), *ALKBH8* (Monies et al., 2019), *CTU2* (Shaheen et al., 2019a), *DALRD3* (Lentini et al., 2020), *ELP2* (Cohen et al., 2015), *ELP3* (Bento-Abreu et al., 2018), *ELP4* (Addis et al., 2015; Reinthaler et al., 2014), *FTSJ1* (methyltransferase) (Freude et al., 2004; Froyen et al., 2007; Guy et al., 2015; Ramser et al.,

2004; Takano et al., 2008), genes encoding all KEOPS subunits (Arrondel et al., 2019; Braun et al., 2017; Domingo-Gallego et al., 2019; Hyun et al., 2018; Lin et al., 2018a), *NSUN2* (NOP2/Sun RNA methyltransferase family member 2) (Abbasi-Moheb et al., 2012; Doan et al., 2019; Fahiminiya et al., 2014; Froukh et al., 2020; Khan et al., 2012; Komara et al., 2015; Martinez et al., 2012), *PUS3* (pseudouridylase synthase 3) (Fang et al., 2020; Froukh et al., 2020; Shaheen et al., 2016), *PUS7* (pseudouridylase synthase 7) (Darvish et al., 2019; de Brouwer et al., 2018; Shaheen et al., 2019b), *TRIT1* (Forde et al., 2020; Kernohan et al., 2017; Yarham et al., 2014), *TRMT1* (Blaesius et al., 2018; Davarniya et al., 2015; Zhang et al., 2020), *TRMT10A* (tRNA methyltransferase 10 homologue A) (Gillis et al., 2014; Igoillo-Esteve et al., 2013; Narayanan et al., 2015; Yew et al., 2015; Zung et al., 2015), and *WDR4* (WD Repeat Domain 4) (Braun et al., 2018; Chen et al., 2018; Shaheen et al., 2015; Trimouille et al., 2017)) have been associated with various neurodevelopmental disorders, including malformation of cortical development (microcephaly, lissencephaly), intellectual disability (ID), primordial dwarfism, Galloway-Murat Syndrome (GAMOS), agenesis of corpus callosum and epilepsy. Although most of those variants have been shown to affect tRNAs modification *in vitro*, their direct implication in disease and the underlying pathophysiological mechanisms have only been elicited for only a few of them (Arrondel et al., 2019; Blanco et al., 2014; Braun et al., 2017; de Brouwer et al., 2018; Ramos et al., 2019).

Adat3 and Wdr4 are respectively the non-catalytic subunits of the heterodimeric enzyme complexes, Adat2/Adat3 (Tad2p/Tad3p in *Saccharomyces cerevisiae*) which edits adenosine (A) to inosine (I) at the wobble position 34 (I_{34}) in mature tRNA having ANN anticodons (Gerber and Keller, 1999), and Mettl1/Wdr4 (Trm8/Trm82 in *S. cerevisiae*), which catalyzes the formation of N(7)-methylguanosine at position 46 (m^7G_{46}) in more than 20 tRNAs in mammals (Alexandrov et al., 2002; Lin et al., 2018b; Zhang et al., 2019). Adat2 and Mettl1 are both catalytically inactive in the absence of Adat3 and Wdr4, respectively, indicating that

heterodimer formation is a prerequisite for I₃₄ and m⁷G₄₆ editing (Alexandrov et al., 2002; Gerber and Keller, 1999). Given the ability of inosine to pair with uracil (U), cytosine (C) or adenosine (A) (Crick, 1966), the A to I conversion at position 34 is essential to expand the decoding capacity of tRNA isoacceptors in organisms that lack the cognate tRNA isoacceptors containing a G or a U at the first position of the anticodon (Grosjean et al., 1996). I₃₄ is, therefore, thought to improve translation fidelity and efficiency (Lyu et al., 2020; Schaub and Keller, 2002). m⁷G₄₆ is a highly prevalent modification found in the variable loop of tRNA where it likely forms interaction with bases at position 13 and 22 in order to stabilize the tRNA structure (Jovine et al., 2000; Sprinzl et al., 1998), to protect tRNA from degradation (Alexandrov et al., 2006) and to ensure efficient codon recognition (Lin et al., 2018b). Illustrating the biological importance of Adat2/Adat3 and Mettl1/Wdr4 complexes, complete deletion or loss of activity of those tRNA modification complexes leads to lethality (Cheng et al., 2016; Lee and Hsieh, 2018; Torres et al., 2015; Tsutsumi et al., 2007), growth retardation (Alexandrov et al., 2006) and/or impaired cell cycle progression (Lee and Hsieh, 2018; Lin et al., 2018b; Tsutsumi et al., 2007; Wu et al., 2006) in several eukaryotes including yeast, human and mouse. In addition, both hWDR4 and hMETTL1 or their mouse or *Drosophila Melanogaster* and *Xenopus Tropicalis* homologues play critical roles in cellular differentiation (Deng et al., 2020; Lin et al., 2018b; Na et al., 2020; Rastegari et al., 2020; Wu et al., 2006). In particular, *Mettl1* or *Wdr4* knockout in mouse embryonic stem cells severely impair their capacity to differentiate into neural lineages (Lin et al., 2018b).

A same homozygous *ADAT3* variant (NM_138422.4: c.430G>A; p.Val144Met) have been reported in 43 patients from 21 consanguineous families presenting with an autosomal recessive syndromic form of intellectual disability (ID), characterized by developmental delay, moderate to severe ID, speech delay, microcephaly, abnormal brain structure, facial dysmorphism and epilepsy (**Table 1**) (Alazami et al., 2013; El-Hattab et al., 2016; Hengel et al., 2020; Sharkia et al., 2018). In addition to this founder mutation, a homozygous duplication in *ADAT3* (NM_138422.4: c.99_106dupGAGCCCGG; p.Glu36Glyfs*44) (Salehi Chaleshtori et

al., 2018) and a compound heterozygous missense *ADAT3* variant that affect a conserved amino acid in the deaminase domain (NM_138422.4: c.587C>T, p.Ala196Val; c.586_587delinsTT, p.Ala196Leu) (Thomas et al., 2019) have been described in 3 patients with similar but milder ID syndrome features. *WDR4* have also been genetically linked to heterogenous neurodevelopmental disorders with varying degrees of severity (**Table 1**). First, an homozygous variant in *WDR4* (NM_033661.4: c.509G >T; p.Arg170Leu) causes primordial dwarfism associated with microcephaly, abnormal gyration, agenesis of corpus callosum and epileptic encephalopathy in two consanguineous families (Shaheen et al., 2015). Second, two biallelic *WDR4* variants (NM_033661.4: c.509G>A, p.Arg170Gln; c.911_927dup, p.Gln310Glyfs*30 and c.491A>C; p.Asp164Ala; c.940dupC; p.Leu314Profs*16) were reported, respectively, in two siblings presenting with a distinct phenotype characterized by ID, growth retardation and progressive microcephaly (Trimouille et al., 2017) and in one patient presenting with ID and motor and speech delay (Chen et al., 2018). Third, a homozygous splice site variant has been described in patients with GAMOS, characterized by brain anomalies (microcephaly, abnormal gyration, cerebellar atrophy) combined with glomerulopathy (Braun et al., 2018). Fourth, *WDR4*, which is located on the human chromosome 21q22.3, has been proposed as a candidate gene for some cognitive phenotypes associated with Down syndrome, the most common genetic cause of ID that results from the trisomy of chromosome 21 (Michaud et al., 2000; Pereira et al., 2009). Except for the p.Val144Met *ADAT3* variant that was shown to alter the tRNAs A₃₄ deaminase activity of the Adat2/Adat3 complex without compromising the formation of the complex (Alazami et al., 2013; Ramos et al., 2019) and the p.Arg170Leu *WDR4* variant that was demonstrated to affect m⁷G₄₆ tRNA modification using patient cells (Shaheen et al., 2015), our knowledge of the molecular effect of *ADAT3* and *WDR4* variants is very limited. Altogether those results highlight a critical role of both *ADAT2/ADAT3* and *METTL1/WDR4* complexes in brain development and function. Yet, the neurodevelopmental processes that required proper function of those tRNA modification complexes haven't been elucidated.

Here we show that ADAT3 and WDR4 regulate radial migration of projection neurons likely through their roles of co-factor within the heterodimeric complexes. We further demonstrate that the catalytic activity of ADAT2 and METTL1 is critical to promote neuronal migration during corticogenesis. We also expand the molecular spectrum of *WDR4* and *ADAT3*-related neurodevelopmental disorders by reporting 2 novel homozygous missense variants and 2 compound heterozygous variants in patients with intellectual disabilities, structural brain anomalies and global growth retardation. Importantly, we identify a compound heterozygous variant in the catalytic subunit *METTL1*, establishing that mutation in both genes required for m⁷G₄₆ modification lead to neurodevelopmental disorder. Using complementation assays, we show that both previously- and newly- reported *ADAT3*, *METTL1* and *WDR4* pathogenic variants alter tRNA modification and impede radial migration of projection neurons through loss of function mechanisms, providing the evidence of a causal relationship between variants in *ADAT3*, *METTL1* and *WDR4* and neurodevelopmental disorders.

Results

Adat2/Adat3 and Mettl1/Wdr4 complexes are expressed ubiquitously during cortical development

We first examined the expression pattern of both catalytic and non-catalytic subunits of the Adat2/Adat3 and Mettl1/Wdr4 heterodimeric complexes during mouse cortical development. Although the levels of all mRNA transcripts tend to increase from embryonic day (E) 12.5 to E18.5 (**Fig. 1A**), immunoblotting using homemade antibodies for Adat3, Adat2 and Wdr4 (**Supplementary Fig. 1A-C**) and commercially available Mettl1 antibody showed rather stable expression of both Adat3 and Adat2 proteins and a progressive decrease of Wdr4 and Mettl1 expression from E12.5 to postnatal day (P) 2 (**Fig. 1B**). Immunolabelling of E18.5 embryo brain section (**Fig. 1C-E**) and of primary cortical neurons at day *in vitro* (DIV) 0 and DIV2 (**Supplementary Fig. 1E**) revealed expression of Adat3, Adat2, Mettl1 and Wdr4 in both progenitors and neurons. Expression of Wdr4 and its partner Mettl1 in both compartments was confirmed by immunoblotting of progenitors (YFP-; CD24-) and neurons (YFP+; CD24+) from Rosa26-loxSTOP-YFP; NEX^{CRE/+} E16.5 cortices by fluorescent-activated cell sorting (**Supplementary Fig. 1D**). Whereas Wdr4 cellular localization was likely restricted to the nucleus in both progenitors and neurons (**Fig. 1E – insets**), Adat2 and Adat3 showed both cytoplasmic and nuclear localization in all cell types (**Fig. 1C,D – insets**) in E18.5 cortical tissue. Analysis of subcellular localization of each protein in primary cortical neurons ascertained the nuclear localization of the Mettl1/Wdr4 complex and the more diffuse expression pattern of the Adat2/Adat3 complex.

Adat3 and Wdr4 regulate radial migration of projection neurons

To evaluate the function of mAdat3 and mWdr4, we assessed the consequences of acute depletion of both mAdat3 and mWdr4 on neuronal migration using *in utero* electroporation

(IUE) of miRNAs or shRNA in E14.5 mouse embryo. Efficacy of two miRNAs and/or shRNAs per gene was confirmed by RT-qPCR and immunoblotting (reduction of 85.3% and 96.5% of protein levels for miR1- and miR2-*Adat3* respectively, and of 82.7% and 84.2% for sh-*Wdr4* and miR1-*Wdr4* respectively) (**Supplementary Fig. 2A-D**). We first performed IUE of plasmid expressing these sh/miRNAs or scramble miRNAs under the control of an ubiquitous pCAGGS promoter together with a NeuroD-IRES-GFP reporter construct, allowing the expression of GFP specifically in post mitotic neurons, in wild-type mouse cortices at E14.5. Four days after IUE, the distribution of GFP+ neurons depleted for *Adat3* or *Wdr4* was significantly impaired with a notable reduction of GFP+ neurons reaching the upper cortical plate (up CP) upon acute depletion of *Adat3* (-32,7% and -21,7 % for miR1- and miR2-*Adat3*, respectively) (**Supplementary Fig. 2E,F**) and *Wdr4* (-13,6% for sh-*Wdr4* and -18,2 % for miR1-*Wdr4*) (**Supplementary Fig. 2G,H**). As pCAGGS is an ubiquitous promoter, impaired neuronal positioning observed upon pCAGGS-driven *Adat3* and *Wdr4* deletion might result from defects arising in progenitors, in their neuronal progeny or in both. IUE of plasmids expressing the same sh/miRNAs under the control of the neuronal promoter NeuroD showed faulty migration of *Adat3*- and *Wdr4*-silenced neurons with a reduction of 21.9%, 22,7%, 19.1% and 22.4% of cells distributed in the upper CP for miR1- and miR2-*Adat3*, sh-*Wdr4* and miR1-*Wdr4*, respectively, suggesting that defect in postmitotic neurons largely contributed to the *Adat3*- and *Wdr4*- dependent migration phenotype in a cell-autonomous manner (**Fig. 2A-D**). Most of the *Adat3*-silenced cells showed a correct positioning with nearly all cells found in the upper layer of the cortex after birth, indicating a delay in migration rather than a permanent arrest (**Fig. 2E**). By contrast, 33.3% of the embryos electroporated with miR1-*Wdr4* displayed a large number of neurons arrested in the white matter and the deep-layers at P2, suggesting that knockdown of *Wdr4* induced a permanent migration defect with an incomplete penetrance (**Fig. 2F**). To further validate the specificity of the migratory phenotype induced by *Adat3*- and *Wdr4*-silencing, we tested the ability of wild-type (WT) *Adat3* and *Wdr4* protein to restore migration defects. Transfection in HEK cell line showed proper expression of wild-type *Wdr4*

protein by western blot (**Supplementary Fig. 3B**). At the opposite, expression of Adat3 alone or together with Adat2 in N2A neuroblastoma cell line revealed the need of Adat2 to stabilize Adat3 (**Supplementary Fig.3C**), in line with the necessity of Adat2 to maintain Adat3 proper folding (Gerber and Keller, 1999; Ramos et al., 2019). We performed co-electroporation of NeuroD-driven miRNAs together with plasmids expressing miRNAs-insensitive Adat3 or Wdr4 under the regulation of a neuronal promotor (DCX and NeuroD respectively) (**Supplementary Fig. 3A,B**). Whereas WT Wdr4 fully restored the defective migration induced by miR1-Wdr4 (**Fig. 3C,D, Supplementary Fig. 3I,J**), co-electroporation of WT Adat3 alone failed to rescue the impaired distribution of *Adat3*-depleted neurons (**Supplementary Fig. 3E,F**). However, *Adat3*-silenced neurons expressing both wild-type Adat3 and Adat2 displayed a correct positioning within the upper cortical plate (**Fig. 3A,B**), indicating that Adat3 ability to restore the migration phenotype depends on the stoichiometric expression of Adat3 and Adat2 *in vivo*. Altogether, these results demonstrate that Adat3 and Wdr4 are cell-autonomously required for proper migration of projection neurons and they suggest a contribution of tRNAs modification to radial migration.

The catalytic activity of Adat3/Adat2 and Mettl1/Wdr4 complexes is required for proper neuronal migration.

To assess whether the migratory function of Adat3 and Wdr4 depends on their function within their respective heterodimeric enzymatic complexes, we next explored the effect of silencing the catalytically active partners, Adat2 and Mettl1, on neuronal migration. We performed acute depletion of *Adat2* and *Mettl1* specifically in neurons or in cortical cells by IUE of NeuroD-driven *Adat2*-miRNAs or pCAGGS-driven *Mettl1*-miRNAs in wild type cortices at E14.5, respectively. The ability of miRNAs to efficiently target *Adat2* was tested by qPCR and immunoblotting (reduction of 83% of protein levels for both miR1- and miR2-*Adat2*) (**Supplementary Fig. 2A,B**). Consistent with a critical role of the complexes in the regulation

of radial migration, the migration defects observed after depletion of *Adat2* and *Mettl1* were comparable to those observed after silencing of *Adat3* and *Wdr4* (-21%, -19.5%, -18.7%, -15.6% of cell reaching the upper cortical plate in miR1-, and miR2-*Adat2* and miR1- and miR2-*Mettl1* condition) (**Fig. 3E-H**). We next addressed whether the *Adat2/Adat3* complex controls neuronal migration through their catalytic activity. We tested for restoration of the phenotype induced by the loss of *Adat3* by expressing wild-type *Adat3* and a catalytically inactive form of *Adat2* (**Supplementary Fig. 3D**) (Gerber and Keller, 1999; Spears et al., 2011). In accordance with the need of the enzymatic activity, co-expression of *Adat3* with wild-type *Adat2* but not with catalytic inactive *Adat2* (*Adat2* CI) rescued the impaired positioning of *Adat3*-depleted cells (**Fig. 3A,B**). Altogether these results demonstrate the catalytic activity of the *Adat2/Adat3* and *Wdr4/Mettl1* complexes is required to exert their function in migrating projection neurons.

Identification of *ADAT3*, *WDR4* and *METTL1* variants

Through the GeneMatcher platform (Sobreira et al., 2015), we identified biallelic variants in *ADAT3*, *WDR4* and *METTL1* in five patients presenting with intellectual disabilities and brain anomalies (**Table 1**). We first found a unreported homozygous variant in *ADAT3* (*ADAT3*, NM_138422.4: c.335G>T, p.Arg128Leu) was found in Patient 1, who has a known consanguineous family history and who presented with severe ID associated with microcephaly and corpus callosum hypoplasia (**Fig. 4A,C**). Concurrently, we reported 2 variants in *WDR4*. Two patients from independent non-consanguineous families, Patient 2 (P2) and Patient 3 (P3), who presented with ID accompanied by microcephaly and global developmental delay, were homozygous carrier for a missense variant at the start codon (NM_033661: c.2T>C, p.iMet1Thr) (**Fig. 4D**). The same missense variant (NM_033661: c.2T>C, p.iMet1Thr) was also identified as a compound heterozygous variant with a splice site variant (NM_033661: c.567-2A>G, p.?) in a third patient (Patient 4 (P4)) presenting with similar clinical features (**Fig. 4D**). The c.2T>C substitution leads to the introduction of a threonine that

can initiate translation, albeit at a lower efficiency than iMet (Kearse and Wilusz, 2017), strongly arguing for *WDR4* haploinsufficiency in the carrier patients. Finally, we identified a compound heterozygous missense variant in *METTL1* in Patient 5 (P5) (NM_005371: c. 360T>G, p.Ile120Met; c.521G>A, p.Arg174Gln) presenting with ID, severe microcephaly, corpus callosum hypoplasia, severe epilepsy and developmental delay (**Fig. 4B, E**). The p.Ile120Met variant was inherited from the healthy father, while the p.Arg174Gln occurred *de novo* (**Fig. 4B**). All variants were predicted pathogenic by commonly-used *in silico* softwares (Polyphen-2, Mutation Taster and SIFT; **Supplementary Fig. 4D**) and co-segregated with the phenotype in each pedigree (**Fig. 4A, B** and data not shown). None of the *ADAT3*, *WDR4* and *METTL1* newly-identified variants is reported in public databases, including dbSNP, 1000 Genomes and gnomAD as biallelic variants. Overall, by identifying novel variants in *ADAT3*, *WDR4* and *METTL1* genes, we expanded the spectrum of neurodevelopmental diseases related to heterodimeric tRNAs modification complexes (**Table 1**).

Variants in *WDR4* and *METTL1* likely impair the complex enzymatic activity

We next investigated how the identified variants in *WDR4* and *METTL1* affect the structure and function of their respective complexes. We first modelled the location of *METTL1* p.Ile120Met and p.Arg174Gln variants to predict their impact on the complex, based on the yeast Trm8-Trm82 crystal structure (Leulliot et al., 2008). As previously reported, R195 of yeast Trm8 (corresponding to p.Arg174 in human) forms a hydrogen bond with a glutamate residue in position 204 (yeast E204; human p.Glu183) in a Trm82-free confirmation (**Fig. 4F, left panel, Supplementary Fig. 4E**). This interaction is no longer possible in the Trm8-Trm82 complex as the E204-Trm8 residue forms a salt bridge with the lysine residue at position 223 of Trm82 (yeast K223-Trm82 corresponding to p.Arg170 in human *WDR4* (**Supplementary Fig. 4F**)). In this so-called ‘active’ conformation, the R195-Trm8 adopts a preferred position for interaction within the β 4- α D loop, which forms the top of the S-adenosyl-methionine (SAM)

binding pocket and that is essential for the methyltransferase activity (**Fig. 4F, right panel**) (Leulliot et al., 2008). Notably, the I139-Trm8 residue (p.Ile120 in hMETTL1 (**Supplementary Fig. 4F**)) is located in the β 4- α A loop that constitutes the bottom of the SAM binding site (**Fig. 4F, right panel**) (Leulliot et al., 2008). Altogether, these results suggest that pathogenic p.Arg174Gln and p.Ile120Met substitution might impair Mettl1/Wdr4 complex activity likely through conformational changes occurring within the SAM binding pocket. To evaluate the ability of the Mettl1/Wdr4 complex to form in pathogenic condition, we performed co-expression study in E.Coli. To facilitate WDR4 expression in E.coli, we used a truncated form of mouse Wdr4 that lacks the 41 N-terminal amino-acids, that are missing in the human WDR4 (**Supplementary Fig. 4F**) and that lacks the 31 C-terminal residues, a region that is predicted as unstructured (Wdr4-N1C1). Co-expression of GST-tagged wild-type or R215L (that corresponds to p.Arg170Leu in human, **Supplementary Fig. 5B**) Wdr4-N1C1 with mouse Mettl1 revealed that the formation of the complex is preserved in both wild-type and mutant conditions (**Fig. 4G**).

Mutant ADAT2/ADAT3 complex fails to properly modify tRNAs

We next interrogated the molecular effect of the ADAT3 variants. We first assessed the effect of the previously reported p.Val144Met and the newly identified p.Arg128Leu *ADAT3* variants on hADAT3 protein levels. We compared hADAT3 protein levels in Lymphoblastoid cell lines (LCLs) generated from a carrier of the homozygous p.Val144Met variant (affected patient depicted in **Supplementary Figure 4A**) and from patient 1 (p.Arg128Leu) to control lymphoblasts generated from sex and aged-match healthy individuals or from healthy parents. Immunoblotting revealed a severe decrease of ADAT3 protein levels in both patient cell lines compared to controls (**Fig. 4H**), suggesting that the mutant ADAT3 proteins are unstable. We further tested the consequences of the ADAT3 variants on the ADAT2/ADAT3 tRNA function. We performed sequencing of Val-AAC and Thr-AGT tDNA isolated from patients and control

LCLs and, as inosine is read as a 'G' by reverse transcriptase (Torres et al., 2015), we sought for the percentage of G₃₄ as a proxy of A₃₄ to I₃₄ editing. We observed a drastic reduction (-69.8% for tRNA-Val-AAC and -97.3% for tRNA-Thr-AGT) of A to I tRNA modification in p.Val144Met LCLs (**Fig. 4I**). Altogether, these results indicate that the p.Val144Met and likely the p.Arg128Leu ADAT3 variant act as loss of function variants and impair the tRNA modification activity of the ADAT2/ADAT3 complexes.

Missense variants in *Adat3*, *Wdr4* impair neuronal migration through loss of function mechanism

To further assess the functional consequences of both previously and newly identified *ADAT3* and *WDR4* variants and to ascertain the predicted loss of function mechanism, we evaluated the ability of the variants to restore the migration phenotype induced by the depletion of *Adat3*, *Wdr4*. As we observed a decrease of protein levels in p.Val144Met and p.Arg128Leu ADAT3 LCLs, we first tested whether low amount of wild-type mouse *Adat3* rescued the migration phenotype observed upon m*Adat3* deletion by IUE of miR1-*Adat3* together with increasing amount of mADAT3. Whereas *Adat3*-silenced neurons expressing 1 unit of m*Adat3* are correctly distributed in the upper cortical plate 4 days after IUE (**Fig. 3A,B**), the expression of two-third of m*Adat3* only partially rescued the faulty migration (**Fig. 5A,B**), suggesting that *Adat3* controls neuronal migration in a dose-dependent manner. To undoubtedly demonstrate the loss of function of the *Adat3* variant, we electroporated V128M and R112L mutant mouse *Adat3* (that corresponds to human p.Val144Met and p.Arg128Leu, respectively (**Supplementary Fig. 5A**)) together with wild-type m*Adat2* in *Adat3*-silenced neurons. All variants showed expression similar to the expression of the wild-type protein, as confirmed by immunoblotting (**Supplementary Fig. 5C**). Both variants failed to fully rescue the altered distribution of *Adat3*-knocked-down neurons, therefore confirming the loss of function of the variants in migrating neurons (**Fig. 5A,B, Supplementary Fig. 3G,H**). Concurrently, we

assessed the functional consequences of p.Ala196Leu (A180L m Adat3 (**Supplementary Fig.5A**)) and p.Ala196Val (A180V m Adat3 (**Supplementary Fig.5A**)) *in vivo* (affected patient depicted in (**Supplementary Figure 4B**)). While the A180V variant restored the migration defects as efficiently as the Adat3 WT construct, the A180L variant did not rescue the phenotype (**Fig. 5A,B, Supplementary Fig. 3G,H**), suggesting Adat3 variants affect Adat3 migratory function at several extent. Similarly, we tested the impact of WDR4 variants on migration. As the p.iMet1Thr WDR4 variant is predicted to negatively affect the translation of the WDR4 protein, we tested the effect of this variant in neuronal migration using complementation assay with increasing amount of wild-type mWdr4. Co-electroporation of mir1-*Wdr4* with increasing doses of Wdr4 (0.25 and 0.5) gradually restored the migration phenotype of *Wdr4*-silenced neurons (**Fig. 5C,D**). These results suggest that a proper dosage of WDR4 is required to ensure its function during cortical migration and support a pathogenic effect of the p.iMet1Thr variant possibly through defective translation of WDR4 protein. Finally, we demonstrated that overexpression of the R215L mWdr4 (that corresponds to the human p.Arg170Leu WDR4 (**Supplementary Fig.5B,D**), affected patient depicted in (**Supplementary Figure 4C**)) in *Wdr4*-silenced neurons did not restored the faulty migration (**Fig. 5C,D, Supplementary Fig. 3I,J**), indicating an altered function of the p.Arg170Leu WDR4 in migrating neurons. Altogether, these results demonstrate that missense hADAT3 and hWDR4 variants impede, to various extent, the radial migration of projection neurons through loss of function mechanisms.

Discussion

Our findings highlight a critical role of the heterodimeric enzyme complexes, Adat2/Adat3 and Mettl1/Wdr4, in the regulation of radial migration of projection neurons. Several lines of evidence suggest that the catalytic activity of both complexes is required for proper neuronal migration. First, we demonstrated that silencing of both the catalytic (Adat2 and Mettl1) and

non-catalytic (Adat3 and Wdr4) subunits of the complexes impaired neuronal migration to similar extent (**Fig. 3**). Second, co-expression of Adat3 together with Adat2 is required to abrogate the phenotype induced by the loss of Adat3 (**Supplementary Fig. 3E, F**), co-expression of Adat2 likely being necessary to stabilize Adat3 *in vivo* (**Supplementary Fig. 3C**). This results notably correlated with *in vitro* findings showing that Adat3 tends to self-associate and aggregate when not assembled with Adat2 (Ramos et al., 2019). Third, co-expression of Adat3 together with a catalytic-inactive form of Adat2 is unable to rescue the *Adat3*-induced migratory phenotype (**Fig. 3A, B**). Fourth, decreased expression of Adat3 is accompanied by a drastic impairment of A to I conversion at the wobble position of tRNAs (**Fig. 4I**). Fifth, Adat3 and Wdr4 protein bearing, respectively, the p.Val144Met (V128M mAdat3) and the p.Arg179Leu (R215L mWdr4) variants, that were shown to affect the tRNAs modification activity of the corresponding complexes (Ramos et al., 2019; Shaheen et al., 2015), lost its ability to restore the faulty migration observed upon *Adat3* depletion. Sixth, patient carrying the newly-identified *METTL1* variant presented with clinical features, that are very similar to those of patients having variants in *WDR4* (**Table 1**), suggesting that any disruption of the *WDR4/METTL1* complex leads to neurodevelopmental disorders.

Our findings also implicate variants in *ADAT3*, *WDR4* and *METTL1* in ID and brain malformation (**Fig. 4, Table 1**). We identified four biallelic variants including two homozygous missense variants and two compound heterozygous variants in five patients. Our functional investigations revealed that both the identified and previously reported variants lead to loss of function. We demonstrated that previously-reported p.Val144Met and newly-identified p.Arg128Leu *ADAT3* variant showed decreased expression levels in patients cells (**Fig. 4H**). Notably, we reported a c.2T>C substitution either at the homozygous state or as a compound heterozygous variant with a splice site variant, that is likely introducing a weak initiation codon (Kearse and Wilusz, 2017), resulting in reduction of *WDR4* expression in patient cells. We therefore used IUE of miRNAs in mouse cortices to assess the functional consequences of

those variants and showed that *Adat3* and *Wdr4* depletion leads to impaired neuronal positioning (**Fig. 2**). We further performed complementation assays, and showed, that, when expressed at equivalent level compared to the WT protein, the p.Val144Met (V128M) and p.Arg128Leu (R112L) ADAT3 variants failed to rescue the knockdown phenotype (**Fig. 5C**), indicating that, in addition to their instability, the remaining protein might lose their activity within the Adat2/Adat3 complex. Consistently, analysis of the crystal structure of the wild-type and V128M Adat3 in complex with Adat2, revealed that the mutant complex harbors a tilted conformation that affects the binding of tRNAs substrates (Ramos, Romier and Godin, personal communication). Although we cannot conclude about a potential impact of neither the p.Ala196Leu (A180L) and p.Ala196Val (A180V) variants on ADAT3 or of the p.Arg170Leu (R215L) variant on WDR4 because of the lack of patients cells, we showed that, at least, the p.Ala196Leu and p.Arg170Leu lose, totally or partially, their function during migration (**Fig. 5C, E**). The loss of function of p.Arg170Leu is in line with work performed in yeast showing that the corresponding K223 residue is interchangeable with an arginine but not with a leucine (Shaheen et al., 2015). Of note, none biallelic null variant have been found in *ADAT2* yet. Strikingly we reported novel compound heterozygous missense variants in *METTL1* that affect two conserved residues positioned in the roof (p.Arg174) and floor (p.Ile120) of the SAM binding pocket, strongly arguing for defective catalytic activity of mutant complexes. In addition the R195 residue (p.Arg174) forms a salt bridge with E204 in yeast, this is thought to stabilize Trm8 (Mettl1) in an inactive conformation (Leulliot et al., 2008). As binding to Trm82 (Wdr4) involves structural rearrangements around those residues to render Trm8 active (Leulliot et al., 2008), it is tempting to speculate that the p.Arg174Gln variant locks METTL1 in an inactive conformation. In addition, given that K223 Trm8 (p.Arg170) is a key residue at the interaction surface between Trm8 and Trm82 as it forms a salt bridge with E204 Trm8 (Leulliot et al., 2008), p.Arg170Leu WDR4 variant is also likely impeding the active conformation of the METTL1/WDR4 complex.

Most of the patients with variants in *ADAT3*, *METTL1* and *WDR4* present with moderate to severe microcephaly, therefore questioning the role of those genes in regulating brain size. Interestingly, loss of function variants in other tRNAs modification enzymes, such as PUS7, NSUN2 and TRMT10A, have been associated with microcephaly in Human patients (Abbasi-Moheb et al., 2012; de Brouwer et al., 2018; Doan et al., 2019; Fahiminiya et al., 2014; Froukh et al., 2020; Gillis et al., 2014; Igoillo-Esteve et al., 2013; Khan et al., 2012; Komara et al., 2015; Martinez et al., 2012; Narayanan et al., 2015; Shaheen et al., 2019b; Yew et al., 2015; Zung et al., 2015). However, the underlying pathological mechanisms were only elicited for NSUN2 with microcephaly observed in NSUN2^{-/-} mice shown to arise from poor survival of both neuronal progenitors and neurons as well as from a decreased soma size of neuron (Blanco et al., 2014). Additional work in mice showed that loss of ncm⁵ and mcm⁵ U₃₄ modifications, catalyzed by the elongator complex, leads to microcephaly through impaired generation of neurons without affecting their survival (Laguesse et al., 2015). As such, to date, no convergent underlying cellular mechanisms has emerged, making it hard to predict how I₃₄ and m⁷G₄₆ contribute to the regulation of brain size.

Strikingly, maintaining a proper level of both Adat2/Adat3 and Mettl1/Wdr4 complexes activity seems to be crucial for cerebral cortex development. Indeed, expression of Wild-type Adat3 or Wdr4 restored the migration phenotype in a dose-dependent manner (**Fig. 5B, E**). What is the minimal level of complex activity required to ensure proper neuronal development? Convergent evidences suggest that cortical development can sustain hemizygosity. First, whereas full knock-out of *Adat3* and *Wdr4* are lethal in mice, loss of one allele (*Adat3^{+/-}* and *Wdr4^{+/-}* mice) does not lead to any brain defects (Del Pozo and Godin, personal communication) (Cheng et al., 2016). Second, human *ADAT3*, *ADAT2*, *WDR4* and *METTL1* genes tolerate loss-of-function variants with many loss-of-function heterozygous variants reported in the gnomAD general population (Genome Aggregation Database, v2.1.1). Consistently, variants in *ADAT3*, *WDR4* and *METTL1* genes identified in patients with neurodevelopmental disorders, were only found at the biallelic state (**Fig. 4, Table 1**). Interestingly, we demonstrated that the missense

ADAT3 variants impaired migration at various extent (Fig. 5C), suggesting that the position of the missense variants more or less alter the function of the complex. As our results exclude any effect of the variants on the formation of the complex (Ramos, Romier and Godin, personal communication), we hypothesized that the variant alters the activity of the complex so that it dictates the severity of the phenotype induced by the given variant. Further analyses are needed to test whether the ability of each variant to restore the phenotype correlates with their capacity to maintain minimal levels of tRNA modification. Whether or not the threshold activity of the complexes required for proper migration or for other developmental process is the same remains to be tested. Overall, our result raised the possibility of a threshold of activity below which the tRNAs modification (I_{34} , m^7G_{46}) would not be sufficient to ensure protein demand during brain development, leading to neurodevelopmental disorders.

Methods

Cloning and plasmid constructs.

miRNAs against coding sequences (CDSs) for mouse *Adat3* (NM_001100606), *Adat2* (NM_025748.4), *Wdr4* (NM_021322.2) and *Mettl1* (NM_010792.1) were generated using BLOCK-iT™ RNAi Designer (<https://rnaidesigner.thermofisher.com/rnaiexpress/>). Sense and antisense oligos (see supplementary table1 for sequences) were annealed and the resulting duplex was subcloned in pCAGGs-mir30 (Addgene plasmid # 12345)(Matsuda and Cepko, 2007) and NeuroD-miR30 vectors digested with Xhol and EcoRI. NeuroD-miR30 vector was generated by replacing the pCAGGs promoter in pCAGGSs-miR30 backbone with NeuroD promoter from the NeuroD-IRES-GFP plasmid (Hand and Polleux, 2011).

Wild-type (WT) mouse *Adat3* (NCBI Reference Sequence NM_001100606), *Adat2* (NM_025748.4), *Wdr4* (NM_021322.2) and *Mettl1* (NM_010792.1) CDSs were amplified from

E16.5 cortices using primers listed in Supplementary Table 1 and cloned into pJET 1.2 blunt vector using CloneJet PCR Cloning kit. They were further subcloned into psiSTRIKE DCX-IRES-GFP (provided by *J. Chelly (IGBMC, Strasbourg, France)*) and pnThx (Diebold et al., 2011) (*Adat3*), pet16B (Novagen (EMD Millipore)) (*Adat2*), NeuroD-IRES-GFP (Hand and Polleux, 2011) (*Adat2*, *Wdr4*, *Mettl1*), pCAGGs-IRES-GFP (Nguyen et al., 2006) (*Adat2*, *Adat3*, *Wdr4*, *Mettl1*) vectors by restriction-ligation. miR1-*Adat3* and miR1-*Wdr4* resistant constructs were obtained by site-directed mutagenesis using the primers indicated in supplementary table 1 and subcloned into the psiSTRIKE DCX-IRES-GFP (*Adat3*), NeuroD-IRES-GFP (*Wdr4*) and pCAGGs-IRES-GFP plasmids. Insensitivity of the vectors was validated by transfection of HEK239T cells together with the miRNA constructs. Mouse *Adat3* V128M, R112L, A180L and A180V variants were created from WT CDS by sequence- and ligation-independent cloning (SLIC) and subcloned into the psiSTRIKE DCX-iresGFP vector. Mouse *Wdr4* R215L variant and catalytically inactive *Adat2* (E73A) (Gerber and Keller, 1999) were generated from the WT *Wdr4* and *Adat2* CDSs respectively by site-directed mutagenesis using the primers listed in supplementary table 1. All the vectors used in this study were prepared using the EndoFree plasmid purification kit (Macherey Nagel).

Mice

All animal studies were conducted in accordance with French regulations (EU Directive 86/609 – French Act Rural Code R 214-87 to 126) and all procedures were approved by the local ethics committee and the Research Ministry (APAFIS#15691-201806271458609). Mice were bred at the IGBMC animal facility under controlled light/dark cycles, stable temperature (19°C) and humidity (50%) condition and were provided with food and water ad libitum. Timed-pregnant WT NMRI (Janvier-labs) and CD1 (Charles River Laboratories) females were used for *in utero* electroporation of the different constructs at embryonic day 14.5 (E14.5).

***In utero* electroporation**

In utero electroporation (IUE) was performed as described previously (Godin et al., 2012; Laguesse et al., 2015). Briefly, pregnant females were anesthetized with isoflurane (2L/min of oxygen; 4% isoflurane in the induction phase followed by 2% isoflurane during surgery; Tem Seg). The uterine horns were exposed, and a lateral ventricle of each embryo was injected using pulled glass capillaries (Harvard apparatus, 1.0OD*0.58ID*100mmL) with Fast Green (1 µg/µl; Sigma) combined with different amounts of DNA constructs using a micro injector (Eppendorf Femto Jet). Plasmids were electroporated into the neuronal progenitors adjacent to the ventricle by 5 electric pulses (40V) for 50 ms at 950 ms intervals using electrodes (diameter 3 mm; Sonidel CUY650P3) and ECM-830 BTX square wave electroporator (VWR international). After electroporation, embryos were placed back in the abdominal cavity and the abdomen was sutured using surgical needle and thread. For E18.5 analysis, pregnant mice were sacrificed by cervical dislocation four days after surgery. For post-natal analysis, electroporated pups were sacrificed two days after birth (P2) by head sectioning. Conditions of IU with plasmids and concentration used are summarized in Supplementary Table 2.

Mouse brain fixation, cutting and immunolabelling

E18.5 and P2 animals were sacrificed by head sectioning and brains were fixed in 4% paraformaldehyde (PFA, Electron Microscopy Sciences) diluted in Phosphate buffered saline (PBS, HyClone) overnight at 4°C. WT E18 cryosections were prepared for immunolabeling as follows: after fixation, brains were rinsed and equilibrated in 20% sucrose in PBS overnight at 4°C, embedded in Tissue-Tek O.C.T. (Sakura), frozen on dry ice, cut coronally at the cryostat (18 µm thickness, Leica CM3050S) and maintained at -80°C until immunolabeling. For *IUE* analyses, vibratome section were prepared as follows: after fixation, brains were washed and embedded in a 4% low-melting agarose solution (Bio-Rad) and cut at a thickness of 60um coronally using a vibrating-blade microtome (Leica VT1000S, Leica Microsystems). Sections

were kept in PBS-azide 0,05% for short-term storage or in an antifreeze solution (30% Ethyleneglycol, 20% Glycerol, 30% DH2O, 20% PO4 buffer) for long-term storage. For immunolabeling cryosections and vibratome sections were permeabilized and blocked with blocking solution (5% Normal Donkey Serum (NDS, Dominic Dutscher), 0,1% Triton-X-100 in PBS) for 1h at room temperature (RT). Sections were then incubated with primary antibodies (see Supplementary Table 3) diluted in blocking solution overnight at 4°C and with secondary antibodies (see Supplementary Table 3) and DAPI (dilution 1/1000, 1mg/mL Sigma) diluted in PBS 0,1% Triton for 1h at RT. Slides were mounted using Aquapolymount mounting medium (Polysciences Inc).

Primary neuronal culture and immunolabeling

Cortices from WT CD1 mice at E15.5 were dissected in cold PBS supplemented with BSA (3 mg/mL), MgSO4 (1 mM, Sigma), and D-glucose (30 mM, Sigma). They were enzymatically dissociated in Neurobasal medium containing papain (20 U/mL, Worthington) and DNase I (100 µg/mL, Sigma) for 20 minutes at 37°C, washed 5 minutes with Neurobasal medium containing Ovomucoide (15 mg/mL, Worthington) and manually triturated in Optimem with 20mM D-glucose. 2×10^5 cells per well were plated in a 24-well plate previously coated overnight at 4°C with poly-D-lysine (1 mg/mL, Sigma). Cells were then either fixed 2h after plating or cultured in Neurobasal medium supplemented with B27, L-glutamine (2 mM) and penicillin-streptomycin (5 U/mL and 50 mg/mL, respectively) till DIV2 and fixed in 4% PFA and 4% sucrose in PBS for 15 minutes at RT. Cells were then blocked for 1 hour in 0,1% Triton X-100, 5% NDS in PBS and primary antibodies (see Supplementary Table 3) were added overnight at 4°C. Next day they were washed and incubated with secondary antibodies (see Supplementary Table 3) and DAPI (dilution 1/1000, 1mg/mL Sigma) for 1 hour at RT. Subsequently, they were mounted in Aquapolymount mounting medium (Polysciences Inc).

Fluorescent-activated cell sorting (FACS)

3 to 4 cortices from Rosa26-loxSTOP-YFP; NEXCRE/+ mouse embryos were dissected at E16 and dissociated as described above. Cells were then resuspended in 500 µl of Staining solution (10% FBS + 0,02% Sodium Azide in PBS) and incubated 20 min on ice in the dark with Anti-CD24-APC (0, 06 µg /100 µl final). Cells were washed two times with HBSS (Gibco) and passed through a 40 µm filter (Filcon FACS). Two different populations were sorted: YFP-/CD24- corresponding to progenitors and YFP+/CD24+, corresponding to neurons. Sorting experiments were carried out in BD Aria II flow cytometer with 488 and 633 lasers to excite YFP and APC respectively. Setting of YFP and CD24 gates was done using littermate YFP- embryos (ROSA26-loxSTOP-YFP;NEXCRE-), which were processed in the same way and stained with the Rat IgG2b-APC isotype control antibody (clone eB149/10H5, ThermoFischer Scientific (#17-4031-82)).

Cell culture and transfections

Human embryonic kidney 293T (HEK293T) cells were cultured in Dulbecco's modified Eagle's medium (DMEM, GIBCO) with 10% foetal calf serum (FCS), penicillin 100 U/mL and streptomycin 100 µg/mL. Mouse neuroblastoma N2A (ATCC) cells were cultured in DMEM (GIBCO) supplemented with 5% Fetal Calf Serum (FCS) and Gentamycin 40µg/ml in a humidified atmosphere containing 5% CO₂ at 37°C. All the cells were incubated in a humidified atmosphere containing 5% CO₂ at 37°C.

For transfection, when cells reached 40-60% confluence, they were transfected using Lipofectamine 2000 (Invitrogen) according to the manufacturer's protocol. 48h post-transfection expression of transfected genes was assessed by RT-qPCR and western blot analysis. To assess miRNAs or shRNA knock-down efficacy and validate specificity of antibodies, HEK293T cells were transfected with 1 µg of pCAGGs-*Adat3*-IRES-GFP,

pCAGGs-*Adat2*-IRES-GFP, pCAGGs-*Wdr4*-IRES-GFP or pCAGGs-*Mettl1*-IRES GFP and 3 µg of pCAGGs-miR30-scramble or pCAGGs-miR30-miRNA targeting *Adat3*, *Adat2*, *Wdr4* or *Mettl1* respectively. To validate miRNA resistant vectors, HEK293T cells were transfected with 1 µg of either pCAGGs-*Adat3*-IRES-GFP (WT or miRNA resistant) or pCAGGs-*Wdr4*-IRES-GFP (WT or miRNA resistant) vector together with 3 µg of pCAGGs-miR30-scramble or pCAGGs-miR30-miRNA targeting *Adat3* or *Wdr4* respectively. For confirmation of expression of mutant vectors 1 µg of the respective psiSTRIKE DCX-IRES-GFP or NeuroD-IRES-GFP vectors were transfected in N2A cells.

RNA extraction, cDNA synthesis and RT-qPCR

Total RNA from brain tissues or cells was extracted using TRIzol reagent (Thermo Fischer Scientific). and submitted to DNaseI treatment (TurboDNase, ThermoFisher). cDNA samples were synthetized with SuperScript IV Reverse Transcriptase (Invitrogen) and quantitative RT-PCR (qRT-PCR) was done with amplified cDNA and SYBR Green Master Mix (Roche) together with 0,1 µM of forward and reverse primers using a Lightcycler® 480 (Roche). For assessment of expression pattern of *Adat3*, *Adat2*, *Wdr4* and *Mettl1* by RT-qPCR, WT NMRI mouse cortices from E12.5-E18.5 were processed as described above and RT-qPCRs were carried using the primers listed in Supplementary Table 1. For assessment of knock-down efficiency by RT-qPCR, total RNA and cDNA was prepared from HEK293T cells transfected with the corresponding vectors as described above and RT-qPCRs were carried using the primers listed in Supplementary Table 1.

Protein extraction and western blot

Proteins from mouse cortices (E12.5 to P2) or from transfected cells (HEK 293T, N2A) were extracted as follows: cells or tissue were lysed in RIPA buffer (50 mM Tris pH 8.0, 150 mM

NaCl, 5 mM EDTA pH 8.0, 1% Triton X-100, 0.5% sodium deoxycholate, 0.1% SDS) supplemented with EDTA-free protease inhibitors (cOmpleteTM, Roche) for 30 min, then cells debris were removed by high speed centrifugation at 4°C for 25 min. Protein concentration was measured by spectrophotometry using Bio-Rad Bradford protein assay reagent. Samples were denatured at 95°C for 10 min in Laemmli buffer (Bio-Rad) with 2% β-mercaptoethanol, then resolved by SDS-PAGE and transferred onto nitrocellulose membranes. Membranes were blocked in 5% milk in PBS buffer with 0.1% Tween (PBS-T) and incubated overnight at 4°C with the appropriate primary antibody in blocking solution. Membranes were washed 3 times in PBS-T, incubated at room temperature for 1 h with HRP-coupled secondary antibodies at 1:10,000 dilution in PBS-T, followed by 3 times PBS-T washes. Visualization was performed by quantitative chemiluminescence using SuperSignal West Pico PLUS Chemiluminescent Substrate (Sigma). Signal intensity was quantified using ImageQuant LAS 600 (GE Healthcare). Primary and secondary coupled HRP antibodies used for western blot are described in Supplementary Table 3. All immunoblot experiments consisted of at least three independent replicates.

Detection of I₃₄ tRNA modification level in human lymphoblastoid lines

Total RNA was extracted from human lymphoblastoid lines with TRIzol reagent (Thermo Fisher Scientific) according to manufacturer's protocol and treated with DNase I (TurboDNase, ThermoFisher). cDNA samples were synthesized with SuperScript IV Reverse Transcriptase (Invitrogen) using tRNA specific reverse primers and tRNA-Val-AAC and tRNA-Thr-AGT specific amplification was carried out by Polymerase Chain reaction (PCR) (Annealing at 60°C) with Phusion Hot Start II High Fidelity DNA polymerase with gene specific primers for tRNA-Val-AAC and tRNA-Thr-AGT (See Supplementary Table 1). cDNA libraries were generated using the Diagenode MicroPlex Library Preparation Kit (C05010014) (following the manufacturer's protocol). Nucleotide barcode sequences were added to reverse primers to

allow discrimination between samples upon sequencing. Sequencing was performed in a HiSeq4000 Illumina sequencer (IGBMC, Strasbourg) as single-read 50 base reads following Illumina's instructions. Image analysis and base calling were performed using RTA 2.7.3 and bck2fastq. Number of reads containing G₃₄ was used to determine the level of I₃₄ modification (I₃₄ is read as G upon sequencing).

Generation of Rabbit antibodies for mouse ADAT3, ADAT2 and WDR4.

WT mouse ADAT3 and ADAT2 full length proteins were expressed by transformation of pnThx-*Adat3*, pet16B-*Adat2* vectors (Diebold et al., 2011) into BL21 (DE3) Rosetta®(DE3) *E. coli* cells (Novagene). Bacterial cultures were grown in 2XLB media for 5-6 hours at 37°C and 200rpm. Temperature was then decreased to 22°C and recombinant protein expression was induced by addition of 0.5 mM IPTG to the LB culture media that was grown O/N at 180rpm. Next day, Cultures were harvested, resuspended in resuspension buffer (200mM NaCl, 10mM Tris pH8) and sonicated on ice. The lysate was centrifuged and the supernatant was incubated with Talon Metal Affinity Resin (Clontech) for 2h at 4°C. The resin was washed with resuspension buffer to get rid of the unbound proteins. Adat3 was eluted from the column by incubating the resin with 3C protease and Adat2 was eluted by by addition of 200mM NaCl, 10mM Tris, 250mM Imidazole (pH8) buffer. Eluted proteins were concentrated using Amicon® Ultra 15ml Centrifugal Filters (Merck) and loaded on HiLoad® 16/600 Superdex® columns (Akta Pure, Purification system) for affinity-based protein purification. Eluted fractions containing mouse ADAT3, ADAT2 proteins were respectively pooled and dialyzed against PBS overnight using 3.5K Slide-A-Lyzer™ G2 Dialysis Cassettes (ThermoFisherScientific). Mouse WDR4 peptide "LKKKRQRSPFPGSPEQTK" previously used for generation of mouse Wdr4 antibody (Lee and Hsieh, 2018) was synthetized in IGBMC peptide synthesis facility and subsequently coupled to Ovalbumin carrier protein using Imject Maleimide-Activated BSA (77115, Thermo Fisher Scientific) prior to injection into the animals. Immunization was done as follows: 300 µg

of either ADAT3, ADAT2 or WDR4 peptides (in a 1:1 phosphate-buffered saline (PBS)/complete Freund adjuvant emulsion) were injected in anesthetized New Zealand female rabbit as 70 intradermal indulation points, with a glass syringe. One month later, 40 ml of blood was drawn every week four times and the serums were collected. Rabbits were boosted with 150 µg of peptide (in a 1:1 PBS/incomplete Freund adjuvant emulsion) and killed 12 days later, under anesthesia. Antibodies were purified from serum with SulfoLink-columns coupled to the immunogens (20325, Thermo Fischer Scientific) according to manufacturer's protocol and specificity validated by Western Blot.

Recombinant overproduction and purification of mWdr4/mMettl1 complexes.

Truncated (N1C1) mouse Wdr4-wt WT and Wdr4-R215L fused to a GST affinity tag were co-expressed with untagged full-length mouse Mettl1 in *E.coli*. Recombinant protein complexes were affinity-purified using Pierce GlutathioneAgarose beads (16102BID, ThermoFischer Scientific) according to manufacturer's protocol. GST-tag was removed by 3C protease (kind gift from Christophe Romier). Affinity-purified protein complexes were subjected to size-exclusion chromatography (Superdex S200 16/60 column) followed by SDS-PAGE analysis of peak fractions.

Image acquisition and analysis

Images for primary neuronal culture and expression pattern analyses were acquired using a TCS SP8 UV (Leica microsystems) using a 63x OIL HC PL APO CS2 and 20x IMM, HC PL APO CS2 objectives respectively and images for neuronal migration and expression pattern

analyses were acquired using a TCS SP8 X (Leica microsystems) confocal microscope using a 20x DRY HC PL APO CS2 objective. For all experiments, a Z-stack of 1,50 μ m was acquired. The image size was 524x524 for neuronal migration analysis and 1024x1024 for primary neuronal culture and expression analysis. Image analysis was done using ImageJ software (NIH). Cell counting was performed in 2 to 4 different brain sections of at least 3 different embryos or pups per condition. Only similarly electroporated regions were considered for further analysis. Cortical areas (upper cortical plate, lower cortical plate, intermediate zone, subventricular zone/ventricular zone) were delimited based on cell density (nuclei count with DAPI staining) using equivalent sized boxes. Number of GFP-positive cells was determined in each cortical area to establish the percentage of positive cells. All the experiments were done in at least three independent replicates.

Statistics

All statistics analyses were performed using GraphPad Prism 6 (GraphPad) and are represented as mean +/- S.E.M. The level of significance was set at $P < 0.05$ in all the statistical tests. All statistical tests used and n size numbers are shown in the figure legends.

Figures Legends

Table 1. Clinical features of patients with *ADAT3*, *WDR4* or *METTL1* variants. Patients identified in the current study are highlighted in bold. *In vivo* functional tests have been

performed for the variants depicted in red. ND: not determined; Comp.Het: Compound heterozygous.

Figure 1. Adat2/Adat3 and Wdr4/Mettl1 expression pattern in the mouse embryonic cerebral cortex. (A) RT-qPCR and (B) Western-Blot analysis performed on mouse WT cortices showing expression of Adat3, Adat2, Wdr4 and Mettl1 throughout development from E12.5 to P2 (n=3-5 brain per stage). Data are represented as means \pm S.E.M. Significance was calculated by one-way ANOVA (Tukey's multiple comparison test), *P < 0.05; **P < 0.01; ***P < 0.001; ****P < 0.0001. (C-E) E18.5 mouse forebrain coronal sections immunolabelled for (C) Adat3, (D) Adat2 and (E) Wdr4 (in green) and Tbr2 (intermediate progenitor marker, red) and counterstained with DAPI (blue) revealing expression of Adat3, Adat2 and Wdr4 in both progenitors and neurons. Close-up views of the white boxed area in CP and VZ/SVZ showing subcellular localization of Adat3, Adat2 and Wdr4 in the nucleus. CP cortical plate, IZ intermediate zone, SVZ subventricular zone, VZ ventricular zone. Scalebars, 100 μ m and 25 μ m for magnifications.

Figure 2. Knockdown of Adat3 or Wdr4 leads to abnormal radial migration of projection neurons. (A, C, E, F) Coronal sections of E18.5 (A, C) or P2 (E, F) mouse cortices electroporated at E14.5 with scramble, *Adat3* (A, E) or *Wdr4* (C, F) mi/shRNA under the NeuroD (ND) (A, C) or pCAGGS (E, F) promoters. GFP-positive electroporated cells are depicted in green. Nuclei are stained with DAPI. Scalebars, 100 μ m. (F) Percentage indicate the penetrance of each phenotype (number of embryos are indicated in brackets). (B, D) Quantification (means \pm S.E.M.) of the percentage of electroporated cells in the different cortical regions (Up CP: upper cortical plate, Lo CP: lower cortical plate, IZ: intermediate zone, SVZ: subventricular zone, WM: White matter) showing effect of (B) *Adat3* and (D) *Wdr4* knockdown on neuronal migration. Data were analyzed by two-way ANOVA (Bonferroni's multiple

comparisons test). Number of embryos analyzed: **B**, NeuroD Scramble, n = 8; NeuroD miR1-*Adat3*, n=9; NeuroD miR2-*Adat3*, n=10; **D**, NeuroD Scramble, n = 9; NeuroD miR1-*Wdr4*, n=7; NeuroD sh-*Wdr4*, n=5. ns non-significant; *P < 0.05; ***P < 0.001; ****P < 0.0001.

Figure 3. Role of Adat3 and Wdr4 in migrating neurons depends on their function within the Adat2/Adat3 and Mettl1/Wdr4 complexes. (A) Coronal sections of E18.5 mouse cortices electroporated at E14.5 with NeuroD (ND) scramble or *Adat3* miRNA together with empty vector or DCX WT Adat3 and NeuroD WT or Catalytically inactive (CI) Adat2. **(B)** Percentage (means \pm S.E.M.) of the positive electroporated cells in upper (Up CP) and lower (Lo CP) cortical plate, intermediate (IZ) and subventricular zone (SVZ) showing the need of catalytic-active Adat2 for Adat3 to rescue the faulty migration of *Adat3*-silenced neurons. **(C)** Representative coronal section of brains electroporated with NeuroD scramble or *Wdr4* miRNAs together with empty or NeuroD *Wdr4* constructs. **(D)** Quantification of the percentage of positive electroporated cells in Up CP, Lo CP and SVZ/IZ showing that expression of WT WDR4 protein is able to rescue *Wdr4*-induced abnormal migration. **(E, G)** Coronal sections of E18.5 mouse cortices electroporated at E14.5 with scramble, *Adat2* (**A, E**) or *Mettl1* (**C, F**) miRNAs under the NeuroD (ND) (**E**) or pCAGGS (**G**) promoters. **(F, G)** Analysis (means \pm S.E.M.) of the percentage of GFP-electroporated cells different regions showing impaired migration of (**F**) *Adat2* and (**D**) *Mettl1*-silenced neurons at E18.5. **(A, C, E, G)** GFP-positive electroporated cells are depicted in green. Nuclei are stained with DAPI. Scalebars, 100 μ m **(B, D, F, H)** Data were analyzed by two-way ANOVA (Tukey's multiple comparison test (**B, D**); Bonferroni's multiple comparisons test (**F, G**)). Number of embryos analyzed: **B**, NeuroD Scramble, n = 6; Empty+ NeuroD *Adat2* + NeuroD miR1-*Adat3* , n=8; NeuroD miR1-*Adat3* + DCX *Adat3* + NeuroD *Adat2*, n=9; NeuroD miR1-*Adat3* + DCX *Adat3* + NeuroD *Adat2* C.I, n= 3; **D**, NeuroD Scramble, n = 5; NeuroD miR1-*Wdr4* + Empty, n=6; NeuroD miR1-*Wdr4* + NeuroD *Wdr4*, n=7; **F**, NeuroD Scramble and NeuroD miR1-*Adat2*, n=8; NeuroD miR2-*Adat2*,

n=9; **H**, pCAGGS Scramble, n=4 ; pCAGGS miR1-*Mettl1*, n=5; pCAGGS miR2-*Mettl1*, n=6. ns non-significant; *P < 0.05; **P < 0.01; ***P < 0.001; ****P < 0.0001.

Figure 4. Adat3, Wdr4 and Mettl1 variants impair protein expression and tRNA modification activity. (A, B) Pedigrees of patients with newly-identified (A) *ADAT3* and (B) *METTL1* variants. (C-E) Schematic representation of human *ADAT3* (C), *WDR4* (D) and *METTL1* (E) protein indicating position of the previously and newly identified (Bold) variants. Variants depicted in the same color were found in the same patient. *In vivo* functional tests have been performed for the variants that are underlined. (F) Structure of the Trm8/Trm82 complex showing that formation of the Trm8/Trm82 complex induces a rearrangement of the Trm8 structure with the loop harbouring R195 undergoing a large movement (double arrow, middle panel) towards the S-adenosyl-methionine (SAM) binding site. Left panel: ribbon representation of the crystallographic structure of Trm8 alone. Right panel: ribbon representation of the crystallographic structure of Trm8/Trm82 complex. Middle panel: superposition of the two crystallographic structures. Important amino acid residues are represented as sticks and labelled. Hydrogen bonds formed by glutamate E204 are represented as dotted lines. (G) Size-exclusion chromatography of affinity-purified WT (blue) or R215 (red) mWDR4/mMETTL1 complexes showing that R215L mutation does not prevent the formation of a stable mWDR4/mMETTL1 complex. (H) Western Blot analysis of p.Val144Met or p.Arg128Leu homozygous patient LCLs revealing reduced ADATt3 protein levels in comparison to controls (Controls, n=8; both mutant conditions, n=3; One-way ANOVA, Bonferroni's multiple comparisons test). (I) Sequencing of tRNA-Val-AAC (left panel) and tRNA-Thr-AGT (right panel) isolated from healthy (purple) or patient (p.Val144Met) (green) LCLs showing a drastic reduction of the percentage of I₃₄ modification in patient cells. (+/-. n=3; p.Val144Met/p.Val144Met, n=4, Unpaired Student's t-test, two-tailed). ns non-significant; *P < 0.05; **P < 0.01; ***P < 0.001.

Figure 5. Missense variants in *Adat3* and *Wdr4* impair neuronal migration. (A) Coronal sections of E18.5 mouse cortices electroporated at E14.5 with NeuroD scramble or *Adat3* miRNAs with DCX Empty or mouse WT *Adat3* at two different concentration (0.5 or 0.75 μ g/ μ l), V128M, R112L, A180L or A180V constructs together with NeuroD Adat2. GFP-positive electroporated cells are depicted in green. Nuclei are stained with DAPI. (C) Coronal section of cortices electroporated with NeuroD scramble or miR1-*Wdr4* with NeuroD empty, increasing amount of *Wdr4* WT (0.25 or 0.5 μ g/ μ l) or R215L constructs. Scalebars, 100 μ m. (B, C, E) Analysis of percentage (means \pm S.E.M.) of electroporated cells in upper (Up CP) and lower (Lo CP) cortical plate, intermediate (IZ) and subventricular zone (SVZ) showing a dose-dependent rescue of *Adat3* and *Wdr4* phenotype with wild-type proteins and absence of rescue with most of the variants. Data were analyzed by two-way ANOVA (Tukey's multiple comparison test). Number of embryos analyzed: **B, C** NeuroD Scramble, n = 7; NeuroD miR1-*Adat3* + Empty, n=5; NeuroD miR1-*Adat3* + DCX WT (0.5 μ g/ μ L), n=4; NeuroD miR1-*Adat3* + DCX WT (0.75 μ g/ μ L), n= 6; NeuroD miR1-*Adat3* + DCX V128M, n=5; NeuroD miR1-*Adat3* + DCX R112L, n=7; NeuroD miR1-*Adat3* + DCX A180L, n=7; NeuroD miR1-*Adat3* + DCX A180V, n=6; **D**, NeuroD Scramble + Empty, n = 5; NeuroD miR1-*Wdr4* + Empty, n=6; NeuroD miR1-*Wdr4* + NeuroD WT (0.25 μ g/ μ L), n=5; NeuroD miR1-*Wdr4* + NeuroD WT (0.5 μ g/ μ L), n=7; NeuroD miR1-*Wdr4* + NeuroD R215L, n=5. ns non-significant; *P < 0.05; **P < 0.01; ***P < 0.001; ****P < 0.0001.

References

Abbasi-Moheb, L., Mertel, S., Gonsior, M., Nouri-Vahid, L., Kahrizi, K., Cirak, S., Wieczorek, D., Motazacker, M.M., Esmaeeli-Nieh, S., Cremer, K., *et al.* (2012). Mutations in NSUN2 cause autosomal-recessive intellectual disability. *Am J Hum Genet* 90, 847-855.

Addis, L., Ahn, J.W., Dobson, R., Dixit, A., Ogilvie, C.M., Pinto, D., Vaags, A.K., Coon, H., Chaste, P., Wilson, S., *et al.* (2015). Microdeletions of ELP4 Are Associated with Language Impairment, Autism Spectrum Disorder, and Mental Retardation. *Hum Mutat* 36, 842-850.

Agris, P.F., Vendeix, F.A., and Graham, W.D. (2007). tRNA's wobble decoding of the genome: 40 years of modification. *J Mol Biol* 366, 1-13.

Alazami, A.M., Hijazi, H., Al-Dosari, M.S., Shaheen, R., Hashem, A., Aldahmesh, M.A., Mohamed, J.Y., Kentab, A., Salih, M.A., Awaji, A., *et al.* (2013). Mutation in ADAT3, encoding adenosine deaminase acting on transfer RNA, causes intellectual disability and strabismus. *J Med Genet* 50, 425-430.

Alexandrov, A., Chernyakov, I., Gu, W., Hiley, S.L., Hughes, T.R., Grayhack, E.J., and Phizicky, E.M. (2006). Rapid tRNA decay can result from lack of nonessential modifications. *Mol Cell* 21, 87-96.

Alexandrov, A., Martzen, M.R., and Phizicky, E.M. (2002). Two proteins that form a complex are required for 7-methylguanosine modification of yeast tRNA. *Rna* 8, 1253-1266.

Arrondel, C., Missoury, S., Snoek, R., Patat, J., Menara, G., Collinet, B., Liger, D., Durand, D., Gribouval, O., Boyer, O., *et al.* (2019). Defects in t(6)A tRNA modification due to GON7 and YRDC mutations lead to Galloway-Mowat syndrome. *Nat Commun* 10, 3967.

Bento-Abreu, A., Jager, G., Swinnen, B., Rue, L., Hendrickx, S., Jones, A., Staats, K.A., Taes, I., Eykens, C., Nonneman, A., *et al.* (2018). Elongator subunit 3 (ELP3) modifies ALS through tRNA modification. *Hum Mol Genet* 27, 1276-1289.

Blaesius, K., Abbasi, A.A., Tahir, T.H., Tietze, A., Picker-Minh, S., Ali, G., Farooq, S., Hu, H., Latif, Z., Khan, M.N., *et al.* (2018). Mutations in the tRNA methyltransferase 1 gene TRMT1 cause congenital microcephaly, isolated inferior vermian hypoplasia and cystic leukomalacia in addition to intellectual disability. *Am J Med Genet A* 176, 2517-2521.

Blanco, S., Dietmann, S., Flores, J.V., Hussain, S., Kutter, C., Humphreys, P., Lukk, M., Lombard, P., Treps, L., Popis, M., *et al.* (2014). Aberrant methylation of tRNAs links cellular stress to neuro-developmental disorders. *EMBO J* 33, 2020-2039.

Braun, D.A., Rao, J., Mollet, G., Schapiro, D., Daugeron, M.C., Tan, W., Gribouval, O., Boyer, O., Revy, P., Jobst-Schwan, T., *et al.* (2017). Mutations in KEOPS-complex genes cause nephrotic syndrome with primary microcephaly. *Nat Genet* 49, 1529-1538.

Braun, D.A., Shril, S., Sinha, A., Schneider, R., Tan, W., Ashraf, S., Hermle, T., Jobst-Schwan, T., Widmeier, E., Majmundar, A.J., *et al.* (2018). Mutations in WDR4 as a new cause of Galloway-Mowat syndrome. *Am J Med Genet A* 176, 2460-2465.

Cantara, W.A., Crain, P.F., Rozenski, J., McCloskey, J.A., Harris, K.A., Zhang, X., Vendeix, F.A., Fabris, D., and Agris, P.F. (2011). The RNA Modification Database, RNAMDB: 2011 update. *Nucleic Acids Res* 39, D195-201.

Chen, X., Gao, Y., Yang, L., Wu, B., Dong, X., Liu, B., Lu, Y., Zhou, W., and Wang, H. (2018). Speech and language delay in a patient with WDR4 mutations. *Eur J Med Genet*.

Cheng, I.C., Chen, B.C., Shuai, H.H., Chien, F.C., Chen, P., and Hsieh, T.S. (2016). Wuho Is a New Member in Maintaining Genome Stability through its Interaction with Flap Endonuclease 1. *PLoS Biol* 14, e1002349.

Cohen, J.S., Srivastava, S., Farwell, K.D., Lu, H.M., Zeng, W., Lu, H., Chao, E.C., and Fatemi, A. (2015). ELP2 is a novel gene implicated in neurodevelopmental disabilities. *Am J Med Genet A* 167, 1391-1395.

Crick, F.H. (1966). Codon--anticodon pairing: the wobble hypothesis. *J Mol Biol* 19, 548-555.

Darvish, H., Azcona, L.J., Alehabib, E., Jamali, F., Tafakhori, A., Ranji-Burachaloo, S., Jen, J.C., and Paisan-Ruiz, C. (2019). A novel PUS7 mutation causes intellectual disability with autistic and aggressive behaviors. *Neurol Genet* 5, e356.

Davarniya, B., Hu, H., Kahrizi, K., Musante, L., Fattahi, Z., Hosseini, M., Maqsoud, F., Farajollahi, R., Wienker, T.F., Ropers, H.H., *et al.* (2015). The Role of a Novel TRMT1 Gene Mutation and Rare GRM1 Gene Defect in Intellectual Disability in Two Azeri Families. *PLoS One* 10, e0129631.

de Brouwer, A.P.M., Abou Jamra, R., Kortel, N., Soyris, C., Polla, D.L., Safra, M., Zisso, A., Powell, C.A., Rebelo-Guiomar, P., Dinges, N., *et al.* (2018). Variants in PUS7 Cause Intellectual Disability with Speech Delay, Microcephaly, Short Stature, and Aggressive Behavior. *Am J Hum Genet* 103, 1045-1052.

de Crecy-Lagard, V., Boccaletto, P., Mangleburg, C.G., Sharma, P., Lowe, T.M., Leidel, S.A., and Bujnicki, J.M. (2019). Matching tRNA modifications in humans to their known and predicted enzymes. *Nucleic Acids Res* 47, 2143-2159.

Deng, Y., Zhou, Z., Lin, S., and Yu, B. (2020). METTL1 limits differentiation and functioning of EPCs derived from human-induced pluripotent stem cells through a MAPK/ERK pathway. *Biochem Biophys Res Commun*.

Diebold, M.L., Fribourg, S., Koch, M., Metzger, T., and Romier, C. (2011). Deciphering correct strategies for multiprotein complex assembly by co-expression: application to complexes as large as the histone octamer. *J Struct Biol* 175, 178-188.

Doan, R.N., Lim, E.T., De Rubeis, S., Betancur, C., Cutler, D.J., Chiocchetti, A.G., Overman, L.M., Soucy, A., Goetze, S., Autism Sequencing, C., *et al.* (2019). Recessive gene disruptions in autism spectrum disorder. *Nat Genet* 51, 1092-1098.

Domingo-Gallego, A., Furlano, M., Pybus, M., Barraca, D., Martinez, A.B., Mora Munoz, E., Torra, R., and Ars, E. (2019). Novel homozygous OSGEP gene pathogenic variants in two unrelated patients with Galloway-Mowat syndrome: case report and review of the literature. *BMC Nephrol* 20, 126.

El-Hattab, A.W., Saleh, M.A., Hashem, A., Al-Owain, M., Asmari, A.A., Rabei, H., Abdelraouf, H., Hashem, M., Alazami, A.M., Patel, N., *et al.* (2016). ADAT3-related intellectual disability: Further delineation of the phenotype. *Am J Med Genet A*.

Fahiminiya, S., Almuriekhi, M., Nawaz, Z., Staffa, A., Lepage, P., Ali, R., Hashim, L., Schwartzentruber, J., Abu Khadija, K., Zaineddin, S., *et al.* (2014). Whole exome sequencing unravels disease-causing genes in consanguineous families in Qatar. *Clinical genetics* 86, 134-141.

Fang, H., Zhang, L., Xiao, B., Long, H., and Yang, L. (2020). Compound heterozygous mutations in PUS3 gene identified in a Chinese infant with severe epileptic encephalopathy and multiple malformations. *Neurol Sci* 41, 465-467.

Forde, K.M., Molloy, B., Conroy, J., Green, A.J., King, M.D., Buckley, P.G., Ryan, S., and Gorman, K.M. (2020). Expansion of the phenotype of biallelic variants in TRIT1. *Eur J Med Genet* 63, 103882.

Freude, K., Hoffmann, K., Jensen, L.R., Delatycki, M.B., des Portes, V., Moser, B., Hamel, B., van Bokhoven, H., Moraine, C., Fryns, J.P., *et al.* (2004). Mutations in the FTSJ1 gene coding for a novel S-adenosylmethionine-binding protein cause nonsyndromic X-linked mental retardation. *Am J Hum Genet* 75, 305-309.

Froukh, T., Nafie, O., Al Hait, S.A.S., Laugwitz, L., Sommerfeld, J., Sturm, M., Baraghiti, A., Issa, T., Al-Nazer, A., Koch, P.A., *et al.* (2020). Genetic basis of neurodevelopmental disorders in 103 Jordanian families. *Clin Genet* 97, 621-627.

Froyen, G., Bauters, M., Boyle, J., Van Esch, H., Govaerts, K., van Bokhoven, H., Ropers, H.H., Moraine, C., Chelly, J., Fryns, J.P., *et al.* (2007). Loss of SLC38A5 and FTSJ1 at Xp11.23 in three brothers with non-syndromic mental retardation due to a microdeletion in an unstable genomic region. *Hum Genet* 121, 539-547.

Gerber, A.P., and Keller, W. (1999). An adenosine deaminase that generates inosine at the wobble position of tRNAs. *Science* 286, 1146-1149.

Gillis, D., Krishnamohan, A., Yaacov, B., Shaag, A., Jackman, J.E., and Elpeleg, O. (2014). TRMT10A dysfunction is associated with abnormalities in glucose homeostasis, short stature and microcephaly. *J Med Genet* 51, 581-586.

Godin, J.D., Thomas, N., Laguesse, S., Malinouskaya, L., Close, P., Malaise, O., Purnelle, A., Raineteau, O., Campbell, K., Fero, M., *et al.* (2012). p27(Kip1) is a microtubule-associated protein that promotes microtubule polymerization during neuron migration. *Dev Cell* 23, 729-744.

Grosjean, H., Auxilien, S., Constantinesco, F., Simon, C., Corda, Y., Becker, H.F., Foiret, D., Morin, A., Jin, Y.X., Fournier, M., *et al.* (1996). Enzymatic conversion of adenosine to inosine and to N1-methylinosine in transfer RNAs: a review. *Biochimie* 78, 488-501.

Guy, M.P., Shaw, M., Weiner, C.L., Hobson, L., Stark, Z., Rose, K., Kalscheuer, V.M., Gecz, J., and Phizicky, E.M. (2015). Defects in tRNA Anticodon Loop 2'-O-Methylation Are Implicated in Nonsyndromic X-Linked Intellectual Disability due to Mutations in FTSJ1. *Hum Mutat* 36, 1176-1187.

Hand, R., and Polleux, F. (2011). Neurogenin2 regulates the initial axon guidance of cortical pyramidal neurons projecting medially to the corpus callosum. *Neural Dev* 6, 30.

Hengel, H., Buchert, R., Sturm, M., Haack, T.B., Schelling, Y., Mahajnah, M., Sharkia, R., Azem, A., Balousha, G., Ghanem, Z., *et al.* (2020). First-line exome sequencing in Palestinian and Israeli Arabs with neurological disorders is efficient and facilitates disease gene discovery. *Eur J Hum Genet*.

Hyun, H.S., Kim, S.H., Park, E., Cho, M.H., Kang, H.G., Lee, H.S., Miyake, N., Matsumoto, N., Tsukaguchi, H., and Cheong, H.I. (2018). A familial case of Galloway-Mowat syndrome due to a novel TP53RK mutation: a case report. *BMC Med Genet* 19, 131.

Igoillo-Esteve, M., Genin, A., Lambert, N., Desir, J., Pirson, I., Abdulkarim, B., Simonis, N., Drielsma, A., Marselli, L., Marchetti, P., *et al.* (2013). tRNA methyltransferase homolog gene

TRMT10A mutation in young onset diabetes and primary microcephaly in humans. PLoS Genet 9, e1003888.

Jovine, L., Djordjevic, S., and Rhodes, D. (2000). The crystal structure of yeast phenylalanine tRNA at 2.0 Å resolution: cleavage by Mg(2+) in 15-year old crystals. J Mol Biol 301, 401-414.

Kearse, M.G., and Wilusz, J.E. (2017). Non-AUG translation: a new start for protein synthesis in eukaryotes. Genes Dev 31, 1717-1731.

Kernohan, K.D., Dyment, D.A., Pupavac, M., Cramer, Z., McBride, A., Bernard, G., Straub, I., Tetreault, M., Hartley, T., Huang, L., et al. (2017). Matchmaking facilitates the diagnosis of an autosomal-recessive mitochondrial disease caused by biallelic mutation of the tRNA isopentenyltransferase (TRIT1) gene. Hum Mutat 38, 511-516.

Khan, M.A., Rafiq, M.A., Noor, A., Hussain, S., Flores, J.V., Rupp, V., Vincent, A.K., Malli, R., Ali, G., Khan, F.S., et al. (2012). Mutation in NSUN2, which encodes an RNA methyltransferase, causes autosomal-recessive intellectual disability. Am J Hum Genet 90, 856-863.

Komara, M., Al-Shamsi, A.M., Ben-Salem, S., Ali, B.R., and Al-Gazali, L. (2015). A Novel Single-Nucleotide Deletion (c.1020delA) in NSUN2 Causes Intellectual Disability in an Emirati Child. J Mol Neurosci 57, 393-399.

Laguisse, S., Creppe, C., Nedialkova, D.D., Prevot, P.P., Borgs, L., Huysseune, S., Franco, B., Duyssens, G., Krusy, N., Lee, G., et al. (2015). A Dynamic Unfolded Protein Response Contributes to the Control of Cortical Neurogenesis. Dev Cell 35, 553-567.

Lee, C.C., and Hsieh, T.S. (2018). WUHO/WDR4 deficiency inhibits cell proliferation and induces apoptosis via DNA damage in mouse embryonic fibroblasts. Cell Signal 47, 16-26.

Lentini, J.M., Alsaif, H.S., Fafeih, E., Alkuraya, F.S., and Fu, D. (2020). DALRD3 encodes a protein mutated in epileptic encephalopathy that targets arginine tRNAs for 3-methylcytosine modification. Nat Commun 11, 2510.

Leulliot, N., Chaillet, M., Durand, D., Ulryck, N., Blondeau, K., and van Tilbeurgh, H. (2008). Structure of the yeast tRNA m7G methylation complex. Structure 16, 52-61.

Lin, P.Y., Tseng, M.H., Zenker, M., Rao, J., Hildebrandt, F., Lin, S.H., Lin, C.C., Chang, J.H., Hsu, C.H., Lee, M.D., et al. (2018a). Galloway-Mowat syndrome in Taiwan: OSGEP mutation and unique clinical phenotype. Orphanet J Rare Dis 13, 226.

Lin, S., Liu, Q., Lelyveld, V.S., Choe, J., Szostak, J.W., and Gregory, R.I. (2018b). Mettl1/Wdr4-Mediated m 7 G tRNA Methylome Is Required for Normal mRNA Translation and Embryonic Stem Cell Self-Renewal and Differentiation. Molecular Cell.

Lyu, X., Yang, Q., Li, L., Dang, Y., Zhou, Z., Chen, S., and Liu, Y. (2020). Adaptation of codon usage to tRNA I34 modification controls translation kinetics and proteome landscape. PLoS Genet 16, e1008836.

Machnicka, M.A., Milanowska, K., Osman Oglou, O., Purta, E., Kurkowska, M., Olchowik, A., Januszewski, W., Kalinowski, S., Dunin-Horkawicz, S., Rother, K.M., et al. (2013). MODOMICS: a database of RNA modification pathways--2013 update. Nucleic Acids Res 41, D262-267.

Martinez, F.J., Lee, J.H., Lee, J.E., Blanco, S., Nickerson, E., Gabriel, S., Frye, M., Al-Gazali, L., and Gleeson, J.G. (2012). Whole exome sequencing identifies a splicing mutation in NSUN2 as a cause of a Dubowitz-like syndrome. *J Med Genet* 49, 380-385.

Matsuda, T., and Cepko, C.L. (2007). Controlled expression of transgenes introduced by in vivo electroporation. *Proc Natl Acad Sci U S A* 104, 1027-1032.

Michaud, J., Kudoh, J., Berry, A., Bonne-Tamir, B., Lalioti, M.D., Rossier, C., Shibuya, K., Kawasaki, K., Asakawa, S., Minoshima, S., *et al.* (2000). Isolation and characterization of a human chromosome 21q22.3 gene (WDR4) and its mouse homologue that code for a WD-repeat protein. *Genomics* 68, 71-79.

Monies, D., Vagbo, C.B., Al-Owain, M., Alhomaidi, S., and Alkuraya, F.S. (2019). Recessive Truncating Mutations in ALKBH8 Cause Intellectual Disability and Severe Impairment of Wobble Uridine Modification. *Am J Hum Genet* 104, 1202-1209.

Na, W., Fu, L., Luu, N., and Shi, Y.B. (2020). Direct activation of tRNA methyltransferase-like 1 (Mettl1) gene by thyroid hormone receptor implicates a role in adult intestinal stem cell development and proliferation during *Xenopus tropicalis* metamorphosis. *Cell Biosci* 10, 60.

Narayanan, M., Ramsey, K., Grebe, T., Schrauwen, I., Szelinger, S., Huentelman, M., Craig, D., Narayanan, V., and Group, C.R.R. (2015). Case Report: Compound heterozygous nonsense mutations in TRMT10A are associated with microcephaly, delayed development, and periventricular white matter hyperintensities. *F1000Res* 4, 912.

Nguyen, L., Besson, A., Heng, J.I., Schuurmans, C., Teboul, L., Parras, C., Philpott, A., Roberts, J.M., and Guillemot, F. (2006). p27kip1 independently promotes neuronal differentiation and migration in the cerebral cortex. *Genes Dev* 20, 1511-1524.

Pereira, P.L., Magnol, L., Sahun, I., Brault, V., Duchon, A., Prandini, P., Gruart, A., Bizot, J.C., Chadeaux-Vekemans, B., Deutsch, S., *et al.* (2009). A new mouse model for the trisomy of the Abcg1-U2af1 region reveals the complexity of the combinatorial genetic code of down syndrome. *Hum Mol Genet* 18, 4756-4769.

Phizicky, E.M., and Alfonzo, J.D. (2010). Do all modifications benefit all tRNAs? *FEBS Lett* 584, 265-271.

Ramos, J., Han, L., Li, Y., Hagelskamp, F., Kellner, S.M., Alkuraya, F.S., Phizicky, E.M., and Fu, D. (2019). Formation of tRNA Wobble Inosine in Humans Is Disrupted by a Millennia-Old Mutation Causing Intellectual Disability. *Mol Cell Biol* 39.

Ramser, J., Winnepenninckx, B., Lenski, C., Errijgers, V., Platzer, M., Schwartz, C.E., Meindl, A., and Kooy, R.F. (2004). A splice site mutation in the methyltransferase gene FTSJ1 in Xp11.23 is associated with non-syndromic mental retardation in a large Belgian family (MRX9). *J Med Genet* 41, 679-683.

Rastegari, E., Kajal, K., Tan, B.S., Huang, F., Chen, R.H., Hsieh, T.S., and Hsu, H.J. (2020). WD40 protein Wuho controls germline homeostasis via TRIM-NHL tumor suppressor Mei-p26 in *Drosophila*. *Development* 147.

Reinthalter, E.M., Lal, D., Jurkowski, W., Feucht, M., Steinbock, H., Gruber-Sedlmayr, U., Ronen, G.M., Geldner, J., Haberlandt, E., Neophytou, B., *et al.* (2014). Analysis of ELP4, SRPX2, and interacting genes in typical and atypical rolandic epilepsy. *Epilepsia* 55, e89-93.

Salehi Chaleshtori, A.R., Miyake, N., Ahmadvand, M., Bashti, O., Matsumoto, N., and Noruzinia, M. (2018). A novel 8-bp duplication in ADAT3 causes mild intellectual disability. *Hum Genome Var* 5, 7.

Schaub, M., and Keller, W. (2002). RNA editing by adenosine deaminases generates RNA and protein diversity. *Biochimie* 84, 791-803.

Shaheen, R., Abdel-Salam, G.M., Guy, M.P., Alomar, R., Abdel-Hamid, M.S., Afifi, H.H., Ismail, S.I., Emam, B.A., Phizicky, E.M., and Alkuraya, F.S. (2015). Mutation in WDR4 impairs tRNA m(7)G46 methylation and causes a distinct form of microcephalic primordial dwarfism. *Genome Biol* 16, 210.

Shaheen, R., Han, L., Faqeih, E., Ewida, N., Alobeid, E., Phizicky, E.M., and Alkuraya, F.S. (2016). A homozygous truncating mutation in PUS3 expands the role of tRNA modification in normal cognition. *Hum Genet*.

Shaheen, R., Mark, P., Prevost, C.T., AlKindi, A., Alhag, A., Estwani, F., Al-Sheddi, T., Alobeid, E., Alenazi, M.M., Ewida, N., et al. (2019a). Biallelic variants in CTU2 cause DREAM-PL syndrome and impair thiolation of tRNA wobble U34. *Hum Mutat* 40, 2108-2120.

Shaheen, R., Tasak, M., Maddirevula, S., Abdel-Salam, G.M.H., Sayed, I.S.M., Alazami, A.M., Al-Sheddi, T., Alobeid, E., Phizicky, E.M., and Alkuraya, F.S. (2019b). PUS7 mutations impair pseudouridylation in humans and cause intellectual disability and microcephaly. *Hum Genet* 138, 231-239.

Sharkia, R., Zalan, A., Jabareen-Masri, A., Zahalka, H., and Mahajnah, M. (2018). A new case confirming and expanding the phenotype spectrum of ADAT3-related intellectual disability syndrome. *European Journal of Medical Genetics*.

Sobreira, N., Schiettecatte, F., Valle, D., and Hamosh, A. (2015). GeneMatcher: a matching tool for connecting investigators with an interest in the same gene. *Hum Mutat* 36, 928-930.

Spears, J.L., Rubio, M.A., Gaston, K.W., Wywial, E., Strikoudis, A., Bujnicki, J.M., Papavasiliou, F.N., and Alfonzo, J.D. (2011). A single zinc ion is sufficient for an active *Trypanosoma brucei* tRNA editing deaminase. *J Biol Chem* 286, 20366-20374.

Sprinzl, M., Horn, C., Brown, M., Ioudovitch, A., and Steinberg, S. (1998). Compilation of tRNA sequences and sequences of tRNA genes. *Nucleic Acids Res* 26, 148-153.

Takano, K., Nakagawa, E., Inoue, K., Kamada, F., Kure, S., Goto, Y., and Japanese Mental Retardation, C. (2008). A loss-of-function mutation in the FTSJ1 gene causes nonsyndromic X-linked mental retardation in a Japanese family. *American journal of medical genetics Part B, Neuropsychiatric genetics : the official publication of the International Society of Psychiatric Genetics* 147B, 479-484.

Thomas, E., Lewis, A.M., Yang, Y., Chanprasert, S., Potocki, L., and Scott, D.A. (2019). Novel Missense Variants in ADAT3 as a Cause of Syndromic Intellectual Disability. *J Pediatr Genet* 8, 244-251.

Torres, A.G., Pineyro, D., Rodriguez-Escriba, M., Camacho, N., Reina, O., Saint-Leger, A., Filonava, L., Batlle, E., and Ribas de Pouplana, L. (2015). Inosine modifications in human tRNAs are incorporated at the precursor tRNA level. *Nucleic Acids Res* 43, 5145-5157.

Trimouille, A., Lasseaux, E., Barat, P., Deiller, C., Drunat, S., Rooryck, C., Arveiler, B., and Lacombe, D. (2017). Further delineation of the phenotype caused by biallelic variants in the WDR4 gene. *Clin Genet.*

Tsutsumi, S., Sugiura, R., Ma, Y., Tokuoka, H., Ohta, K., Ohte, R., Noma, A., Suzuki, T., and Kuno, T. (2007). Wobble inosine tRNA modification is essential to cell cycle progression in G(1)/S and G(2)/M transitions in fission yeast. *J Biol Chem* 282, 33459-33465.

Wu, J., Hou, J.H., and Hsieh, T.S. (2006). A new Drosophila gene wh (wuho) with WD40 repeats is essential for spermatogenesis and has maximal expression in hub cells. *Dev Biol* 296, 219-230.

Yarham, J.W., Lamichhane, T.N., Pyle, A., Mattijssen, S., Baruffini, E., Bruni, F., Donnini, C., Vassilev, A., He, L., Blakely, E.L., *et al.* (2014). Defective i6A37 modification of mitochondrial and cytosolic tRNAs results from pathogenic mutations in TRIT1 and its substrate tRNA. *PLoS Genet* 10, e1004424.

Yew, T.W., McCreight, L., Colclough, K., Ellard, S., and Pearson, E.R. (2015). tRNA methyltransferase homologue gene TRMT10A mutation in young adult-onset diabetes with intellectual disability, microcephaly and epilepsy. *Diabet Med.*

Zhang, K., Lentini, J.M., Prevost, C.T., Hashem, M.O., Alkuraya, F.S., and Fu, D. (2020). An intellectual disability-associated missense variant in TRMT1 impairs tRNA modification and reconstitution of enzymatic activity. *Hum Mutat* 41, 600-607.

Zhang, L.S., Liu, C., Ma, H., Dai, Q., Sun, H.L., Luo, G., Zhang, Z., Zhang, L., Hu, L., Dong, X., *et al.* (2019). Transcriptome-wide Mapping of Internal N(7)-Methylguanosine Methylome in Mammalian mRNA. *Mol Cell* 74, 1304-1316 e1308.

Zung, A., Kori, M., Burundukov, E., Ben-Yosef, T., Tatoor, Y., and Granot, E. (2015). Homozygous deletion of TRMT10A as part of a contiguous gene deletion in a syndrome of failure to thrive, delayed puberty, intellectual disability and diabetes mellitus. *Am J Med Genet A* 167, 3167-3173.

Supplementary material

Content:

- Supplementary Figure legends
- Supplementary Table 1 : List of sense and antisense oligos used in this work.
- Supplementary Table 2 : Condition of *in utero* electroporation used in this work.
- Supplementary Table 3 : List of primary and secondary antibodies used in this work.

Supplementary Figure legends

Supplementary Figure 1. Adat3, Adat2 and Wdr4 antibody validation and *in vitro* cortical immunostainings. (A-C) Western blot analysis of HEK293T cells protein lysates confirming the specificity of homemade antibodies. Cells were transfected with pCAGGs (A) Adat3, (B) Adat2 and (C) Wdr4 constructs together with scramble, miRNA or shRNA targeting each gene. (D) Western blot of extracts from progenitors (YFP-; CD24-, expressing Pax6 and Tbr2 transcription factors) and neurons (YFP+; CD24+, expressing β -III-tubulin) isolated by FACS from Rosa26-loxSTOP-YFP; NEX E16.5 cortices showing both Wdr4 and Mettl1 expression in cortical neurons and progenitors (n=3 independent experiments). GAPDH was used as a loading control. (E) Representative cortical neurons immunostained for Adat3 (red), Adat2 (red), Wdr4 (red), Mettl1 (red), Tbr2 (green), α -tubulin (green) and β -III-tubulin (gray) and counterstained with Dapi (blue) at 0 or 2 days *in vitro* (DIV). Arrows point to neurons (cells positive for β -III-Tubulin). Arrowheads point to intermediate progenitors (cells positive for Tbr2). Scalebars, 25 μ m.

Supplementary Figure 2. Acute depletion of *Adat3* and *Wdr4* impairs neuronal migration. (A-D) Validation of knockdown efficiency of *Adat3*, *Adat2* and *Wdr4* miRNAs and shRNAs by (A, C) RT-qPCR and (B, D) Western blot analysis (n=3 for each condition; One-way ANOVA (Bonferroni's multiple comparisons test)). Actin and α -Tubuline (α -Tub) were used as loading controls. (E, G) Coronal sections of E18.5 mouse cortices electroporated at E14.5 with Scramble, *Adat3* or *Wdr4* miRNAs or *Wdr4* shRNA under pCAGGS promoter. GFP-positive electroporated cells are depicted in green. Nuclei are stained with DAPI. Scalebars, 100 μ m. (F, H) Percentage (means \pm S.E.M.) of electroporated cells in upper (Up CP) and lower (Lo CP) cortical plate, intermediate (IZ) and subventricular zone (SVZ) showing altered distribution of (F) *Adat3* and (H) *Wdr4*-silenced cells. Data were analyzed by two-way ANOVA (Bonferroni's multiple comparisons test). Number of embryos analyzed: F, pCAGGS Scramble, n=4 ; pCAGGS miR1-*Adat3*, n=8; pCAGGS miR2-*Adat3*, n=7; H, pCAGGS Scramble, n=11; pCAGGS miR1-*Wdr4*, n=8; pCAGGS sh-*Wdr4*, n=6. ns non-significant; *P < 0.05; **P < 0.01; ***P < 0.001; ****P < 0.0001.

Supplementary Figure 3. Overexpression of WT and missense *Adat3* and *Wdr4* variants does not impair neuronal migration. (A-B) Western blot analysis of N2A cells protein lysates validating miR1-*Adat3* (A) and miR1-*Wdr4* (B) resistant *Adat3* and *Wdr4* constructs. (C) Western Blot analysis of protein extracts from N2A cells transfected with WT or V128M mouse *Adat3* plasmids together with empty or *Adat2* constructs demonstrating the need of *Adat2* for *Adat3* expression. (D) Western Blot analysis of N2A cells transfected with WT or C1 *Adat2* confirming similar expression of both proteins. (E, G, I) Coronal sections of E18.5 mouse cortices electroporated at E14.5 with NeuroD (ND) Scramble and the *Adat3*, *Adat2* and *Wdr4* constructs as indicated. GFP-positive electroporated cells are depicted in green. Nuclei are stained with DAPI. Scalebars, 100 μ m. (F, H, I) Quantification of the percentage (means \pm S.E.M.) of electroporated cells in upper (Up CP) and lower (Lo CP) cortical plate, intermediate

(IZ) and subventricular zone (SVZ) showing (**F**) the requirement of both Adat3 and Adat2 to rescue the migration phenotype induced by *Adat3* knock-down and (**H, J**) the correct positioning of cells overexpressing WT or mutant (**H**) Adat3 or (**J**) Wdr4 proteins. Data were analyzed by two-way ANOVA (Tukey's multiple comparison test). Number of embryos analyzed: **F**, NeuroD Scramble, n =6; NeuroD Scramble + NeuroD Adat2, n=7; NeuroD miR1-*Adat3* + Empty , n=8; NeuroD miR1-*Adat3* + DCX Adat3, n=3; NeuroD miR1-*Adat3* + DCX Adat3 + NeuroD Adat2, n=8; **H**, Empty, n= 6; Empty + NeuroD Adat2, n= 7; DCX WT (1 μ g/ μ L) + NeuroD Adat2, n=8; DCX V128M + NeuroD Adat2, n=5; DCX R112L + NeuroD Adat2, n=6; DCX A180L + NeuroD Adat2, n=6; DCX A180V + NeuroD Adat2, n=5; **J**, Empty, n=5; Neuro Wdr4 WT, n=6; NeuroD Wdr4 R215L, n=5. ns non-significant; **P < 0.01.

Supplementary Figure 4. Identification of *ADAT3*, *WDR4* and *METTL1* variants. (A-C)

Pedigrees of patients with previously published (**A, B**) *ADAT3* and (**C**) *WDR4* variants analyzed in the study. (**D**) *In silico* prediction of sequence changes identified in patients with SIFT, Mutation taster and Polyphen-2. (**E, F**) Alignment of (**E**) *METTL1* and (**F**) *WDR4* proteins across several species (human, mouse, yeast) showing the conservation of (**E**) p.Ile120 and p.Arg174 *METTL1* residues and (**F**) p.Arg170 *WDR4* mutated amino acid.

Supplementary Figure 5. Expression of *ADAT3* and *WDR4* mouse mutated proteins. (A, B)

(A) Alignment of *ADAT3* (**A**) and *WDR4* (**B**) protein across human and mouse showing the conservation of the (**A**) p.Arg128, p.Val144, p.Ala196 *ADAT3* residue and (**B**) the p.Arg170 amino acid among both species. (**C, D**) Western blot analysis of N2A cells transfected with miRNA-resistant WT and mutant (**C**) DCX Adat3 or (**D**) NeuroD (ND) Wdr4 protein showing equivalent expression of indicated constructs.

Supplementary Table 1 : List of sense and antisense oligos used in this work.

miRNA and shRNA oligos	
Scramble#1 sense	5'TCGAGAaggatattgtgtgacagtgagcgAAATGTACTGCGCGTGGAGACtagtg aagccacagatgtGTCTCCACGCGCAGTACATT Tgcctactgcctcg 3'
Scramble #1 antisense	5'AATTCCcgaggcagtaggcAAATGTACTGCGCGTGGAGACtagtgcctactgtggcttcact aGTCTCCACGCGCAGTACATT TgcctactgtcaacagcaatatacctC 3'
Scramble#2 sense	5'TCGAGAaggatattgtgtgacagtgagcgATCTCGCTGGGCGAGAGTAAGtagt gaagccacagatgtACTTACTCTGCCAAGCGAGAGTgcctactgcctcg 3'
Scramble#2 antisense	5'AATTCCcgaggcagtaggcCTCTCGCTGGGCGAGAGTAAGtagtgcctactgtcaacagcaatatacctC 3'
Adat3 miR1 sense	5'TCGAGAaggatattgtgtgacagtgagcgGAGCTGATACTGGCCTATGCTtagtga agccacagatgtAGCATAGGCCAGTATCAGCTC tgcctactgcctcg 3'
Adat3 miR1 antisense	5'AATTCCcgaggcagtaggcAGAGCTGATACTGGCCTATGCTtagtgcctactgtcaacagcaatatacctC 3'
Adat3 miR2 sense	5'TCGAGAaggatattgtgtgacagtgagcgCCCTATGTGTGCAGTGCTATtagtga agccacagatgtATAGCCAGTGCACACATAGGGTgcctactgcctcg 3'
Adat3 miR2 antisense	5'AATTCCcgaggcagtaggcCCCTATGTGTGCAGTGCTATtagtgcctactgtcaacagcaatatacctC 3'
Adat2 miR1 sense	5'TCGAGAaggatattgtgtgacagtgagcgTGGTCGTCTATGGCTGTCAGAtagtga agccacagatgtTCTGACAGCCATAGACGACCAAtgcctactgcctcg 3'
Adat2 miR1 antisense	5'AATTCCcgaggcagtaggcTGGTCGTCTATGGCTGTCAGAtacatgtggcttcacta TCTGACAGCCATAGACGACCAcgcctactgtcaacagcaatatacctC 3'
Adat2 miR2 sense	5'TCGAGAaggatattgtgtgacagtgagcgCCTAACATTGCCTCTGCTGAtagtga agccacagatgtTCAGCAGAGGCAATGTTAGGtgcctactgcctcg 3'
Adat2 miR2 antisense	5'AATTCCcgaggcagtaggcCCTAACATTGCCTCTGCTGAtacatctgtggcttcacta TCAGCAGAGGCAATGTTAGGtgcctactgtcaacagcaatatacctC 3'
Wdr4 sh sense	5'TCGAGAaggatattgtgtgacagtgagcgACCGCATAGCATCGAGTCTTCTtagtga agccacagatgtGAAGAGACTCGATGCTATGGGGTgcctactgcctcg 3'
Wdr4 sh antisense	5'AATTCCcgaggcagtaggcCCCGCATAGCATCGAGTCTTCTtagtgcctactgtggcttcacta GAAGAGACTCGATGCTATGGGGTgcctactgtcaacagcaatatacctC 3'
Wdr4 miR1 sense	5'TCGAGAaggatattgtgtgacagtgagcgGCCGAGTGCACATCACTGACAAAtagtga agccacagatgtTTGTCAGTGTCACTCGGCTgcctactgcctcg 3'
Wdr4 miR1 antisense	5'AATTCCcgaggcagtaggcGCCGAGTGCACATCACTGACAAAtacatgtggcttcacta TTGTCAGTGTCACTCGGCTgcctactgtcaacagcaatatacctC 3'
Mettl1 miR1 sense	5'TCGAGAaggatattgtgtgacagtgagcgAAATGGACTGGCTGAGCTTAtacatgtggcttcacta agccacagatgtTAAAGCTCAGACCAGTCCATT Tgcctactgcctcg 3'
Mettl1 miR1 antisense	5'AATTCCcgaggcagtaggcAAATGGACTGGCTGAGCTTAtacatgtggcttcacta TAAAGCTCAGACCAGTCCATT TgcctactgtcaacagcaatatacctC 3'
Mettl1 miR2 sense	5'TCGAGAaggatattgtgtgacagtgagcgGTTCTTGCTCCGCTTATTCAtagtga agccacagatgtTGAATAAGCGGAGCAAAGAACtgcctactgcctcg 3'
Mettl1 miR2 antisense	5'AATTCCcgaggcagtaggcGTTCTTGCTCCGCTTATTCAtagtgcctactgtcaacagcaatatacctC 3'

Cloning of Adat3, Adat2, Wdr4 and Mettl1 CDSs from mouse cortices		
	Forward sequence	Reverse sequence
Adat3	5'ATGCAGCCCACCTCAGGCT3'	5'CTATGGGTGGGGTCCAGCT3'

<i>Adat2</i>	5'ATGGAGGAGAAGGTGGAGTCCAC 3'	5'TCAGGATTCTGACAATCCTT TTCCG3'
<i>Wdr4</i>	5'ATGGCAGCTCTGCGGG 3'	5'TCAGCAACTAAGGGCTGACTG G 3'
<i>Mettl1</i>	5'ATGATGGCGGGAGCCGAAG3'	5'CTAAGGCAGGGTGGGTTGG3'

Generation of microRNA resistant vectors			
Forward sequence	Reverse sequence (mutagenic)		
5'AAGCGCCAGACGTCCCGCCTC3'	5'GTCCAGGACAGGTGCAGCGTA AGCGGTATCAGCTCAC3'		
<i>Wdr4</i> miR1	5'AGGGCGCAGCGCGTCGCACGTG TCCG3'	5'TCCTGTTGGCGCTAGTAAGCG ATGTCACTCGCC3'	

Cloning of gene variants		
	Forward sequence	Reverse sequence
<i>Adat3</i> p.R112L	5'CGCTCTCTGGCGGAGCTCCTTCC CTTGCCGGCCGTGGACCCACG3'	5'CAAGGGAAGGAGCTCCGCCAG AGAGCG3'
<i>Adat3</i> p.V128M	5' CCTGGTGCCTATGCCTGCC 3'	5' AAAGGTGTGCCAGGCCACGT 3'
<i>Adat3</i> p.A180V	5'CCCACATGGAACGGGTGGTATGT GCGGCCAG3'	5'CGCACATACCACCCGTTCCAT GTGGGTTTG3'
<i>Adat3</i> p.A180L	5'CCCACATGGAACGGGTGGTATGT GCGGCCAG3'	5'CGCACATACCAACCGTTCCAT GTGGGTTTG3'
<i>Adat2</i> p.E73A	5'ATCAGGTCTAGACTGGTGTCA CAGC 3'	5' CAATGCCACCATGGCAGCATG 3'
<i>Wdr4</i> p.R215L	5'ATGAGAAGATCCTGGTCAGCTG3'	5'CCGGTCTGCAGTAAGCACAA 3'

RT-qPCR		
	Forward sequence	Reverse sequence
<i>Adat3</i>	5'CTCAGTCGAGCCCCGTTG3'	5'CGGCTCTGCTCCTCACTTT3'
<i>Adat2</i>	5'GCGCCTTATGAAAATCCCGC3'	5'AGGGATGCACTGAAACGGTC3'
<i>Wdr4</i>	5'CTCCTGGACGGCACGC3'	5'ATCACTGCCGTAGTGGAGA3'
<i>Mettl1</i>	5'TGAGAGTCGGGGGCCTG3'	5'CGCTCAAACAGTGGGTGTT3'
<i>Gapdh</i>	5'GCACAGTCAAGGCCGAGAAT3'	5'GCCTTCTCCATGGTGGTGAA3'
<i>HPRT1</i>	5'AGGCGAACCTCTCGGCTTC3'	5'TCATCATCACTAATCACGACGC C3'

Detection of I34 tRNA modification level in human lymphoblastoid lines		
	Forward sequence	Reverse sequence
<i>tRNA-Val-AAC</i>	5' GTTCCGTAGTGTAGTGG 3'	5'TGGTGTTCGCCCGGGTTT 3'
<i>tRNA-Thr-AGT</i>	5' CGCCGTGGCTTAGTTG 3'	5'ACCGCTGGGATTCGAAC3'

Supplementary Table 2 : Condition of *in utero* electroporation used in this work.

Ubiquitous Knock-down experiments	
Plasmid	Amount
NeuroD-IRES-GFP	1 µg/µl
pCAGGs-miR30-miRNA or pCAGGs-miR30-scramble	3 µg/µl

Neuron-specific Knock-down experiments	
Plasmid	Amount
NeuroD-IRES-GFP	1 µg/µl
NeuroD-miR30-miRNA or NeuroD-miR30-scramble	3 µg/µl
Neuron-specific Knock-down rescue experiments (<i>Adat3</i>)	
Plasmid	Amount
NeuroD-IRES-GFP	0.75 µg/µl
NeuroD-IRES-GFP or NeuroD- <i>Adat2</i> -IRES-GFP (WT or C.I.)	0.5 µg/µl
NeuroD-miR30-miRNA or NeuroD-miR30-scramble	3 µg/µl
psiSTRIKE DCX- <i>Adat3</i> (WT or mutant) miRNA insensitive IRES-GF or psiSTRIKE DCX-IRES-GFP	0.75 µg/µl
Neuron-specific Knock-down rescue experiments (<i>Wdr4</i>)	
Plasmid	Amount
NeuroD-IRES-GFP	1.5 µg/µl
NeuroD-IRES-GFP or NeuroD- <i>Wdr4</i> -IRES-GFP (WT or mutant)	0.5 µg/µl
NeuroD-miR30-miRNA or NeuroD-miR30-scramble	3 µg/µl

Supplementary Table 3 : List of primary and secondary antibodies used in this work.

Primary antibody	Host	Dilution	Antigen retrieval (IHC)	Used for	Provenance	Reference
GFP	Chicken	1/500	Ø	IHC	Abcam	GFP-1020
Pax6	Rabbit	1/500	Ø	IHC	Biolegends	901301
Tbr2	Rat	1/250	Ø	IHC	EBiosciences	14-4875-80
Tbr1	Rabbit	1/500	Ø	IHC	Abcam	ab31940
α-Tubulin	Mouse	1/500	Ø	IHC, WB	Merck	024M4767V
Adat3	Rabbit	1/500	2N HCl	IHC, WB	Homemade	Ø
Adat2	Rabbit	1/500	2N HCl	IHC, WB	Homemade	Ø
Wdr4	Rabbit	1/500	Ø	IHC, WB	Homemade	Ø
Mettl1	Rabbit	1/500	Ø	WB, IF	Merck	HPA020914

Secondary antibody	Host	Dilution	Used for	Provenance	Reference
Actin coupled HRP	Mouse	1/100 000	WB	Sigma-Aldrich	A3854
Goat-mouse-HRP	Mouse	1/10 000	WB	ThermoFisher Sc.	G-21040
Goat-rabbit-HRP	Rabbit	1/10 000	WB	ThermoFisher Sc.	G-21234
Goat-rat-HRP	Rat	1/10 000	WB	ThermoFisher Sc.	62-9520
Donkey-goat-488	Goat	1/1000	IF	ThermoFisher Sc.	A-11055
Donkey-mouse-488	Mouse	1/1000	IF	ThermoFisher Sc.	A-21202

Donkey-mouse-555	Mouse	1/1000	IF	ThermoFisher Sc.	A-31570
Donkey-rabbit-488	Rabbit	1/1000	IF	ThermoFisher Sc.	R-37118
Donkey-rabbit-555	Rabbit	1/1000	IF	ThermoFisher Sc.	A-31572
Donkey-rat-488	Rat	1/1000	IF	ThermoFisher Sc.	A-21208
Ki67 coupled-570	Rat	1/500	IF	eBioscience	41 5698 80

	This study	Alazami et al 2013	Elt Hattab et al 2016	Sharkia et al 2018	Hengel et al 2020	Salehi Chaleshtori et al 2018	Thomas et al 2019	This study	This study	This study	Shaheen et al 2015	Trimouille et al 2018	Chen et al 2018	Braun et al 2018	This study
Patients	1, 1F	24, 12M, 12F	15, 8M, 7F	2, 1M, 1F	2, NA	1, 1F	2, 1M, 1F	1, 1M	1, 1F	2, 2F	2, 2F	1, 1M	4, sex NA	1, XY but female genitalia	
Age at diagnosis	Patient 1 2y	2-24y	1-24y	14-15y	NA	6y	7-12y	Patient 2	Patient 3	Patient 4 4y	4m	After birth	1y	4-15y	Patient 5 2y
Genetics	Hom	Hom	Hom	Hom	Hom	Hom	Comp.Het	Hom	Hom	Comp.Het	Hom	Comp. Het	Comp. Het	Hom	Comp.Het
Type	ADAT3	ADAT3	ADAT3	ADAT3	ADAT3	ADAT3	ADAT3	WDR4	WDR4	WDR4	WDR4	WDR4	WDR4	WDR4	METTL1
Gene	c.335G >T (NM_138422)	c.430G>A (NM_138422)			c.99_106du pGAGCCC GG (NM_138422)	c.587C>T ; c586_587d elinsTT (NM_138422)	c.2T>C (NM_033 661)	c.2T>C (NM_033 661)	c.2T>C; c.567-2A>G (NM_033 661)	c.509G >T (NM_033 661)	c.509G >A; c.911_92 7dup (NM_033 661)	c.491A >C; c.940dup C (NM_033 661)	c.454-2A>C, splice site (NM_033 661)	c.521G>A; c.360T>G (NM_005371)	
Protein	p.Arg 128Leu	p.Val144Met			p.Glu36Gly fs*44	p.Ala196 Val; p.Ala196 Leu	p.Met1 Thr	p.Met1 Thr	p.Met1 Thr	p.Arg170 Leu	p.Arg170 Gln; p.Gln310 Glyfs*30	p.Asp164 Ala; p.Leu314 Profs*16	splice site variant	p.Arg174Gln; p.Ile120Met	
Clinical features															
Intellectual disability	1/1	24/24	15/15	2/2	2/2	1/1	2/2	1/1	1/1	1/1	2/2	2/2	1/1	ND	1/1
Epilepsy	0/1	ND	2/13	ND	ND	ND	ND				2/2	0/2	0/1	0/4	1/1
Hypotonia	1/1	10/24	6/15	2/2	2/2	ND	2/2				2/2	ND	0/1	ND	0/1
Microcephaly	1/1	11/24	11/15	2/2	NA	1/1	1/2	1/1	1/1	1/1	2/2	2/2	1/1	4/4	1/1
Corpus callosum hypoplasia	1/1	ND	9/13	1/2	ND	ND	ND				2/2	0/2	0/1	ND	1/1
Face abnormalities	1/1	ND	5/15	2/2	ND	1/1	0/2				2/2	2/2	0/1	ND	1/1
Motor development delay	0/1	ND	15/15	2/2	ND	ND	2/2				2/2	2/2	1/1	ND	0/1
Language delay	1/1	ND	15/15	ND	ND	1/1	2/2				ND	2/2	1/1	ND	1/1
Sleep disturbances	ND	ND	ND	ND	ND	ND	ND				ND	2/2	0/1	ND	ND
Growth retardation	1/1	22/24	11/15	2/2	ND	ND	2/2	1/1	1/1	1/1	2/2	2/2	1/1	4/4	1/1

Figure 1

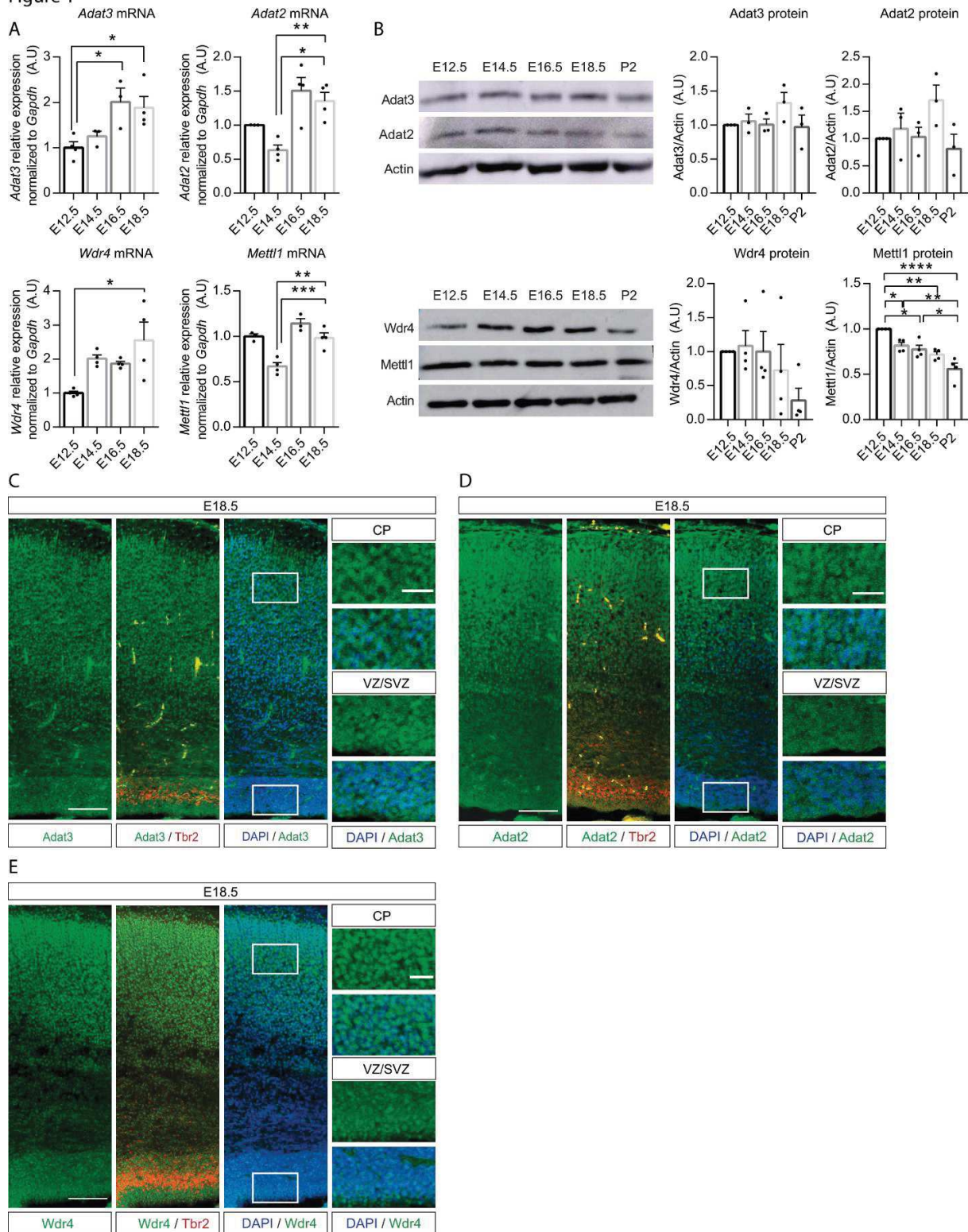


Figure 2

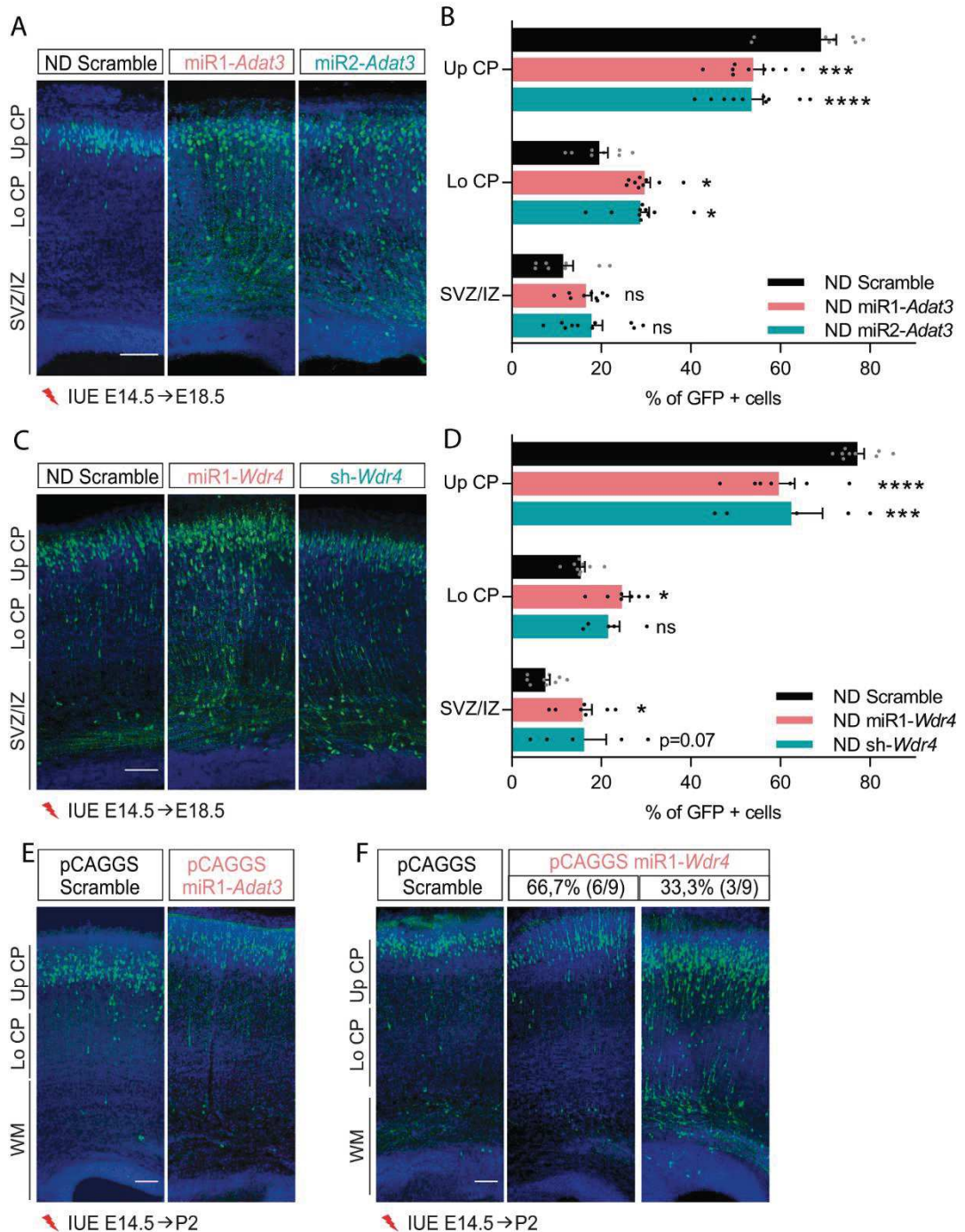


Figure 3

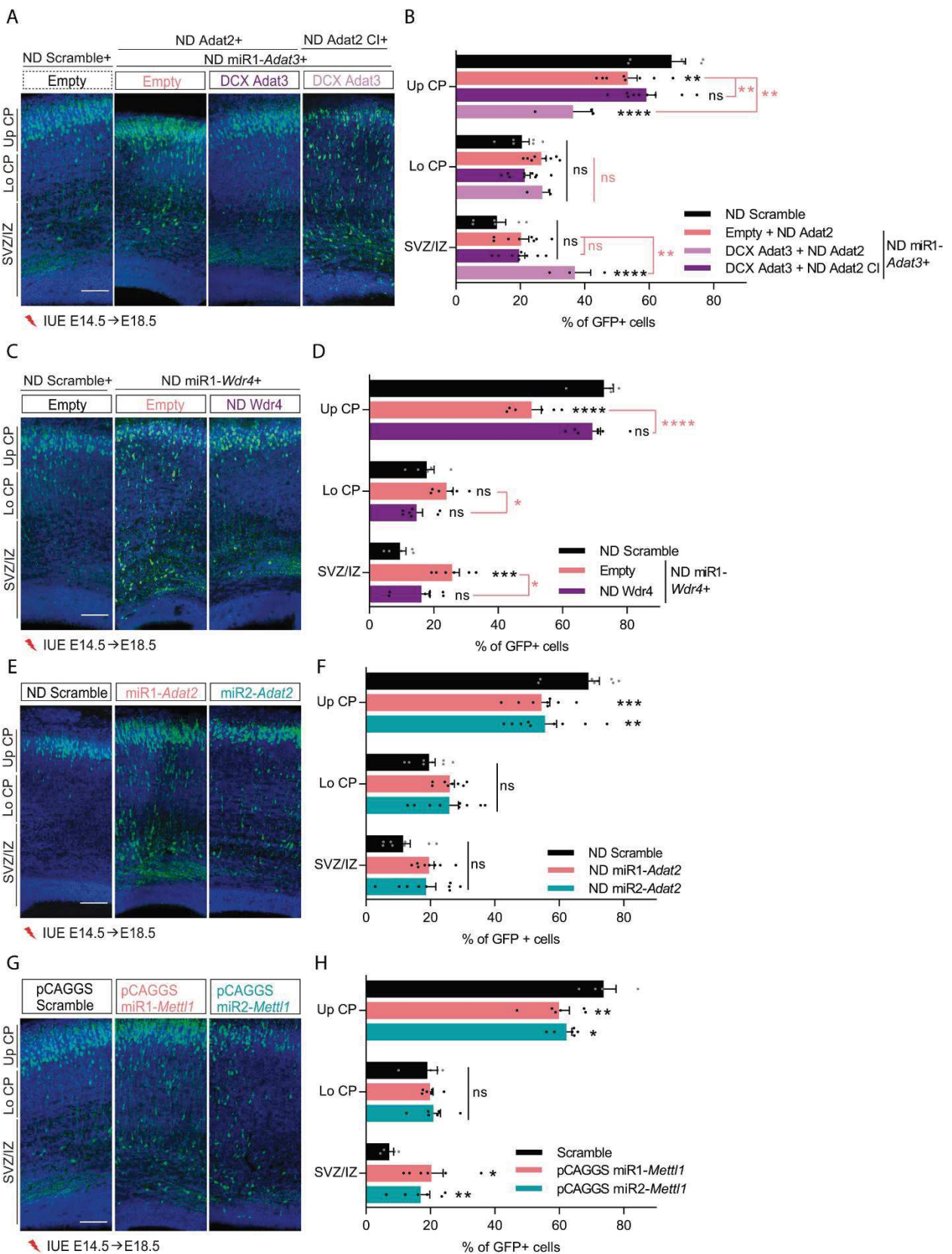


Figure 4

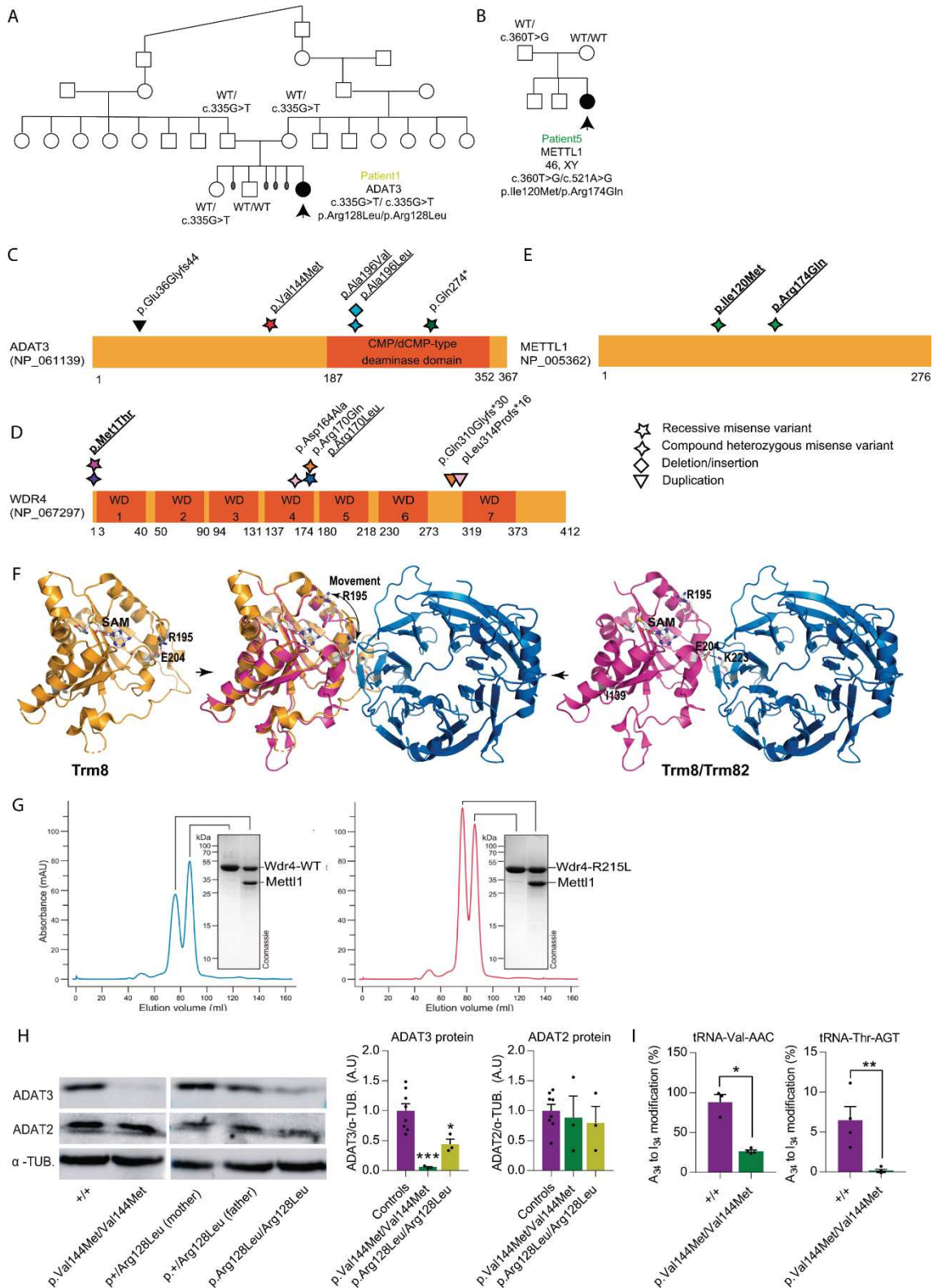
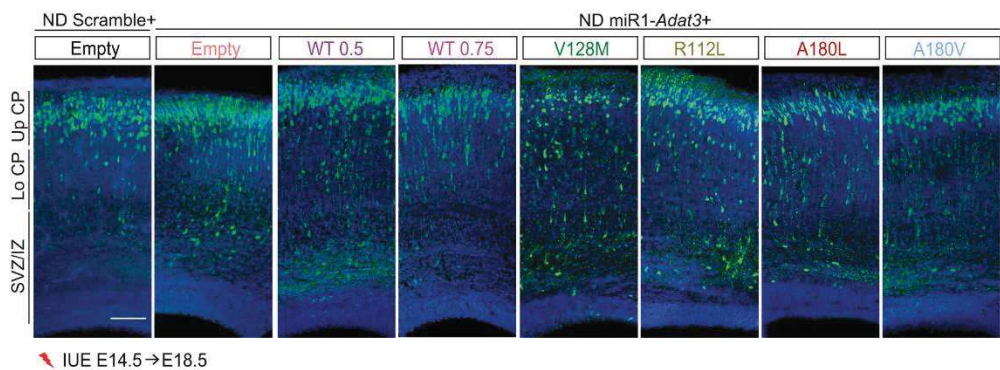
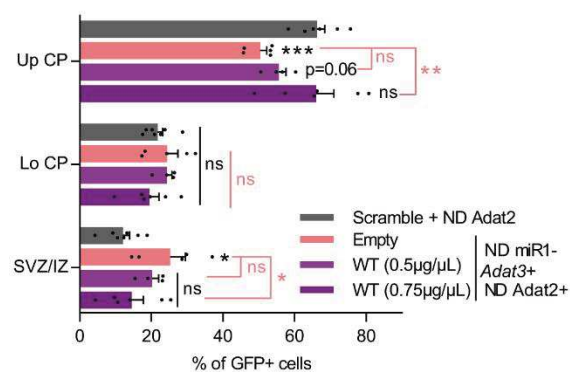


Figure 5

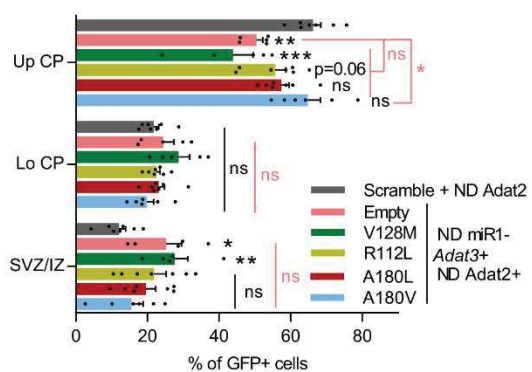
A



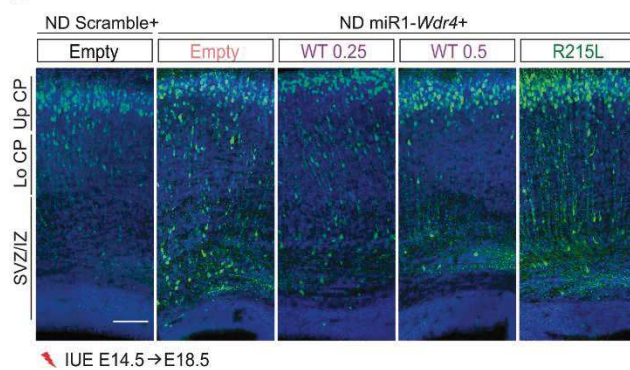
B



C



D



E

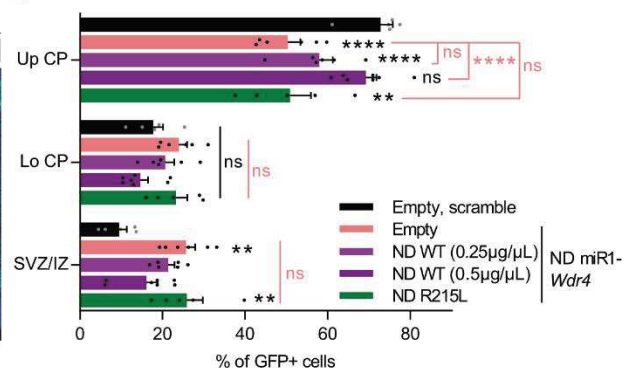


Figure S1

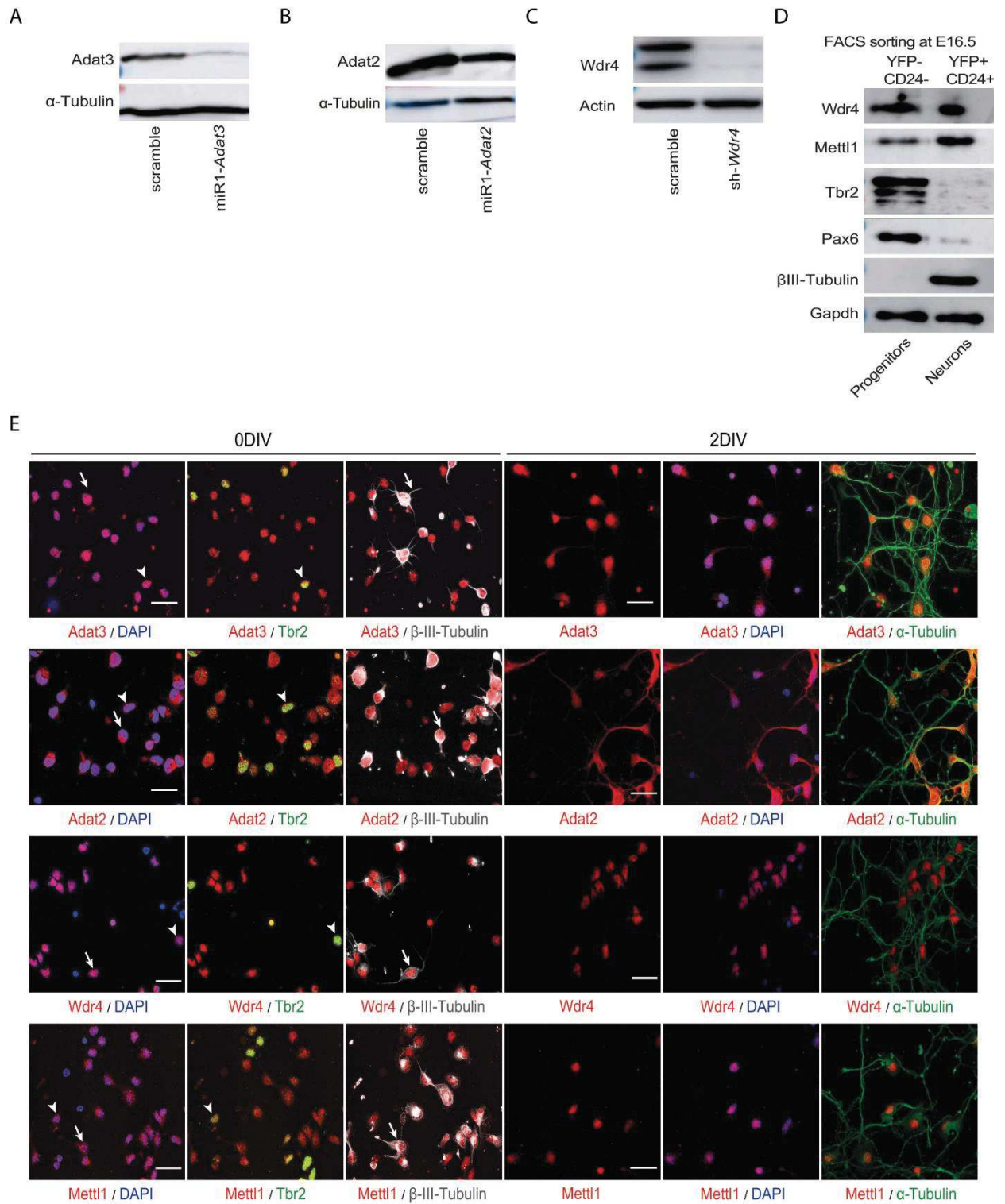


Figure S2

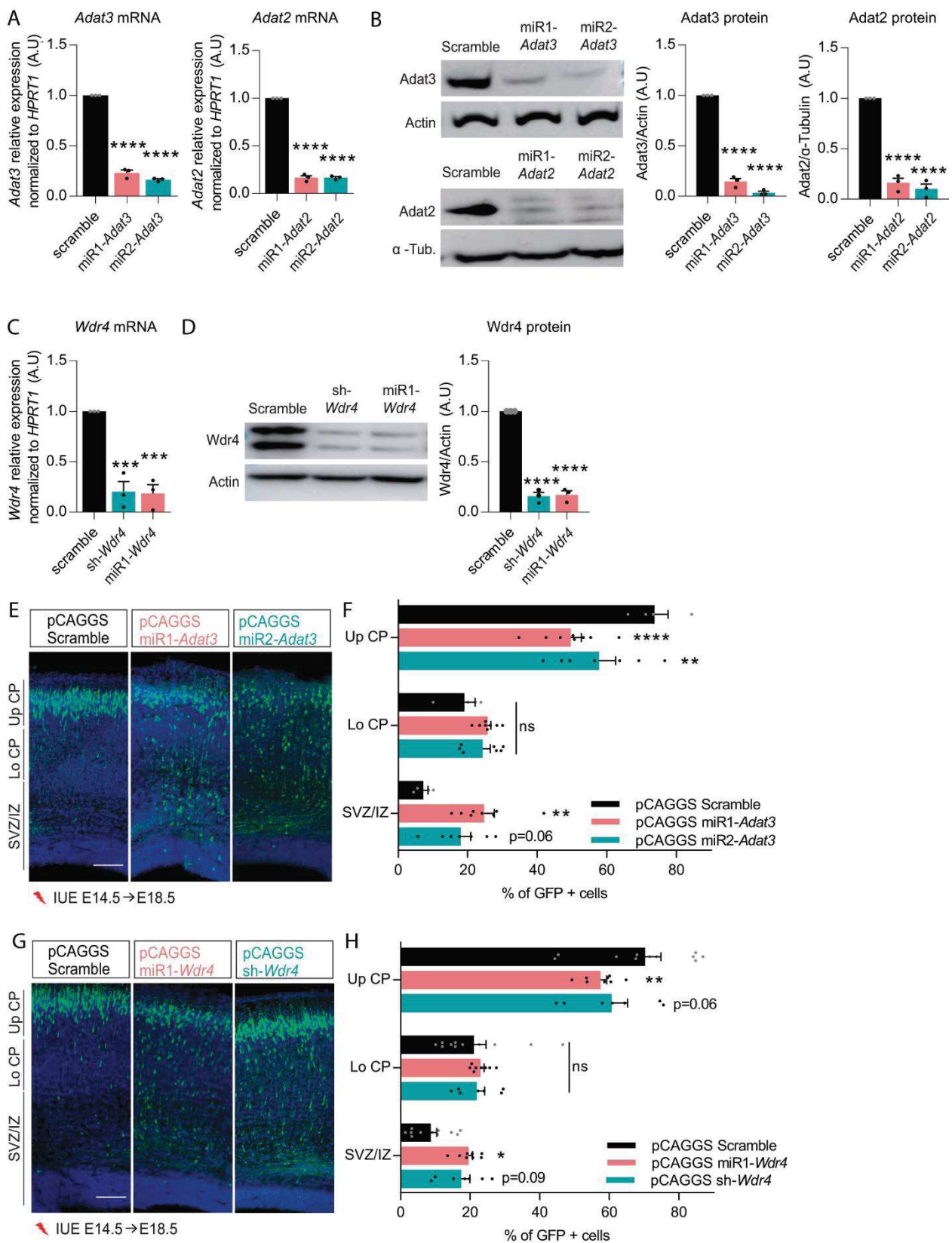


Figure S3

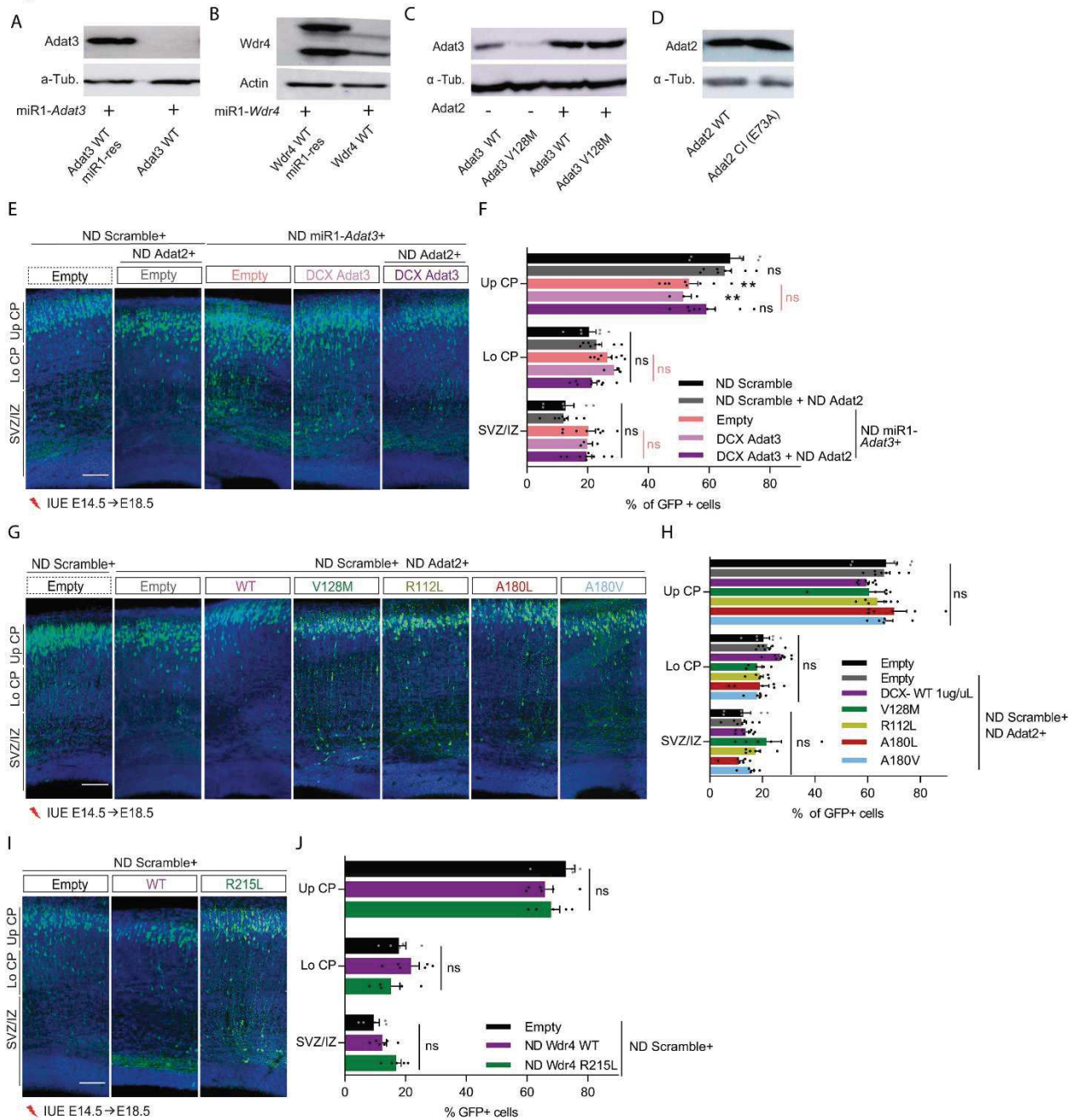
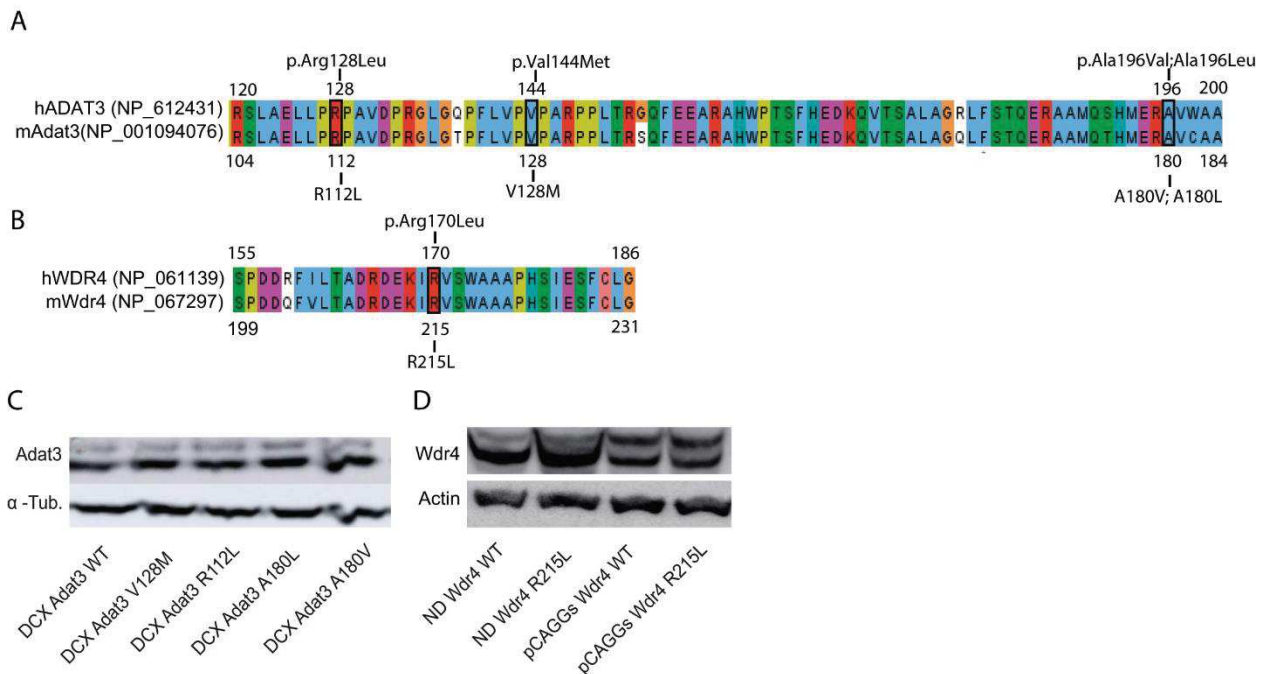


Figure S5



Preliminary results: Characterization of an *ADAT3*
p.V128M homozygous Knock-in mice line

Preliminary results: Characterization of an *ADAT3* p.V128M homozygous Knock-in mice line

Jordi Del Pozo Rodriguez^{1,2,3,4}, Efil Bayam^{1,2,3,4}, Peggy Tilly^{1,2,3,4}, Binnaz Yalcin^{1,2,3,4}, Marie-Christine Birling⁵ and Juliette D.Godin^{1,2,3,4}.

1. Institut de Génétique et de Biologie Moléculaire et Cellulaire, Illkirch, France.
2. Centre National de la Recherche Scientifique, UMR7104, Illkirch, France.
3. Institut National de la Santé et de la Recherche Médicale, INSERM, U1258, Illkirch, France.
4. Université de Strasbourg, Strasbourg, France.
5. Institute Clinique De La Souris, Illkirch, France.

Rational

ADAT3 stands for Adenosine Deaminase tRNA-specific 3, and forms a complex with *ADAT2* (Adenosine Deaminase tRNA-specific 2) to catalyze the formation of Inosine 34 (I34) of all mature tRNAs with the anticodon starting with A (tRNA ANN) at the wobble position (Gerber & Keller, 1999). Recently, several mutations in *ADAT3* were described in human patients presenting with microcephaly, intellectual disability (ID), strabismus and developmental delay as major phenotypes (Alazami et al., 2013; El-Hattab et al., 2016; Hengel et al., 2020; Salehi Chaleshtori et al., 2018; Rajech Sharkia, Abdelnaser Zalan, Azhar Jabareen-Masri, Hazar Zahalka, & Muhammad Mahajnah, 2018; Thomas et al., 2019). p.Val144Met *ADAT3* homozygous variant was found in a total of 43 patients, mostly in consanguineous Arab families (Alazami et al., 2013; El-Hattab et al., 2016; Hengel et al., 2020; Rajech Sharkia et al., 2018). It is thought to originate from a common founder, mutation having occurred between 65th to 111th generation ago. Interestingly, in silico modeling revealed significant changes in the conformation of the mutant p.Val144Met *ADAT3* protein that are thought to disturb the *ADAT2-ADAT3* heterodimer and/or tRNA binding (Alazami et al., 2013). More recently, it was shown that p.Val144Met *ADAT3* retains its ability to interact with *ADAT2*. However mutant protein

display aberrant subcellular localization, association with cytoplasmic chaperonins (HSP60 and TriC) and propensity to aggregate (Ramos et al., 2019). Moreover, analysis of I_{34} tRNAs level in WT and p.Val144Met patient cells has shown a severe decrease of deamination in patient cells in some tRNAs (tRNA-Val-AAC, tRNA-Thr-AGT, tRNA-Ile-AAU and tRNA-Leu-AAG)(Ramos et al., 2019)(Del pozo et al, in preparation). *In vivo*, mouse protein mutated on the corresponding amino acid (V128M) failed to rescue neuronal migration defects induced by *Adat3* silencing (Del pozo et al, in preparation). Altogether these results indicate that V128M mutation negatively affects ADAT3 function likely resulting in defects in tRNA editing and protein translation.

Here, we generated a V128M *Adat3* knock-in (KI, *Adat3*^{V128M/V128M}) mouse line which represent an hypomorphic mutation, while null mutations may be incompatible with life, *ADAT3* and *ADAT2* being essential genes in yeast and human cell lines (Torres et al., 2014; Tsutsumi et al., 2007). Using this model we investigated how *Adat3* mutation and the consequent defects in tRNAs I_{34} modification contribute to brain malformation.

Results

Mouse *Adat3* KI/KI homozygous mice display lower *Adat3* protein levels but do not show neuroanatomical defects and migration defects.

To create a stable mammalian model to study ADAT3 neurodevelopmental phenotypes, we generated a constitutive knock-in mouse line (*Adat3*^{V128M/V128M}) bearing the V128M disease-causing mutation (KI/KI). In this model, the V128M variant is expressed at the homozygous state in the C57BL/6N mouse genetic background (Fig. 1A). Genotypes were confirmed by PCR and DNA sequencing. Both *Adat3*^{+/V128M} (KI/+) and *Adat3*^{V128M/V128M} (KI/KI) male and female mice were fertile and crossed to generate the disease model KI/KI. At Embryonic day 18 (E18) the expected Mendelian segregation was observed (data not shown). Both *Adat3*^{+/+} and *Adat3*^{KI/KI} displayed a normal lifespan (data not shown).

We first assessed Adat3 protein level at E18 in three central nervous system tissues: Cortex, hippocampus and ganglionic eminences (GE) (Fig. 1B, C and Fig. S1B, C). By Western Blot analysis, we observed a clear reduction in Adat3 protein level of around 80% in *Adat3^{KI/KI}* mice in the three tissues analyzed when compared to WT littermates. Preliminary immunoblotting for Adat2 suggested a reduced Adat2 protein level in the three tissues analyzed from KI/KI animals.

Given that all the patients carrying the p.Val144Met variant (NM_138422.4) present with severe brain anomalies, including microcephaly, arachnoid cyst (cerebrospinal fluid covered by arachnoidal cells and collagen), brain atrophy, dilatated ventricles and dysmyelination (Alazami et al., 2013; El-Hattab et al., 2016; Hengel et al., 2020; R. Sharkia, A. Zalan, A. Jabareen-Masri, H. Zahalka, & M. Mahajnah, 2018) we first sought for neuroanatomical defects in wild-type and *Adat3^{KI/KI}* embryos at mid (E14.5) and late (E18.5) corticogenesis stages. Analysis of thickness of the cortex, the cortical plate or of the ventricular, subventricular and intermediate zones did not reveal any difference between WT and *Adat3^{KI/KI}* embryos neither at E14.5 or E18.5 (Fig. 1 D-K). We further examined finer-scale neuro-morphological features in *Adat3^{KI/KI}* 16-week old males using a recently developed approach that consisted in a systematic quantification of 40 brain parameters across 22 unique brain regions in the same sagittal brain region at Lateral +0.60 mm (Supplementary Table 1 and 2). There were no mutant neuroanatomical parameters significantly different from WT, suggesting that the *Adat3* V128M mutation does not alter the size and the morphology of the murine brain, at least in males (Fig. 1L,M).

Considering that the V128M variant acts as a loss of function variant for the role of Adat3 in regulating radial migration of projection neuron (Del Pozo Rodriguez, in preparation, article 1), we investigated the neuronal migration in *Adat3^{KI/KI}* E18.5 embryos. We compared the distribution of 5-Ethynyl-2'-deoxyuridine (EdU)-positive neurons in upper

and lower cortical plate and in subventricular and intermediate zones in *Adat3*^{KI/KI} mice and their wild-type E18.5 littermates (Fig. 1 N, O). In E18.5 embryos born from mice injected with EdU at E14.5, near half of EdU-positive neurons have reached the upper cortical plate, with no difference between control and mutant brains, suggesting that radial migration is not impaired in a constitutive knock-in *Adat3* V128M mouse model.

***Adat3*^{V128M/V128M} mouse cortices affect progenitors' biology at late embryonic stages**

We next addressed the consequence of constitutive expression of the V128M variant in cortical progenitors. We performed immunohistochemistry to label neuronal progenitors' population, including Apical (APs) and Intermediate progenitors (IPs) using Pax6 and Tbr2, respectively. Cells that retain expression of both markers (Pax6/tbr2 double positive) are newborn intermediate progenitors. Analysis at E14.5 in control (*Adat3*^{+/+}) and KI (*Adat3*^{KI/KI}) cortices did not reveal any difference in the number of APs, IPs and newborn IPs (Fig. 2A, C-E). In addition, similar number of Tbr1-positive neurons (Fig 2B, F) indicated that neurogenesis is not impaired at early developmental stages. In contrast, at later stage (E18.5), we observed an increase in both APs (+18,17%) and newborn IPs (+ 9,64%) in *Adat3*^{KI/KI} cortices compared to wild-type littermates (Fig. 2G, I, J). In accordance with an absence of defects in progenitor's biology at early stage, the number of neurons (Tbr1⁺, Fig. 2 L,M) was not affected. Neither upper layer (Satb2⁺, Fig. 2H, K)) or deep layer (Ctip2⁺, Fig. 2L,N) projection neurons numbers was affected.

Constitutive expression of V128M variant affect proliferation of cortical progenitors.

To further characterize the effect of V128M expression in progenitor, we assessed their proliferation. Immunolabelling with Ki67, a proliferation marker, at E14.5 showed equivalent number of cycling progenitors upon expression of *Adat3* V128M variant (Fig.

3A, C). We next carried out a co-labeling with EdU, which was administrated in pregnant dams for 18h. While number of Edu+ cells were not affected in *Adat3*^{KI/KI} embryos (Fig. 3A, B), the percentage of cell exiting the cell cycle, calculated as the percentage of Edu+ cells that are not proliferating after 18h (EdU⁺Ki67⁻/EdU⁺) was decreased by 32,14 % in mutant cortices compared to wild-type, suggesting that mutant progenitors might be retained in cell cycle longer than wild-type progenitors (Fig. 3A, D). In line with these results, and with the observed increased progenitor number at E18.5, the number of cells in proliferation (Ki67⁺) at E18.5 was higher in the KI/KI model (Fig. 3E, F). In contrast, the absolute number of progenitors in mitosis (Fig. 3G) as well as the fraction of progenitors undergoing mitosis (mitotic index ((PH3⁺/ Ki67⁺)*100), Fig. 3H) were unchanged in *Adat3*^{KI/KI} embryos compared to the control.

***Adat3*^{V128M/V128M} mouse cortices did not show major cell fate defects**

We next assessed whether V128M mutant Adat3 affects the fate of progenitors in the developing cortex. We performed intraperitoneal injections of EdU 18h before analysis of the progeny of targeted cells at E14.5 by immunohistochemistry. WT and *Adat3*^{KI/KI} were stained for EdU, markers of progenitors (Tbr2, Pax6) and of newborn neurons (Tbr1) (Fig. 4). *Adat3*^{KI/KI} and WT cortices showed similar number of APs (Pax6⁺Tbr2⁻ Fig. 4A, B; Tbr2⁻Tbr1⁻ Fig. 4C, D), IPs (Pax6⁺Tbr2⁺ and Pax6⁻Tbr2⁺ Fig. 4A, B; Tbr2⁺Tbr1⁻ Fig. 4C, D) and neurons (Pax6⁻Tbr2⁻ Fig. 4A, B; Tbr2⁺Tbr1⁺ and Tbr2⁻Tbr1⁺ Fig. 4C, D). This suggests that constitutive expression of V128M Adat3 mutant did not impair cortical neurogenesis at E14.5.

Acute depletion of Adat3 in WT cortices by *In utero* electroporation of miRNAs leads to defects in cell cycle exit and cell specification.

As level of Adat3 are severely decreased in *Adat3*^{V128M/V128M} cortices, we tested whether acute depletion of Adat3 in apical progenitors impairs progenitor's biology and

neurogenesis. We silenced *Adat3* by in utero electroporation of *Adat3*-targeting miRNAs under the ubiquitous pCAGGS promoter at E13.5 (Fig. 5A). Two days after in utero electroporation, the percentage of proliferative (Ki67⁺) GFP-positive *Adat3*-depleted cells increased with both miRNAs tested compared to the scramble condition (Fig. 5B). In accordance, the percentage of cell exiting the cell cycle decreased upon *Adat3* deletion (Fig. 5C). We further assessed the consequences of *Adat3* depletion on fate of cortical progenitors by performing immunolabelling of GFP-electroporated cells with both progenitors (Tbr2, Pax6) and newborn neurons (Tbr1) markers at E15.5, 2 days after in utero electroporation (Fig. 5D, F). The number of APs (Pax6⁺Tbr2⁻; Tbr2⁻Tbr1⁻) and IPs (Pax6⁺Tbr2⁺; Pax6⁻Tbr2⁺; Tbr2⁺Tbr1⁻) remained unchanged upon *Adat3* depletion (Fig. 5E, G). This was surprising, since the percentage of generated neurons (Tbr2⁻, Pax6⁻, Tbr2⁺Tbr1⁺; Tbr2⁻Tbr1⁺) tended to decrease upon *Adat3* depletion compared to the control condition. Overall, those results suggest that loss of *Adat3* in apical progenitors favored their proliferation at the expense of the neuron production.

Conclusion

ADAT3^{V144M/V144M} patients present, in the majority of the cases, with microcephaly accompanied with other cerebral abnormalities. The results obtained during the characterization of the *Adat3*^{KI/KI} line show that this mouse line is not recapitulating most of the defects observed in patients. Despite presenting lower ADAT3 protein levels compared to WT, *Adat3*^{KI/KI} mice do not present clear brain abnormalities neither at embryonic stages (morphometric analysis of the cerebral cortex at E18.5 (Fig1 D-K) nor in 16-week old adult stage (neuroanatomical analysis in 16 week-old mice (Fig. 1N)). Other mouse models have also been shown to not fully recapitulate patient associated phenotypes. One example is Filamin A (*Flna*) KO mice, which do not present periventricular heterotopia, a common feature in human patients (REFS missing). On the other hand, acute knockdown of *Flna* in rats lead to ectopic neurons recapitulating the

human phenotype (Carabalona et al., 2012). There exist several alternatives that could probably recapitulate the human phenotype observed in *ADAT3* p.Val144Met patients: Among them there is for example the use of ferret or primates as animal models (gyrencephalic species), which are closer to humans (presence of gyri and sulci and additional cell types), or the use of *in vitro* models, such as human cortical organoids derived from hESCs (Cakir et al., 2019).

However, the detection of a decreased cell cycle exit in *Adat3*^{KI/KI} cortices as well as the increase in the number of cortical progenitors at E18.5 provides important insights about possible pathomechanisms driving the human disease. Nevertheless, further developmental time-points should be studied to fully characterize this phenotype. As there is an impairment of cell cycle exit at E14.5 and E15.5, this could possibly be associated to defects in the generation of layer IV pyramidal or upper layer callosal neurons (generation peak respectively at E14.5 and E15.5).

Interestingly, the decreased cell cycle exit is not reflected with any change in terms of cell specification or neuronal populations, among the ones studied at E18.5. IUE studies of miRNAs in WT cortices further confirmed minor cell cycle defects upon depletion of *Adat3* and also reflected a reduced cell specification towards the Pax6⁻Tbr2⁻ lineage, which is not observed in the *Adat3*^{KI/KI} model. This difference could be due to the time of the analysis: while the study with the KI/KI model was carried out at E14.5 (with an injection of EdU 18h before), the study in WT cortices by IUE was performed at E15 (electroporation done at E13). These differences could partially account to the discrepancies observed, particularly if the function of *Adat3* is of special relevance in some specific embryonic stages. In addition to this discrepancy, it is surprising not to observe a phenotype in radial migration in this line, since neuronal radial migration is one of the main phenotypes observed after the depletion of *Adat3* levels in the brain

(Article1). This could be due to compensatory mechanisms that might occur in a context of sustained Adat3 malfunction which do not occur in a context of acute Adat3 depletion. Altogether, these results indicate that this mouse line is probably not the best for modeling human disease, however, it may provide relevant insights into how Adat3 p.V128M mutation can affect the proliferation and specification of cortical progenitors and the molecular mechanisms driving the human disease.

Material and methods

Cloning and plasmid constructs.

miRNAs against coding sequences (CDSs) for mouse *Adat3* (NM_001100606) were generated using BLOCK-iT™ RNAi Designer (<https://rnaidesigner.thermofisher.com/rnaexpress/>) Sense and antisense (see table below for sequences) oligos were annealed and the resulting duplex was subcloned in pCAGGs-mir30 (Addgene plasmid # 12345)(Matsuda & Cepko, 2007) and NeuroD-miR30 vectors digested with Xhol and EcoRI.

<i>Adat3</i> miR1 antisense	5'AATTCcgaggcagtaggcaGAGCTGATACTGGCCTATGCTtacatctgtggcttcactaAGCATAGGCCAGTATCAGCTCcgctcactgtcaacagcaatataccttC 3'
<i>Adat3</i> miR2 sense	5'TCGAGaaggatattgctgtgacagtgagcgCCCTATGTGTGCACTGGCTATggcttcactaTATtagtgaagccacagatgtAGCCAGTGCACACATAGGGgcctactgcctcgG 3'
<i>Adat3</i> miR2 antisense	5'AATTCcgaggcagtaggcaCCCTATGTGTGCACTGGCTATTacatctgtggcttcactaATAGCCAGTGCACACATAGGGcgctcactgtcaacagcaatataccttC 3'

Mice

All animal studies were conducted in accordance with French regulations (EU Directive 86/609 – French Act Rural Code R 214-87 to 126) and all procedures were approved by the local ethics committee and the Research Ministry (APAFIS#15691-201806271458609). Mice were bred at the IGBMC animal facility under controlled light/dark cycles, stable temperature (19°C) and humidity (50%) condition and were provided with food and water ad libitum. Timed-pregnant CD1 (Charles River Laboratories) females were used for in utero electroporation of the different constructs at embryonic day 13.5 (E13.5). For E14.5, E15.5 and E18.5 analysis, pregnant mice were sacrificed by cervical dislocation.

Adat3 KI/KI model

The *Adat3* knock-in mice expressing the p.Val128Met (*Adat3*^{V128M/+}) variant were generated at the Institut Clinique de la Souris (<http://www.icsmci.fr/en/>). C57BL/6N mouse fertilized oocytes were microinjected with a mix of single-guide RNA (sgRNA), Cas9 mRNA and donor single-stranded donor oligonucleotide (ssODN). Guide RNA (gRNA) (Sequence: 5' Tggcctgggcacacccttcgg 3', PAM sequence underlined) was synthesized and validated *in vitro*.

A ssODN containing the mutation and generating a Rsal site for genotyping was ordered from Merck (60 bps homology both in 5' and 3'). ssODN Sequence:

5'ccgcgcgtctggcgagctcctccaggccggccgtggacccacgtggctggcacaccccttccctgtacctatgcctgcccggcccccctcacccgaagccagttgaggaggcacgagcccactggccta3'; non homologous bases are colored, p.V128M mutation is shown in red and Rsa1 site underlined. For identification of F0 founders, tail clips of each animal were analyzed by polymerase chain reaction and genotyped (as described below). Three of them were bred to obtain germ line transmission. Line was established from a slightly mosaic (not heterozygous) founder, for which only the expected allele was detected with the wild type allele and gave germ line transmission.

Genotyping was done as follows: genomic DNA was extracted from tail biopsies using PCR reagent (Viagen) supplemented with Proteinase K (1 mg/mL), heated at 55°C for 5 h. Proteinase K was inactivated for 45 min at 85°C, and cell debris was removed by centrifugation. Amplification of mADAT3 targeted locus was performed by PCR using the following primers: mADAT3 forward: 5'-ACCTGTCCTGGACAAGCGCCAGACG-3', mADAT3 reverse: 5'-AGGTCACAGGAACCGCGGCCCTGCC-3'. PCR products were digested with RsaI : As a RsaI site has been inserted in the knock-in allele but not in the wild type allele. The presence of the wild type and knock-in alleles was indicated by a 585bp product and two fragments of 351 and 234nbp products, respectively, which were detected on a 2% agarose gel.

Neuroanatomical characterization

Mouse brains were following anaesthesia and decapitation. In all steps of the neuroanatomical studies, the animal's genotypes were blind to the experimenters. Standard operating procedures are described in more details elsewhere (Collins et al., 2018). Neuroanatomical studies were carried out using 13 male mice of which, 7 were Adat3^{+/+} and 6 Adat3^{KI/KI} mice. These mice were of 16-week of age bred on B6N background. Mouse brain samples were immersion-fixed in 10% buffered formalin for 48 hours, before paraffin embedding and sectioning at 5µm thickness using a sliding

microtome (Leica RM 2145). Sagittal sections were collected at Sagittal +0.6mm. Brain sections were double-stained using luxol fast blue for myelin and cresyl violet for neurons, and scanned at cell-level resolution using the Nanozoomer whole-slide scanner (Hamamatsu Photonics, Shizuoka, Japan). Co-variates, for example sample processing dates and usernames were collected at every step of the procedure and used to identify data drifts. Using in-house ImageJ plugins, an image analysis pipeline was used to standardize measurements of areas and lengths. Each image was quality controlled for the accuracy of sectioning relative to the reference atlas and controlled for asymmetries and histological artefacts. For parasagittal sections, we quantified 22 unique brain structures at Lat +0.6mm. The list of measures is provided in Figure 1N. All samples were also systematically assessed for cellular ectopia (misplaced neurons). Data were analysed using a two-tailed Student t-test assuming equal variance to determine whether a brain parameter is associated with neuroanatomical defect or not.

EdU injection and staining

Pregnant mice were intraperitoneally injected with EdU (5-ethynyl-2"-deoxyuridine solution, Invitrogen) diluted in NaCl 0.9% at the dose of 40mg EdU/kg of body weight and embryos were harvested and fixed at the indicated timepoint. For migration experiments, EdU injection was carried out at E14.5 and embryos were collected at E18.5. For proliferation and cell fate analyses EdU was injected 18h before embryo collection, which was performed at E14.5, E15.5 or E18.5 depending on the experiment. EdU staining was done using Click-iT EdU Alexa Fluor 647 Imaging Kit (Invitrogen) according to manufacturer's protocol.

Mouse brain fixation, cutting and immunolabelling

E14.5 and E18.5 animals were sacrificed by head sectioning and brains were fixed in 4% paraformaldehyde (PFA, Electron Microscopy Sciences) in Phosphate buffered

saline (PBS, HyClone) overnight at 4°C. after fixation, brains were rinsed and equilibrated in 20% sucrose in PBS overnight at 4 °C, embedded in Tissue-Tek O.C.T. (Sakura). Frozen on dry ice and coronal sections were cut at the cryostat (14 to 18 µm thickness, Leica CM3050S) and processed for immunolabeling. Sections were maintained at -80 °C. For certain immunolabelings (see Supplementary Table 3), an antigen retrieval was performed by boiling sections in sodium citrate buffer (0.01 M, pH 6) during 15 min. Cryo-sections were permeabilized and blocked with 5% Normal Donkey Serum (NDS, Dominic Dutsher), 0.1% Triton-X-100 in PBS. Slides were incubated with primary antibodies diluted in blocking solution overnight at 4°C and secondary antibodies diluted in PBS-0.1% Triton one hour at room temperature, whereas cell nuclei were identified using DAPI (1mg/ml Sigma). Slices were mounted in Aquapolymount mounting medium (Polysciences Inc). All primary and secondary antibodies used for immunolabeling are described in Supplementary Table 3.

***In utero* electroporation**

In utero electroporation (IUE) was performed as described previously (Godin et al., 2012; Laguesse et al., 2015). Briefly, CD1 pregnant females were anesthetized with isoflurane (2L/min of oxygen; 4% isoflurane in the induction phase followed by 2% isoflurane during surgery; Tem Segal). The uterine horns were exposed, and a lateral ventricle of each embryo was injected using pulled glass capillaries (Harvard apparatus, 1.0OD*0.58ID*100mmL) with Fast Green (1 µg/µl; Sigma) combined with different amounts of DNA constructs using a micro injector (Eppendorf Femto Jet). Plasmids were electroporated into the neuronal progenitors adjacent to the ventricle by 5 electric pulses (40V) for 50 ms at 950 ms intervals using electrodes (diameter 3 mm; Sonidel CUY650P3) and ECM-830 BTX square wave electroporator (VWR international). For ubiquitous E13.5 to E15.5 Knock-down experiments we injected 0.2 µg/µl of pCAGGs-

IRES-GFP together with 3 µg/µl of either pCAGGs-miR30-miRNA-Adat3 (Del Pozo Rodriguez et al, in preparation, Article1) or pCAGGs-miR30-scramble.

Protein extraction and western blot

Proteins from mouse brain cortices, hippocampus or ganglionic eminences (GE) (E18.5) were extracted as follows: tissue was lysed in RIPA buffer (50 mM Tris pH 8.0, 150 mM NaCl, 5 mM EDTA pH 8.0, 1% Triton X-100, 0.5% sodium deoxycholate, 0.1% SDS) supplemented with EDTA-free protease inhibitors (cOmplete™, Roche) for 30 min, then cells debris were removed by high speed centrifugation at 4°C for 25 min. Protein concentration was measured by spectrophotometry using Bio-Rad Bradford protein assay reagent. Samples were denatured at 95°C for 10 min in Laemmli buffer (Bio-Rad) with 2% β-mercaptoethanol, then resolved by SDS-PAGE and transferred onto nitrocellulose membranes. Membranes were blocked in 5% milk in PBS buffer with 0.1% Tween (PBS-T) and incubated overnight at 4°C with the appropriate primary antibody in blocking solution. Membranes were washed 3 times in PBS-T, incubated at room temperature for 1 h with HRP-coupled secondary antibodies at 1:10,000 dilution in PBS-T, followed by 3 times PBS-T washes. Visualization was performed by quantitative chemiluminescence using SuperSignal West Pico PLUS Chemiluminescent Substrate (Sigma). Signal intensity was quantified using ImageQuant LAS 600 (GE Healthcare). Primary and secondary coupled HRP antibodies used for western blot are described in Supplementary Table 3. All immunoblot experiments consisted of at least three independent replicates.

Image acquisition and analysis

Images were acquired using a TCS SP8 X (Leica microsystems) confocal microscope using a 20x DRY HC PL APO CS2 objective. For all experiments, a Z-stack of 1.50 µm was acquired. The image size was 524x524. Image analysis was done using ImageJ

software (NIH). Cell counting was performed in 3 to 5 different brain sections of at least 3 different embryos per condition. For in utero electroporation analyses, only similarly electroporated regions were considered for further analysis. Cortical areas (upper cortical plate, lower cortical plate, intermediate zone, subventricular zone/ventricular zone) were delimited based on cell density (nuclei count with DAPI staining) using equivalent sized boxes. For migration analyses, number of Edu- or GFP-positive cells was determined in each cortical area to establish the percentage of positive cells.

Morphometric cortices analyses and cell quantification based on marker stainings in embryonic brain sections were both determined using the Measure and cell counter functions respectively of ImageJ software in defined regions of interest with anatomically matched positions in experimental groups. Limits of the different cortical areas staining were determined by DAPI staining (1mg/ml Sigma).

Statistics

All statistics analyses were performed using GraphPad Prism 6 (GraphPad) and are represented as mean +/- S.E.M. The level of significance was set at $P < 0.05$ in all the statistical tests. All statistical tests used and n size numbers are shown in the figure legends.

Figure legends

Figure 1. The *Adat3*^{V128M/V128M} mouse line does not show apparent neuroanatomical anomalies. (A) Genomic region and CRISPR strategy (use of gRNA and ssODN) for gene editing to establish the *Adat3*^{V128M/V128M} mouse line (KI/KI). Chromatogram results of Sanger sequencing of RNA isolated from *Adat3*^{V128M/V128M} mouse confirms the presence of the mutation in the line. (B, C) Western Blot analysis of +/+, +/KI and KI/KI cortical extracts showing reduced Adat3 protein level in KI/KI embryos at E18.5 (n=3 for each genotype; One-way ANOVA with Tukey's multiple comparison test). (D-K) E14.5 (D) or E18.5 (K) coronal sections of WT (+/+) and KI/KI cortices counterstained with DAPI (Blue) showing similar thickness of (E,I) cortex (White arrow), (F,J) cortical plate (CP) and (G,K) Ventricular (VZ) Subventricular (SVZ), intermediate (IZ) zones (E14.5: +/+, n=5; KI/KI, n= 4; E18.5: +/+, n=3; KI/KI, n= 4; Unpaired two-tailed Student t-test). (L) Top: A schematic representation of the section of interest at Lateral +0.60mm is shown. White colouring indicates a p-value higher than 0.05 and grey shows not enough data to calculate a p-value. Bottom: Histogram comparing male *Adat3*^{V128M/V128M} mice to matched WT and showing variation (decreased-minus scale or increased-positive scale) in areas and lengths expressed as percentage of WT together with a colour map indicating the significance level. (M) List of parameters measured at Lateral -0.60 mm. (N) E18.5 mouse brain coronal sections stained for EdU (gray) 4 days after EdU injection. Nuclei are stained with DAPI (blue). (O) Analysis of the percentage of EdU⁺ cells in upper (Up CP) and lower (Lo CP) cortical plate, intermediate (IZ) and subventricular zone (SVZ) showing comparable distribution of EdU⁺ cells in WT littermates (n=3 (+/+)) and KI/KI n=3 littermates (Two-way ANOVA with Bonferroni's multiple comparison test). **p<0.01; *p<0.05; ns: not significant. Scale bars: 100µm. Graphs depict means ± SEM.

Figure 2. *Adat3*^{V128M/V128M} mouse cortices affect progenitors biology at late embryonic stages. (A,B,G,H,L) Coronal sections of E14.5 mouse cortices stained (A,G)

with progenitor makers (Pax6 in green and Tbr2 in red) or (B,H,L) with the neuronal markers (B,L) Tbr1 (green), (H) Satb2 (red) and (L) Ctip2 (red). Nucleus are counterstained with Dapi (blue). (C-K) Analysis of number of (C,I) apical (Pax6⁺), (D) intermediate (Tbr2⁺), (E, J) new-born intermediate (Pax6⁺, Tbr2⁺) progenitors or (F,K,M-N) neurons (Tbr1⁺; Satb2⁺, Ctip2⁺) show similar progenitors and neurons number at E14.5 and a slight increase of progenitors number at E18.5 (+/+, n=4; KI/KI, n= 3; Unpaired two-tailed Student t-test). ***p < 0.001; *p < 0.05; ns not significant. Scale bars: 100μm (whole cortex) and 25μm (VZ/SVZ/IZ insight). Graphs depict means ± SEM.

Figure 3. *Adat3*^{V128M/V128M} cortices display abnormal progenitor cell cycle exit at E14.5 and increased number of proliferating cells at E18.5. (A) E14.5 WT and KI/KI mouse coronal sections, collected 18h after EdU injection in pregnant mice and immunostained for EdU (gray), Ki67 (proliferation marker, yellow) and Dapi (blue). (B-D) Quantification of the number of (B) proliferating cells (Ki67⁺), (C) EdU-positive cells, and (D) of the % of cell cycle exit, showing abnormalities in cell cycle exit in KI/KI cortices at E14.5. (E) E18 KI/KI mouse coronal brain sections costained with Ki67 (yellow), Phospho histone 3 (PH3) (a mitosis cell marker, red) and Dapi (blue). Quantitative analysis of (F) the total number of proliferating cells (Ki67⁺), (G) the total number of PH3⁺ cells and (H) the mitotic index, showing increased cell proliferation in E18.5 KI/KI embryos. (For each analysis, n=3 (+/+); n=4 (KI/KI); Unpaired two-tailed Student t-test). **p < 0.01; *p < 0.05; ns not significant. Scale bars: 100μm (A) and 25μm (E). Graphs depict means ± SEM.

Figure 4. *Adat3*^{V128M/V128M} animals do not display major defects in cell fate. (A,C) E14.5 WT and KI/KI mouse coronal sections, collected 18h after EdU injection in pregnant mice and immunostained for EdU (gray), Pax6 (green), Tbr2 (red) or Tbr1 (green). Nuclei were counterstained with Dapi (blue). (B, D) Percentage of Edu-positive cells co-expressing or not (B) Pax6 and Tbr2 or (D) Tbr2 and Tbr1 in E14.5 WT and *Adat3*^{KI/KI} cortices subjected to Edu injection 18h earlier, showing no difference in cell

fate between KI/KI and WT littermates. Scalebar = 100 μ m. (for each analysis, n=5 (+/+); n=5 (KI/KI); Two-way ANOVA with Bonferroni's multiple comparison test). Graphs depict means \pm SEM.

Figure 5. Acute depletion of *Adat3* in WT cortices by IUE impairs cell cycle exit and proliferation. (A) Coronal brain sections of E15.5 mouse embryo electroporated at E13.5 with pCAGGs scramble or miRNA (miR) constructs and injected with EdU 18h before sacrifice were stained for Ki67 (red) and Edu (gray). GFP-positive electroporated cells are depicted in green and nuclei are labelled with DAPI (blue). (B, C) Quantification of the percentage of GFP+ cells proliferating (GFP+, Ki67+) and exiting cell cycle showing a tendency for an increased proliferation and decreased cell cycle exit. (for each analysis, +/+, n=6; KI/KI, n=8); Unpaired two-tailed Student t-test). (D,F) Coronal brain sections of E15.5 mouse embryo electroporated at E13.5 with pCAGGs scramble or miRNA (miR) constructs were immuno-labelled for Pax6 (D, gray), Tbr2 (D,F, red) and Tbr1 (F, gray). GFP-positive electroporated cells are depicted in green and nuclei are labelled with DAPI (blue). (E,G) According to the marker they co-express, GFP+ cells were classified as APs (Tbr2⁻, Pax6⁺ or Tbr2⁺, Tbr1⁻), newborn IPs (Tbr2⁺, Pax6⁺ or Tbr2⁺, Tbr1⁻), IPs (Tbr2⁺, Pax6⁻ or Tbr2⁺, Tbr1⁺) or neurons (Tbr2⁻, Pax6⁻ or Tbr2⁻, Tbr1⁺). Scramble-expressing and *Adat3*-depleted (miR1 or miR2) cells show similar fate. One-Way ANOVA with Dunett's multiple comparison test) (n=6 for each condition) ***p < 0.001; *p < 0.05. ns: non significant. Scale bars: 100 μ m. Graphs depict means \pm SEM.

References

Alazami, A. M., Hijazi, H., Al-Dosari, M. S., Shaheen, R., Hashem, A., Aldahmesh, M. A., . . . Alkuraya, F. S. (2013). Mutation in ADAT3, encoding adenosine deaminase acting on transfer RNA, causes intellectual disability and strabismus. *J Med Genet*, 50(7), 425-430. doi:10.1136/jmedgenet-2012-101378

Cakir, B., Xiang, Y., Tanaka, Y., Kural, M. H., Parent, M., Kang, Y. J., . . . Park, I. H. (2019). Engineering of human brain organoids with a functional vascular-like system. *Nat Methods*, 16(11), 1169-1175. doi:10.1038/s41592-019-0586-5

Carabalona, A., Beguin, S., Pallesi-Pocachard, E., Buhler, E., Pellegrino, C., Arnaud, K., . . . Cardoso, C. (2012). A glial origin for periventricular nodular heterotopia caused by impaired expression of Filamin-A. *Hum Mol Genet*, 21(5), 1004-1017. doi:10.1093/hmg/ddr531

Collins, S. C., Wagner, C., Gagliardi, L., Kretz, P. F., Fischer, M. C., Kessler, P., . . . Yalcin, B. (2018). A Method for Parasagittal Sectioning for Neuroanatomical Quantification of Brain Structures in the Adult Mouse. *Curr Protoc Mouse Biol*, 8(3), e48. doi:10.1002/cpmo.48

El-Hattab, A. W., Saleh, M. A., Hashem, A., Al-Owain, M., Asmari, A. A., Rabei, H., . . . Alkuraya, F. S. (2016). ADAT3-related intellectual disability: Further delineation of the phenotype. *Am J Med Genet A*. doi:10.1002/ajmg.a.37578

Gerber, A. P., & Keller, W. (1999). An adenosine deaminase that generates inosine at the wobble position of tRNAs. *Science*, 286(5442), 1146-1149.

Godin, J. D., Thomas, N., Laguesse, S., Malinouskaya, L., Close, P., Malaise, O., . . . Nguyen, L. (2012). p27(Kip1) is a microtubule-associated protein that promotes microtubule polymerization during neuron migration. *Dev Cell*, 23(4), 729-744. doi:10.1016/j.devcel.2012.08.006

Hengel, H., Buchert, R., Sturm, M., Haack, T. B., Schelling, Y., Mahajnah, M., . . . Schols, L. (2020). First-line exome sequencing in Palestinian and Israeli Arabs with neurological disorders is efficient and facilitates disease gene discovery. *Eur J Hum Genet*. doi:10.1038/s41431-020-0609-9

Laguesse, S., Creppe, C., Nedialkova, D. D., Prevot, P. P., Borgs, L., Huysseune, S., . . . Nguyen, L. (2015). A Dynamic Unfolded Protein Response Contributes to the Control of Cortical Neurogenesis. *Dev Cell*, 35(5), 553-567. doi:10.1016/j.devcel.2015.11.005

Matsuda, T., & Cepko, C. L. (2007). Controlled expression of transgenes introduced by in vivo electroporation. *Proc Natl Acad Sci U S A*, 104(3), 1027-1032. doi:10.1073/pnas.0610155104

Ramos, J., Han, L., Li, Y., Hagelskamp, F., Kellner, S. M., Alkuraya, F. S., . . . Fu, D. (2019). Formation of tRNA Wobble Inosine in Humans Is Disrupted by a Millennia-Old Mutation Causing Intellectual Disability. *Mol Cell Biol*, 39(19). doi:10.1128/MCB.00203-19

Salehi Chaleshtori, A. R., Miyake, N., Ahmadvand, M., Bashti, O., Matsumoto, N., & Noruzinia, M. (2018). A novel 8-bp duplication in ADAT3 causes mild intellectual disability. *Hum Genome Var*, 5, 7. doi:10.1038/s41439-018-0007-9

Sharkia, R., Zalan, A., Jabareen-Masri, A., Zahalka, H., & Mahajnah, M. (2018). A new case confirming and expanding the phenotype spectrum of ADAT3-related intellectual disability syndrome. *European Journal of Medical Genetics*. doi:10.1016/j.ejmg.2018.10.001

Sharkia, R., Zalan, A., Jabareen-Masri, A., Zahalka, H., & Mahajnah, M. (2018). A new case confirming and expanding the phenotype spectrum of ADAT3-related intellectual disability syndrome. *Eur J Med Genet*. doi:10.1016/j.ejmg.2018.10.001

Thomas, E., Lewis, A. M., Yang, Y., Chanprasert, S., Potocki, L., & Scott, D. A. (2019). Novel Missense Variants in ADAT3 as a Cause of Syndromic Intellectual Disability. *J Pediatr Genet*, 8(4), 244-251. doi:10.1055/s-0039-1693151

Torres, A. G., Pineyro, D., Filonava, L., Stracker, T. H., Batlle, E., & Ribas de Pouplana, L. (2014). A-to-I editing on tRNAs: biochemical, biological and evolutionary implications. *FEBS Lett*, 588(23), 4279-4286. doi:10.1016/j.febslet.2014.09.025

Tsutsumi, S., Sugiura, R., Ma, Y., Tokuoka, H., Ohta, K., Ohte, R., . . . Kuno, T. (2007). Wobble inosine tRNA modification is essential to cell cycle progression in G(1)/S and G(2)/M transitions in fission yeast. *J Biol Chem*, 282(46), 33459-33465. doi:10.1074/jbc.M706869200

Figure 1

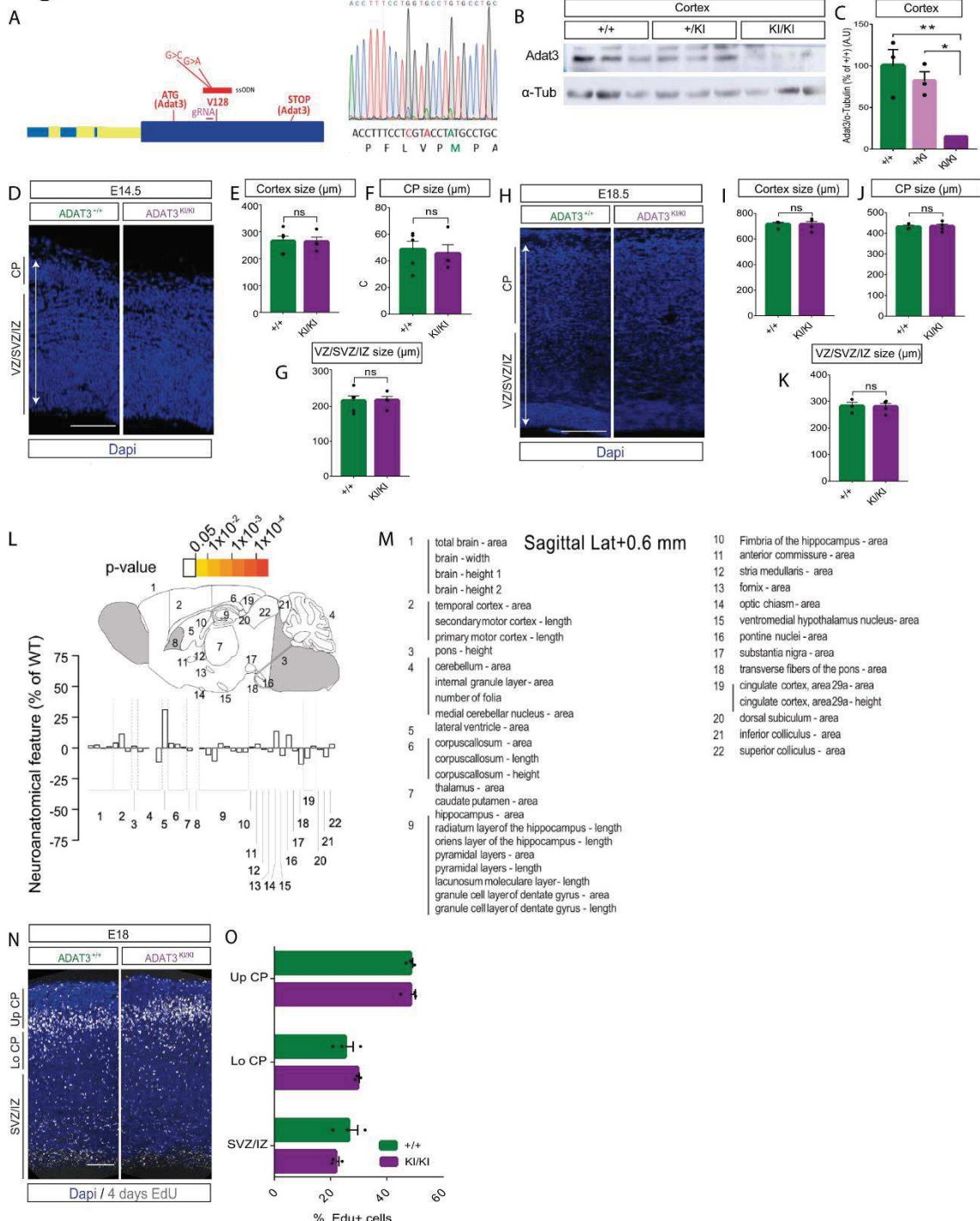


Figure 2

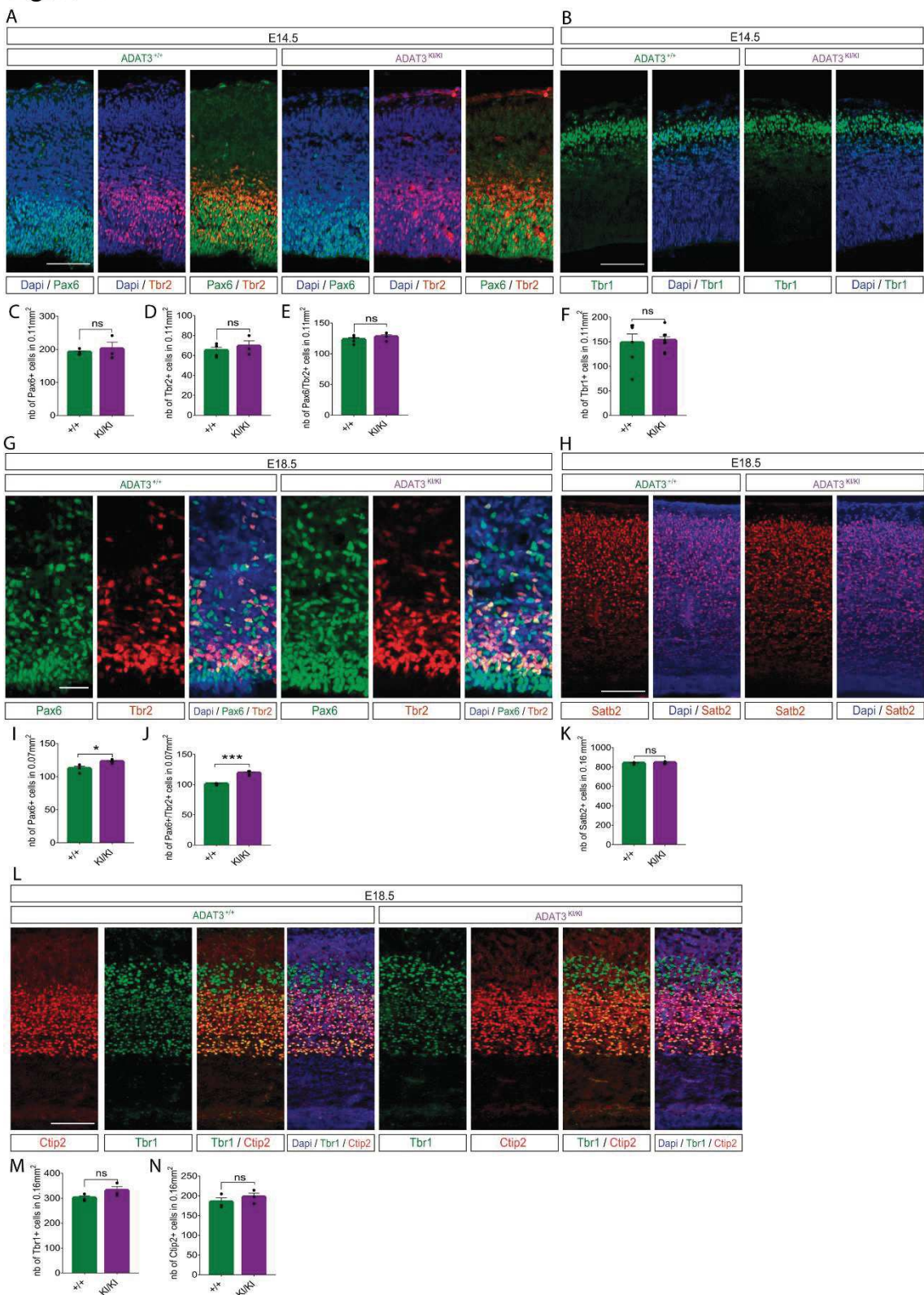
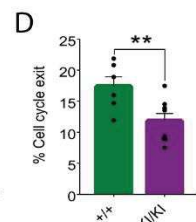
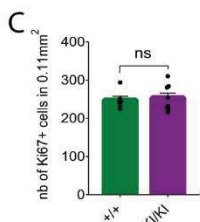
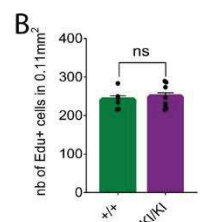
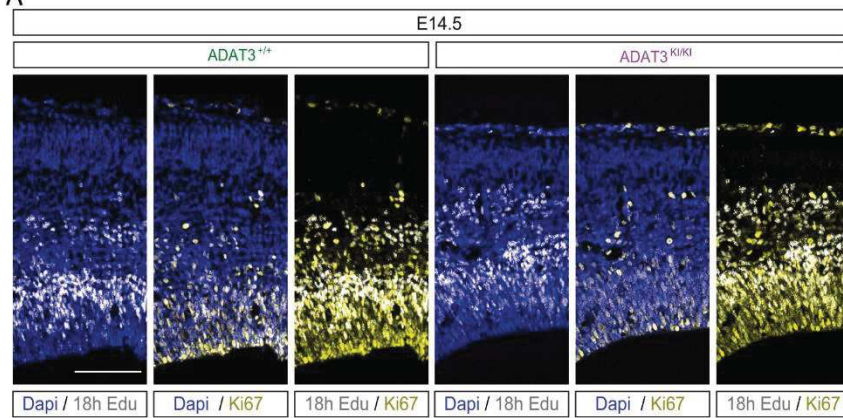


Figure 3

A



E

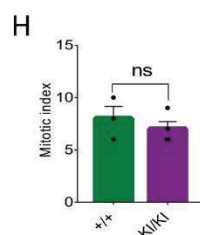
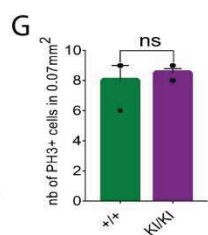
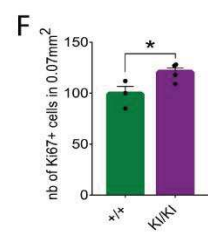
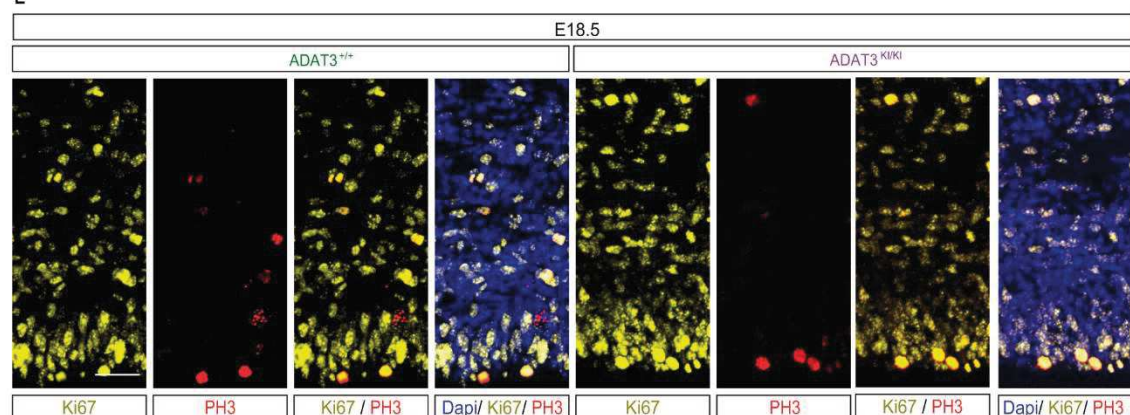


Figure 4

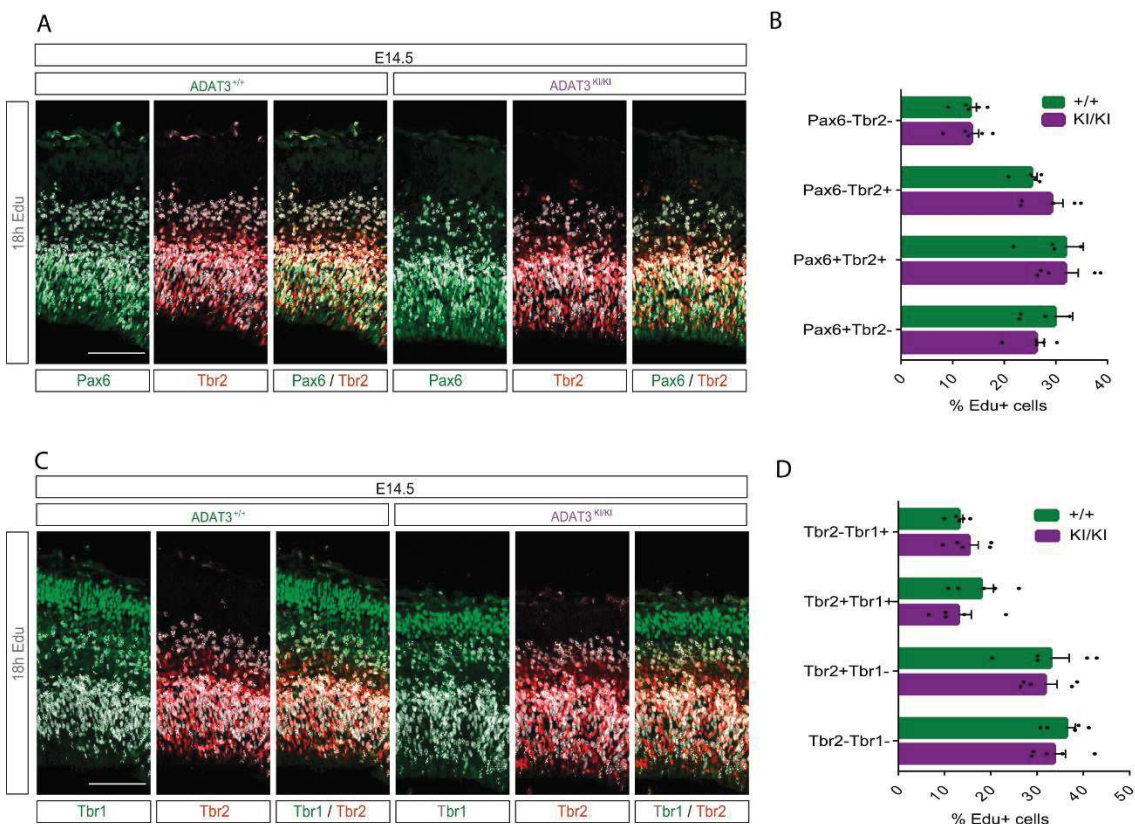
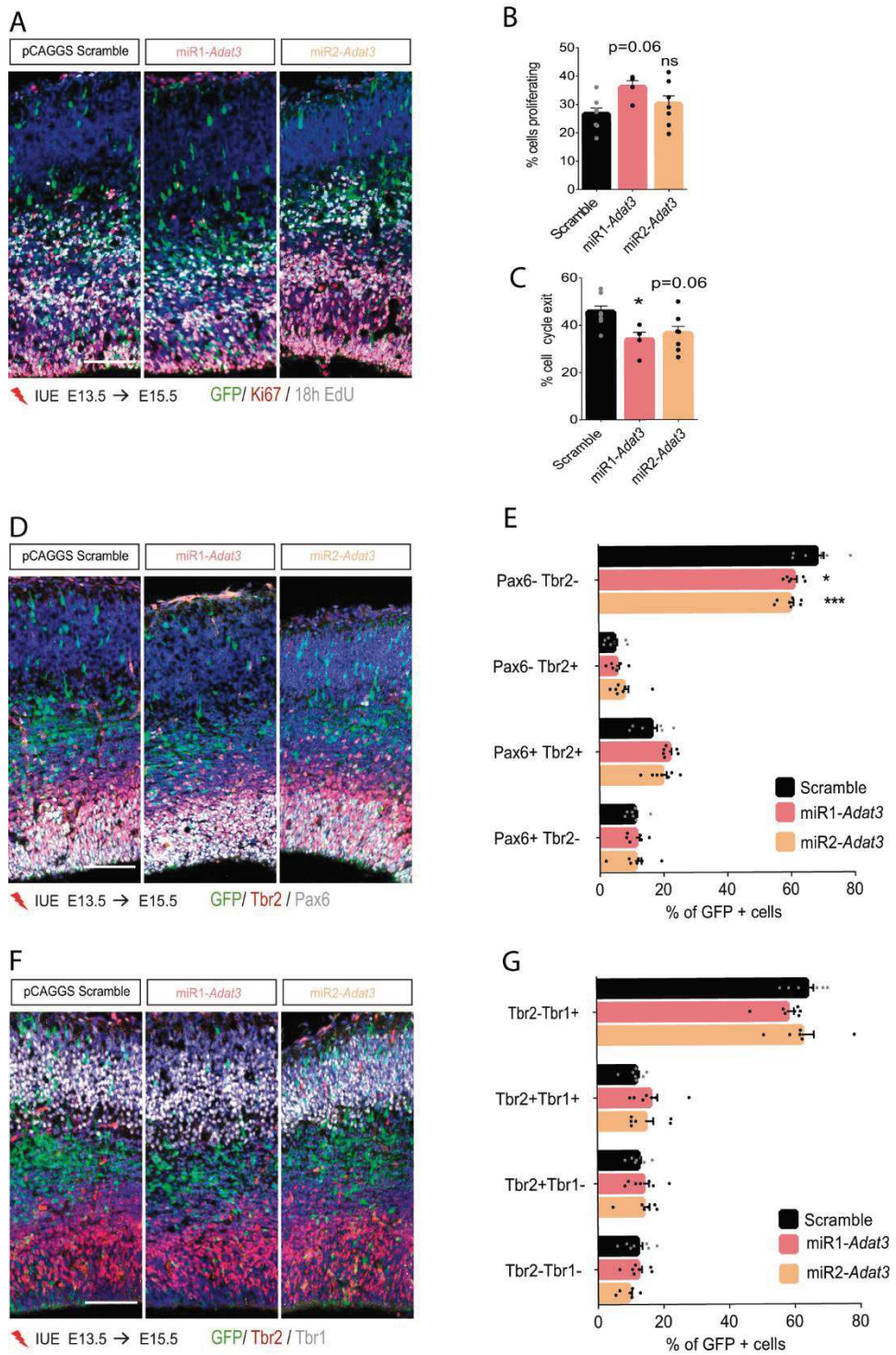


Figure 5



Supplementary information

Figure.S1

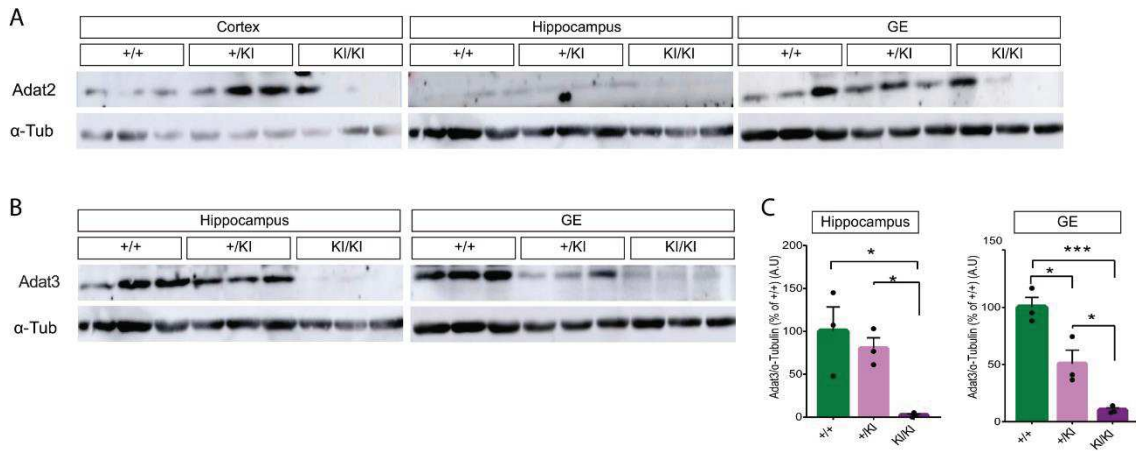


Figure S1. Immunoblot showing Adat2 and Adat3 protein expression in different brain structures. (A) Western blot to detect Adat2 protein level in different brain structures (cortex, hippocampus and GE) from WT, +/KI and KI/KI animals. (B) Western blot to detect Adat3 protein level in hippocampus and GE. (C) Quantification of Adat3 expression normalized by α -tubulin protein level. (n=3 (+/+); n=3 (KI/KI); One-way ANOVA) ***p < 0.001; *p < 0.05. Graphs depict means \pm SEM.

Supplementary Table 1- List of 40 brain parameters across 22 unique brain regions analysed in the neuroanatomical analyses.

Parameter	Description	Unit
4_TB_area	Total brain area	cm ²
4_TC_area	Total cerebellar area	cm ²
4_LV_area	Lateral ventricle area	cm ²
4_cc_area	Corpus callosum area	cm ²
4_cc_cellcount	Cell count of the corpus callosum	digit
4_cc_cellarea	Total cell area of the corpus callosum	cm ²
4_cc_celldens	Cell density of the corpus callosum	digit
4_cc_avgcellarea	Average cell area of the corpus callosum	cm ²
4_cc_cellcirc	Cell circularity of the corpus callosum	digit
4_cc_cellsol	Cell solidity of the corpus callosum	digit
4_TCTX_area	Total cortical area	cm ²
4_TCTX_cellcount	Cell count of the cortex	digit
4_TCTX_cellarea	Total cell area of the cortex	cm ²
4_TCTX_celldens	Cell density of the cortex	digit
4_TCTX_avgcellarea	Average cell area of the cortex	cm ²
4_TCTX_cellcirc	Cell circularity of the cortex	digit
4_TCTX_cellsol	Cell solidity of the cortex	digit
4_TTh_area	Total thalamic area	cm ²
4_TTh_cellcount	Cell count of the thalamus	digit
4_TTh_cellarea	Total cell area of the thalamus	cm ²
4_TTh_celldens	Cell density of the thalamus	digit
4_TTh_avgcellarea	Average cell area of the thalamus	cm ²
4_TTh_cellcirc	Cell circularity of the thalamus	digit
4_TTh_cellsol	Cell solidity of the thalamus	digit
4_CPu_area	Caudate putamen area	cm ²
4_CPu_cellcount	Cell count of the caudate putamen	digit
4_CPu_cellarea	Total cell area of the caudate putamen	cm ²
4_CPu_celldens	Cell density of the caudate putamen	digit
4_CPu_avgcellarea	Average cell area of the caudate putamen	cm ²
4_CPu_cellcirc	Cell circularity of the caudate putamen	digit
4_CPu_cellsol	Cell solidity of the caudate putamen	digit
4_HP_area	Hippocampus area	cm ²
4_HP_cellcount	Cell count of the hippocampus	digit
4_HP_cellarea	Total cell area of the hippocampus	cm ²
4_HP_celldens	Cell density of the hippocampus	digit
4_HP_avgcellarea	Average cell area of the hippocampus	cm ²
4_HP_cellcirc	Cell circularity of the hippocampus	digit
4_HP_cellsol	Cell solidity of the hippocampus	digit
4_TILpy_area	Area of pyramidal cells of the hippocampus	cm ²
4_TILpy_cellcount	Cell count of the pyramidal cells of the hippocampus	digit
4_TILpy_cellarea	Total cell area of the pyramidal cells of the hippocampus	cm ²
4_TILpy_celldens	Cell density of the pyramidal cells of the hippocampus	digit
4_TILpy_avgcellarea	Average cell area of the pyramidal cells of the hippocampus	cm ²
4_TILpy_cellcirc	Cell circularity of the pyramidal cells of the hippocampus	digit
4_TILpy_cellsol	Cell solidity of the pyramidal cells of the hippocampus	digit
4_DG_area	Dentate gyrus area	cm ²
4_DG_cellcount	Cell count of the dentate gyrus	digit
4_DG_cellarea	Total cell area of the dentate gyrus	cm ²
4_DG_celldens	Cell density of the dentate gyrus	digit
4_DG_avgcellarea	Average cell area of the dentate gyrus	cm ²
4_DG_cellcirc	Cell circularity of the dentate gyrus	digit
4_DG_cellsol	Cell solidity of the dentate gyrus	digit
4_fi_area	Area of the fimbria of the hippocampus	cm ²
4_fi_cellcount	Cell count of the fimbria of the hippocampus	digit
4_fi_cellarea	Total cell area of the fimbria of the hippocampus	cm ²
4_fi_celldens	Cell density of the fimbria of the hippocampus	digit
4_fi_avgcellarea	Average cell area of the fimbria of the hippocampus	cm ²

4_fi_cellicirc	Cell circularity of the fimbria of the hippocampus	digit
4_fi_cellsol	Cell solidity of the fimbria of the hippocampus	digit
4_aca_area	Anterior commissure area	cm2
4_aca_cellcount	Cell count of the anterior commissure	digit
4_aca_cellarea	Total cell area of the anterior commissure	cm2
4_aca_celldens	Cell density of the anterior commissure	digit
4_aca_avgcellarea	Average cell area of the anterior commissure	cm2
4_aca_cellcirc	Cell circularity of the anterior commissure	digit
4_aca_cellsol	Cell solidity of the anterior commissure	digit
4_sm_area	Stria medullaris area	cm2
4_sm_cellcount	Cell count of the stria medullaris	digit
4_sm_cellarea	Total cell area of the stria medullaris	cm2
4_sm_celldens	Cell density of the stria medullaris	digit
4_sm_avgcellarea	Average cell area of the stria medullaris	cm2
4_sm_cellcirc	Cell circularity of the stria medullaris	digit
4_sm_cellsol	Cell solidity of the stria medullaris	digit
4_f_area	Fornix area	cm2
4_f_cellcount	Cell count of the fornix	digit
4_f_cellarea	Total cell area of the fornix	cm2
4_f_celldens	Cell density of the fornix	digit
4_f_avgcellarea	Average cell area of the fornix	cm2
4_f_cellcirc	Cell circularity of the fornix	digit
4_f_cellsol	Cell solidity of the fornix	digit
4_och_area	Optic chiasm area	cm2
4_och_cellcount	Cell count of the optic chiasm	digit
4_och_cellarea	Total cell area of the optic chiasm	cm2
4_och_celldens	Cell density of the optic chiasm	digit
4_och_avgcellarea	Average cell area of the optic chiasm	cm2
4_och_cellcirc	Cell circularity of the optic chiasm	digit
4_och_cellsol	Cell solidity of the optic chiasm	digit
4_VMHvl_area	Area of ventromedial nucleus of the hypothalamus	cm2
4_VMHvl_cellcount	Cell count of the ventromedial nucleus of the hypothalamus	digit
4_VMHvl_cellarea	Total cell area of the ventromedial nucleus of the hypothalamus	cm2
4_VMHvl_celldens	Cell density of the ventromedial nucleus of the hypothalamus	digit
4_VMHvl_avgcellarea	Average cell area of the ventromedial nucleus of the hypothalamus	cm2
4_VMHvl_cellcirc	Cell circularity of the ventromedial nucleus of the hypothalamus	digit
4_VMHvl_cellsol	Cell solidity of the ventromedial nucleus of the hypothalamus	digit
4_Pn_area	Pontine nuclei area	cm2
4_Pn_cellcount	Cell count of the pontine nuclei	digit
4_Pn_cellarea	Total cell area of the pontine nuclei	cm2
4_Pn_celldens	Cell density of the pontine nuclei	digit
4_Pn_avgcellarea	Average cell area of the pontine nuclei	cm2
4_Pn_cellcirc	Cell circularity of the pontine nuclei	digit
4_Pn_cellsol	Cell solidity of the pontine nuclei	digit
4_SN_area	Substantia nigra area	cm2
4_SN_cellcount	Cell count of the substantia nigra	digit
4_SN_cellarea	Total cell area of the substantia nigra	cm2
4_SN_celldens	Cell density of the substantia nigra	digit
4_SN_avgcellarea	Average cell area of the substantia nigra	cm2
4_SN_cellcirc	Cell circularity of the substantia nigra	digit
4_SN_cellsol	Cell solidity of the substantia nigra	digit
4_fp_area	Area of fibre of pons	cm2
4_fp_cellcount	Cell count of the fibre of pons	digit
4_fp_cellarea	Total cell area of the fibre of pons	cm2
4_fp_celldens	Cell density of the fibre of pons	digit
4_fp_avgcellarea	Average cell area of the fibre of pons	cm2
4_fp_cellcirc	Cell circularity of the fibre of pons	digit
4_fp_cellsol	Cell solidity of the fibre of pons	digit
4_Cg_area	Cingulate cortex area	cm2

4_Cg_cellcount	Cell count of the cingulate cortex	digit
4_Cg_cellarea	Total cell area of the cingulate cortex	cm2
4_Cg_celldens	Cell density of the cingulate cortex	digit
4_Cg_avgcellarea	Average cell area of the cingulate cortex	cm2
4_Cg_cellcirc	Cell circularity of the cingulate cortex	digit
4_Cg_cellsol	Cell solidity of the cingulate cortex	digit
4_DS_area	Dorsal subiculum area	cm2
4_DS_cellcount	Cell count of the dorsal subiculum	digit
4_DS_cellarea	Total cell area of the dorsal subiculum	cm2
4_DS_celldens	Cell density of the dorsal subiculum	digit
4_DS_avgcellarea	Average cell area of the dorsal subiculum	cm2
4_DS_cellcirc	Cell circularity of the dorsal subiculum	digit
4_DS_cellsol	Cell solidity of the dorsal subiculum	digit
4_InfC_area	Inferior colliculus area	cm2
4_InfC_cellcount	Cell count of the inferior colliculus	digit
4_InfC_cellarea	Total cell area of the inferior colliculus	cm2
4_InfC_celldens	Cell density of the inferior colliculus	digit
4_InfC_avgcellarea	Average cell area of the inferior colliculus	cm2
4_InfC_cellcirc	Cell circularity of the inferior colliculus	digit
4_InfC_cellsol	Cell solidity of the inferior colliculus	digit
4_SupC_area	Superior colliculus area	cm2
4_SupC_cellcount	Cell count of the superior colliculus	digit
4_SupC_cellarea	Total cell area of the superior colliculus	cm2
4_SupC_celldens	Cell density of the superior colliculus	digit
4_SupC_avgcellarea	Average cell area of the superior colliculus	cm2
4_SupC_cellcirc	Cell circularity of the superior colliculus	digit
4_SupC_cellsol	Cell solidity of the superior colliculus	digit
4_Med_area	Area of the medial cerebellar nucleus	cm2
4_Med_cellcount	Cell count of the medial cerebellar nucleus	digit
4_Med_cellarea	Total cell area of the medial cerebellar nucleus	cm2
4_Med_celldens	Cell density of the medial cerebellar nucleus	digit
4_Med_avgcellarea	Average cell area of the medial cerebellar nucleus	cm2
4_Med_cellcirc	Cell circularity of the medial cerebellar nucleus	digit
4_Med_cellsol	Cell solidity of the medial cerebellar nucleus	digit
4_TILpy_length	Total internal length of pyramidal cell layer of the hippocampus	cm
4_DG_length	Dentate gyrus length	cm
4_cc_length	Total outer length of the corpus callosum	cm
4_Mol_length	Length of the molecular layer of the hippocampus	cm
4_Rad_length	Length of the radium layer of the hippocampus	cm
4_Or_length	Length of the oriens layer of the hippocampus	cm
4_cc_height	Corpus callosum thickness	cm
4_M2_length	Length of the secondary motor cortex	cm
4_M1_length	Length of the primary motor cortex	cm
4_Cg_height	Height of the cingulate cortex	cm
4_TB_width	Width of the total brain	cm
4_TB_height_CS1	Height of the total brain at CS1 (coronal critical section 1)	cm
4_TB_height_CS2	Height of the total brain at CS2 (coronal critical section 2)	cm
4_Pons_height	Height of the pons	cm
4_IGL_area	Area of the internal granular layer of the cerebellum	cm2
4_Folia	Number of folia	digit

Supplementary Table 2 - Full raw experimental data for male Adat3 V128M knock-in mice at 16-week of age.

Sex	Male	Male	Male	Effect_size	T-TEST											
Age	16 weeks	16 weeks	16 weeks													
Barcode	A00008707	A00008710	A00008723	A00008728	A00008734	A00008746	A00008747	A00008704	A00008711	A00008725	A00008729	A00008730	A00008736	A00008736		
Gene	ADAT3	ADAT3	ADAT3													
Genotype	WT/WT	KI/KI	KI/KI	KI/KI	KI/KI	KI/KI	KI/KI	KI/KI								
4_TB_area	0,254630068	0,2616	0,2719	0,272144546	0,3002	0,279645458	0,277179449	0,249039913	0,2566	0,284595638	0,301597844	0,301790095			1,761506986	0,710175263
4_TB_width	0,530122921	0,529956427	0,581154827	0,573529412	0,552196805	0,576252723	0,561592229	0,553805239	0,5436	0,590413943	0,583514887	0,582425563			2,316585152	0,319484627
4_TB_height_CS1	0,392058734	0,42912868	0,452760095	0,426407221	0,463827278	0,453803239	0,45049213	0,407621914	0,416337824	0,437383771	0,467909466	0,453304304			-0,420312253	0,90209115
4_TB_height_CS2	0,491631514	0,494322735	0,527600127	0,481743548	0,520841838	0,521204699	0,517621445	0,486625431	0,501836985	0,522837574	0,527191908	0,526284755			1,004831246	0,640578773
4_TCTX_area	0,028267149	0,029697648	0,029666887	0,027516654	0,031971371	0,028254655	0,031251059	0,028983998	0,02946854	0,032837449	0,031736733	0,030383868			3,944045259	0,250334531
4_M2_length	0,107088718	0,098504926	0,09728	0,106781907	0,080808075	0,123349107	0,089811909	0,114742576	0,093933583	0,134299336	0,109269474	0,107448085			11,36197183	0,206840022
4_M1_length	0,111204609	0,117249512	0,112738483	0,111579807	0,119415486	0,12423459	0,117027794	0,116841294	0,105955459	0,119020676	0,10863156	0,114301265			-2,802866498	0,316693987
4_Pons_height	0,217067536	0,193982424	0,210242677			0,242975164	0,211873379	0,218803961	0,220918825	0,2116		0,222328066			1,479581424	0,717621676
4_TC_area	0,059832194	0,05575	0,070126197	0,064575361		0,064413027	0,068625701	0,058375841		0,064175762	0,063512055				-2,920560255	0,536639073
4_IGL_area	0,0301	0,0273	0,03429	0,03020443		0,032559036	0,031671536			0,03148	0,030397136				-0,265194893	0,943908086
4_Folia	8	8	8	8		8	8	8		8	8	8			0	
4_Med_area		0,000545733	0,000293305	0,000468708	0,001744305	0,00198569	0,000457472		0,000875107	0,000941558	0,000613088				-11,56837779	0,751688817
4_LV_area	0,007616508	0,004693849	0,010991916	0,00914358	0,007864932	0,006398557	0,011053991	0,010074363	0,010527486	0,004654756	0,012561968	0,016281669			31,12182914	0,266466295
4_cc_area	0,00935514	0,010005764	0,009777364	0,009955462	0,011848585	0,008739044	0,009740927	0,007842076	0,009905	0,009923593	0,010687175	0,013027382			3,625680664	0,707395458
4_cc_length	0,502335693	0,490904493	0,470510577	0,494151742	0,562752071	0,500520021	0,496908016	0,46941218	0,488940888	0,511078685	0,515036937	0,601988985			2,926580849	0,580528815
4_cc_height	0,02121	0,02170919	0,0211	0,02879866	0,022739288	0,019832435	0,021263828	0,015131175	0,021043852	0,022673752	0,023605148	0,030001868			0,500922415	0,967511998
4_TTh_area	0,025281456	0,02555	0,02810315		0,03211699	0,028168261	0,030040291	0,024986349	0,026807879	0,02623	0,03061	0,029323219			-2,192608032	0,687220966
4_CPu_area				0,000836109	0,001427953											

4_HP_area	0,012056913	0,011946362	0,011358741	0,012033468	0,014698389	0,01194	0,011657697	0,009505484	0,011106809	0,011986365	0,012934017	0,015264134		-0,672221783	0,940147497
4_Rad_length	0,019140926	0,020261194	0,022179888	0,023336553	0,026126004	0,021227378	0,02098547	0,017961627	0,020229561	0,018369902	0,021680954	0,024992062		-5,696079837	0,443618446
4_Or_length	0,009675	0,01241	0,01101	0,012171013	0,012917703	0,010938278	0,009950793	0,009626098	0,010050667	0,008870265	0,011011788	0,010831518		-10,78287098	0,075153177
4_TILpy_area	0,000890247	0,0010236	0,000812407	0,001051	0,001130495	0,000991	0,000890996	0,000845601	0,000864167	0,000854462	0,001101399	0,001253678		3,494752748	0,710046
4_TILpy_length	0,158982951	0,183219956	0,160940318	0,169564545	0,202168735	0,171673389	0,153684004	0,156465614	0,174532139	0,151309725	0,181415158	0,2033		1,132928542	0,867425302
4_Moi_length	0,01040202	0,011370868	0,009797251	0,014151585	0,01251871	0,011157981	0,009933324	0,009116887	0,011067265	0,010522974	0,009572677	0,014968023		-2,501877086	0,819473527
4_DG_area	0,001211199	0,001171	0,001144793	0,001168608	0,001253511	0,001268878	0,001156723	0,000838291	0,001048084	0,001240276	0,001363906	0,001278434		-3,559819132	0,679004323
4_DG_length	0,151178878	0,134114257	0,126542937	0,1527	0,156039689	0,149390749	0,139898086	0,11728269	0,139475143	0,136971759	0,148521713	0,1542243		-3,44588266	0,530662285
4_fi_area	0,003066778	0,00480868	0,003587	0,003018394	0,003980354	0,003949706	0,003453413	0,003755173	0,003797056	0,003997402	0,003222256	0,003814314		0,604525345	0,935486644
4_aca_area	0,000750563	0,00082619	0,000858627	0,000881182	0,001000956	0,0008543	0,00086443	0,000781861	0,000897003	0,000935598	0,000926966	0,00090397		3,1030733	0,514710371
4_sm_area	0,001092649	0,0008143	0,001910026	0,002112	0,001005586	0,002626762	0,001599219	0,002630789	0,000418766	0,002972676	0,000921803	0,000937949		-1,126878963	0,975884
4_f_area	0,000514679	0,000392933	0,000506761	0,00065053	0,000573925	0,0008436	0,000459296	0,000488719	0,000460356	0,0005356	0,000689579	0,000552185		-3,163828822	0,800421879
4_och_area	0,00236814	0,000869789	0,000782658			0,000761083	0,000757048	0,000799175	0,001293994	0,002116758	0,000820226			13,52250196	0,744397284
4_VMHvl_area			0,002126288		0,000748154	0,001744213	0,002395519		0,001558		0,00173353			-6,15137292	0,78858388
4_Pn_area	0,002957981	0,002826857	0,00266988	0,001632175		0,002278481	0,002641329	0,002959858	0,00251	0,002725175	0,00285011			10,40209498	0,274770976
4_SN_area	0,001078943	0,001876426	0,002434416		0,001536288	0,002099461	0,001828606	0,001681263	0,002185		0,001433604			-2,343861421	0,890162141
4_fp_area	0,0018207	0,001962912	0,002451561			0,002955615	0,0018925	0,002183917	0,001998538	0,002456409	0,001058176			-13,19092313	0,463559157
4_Cg_area	0,004608	0,004057008	0,0053259	0,004717448	0,00512611	0,004666	0,005272	0,004214778	0,004137	0,004336328	0,005035			-8,16354512	0,183999995
4_Cg_height	0,077652288	0,077516215	0,068609831	0,06817254	0,07125686	0,075407085	0,07511	0,083276636	0,067628249	0,083049848	0,077380142	0,060824602		1,420692271	0,832736674
4_DS_area	0,0005965	0,000633434	0,000432108	0,000645052	0,000810548	0,000691047	0,0004499	0,00052425	0,0005823	0,0005259	0,000496939	0,000875358		-1,219727943	0,933534412
4_InfC_area	0,006044	0,004865091	0,003904	0,007284384	0,007222447	0,006714723	0,004254851	0,003784187	0,005536	0,005202177	0,006865221			-7,101658085	0,636548248
4_SupC_area	0,031120996	0,035392623	0,03523		0,043839055	0,039522159	0,036878812	0,03208	0,03514	0,040777659	0,044270204			2,891271337	0,755146746

Supplementary Table 3- List of primary and secondary antibodies used in this work

Primary antibody	Host	Dilution	Antigen retrieval (IHC)	Used for	Provenance	Reference
Ctip2	Rat	1/500	Ø	IHC	Abcam	ab18465
Caspase-3	Rabbit	1/100	Ø	IHC	R and D system	AF835
GFP	Chicken	1/500	Ø	IHC	Abcam	GFP-1020
Pax6	Rabbit	1/500	Ø	IHC	Biolegends	901301
Tbr2	Rat	1/250	Ø	IHC	EBiosciences	14-4875-80
phospho Histone H3	Rabbit	1/500	Ø	IHC	Millipore	06-570
Tbr1	Rabbit	1/500	Ø	IHC	Abcam	ab31940
Satb2	Mouse	1/400	Ø	IHC	Abcam	ab51502
α-Tubulin	Mouse	1/500	Ø	IHC, WB	Merck	024M4767V
Adat3	Rabbit	1/500	2N HCl	IHC, WB	Homemade	Article 1
Adat2	Rabbit	1/500	2N HCl	IHC; WB	Homemade	Article 1

Secondary antibody	Host	Dilution	Used for	Provenance	Reference
Actin coupled HRP	Mouse	1/100 000	WB	Sigma-Aldrich	A3854
Goat-mouse-HRP	Mouse	1/10 000	WB	ThermoFisher Sc.	G-21040
Goat-rabbit-HRP	Rabbit	1/10 000	WB	ThermoFisher Sc.	G-21234
Goat-rat-HRP	Rat	1/10 000	WB	ThermoFisher Sc.	62-9520
Donkey-goat-488	Goat	1/1000	IF	ThermoFisher Sc.	A-11055
Donkey-mouse-488	Mouse	1/1000	IF	ThermoFisher Sc.	A-21202
Donkey-mouse-555	Mouse	1/1000	IF	ThermoFisher Sc.	A-31570
Donkey-rabbit-488	Rabbit	1/1000	IF	ThermoFisher Sc.	R-37118
Donkey-rabbit-555	Rabbit	1/1000	IF	ThermoFisher Sc.	A-31572
Donkey-rat-488	Rat	1/1000	IF	ThermoFisher Sc.	A-21208
Ki67 coupled-570	Rat	1/500	IF	eBioscience	41 5698 80

PART3

DISCUSSION &

PERSPECTIVES

Here, I present for the first time work directly showing a function of the *Adat2/3* and *Wdr4/Mettl1* complexes in the developing cerebral cortex. During the next sections I will discuss about my PhD thesis findings.

1. Functions of *Adat2/3* and *Wdr4/Mettl1* in the cerebral cortex

The fine spatio-temporal analysis of the *Adat2*, *Adat3*, *Wdr4* and *Mettl1* throughout cortical development in mice (Article 1) together with E14.5 *In situ* hybridization data from GenePaint (<https://gp3.mpg.de/>) (data not shown) shows that all genes are expressed both in cortical progenitors and neurons. Their expression pattern plus the phenotypes in patients with *ADAT3*, *WDR4* or *METTL1* suggest a role during both progenitor division and radial migration.

1.1 Radial neuronal migration

Upon ubiquitous silencing of *Adat3* or *Wdr4*, we observed an impaired distribution of *Adat3* silenced cells in the cortex with an accumulation in the IZ and lower CP at E18.5. To note, *Adat3* depleted cells reach their correct position after birth (analysis at P2), suggesting that *Adat3* knock-down leads to a delay rather than to a total arrest of migration. Unlike *Adat3*, post-natal analyses of *Wdr4* Knock-down at P2 did not lead to all the cells reaching their final position in the cortex in all cases. Results at P2 were heterogeneous: Whereas 6 embryos (33%) showed correct cell positioning, 3 of them (33%) showed a clear accumulation of some cells in the IZ. This heterogeneity in the results is similar to the one reported in *Wdr4* KO mice (Cheng et al., 2016): Cheng and colleagues reported lethality at E9.5 or E10.5 and different severity of the phenotypes depending on the embryos. Although these results should be confirmed by analyzing more litters, one may hypothesize that severity or penetrance of the phenotype upon *Wdr4* impairment is variable between individuals based on environmental or genetic factors. Another possibility that could account for incomplete penetrance of the phenotype would be that expression of the miRNAs or IUE might have been slightly different between the embryos.

Upon neuron-specific silencing of *Adat3* and *Wdr4*, we observed respectively the same migration phenotype to the one observed upon ubiquitous silencing, which suggests a function of both *Adat3* and *Wdr4* in neurons (analyses at E18.5). Altogether, these results evidence that *Adat3* and *Wdr4* are required for proper neuronal migration.

1.1.1 How to determine which phases of radial migration are impaired?

The migration defects observed upon knockdown of *Adat2*, *Adat3*, *Wdr4* or *Mettl1* could potentially be associated to all the phases involved in neuronal radial migration. However, as there is not a very prominent accumulation of cells in the IZ, I hypothesize that it could be mainly associated to the locomotion or terminal translocation phases. It might also be caused by a worsened cellular fitness that could have an effect throughout all the process. It would be particularly interesting to carry out time-lapse experiments to determine which phases of radial migration are specifically affected upon their depletion. To gain further insights into the function of the complexes in radial migration, it would be valuable to assess whether expression of *Adat2*, *Adat3*, *Wdr4* or *Mettl1* might vary between different phases of neuronal radial migration. Towards that purpose, we could analyse microarray data of cells that were FACS-sorted 1,2 or 3 days after IUE at E14.5 (Data from (Ohtaka-Maruyama et al., 2018)) and determine if their level of expression varies between different radial migration phases. Such experiments together with the time-lapse would help determine which are the phases that are mostly impaired.

1.1.2 Is the function of *Adat3* and *WDR4* in migrating neurons dependent on their catalytic partners *Adat2* and *Mettl1*?

Adat3 and *Wdr4* function in radial migration is likely related to their role in *Adat2/3* and *Wdr4/Mettl1* complexes since same migration phenotype was observed after depleting *Adat2* in neurons or *Mettl1* ubiquitously in the cortex (analyses at E18.5) to those obtained with *Adat3* and *Wdr4* respectively. Several evidences support the need of *Adat2* co-expression for proper *Adat3* folding and its implication in neuronal migration function of *Adat3*: 1) stoichiometric levels of ADAT2 and ADAT3 are required to produce adequate folding of ADAT3 and function. Indeed a) Expression of soluble ADAT3 in *E.Coli* has been found to require co-expression of ADAT2 (Delker et al., 2013; Rubio et al., 2007); b) ADAT2 is able to prevent self-association WT ADAT3 and reduce its interaction with cellular chaperonins (J. Ramos et al., 2019); c) I showed that expression of ADAT3 WT in N2A cells is higher if co-expressed with ADAT2; 2) we found that *Adat3* expression alone was not able to rescue the migration phenotype. Nonetheless, when *Adat3* was co-expressed with *Adat2* WT a rescue of the phenotype was observed. Interestingly, rescue of *Adat3* WT was dependent on the dosage of the vector (Discussed in 2).

Interestingly, *Wdr4* was never shown to require *Mettl1* co-expression, its expression alone (without *Mettl1* co-expression) was sufficient to rescue the migration phenotype which suggests that unlike the *Adat3*, *Wdr4* does not need co-expression of the other subunit.

Interestingly, like in the case of Adat3, rescue of the phenotype by Wdr4 expression was also dependent on the dosage of the vector (Discussed in 2). My results suggest Adat3 and Wdr4 function in neuronal migration is linked to their respective partners.

1.1.3 Are their deaminase and methylation activities involved?

Observing a similar result upon *Adat2* and *Mettl1* silencing (which bear the catalytic activity) supports that the radial migration phenotype is likely due their respective deaminase and methylation activities. In the case of Adat3 rescue experiments, we proved that co-expression of Adat2 WT rescued the migration phenotype, whereas, co-expression of Adat2 catalytically inactive (E73A) did not. To gain further insights into the function of Adat2 in migration, it may be worth performing rescue experiments of the phenotype observed upon *Adat2* silencing with Adat2 WT and catalytically inactive. Observation of a phenotype with catalytically inactive but not with the WT form would definitely prove that this function is dependent on Adat2 catalytic activity.

Interestingly, Adat3 V128M and Wdr4 R215L variants failed to rescue the migration defect upon knockdown of Adat3 and Wdr4 by miRNAs respectively. These two variants were reported to lead to decreased I₃₄ and m⁷G₄₆tRNA modifications respectively in patients derived cells (Publication1, (J. Ramos et al., 2019; Shaheen et al., 2015)) which further suggests that the lack of these tRNA modifications could participate to the defects in migration. Altogether, these results suggest that Adat3 and Wdr4 function in neuronal migration is related to its tRNA modification activity, nevertheless other activities of the complex cannot be excluded (Discussed further in 3.2).

We are currently performing similar experiments for Mettl1. We will silence Mettl1 using NeuroD miRNAs and perform phenotype rescue experiments with *METTL1* p.Ile120Met and p.Arg174Gln variants (which are expected to lead to lower tRNA modification levels, discussed in 5.1) . These experiments, together with assessment of rescue with Mettl1 catalytically inactive form (Cartlidge et al., 2005), are expected to provide further insights into need of Mettl1 catalytic activity in migration. If Wdr4 and Mettl1 migration functions are doing their function in migration as a heterodimer we would expect to obtain similar results to those obtained with Wdr4 in the new Mettl1 experiments.

1.2 Cellular proliferation/fate

The expression of *Adat3/2* and *Wdr4/Mettl1* in cortical progenitors and the high percentage of microcephaly in patients with *ADAT3*, *WDR4* and *METTL1* mutation indicated a possible function of the complex in regulation of cell proliferation and/or cell fate.

In Preliminary results 1 I studied the roles of *Adat3* in cortical progenitors by 1) Analyzing , proliferation, fate and survival 2 days after IUE of pCAGGS-miRNA (E13 to E15 analyses) in WT mice cortices; 2) By analizing progenitors biology in the *Adat3* KI line. My IUE results revealed a decrease in cell cycle exit and increased number of cells proliferating. Furthermore, I showed an altered formation of Pax6⁺Tbr2⁻ (Neurons), nevertheless, when the same experiments were carried out using Tbr2 (Marker for IPs) and Tbr1 (neuron marker) co-labeling no differences were observed between control and miRNA conditions. Consistently with the results obtained by IUE experiments, I also observed an alteration of cell cycle exit in the KI line. I identified several impairments in the cortices of KI/KI mice compared to WT littermates: 1) Decrease in cell cycle exit in cortical progenitors at E14.5; 2) An increased number of intermediate progenitors as well as an increase in the number of cells proliferating at E18.5. Nevertheless, I observed no alteration in progenitors at E14.5, no alterations in the neuronal populations studied both at E14.5 and E18.5, and no cell fate defects between at E14.5 (18h EdU) in this line. The discrepancies in cell fate experiments between the IUE experiments in WT mice and the KI model could be due to compensatory mechanisms in the KI line (discussed later in section 5.2.4). In addition, these differences, could also be explained by the difference in timing E14.5 (Edu18h) in the KI line and E13.5 to E15.5 in the IUE experiments. Altogether, these results show that *Adat3* p.V128M or depletion of *Adat3* levels by miRNAs affects progenitor's biology by impairing their cell cycle by E13.5-E14.5 embryonic stages. This impairment is leading to consequences in later stages of cortical development which include decrease formation of Pax6⁺Tbr2⁻ cells (neurons) by E15.5 (*Adat3* depletion) and increased number of progenitors and proliferating cells by E18.5 (*Adat3* p.V128M). My results with the IUE experiments and the KI line suggest that *Adat3* is important during neurogenesis.

Further studies should be performed in other developmental timepoints to fully characterize *Adat3* function in progenitors. Considering I observed a cell cycle defect at E14.5 and E15.5 it would be particularly relevant to assess cell cycle exit at E12.5, E13.5 and E16.5 and determine if this defect is still present in these stages and if it is more or less severe in these other developmental timepoints. Such differences between developmental timepoints in cell cycle-related parameters have already been reported in the literature. Rodriguez and co-workers (Rodriguez et al., 2012) for example, carried out studies for the transmembrane protein glycerophosphodiester phosphodiesterase 2 (Gde2). By comparing Gde2 WT and KO mice they showed a reduction of cell cycle exit at E12.5, no alterations at E13.5 and E14.5 and an increased cell cycle exit by E15.5 in their KO model. They also observed increased number of cycling cortical progenitors at E13.5 but not at E14.5. Their results evidence that cell cycle related defects in progenitors are very time-dependent. Authors showed that these cell cycle

defects correlated with an increase in superficial layer neurons at E17.5 (Rodriguez et al., 2012). As the defects that I observe in cell cycle exit are occurring later at E14.5 and E15.5, I hypothesize that outer layer neurons, such as layer IV pyramidal or upper layer callosal neurons (generation peak at E14.5 and E15.5 respectively) formation would be mostly impaired. To address this question, it would be interesting to study specific neuronal populations to see if there are any particular defects by looking at other neuronal markers from the ones I studied in this preliminary characterization of the model. It could be also particularly interesting to determine if gliogenesis is impaired upon *Adat3* depletion/dysfunction, since *Adat3* and *Adat2* peak of expression in mouse cortices by RT-qPCR occurred at E16.5 (At E17.5 there is a switch from neurogenic to gliogenic divisions (Qian et al., 2000)).

Similar experiments for *Adat2*, have not been performed yet. Nevertheless, recent work of Bornelöv and co-workers (Bornelov et al., 2019) supports a role of *Adat2* in cortical progenitors. Authors reported a majority of ADAT dependent codons enriched in the A-site of the ribosome in differentiating ESCs and a majority of them in the P-site in self-renewing ESCs. The lower frequency of ADAT codons in the A site in self-renewing ESCs indicates a faster translocation to the P-site. *ADAT2* mRNA transcript level was higher in self-renewing ESCs compared to differentiating ESCs. In accordance, I_{34} -modification levels were also higher in self-renewing ESCs (83-86%) than in differentiating ESCs (60-79%) (Bornelov et al., 2019). The time for the ribosome to ensure that a tRNA found in the A-site is indeed the cognate tRNA for the codon is considered as one of the major rates for translation elongation (Khade et al., 2011; Shah et al., 2013). Their results therefore suggest that higher I_{34} content in self-renewing cells might allow a faster translation in self-renewing cells.

Consistently, I speculate cortical progenitors might present like ESCs higher I_{34} -modification levels than neurons. This higher content of I_{34} modified tRNAs could allow a faster translation of several mRNAs, probably some of which could be related to cell cycle and specification. Such experiments could be performed by FACS sorting cortical progenitors and neurons (for example using Rosa26-loxSTOP-YFP; NEXCRE/+ mice, like in Article1) and performing tRNA sequencing on both populations to determine both the level of A_{34} and I_{34} tRNAs.

Results from Bornelöv and co-workers and my results are in agreement with work by Tsutsumi and colleagues, which showed that mutation in the deaminase domain of *Tad3* (*ADAT3* homolog in yeast) impairment lead to cell cycle arrest. In particular they showed that cell cycle arrest was caused by arrest in G1/S and G2/M cell cycle transition (Tsutsumi et al., 2007). Based on my results and the results from Bornelöv and co-workers, I hypothesize that some translational programs, probably of proteins highly enriched in “ADAT” codons, are affected

upon *Adat3* depletion and this is leading to the defect in cell cycle and neurogenesis (For further discussion on this topic see 3.1.2).

It remains to be determined which phase of cell cycle might be impaired upon *Adat3* dysfunction, if these defects are related to its I_{34} activity and which could be the potential cellular pathways involved. To address these questions measurement of the number of cells in different cell cycle phases in the model could be performed. For example, quantification of number of cells in S-phase could be performed by injection of EdU or BrDU 1h before sacrifice and their subsequent labeling and quantification. Martynoga and colleagues reported that injection of two different halogenated thymidine analogues (such as Edu and BrdU) allowed the calculation of cell cycle kinetic parameters, including total cell cycle time and length of the S-phase (Martynoga et al., 2012). Such quantifications at different developmental timepoints in the KI model could contribute to further determine how *Adat3* impairment affects cell cycle. Determining if *Adat3*-related cell cycle defects in cortical progenitors are related to its I_{34} activity could be performed for example by knockdown of *Adat2* by IUE in WT cortices: Which could be combined with a knockdown of *Adat2* and overexpression of catalytically inactive *Adat2* to further confirm the implication of the deaminase activity. Furthermore, the study of an *Adat2* cKO model with *Adat2* depleted in cortical progenitors could also contribute to answer that question. The potential cellular pathways involved could be identified for example by performing ribosome profiling on *Adat3* or *Adat2* cKO models with *Adat3* or *Adat2* depleted in cortical progenitors.

Regarding *Wdr4* and *Mettl1* several evidences support a role in cell proliferation/specification. Depletion of *WDR4* has been shown to impair cell cycle exit in flies (Wu et al., 2006) and mouse embryonic fibroblasts (C. C. Lee et al., 2018). *Mettl1* has been shown to regulate stem cell formation/proliferation during intestinal remodeling in *Xenopus tropicalis* (Na et al., 2020) and limit differentiation and functioning of endothelial progenitor cells (Y. Deng et al., 2020). Furthermore, Lin and colleagues reported that m^7G_{46} tRNA modification is required for mESCs mRNA translation, self-renewal and differentiation towards neural lineages (Lin et al., 2018). The authors revealed that genes associated to cell cycle and brain abnormality are regulated by *Mettl1* at a translational level (discussed further in 3.1.2). These defects in cell cycle are associated to a lower number of cells in G1 and a higher number of cells in the G2/M transition in *Mettl1* KO mESCs. Like in the case of ADAT, their data suggests that m^7G_{46} is essential during ESC self-renewal and differentiation (Lin et al., 2018). Finally, in a recent publication, it was shown that METTL1-mediated m^7G silencing in human induced pluripotent stem cells (hiPSCs) impairs neuroectoderm formation while accelerating mesoderm differentiation and vasculogenesis (Y. Deng et al., 2020).

It would be particularly interesting to quantify if like in the case of I_{34} , content of m^7G_{46} in tRNAs is higher self-renewing cells than in differentiating cells. For that purpose, cortical progenitors and neurons could be FACS sorted (as described above) and m^7G MeRIP-Seq or m^7G TRAC-Seq (Lin et al., 2018) could be performed.

Altogether, my work plus the work just mentioned provide further knowledge about the role of I_{34} and m^7G_{46} highlight the implication of these two modifications for self-renewing and cellular differentiation. It would be interesting to carry out similar experiments to those carried out for *Adat3* (E13.5-E15.5 IUE to analyze cell fate and proliferation defects) for *Adat2*, *Wdr4* and *Mettl1* as a starting point to get insights into the role of these genes in cortical progenitor's biology. The use of cKO models (see 2.1) would be particularly advantageous for studying the lack of these genes in cortical progenitor's biology. Another possibility could be the use of human cortical organoids derived from hESCs, which would allow to study the function of the genes in the cortex directly in a human context and would allow to obtain higher amount of samples for downstream analyses (Cakir et al., 2019). Considering the arrest in several cell cycle phases, I hypothesize cortical progenitors will take longer to exit cell cycle and as a result will differentiate towards neural lineages at later stages. Another possibility would be to observe some cell death in cortical progenitor's upon impairment of *Adat3*, *Adat2*, *Wdr4* or *Mettl1*. This could be assessed for example co-labeling with Caspase3 (apoptosis marker) and progenitors' markers such as Pax6 or Tbr2. Observing a convergence between both complexes could support the present of a common similar pathway underlying I_{34} and m^7G_{46} in progenitor's (further discussed in 3.1 and 3.2). Altogether, the further study of these genes in progenitor's biology could help to some of the patient related phenotypes, such as microcephaly.

2 Does dosage of the *Adat2/3* and *Wdr4/Mettl1* complex matter?

Strikingly, I observed that the ability of *Adat3* to rescue the migration phenotype is dose dependent. Indeed, while a concentration of DCX *Adat3* WT vector of $0.5\mu\text{g}/\mu\text{L}$ was not sufficient to rescue the migration phenotype induced by *Adat3* KD, concentrations of $0.75\mu\text{g}/\mu\text{L}$ and $1\mu\text{g}/\mu\text{L}$ rescued the migration phenotype. Like in the case of *Adat3*, *Wdr4* dosage levels seem to be particularly sensitive, with overexpression of *Wdr4* WT form at $1\mu\text{g}/\mu\text{L}$ leading to a radial migration phenotype (data not shown) but not at $0.5\mu\text{g}/\mu\text{L}$ (rescue of the phenotype with

WT variant). By contracts, results show that *Wdr4* WT when overexpressed at 0.25 μ g/ μ L is not enough to rescue the migration phenotype induced upon *Wdr4* miRNA.

Interestingly, NeuroD *Wdr4* WT at 0.25 μ g/ μ L was used as an approach to model *Wdr4* p.Met1Thr variant: *Wdr4* p.Met1Thr has been found in homozygosity and as a compound heterozygous variant (p.Met1Thr; c.567-2A>G) in patients. Interestingly, conversion of the first residue of a peptide sequence from methionine to threonine is thought to act as a weak initiator leading to a reduced expression of the gene (Kearse et al., 2017). Thus, supporting an haploinsufficiency effect of p.Met1Thr in carrier patients. Not observing a rescue with NeuroD *Wdr4* WT at 0.25 μ g/ μ L suggests that this might be what occurs in patients bearing *WDR4* pMet1Thr variant. It remains to be validated however, whether *WDR4* p.Met1Thr variant is leading to a weak initiator effect. For that, in vitro cell cultures will be transfected with plasmids containing *WDR4* WT or p.Met1Thr variants and *WDR4* protein levels will be assessed by Western Blot.

Other arguments that support the importance of dosage in these genes are: 1) The decrease in *ADAT3* in cells derived from patients with homozygous mutations in p.Val144Met and p.Arg112Leu display lower *ADAT3* protein levels (Discussed in 5.1.2); 2) The decreased levels of *Adat3* V128M in the KI line (which seems to lead also to lower *Adat2* levels, supporting the relevance of stoichiometry of the complex (still preliminary results) and 3) The implication of *Wdr4* as a candidate gene contributing to down syndrome phenotype (M. Sultan et al., 2007), that is caused by a trisomy of the chromosome 21 in Human.

Interestingly, *WDR4* is part of the locus triplicated in Down syndrome, which suggests that not only its decrease, but also its increase might be deleterious. However, *WDR4* implication in down syndrome is not demonstrated yet, towards this purpose, it would be particularly interesting to compare a model with three *Wdr4* alleles to a model with only one allele. The TS1Yah is a down syndrome mouse model which is trisomic for the 12 genes (Including *Wdr4*) encompassing the *Abcg1-U2af1* genetic interval found in HSA21 sub-telomeric region (Goodliffe et al., 2016). Breeding of the TS1Yah1 mouse line with *Wdr4*/+ mice (Briefly discussed in 2.1) could allow for analysis of the down syndrome related phenotypes in TS1Yah after genetic rescue of *Wdr4*. Subsequent analysis of cortical development and behavioral phenotypes in their offspring would determine if down syndrome related phenotypes in TS1Yah mice are due to *Wdr4* dosage.

Overall, my results suggest that *Adat3* (thus *Adat2*) and *Wdr4* levels should be tightly regulated when trying to express the proteins to ensure proper function of both genes.

2.1 Use of conditional knock-out animals as models?

We tried to generate an *Adat3* KO mouse line with the idea of studying heterozygous mice, as homozygous knock-out animals were expected to be lethal (A. P. Gerber et al., 1999). Nevertheless, *Adat3* knockout animals were lethal even in heterozygosity. In the *Adat3* KI line I reported a decrease of *Adat3* levels of 85.16% by Western-Blot in the cortex. Despite this line presenting low levels of a less functional *Adat3*, some functions for which *Adat3* is implicated (such as radial migration) could not be recapitulated in this line. I hypothesize that in the *Adat3* KI line, probably the threshold of activity/level of *Adat3* p.V128M is enough for most of *Adat3* related functions in mice, which partially hampers the study of some of the effects upon *Adat3* depletion. My results about the lethality of *Adat3* knockout animals in heterozygosity suggest *Adat3* may play important functions in other organs, such as the testis or ovaries, limiting germ line transmission for example. To assess all the *Adat3* related functions/processes in mammals it would be of great help to use a conditional knock-out model, in a way that tissue specific *Adat3* knock-out could be performed. Towards this aim in the lab we generated a mouse model with *Adat3* exon 2 floxed (LoxP-Exon2-LoxP) model to carry out tissue specific deletion of *Adat3*. Analysis after crossing this line with *Nex-Cre* and *Nestin-Cre* mice lines will allow to assess the effect of completely depleting *Adat3* in neurons and progenitors and are planned to be performed soon.

As mentioned before, *Wdr4* knock-out animals are lethal at embryonic stage E9.5-E10.5(Cheng et al., 2016). Interestingly, we checked for possible phenotypes in a *Wdr4* knock-out heterozygous mouse line and observed that animals were fertile and had a normal lifespan and no differences in brain development or other organs in comparison to WT littermates (data not shown). In terms of brain development, we checked for expression of *Pax6*, *Tbr2* and *Tuj1* markers at E14.5 and E18.5 in heterozygous and WT cortices and observed no differences. This further supports that one WT allele of the gene is enough for supplying the dosage of *Wdr4* that cells need. It remains unknown whether *Mettl1* Knock-out animals would be lethal as well, however, as it is the catalytic subunit of the complex it seems tempting to speculate that this would be the case. I therefore think that *Wdr4* or *Mettl1* cKO would be particularly of interest for further assessing the function of the complex and determining whether *Wdr4* and *Mettl1* converge in all their functions. I hypothesize cKO animals would be a better model than Knock-in animals (modelling the human variants) since as reported for *Adat3* p.V128M knock-in mouse they might not recapitulate all patient features. *Wdr4* drosophila homologue (*wuho*) mutants were shown to be infertile (Wu et al., 2006) , another drawback for the possible generation of Knock-in animals for *Wdr4* and *Mettl1* is that they might be sterile.

The use of a cKO animal models for these genes could also be particularly advantageous for performing for example ribosome profiling (Ingolia, 2014; Ingolia et al., 2012) and assessing how lack of these genes might affect translational programs and which are the cellular pathways mostly affected in the models. Furthermore, cKO models could be used for example for performing acute depletion experiments in a cohort of cells, for example by IUE of Cre expressing vectors.

3. Which are the functions and downstream pathways behind the phenotypes?

In the next lines I will discuss about which functions of the complexes could explain and how the observed phenotypes in mice and human patients.

3.1 tRNA modification: I₃₄ and m⁷G₄₆

The fact that the main activity of both complexes is tRNA modification, the convergence of phenotypes with both subunits and the impairment of I₃₄ and m⁷G₄₆ observed in cells derived from human patients (ADAT3 p.Val144Met (Article 1 and (J. Ramos et al., 2019) and WDR4 p.Arg170Leu (Shaheen et al., 2015)) supports that the main function behind the observed phenotypes in patients is the impairment of these tRNA modifications.

Notably, *in vivo* loss of WDR4 might have more permanent consequences (at least for migration). This might reflect that loss of m⁷G₄₆ has more impact on tRNAs. Indeed, m⁷G₄₆ absence could lead to the degradation of an important pool of tRNAs. m⁷G₄₆ appears to be more important in mammals than in yeast for example, recently, Lin and colleagues reported that in mice up to 22 tRNAs are modified by m⁷G₄₆ while only 11 are modified in yeast (Lin et al., 2018). Lacking several tRNAs could have severe consequences during radial migration of neurons, which could be irreversible in some cases (embryos that show a phenotype at P2).

Interestingly, different ADAT tRNAs seem to be differently affected by I₃₄ since percentage of I₃₄ containing tRNAs varies depending on the tRNA specie analyzed, for example, in our analyses all of tRNA-Val-AAC displayed I₃₄ whereas in the case of tRNA-Thr-AGT, only 5% of the reads contained this modification. Reduction of this modification upon p.V144M mutation also seem to vary depending on the tRNA specie, since we observed reductions of 70% and 97% for tRNA-Val-AAC and tRNA-Thr-AGT respectively. Therefore, ADAT3 malfunction could have a differential effect on different tRNAs. For the WDR4/METTL1 complex it was shown that Mettl1 KO also affected tRNAs differentially, whereas ValTAC, ValAAC, ValCAC,

ProCGG, ProAGG, and IleAAT, decreased more than 2-fold levels of other METTL1 substrates were more modestly decreased (Lin et al., 2018). These findings suggest that different tRNAs are differentially affected by lack of Adat2/3 or Wdr4/Mettl1, probably due to their binding to the complex or stability. Function of I₃₄ and m⁷G₄₆ modifications could be related to their effect on protein translation or to other downstream mechanisms. These two options are discussed in the next sections.

3.1.2 Effect I₃₄ and m⁷G₄₆ tRNA modifications in protein translation

As Adat3/Adat2 and Wdr4/Mettl1 are catalysing tRNA modifications, it is tempting to speculate that the phenotypes might be due to an altered translation of group of proteins that could play an important role in any of the phases involved in neuronal migration or cell cycle regulation. Possibly these proteins could be part of groups of proteins that have already been shown to regulate these processes, such as transcriptional regulators, cellular signalling proteins, cytoskeleton components, or extracellular matrix and transmembrane proteins among others.

Several publications show the relevance of I₃₄ and m⁷G₄₆ for translation. Although some publications point at specific protein targets that are affected, it is still unclear if global protein defects might also occur. In one publication, Lyu and colleagues (Lyu et al., 2020) carried out ribosome profiling in *adat2* silenced *Neurospora crassa* cells and showed that upon I₃₄ reduction there were major ADAT-related tRNA profile changes (resulting in codon optimality for translation elongation changes), changes at the translation kinetic level (increased genome-wide codon usage-biased ribosome pausing) which results in changes at the proteome level. They assessed proteome changes upon *adat2* silencing and determined a decreased in citrate cycle, pyruvate metabolism, endocytosis, glycolysis/gluconeogenesis and proteins related to the proteasome and ribosome. On the other hand, they report an upregulation of genes involved in 2-oxocarboxylic acid metabolism, aminoacyl tRNA biosynthesis, and biosynthesis of antibiotics, secondary metabolites and amino acids. All these changes in cellular metabolism could affect progenitor's biology, compromising their proliferation (in accordance with my results for a reduced cell cycle exit in *Adat3* knockdown and KI). In neurons, such changes could affect also the overall energy disposal for the cells and protein synthesis leading to global changes in protein synthesis and cellular fitness. Most of the metabolic pathways impaired are related to glucose metabolism. Glucose is an essential substrate for the brain, where metabolism of acetyl-CoA by the citrate cycle leads to the synthesis of glutamate and γ-aminobutyric acid the neurotransmitters (Haslam et al., 1963), as a consequence, disorders of brain glucose metabolism are often associated with impaired neuronal excitability (Jakkamsetti et al., 2019). Therefore, epilepsy in patients with *ADAT3* mutations could be related to

impairment of the formation of these neurotransmitters. To gain further insights into metabolic changes upon I_{34} reduction I propose to perform metabolomics analyses (A. Zhang et al., 2012) on samples derived from cKO, human organoids or KI animals. In a recent thesis (L. Ribas de Pouplana lab IRB, Barcelona, <http://hdl.handle.net/10803/668499>) silencing of *ADAT2* lead to impaired cellular proliferation (in accordance with *Adat3* phenotype in cortical progenitors) and affected the expression of genes coding for ECM components, such as mucins. Their results suggest that *ADAT2* is required for the proper translation of ECM genes enriched in *ADAT* codon stretches. Importantly, ECM components are crucial during cortical development: ECM components regulate cell shape, proliferation, differentiation and migration during cortical development (Long et al., 2019). Functions of *ADAT2/3* in patients and during cortical developmental could thus be related to functions of ECM proteins. I therefore suggest, assessing the expression levels of several ECM proteins in cKO, organoids or even the *Adat3* V128M KI model and see if these results correlate with Rodriguez-Escriba's. Once alteration in one or several ECM proteins have been identified, complementation experiments could be performed with the identified ECM proteins to decipher whether or which phenotypes could be more related to ECM protein mistranslation. Altogether, these changes in the proteome could account for the phenotypes in *ADAT3* patients and its further study should contribute to better understand the human disease. In another publication, Lin and colleagues (Lin et al., 2018) revealed that in a context of lack of m^7G_{46} (*Mettl1* KO mESCs) there is increased ribosome pausing at m^7G tRNA-dependent codons. In particular, there was an increased ribosome occupancy at P sites, which suggests that lack of this modification may impede ribosomal translocation. The authors revealed that genes associated to cell cycle and brain abnormality are regulated by *Mettl1* at a translational level. Among the Top genes with a higher fold change by ribosome profiling there is for example *Ubxn11*, *Drd2* (Top2 genes with higher fold change) (Lin et al., 2018). These two genes are particularly interesting for the phenotypes observed in mice and patients. *Ubxn11* is predicted to be involve in the reorganization of actin cytoskeleton by *Rnd1*, *Rnd2* and *Rnd3* and to promote RhoA activation (<https://www.uniprot.org>). On the other hand, *Cd24a* is a cell adhesion molecule which plays a pivotal role in cell differentiation of different cell types. *Cd24a* has been shown to regulate proliferation of neuronal committed progenitors in the cortical SVZ (Nieoullon et al., 2005). In a recent publication, Deng and co-workers (Y. Deng et al., 2020) in line with their results showed that reduction of *METTL1* levels in hiPSCs is required for self-renewal by regulating cell cycle genes and that its reduction lead to an decreased expression of neuroectoderm-specific genes (including *OTX2*, *PAX6*, *SOX1* and *MEIS1*) and an increase expression of mesoderm-specific genes (including *TBX6*, *MEOX1*, *PECAM1* and *NKX2-5*)(Y. Deng et al., 2020). Mistranslation of these genes (among others) could potentially explain the migration and proliferation defects in the cortex. I therefore

propose to perform, like in the case of the ADAT2/3 complex, complementation assays with these genes and other interesting candidates from and assess if the phenotypes observed after impairment of WDR4 or METTL1 functions could be rescued by their overexpression.

Another possibility for both I₃₄ and m⁷G₄₆ apart from specific effect on translation, would be that instead, there would be an impact on all the proteome. Nedialkova & Leidel (Nedialkova et al., 2015) showed that loss of mcm⁵ in U₃₄ (which is also leading to impairment of neurogenesis (Laguesse et al., 2015)) causes widespread protein aggregation in vivo.

3.1.3 Possible downstream mechanisms of ADAT2/ADAT3 and WDR4/METTL1 dependent-tRNA defects?

Patients with mutations in *ADAT3*, *WDR4* and *METTL1* display an autosomal recessive type of inheritance and clearly overlap in several phenotypes, majorly, ID, microcephaly and developmental delay. These facts together with observing a similar phenotype in migration and implications of both complexes in cellular proliferation and regulation of cell cycle raise the hypothesis of common downstream mechanisms which drive the disease. It could be that both complexes partially overlap in the changes in the proteome that they might induce upon their dysfunction. It would also be possible that in both cases there is a similar cellular effect, such as ribosome stalling, aggregation of a particular type of cellular proteins or induction of similar tRNA derived fragments for example. Another possibility that could account for these similarities between both complexes could be that the initial cellular effect upon malfunction of the complexes were different but afterwards they end up converging in a similar cellular pathway, for example transcriptional response by ATF4 (a transcription factor implicated in amino acid starvation response whose homolog in *Neurospora crassa* was shown to be an effector to *adat2* silencing)(Lyu et al., 2020). Unfortunately, these are just hypotheses for which there is not a clear answer yet and in order to answer them further research on the field should be done.

Ribosome profiling for *ADAT2/3* or *WDR4/METTL1* data in the brain would contribute to identify the main targets. I therefore suggest performing ribosome profiling in cKO models for these genes in the brain at different developmental timepoints to identify several genes which could be implicated in the phenotype. Once identified, codons of such genes could be modified to a non-*ADAT2/3/WDR4/METTL1* dependent profile (Rapino et al., 2018) (in a way that they would be recognized by tRNA isodecoders which do not require *ADAT2/3* or *WDR4/METTL1* modifications and then they could subsequently be overexpressed in different models (Knock-in models, cKO models, patient derived cell types) to assess possible rescues of the

phenotype. However, an important drawback of this approach would be that by modifying their codon usage, the rate of translation of those genes might be altered too.

Lack of several tRNA modifications, such as U₃₄, have been shown to lead increased ribosome pausing and protein misfolding and aggregates (Nedialkova et al., 2015). As Ribosome profiling has also determined ribosome pausing in an *adat2* (Lyu et al., 2020) or *Mett1* (Lin et al., 2018) silenced context, protein misfolding or aggregation could be the result of lack of their modifications. Assessment of protein aggregation could be performed for example by checking cells or tissues with impaired function of these gene by electronic microscopy or fluorescence microscopy, in the last case after staining with hydrophobic probe Nile red for example (Demeule et al., 2007).

Lack of I₃₄ or m⁷G₄₆ could promote the generation of small tRNAs interfering in some cellular functions (such as apoptosis). NSUN2 is known to catalyze m5C in the anticodon of tRNAs and prevent their cleavage by Angiogenin (Blanco et al., 2014). Importantly, more enzymes are expected to generate tRNA fragments, most of which are not identified. Lack of ADAT2/3 and WDR4/METTL1 catalyzed tRNA modifications could also induce the generation of such tRNA fragments. I therefore propose to assess tRNA fragment levels in RNAs extracted from cKO mice tissue or patient cells to determine if this is the case. Towards this aim, tRNA sequencing in the mentioned samples could be performed.

3.2 Other functions than catalyzing I₃₄ and m⁷G₄₆ tRNA modifications?

Importantly, other functions apart from catalyzing I₃₄ or m⁷G₄₆ tRNA modifications have been described for both complexes which could also explain and participate in ADAT2/ADAT3 and WDR4/METTL1 roles in the cells.

Regarding the ADAT2/ADAT3 complex it was shown that in *Trypanosoma brucei* it can catalyze C to U deamination in some tRNAs in addition to single-stranded DNA. Rubio and colleagues showed that, at least for tRNA-Thr, cytosine 32 is methylated to m³C by ADAT2/3 and TRM140, once methylation has occurred this base is deaminated by the same set of enzymes leading to the formation of m³U. Interestingly, interaction of TRM140 with ADAT2/3 keeps the mutagenic activity (Rubio et al., 2017; Rubio et al., 2007). Regarding these functions there are many questions that remain open? Are these functions also conserved in higher eukaryotes such as mice or human? If yes, is the ADAT2/ADAT3 complex using its mutagenic activity in any cellular context? Is role of ADAT2/ADAT3 in the catalysis of m³U₃₂ tRNA-Thr also conserved for other tRNAs? If yes, are all “ANN” anticodon containing tRNAs or are there

other tRNAs that are potentially modified as well by ADAT2/3? Which is the exact biological function of this modification? Our tRNA-seq experiments from patient derived cells (discussed in 5.1.2) will potentially answer some of these questions for the first time in humans.

It is clear though that ADAT2 and ADAT3 work as a heterodimer to carry out these functions. However, it was shown in publication 1 and work by Torres and colleagues (Torres et al., 2015) that ADAT2 and ADAT3 do not always colocalize, with the possibility of one of the subunits being localized only to the nucleus and the other one more in the cytoplasm. If ADAT2 and ADAT3 require each other for all the cellular functions in which they participate why are they sometimes located in different cellular compartments? Is it just because ADAT3 needs co-assembly of ADAT2 to avoid precipitation as stated by Ramos and colleagues (J. Ramos et al., 2019) or could it be that one of the subunits is doing other functions when not found in the same compartment as the other one? All these questions remain still unclear.

Interestingly, our collaboration with Christophe Romier's group (IGBMC, Strasbourg), has revealed for the first time the structure of the Adat2/3 complex (data not shown), modeling on the structure have revealed that it is quite unlikely that the Adat2/3 complex recognizes other substrates apart from tRNAs (data not shown). This finding, suggest Adat2/3 tRNA modification is the main function behind the observed phenotypes for this complex. It also suggests Adat2/3 is more stringent in terms of substrate recognition than the Wdr4/Mettl1 complex

Other functions and interactions apart from catalysis of m^7G_{46} in tRNAs were published for both WDR4 and METTL1 (for extensive detail check section 2.6.3 of the introduction). Some examples include work from Cheng and colleagues, who showed that WDR4 silencing led to genome instability. Interestingly, METTL1 silencing did not lead to the same results, which suggests that WDR4 function in genome maintenance is METTL1 independent) (Cheng et al., 2016). On the other hand, METTL1 has been shown to be activated by Thyroid hormone 3 (Na et al., 2020) and repressed by insulin signaling (Cartlidge et al., 2005; Na et al., 2020) as well as to inhibit the MAPK signaling pathway (Y. Deng et al., 2020) and catalyze m^7G modifications in mRNAs and miRNAs promoting their translation and correct processing respectively (Pandolfini et al., 2019; L. S. Zhang et al., 2019). Importantly, WDR4 has been shown to participate in the methylation of mRNAs and miRNAs, however, its role in Thyroid hormone 3, insulin and MAPK signaling is currently unknown.

Some of the functions associated to WDR4 and METTL1 could also have a role in the observed phenotypes. DNA repair for example is crucial for genome stability in the developing cortex, it was recently shown that genome stability in neural progenitors contributes to their neuronal

differentiation during cortical development (Onishi et al., 2017). *Wdr4* function in genome stability and DNA damage could be associated to the human phenotype by leading to cell death and affecting progenitor division leading to microcephaly. MAPK signaling has also been shown to be important during cortical development, for example its malfunction has been proven to impairs cortical layer 5 circuit development and pyramidal neuron excitability (Xing et al., 2016). As previously reviewed in sections 1.4.2.3.5 and 1.5.2.4.1 of the introduction miRNAs have already been shown to be involved in transcriptional regulation of neurogenesis and radial migration respectively. Therefore, suggesting *Wdr4/Mettl1* functions in radial migration and cortical progenitors could be associated to miRNAs.

Interestingly, unlike *ADAT3* and *ADAT2*, *WDR4* and *METTL1* have been associated to migration defects in other cellular contexts. Pandolfini and colleagues (Pandolfini et al., 2019) showed that *METTL1* promotes let-7 miRNA family processing via m⁷G methylation: Presence of m⁷G in miRNAs was shown to promote their correct processing. In addition, they assessed migration of A549 (human lung adenocarcinoma) cells upon knockdown of *METTL1* and determined that cells showed a higher migration capacity but not affected cellular proliferation. To note, the increased migration phenotype was rescued by expression of WT *METTL1* but not its catalytically inactive variant which suggests that the catalytic activity of *METTL1* is involved in the migration phenotype (Pandolfini et al., 2019). It remains therefore controversial whether the effect that I observed upon depletion of *Wdr4* and *Mettl1* by IUE of miRNAs in mice embryos is strictly related to their tRNA modification activity. It would be interesting to assess whether this effect is due to its modifying activity over tRNA, miRNA or mRNA or a combined effect of all.

Interestingly, let-7 miRNA family has been already shown to participate in neuronal radial migration and cell cycle regulation in the cerebral cortex. For example, let-7d was shown to target the neural stem cell regulator TLX and regulate neural cell fate and neurogenesis (C. Zhao et al., 2013). Specifically, the authors showed that let-7d overexpression *in vivo* resulted in reduced TLX expression in cells and up-regulated miR-9 expression which promoted premature neuronal differentiation and migration (C. Zhao et al., 2013). In order to assess whether Mettl1 function in the cortex is linked to the let-7 family of miRNAs it could be determined if some of the phenotypes upon modification of the activity of some of the miRNAs comprising the let-7 miRNA family are recapitulated by modifying Mettl1 activity: For example reduced TLX expression, miR-9 upregulation and premature neuronal differentiation in the case of let-7d. In addition, similar IUE experiments to the ones performed for *Wdr4/Mettl1* could be performed reducing (antagomiRs) their levels. Complementation assays by

overexpressing the miRNAs (plasmidic vector) in a context of reduced *Wdr4* or *Mettl1* could also be very informative.

Furthermore, I propose to perform miRNA/mRNA m⁷G profiling experiments (L. S. Zhang et al., 2019) in *Wdr4* or *Mettl1* cKO mice at different developmental stages and compare them to WT mice embryos. Comparison of the results with the miRNAs identified by Pandolfini and colleagues (Pandolfini et al., 2019) to be modified by METTL1 could help identify further miRNAs that could be involved. If several miRNAs were identified their targets could be predicted (using for example TargetScan, Diana-microT v3.0 and MicroRNA.org websites) to identify further downstream targets implicated.

Overall, these findings prove that METTL1 and WDR4 participate in a plethora of functions in the cell, they suggest that the complex might impact protein synthesis and transcription based on different types of signaling in living organism through which they might regulate several cellular pathways in the cell (such as MAPK) and different cellular functions such as proliferation or migration.

Although there are some functions of ADAT2/3 and WDR4/METTL1 which could be independent on the other subunit of the complex my findings in publication 1 for radial migration phenotype suggest that their function in migration is directly related to the other subunit of the complex (discussed in 1.1.1). Nonetheless, The P2 migration analyses revealed a difference between the results of Adat3 and *Wdr4*. This raises 2 hypotheses: 1) Stronger effect of loss of m⁷G modification than I₃₄ modification in vivo (see discussion above) or 2) other functions of *Wdr4* not-related to tRNA, such as miRNA or mRNA modification among others.

3.3 How to determine if the functions of the complexes are linked to their tRNA modifying activity?

As mentioned before, Adat2/3 functions in the cortex appear to be associated to its tRNA modifying function. Nevertheless, it is not that clear for *Wdr4*/*Mettl1*. To determine whether the observed phenotypes of this complex are strictly related to tRNA modification or also to mRNA and miRNA modification several experiments could be performed. Considering that Pandolfini and colleagues reported let-7 miRNA family as one of the main miRNA families affected upon *METTL1* knockdown (Pandolfini et al., 2019) studying its involvement by rescue experiments in which their levels are enhanced or reduced in cortices could be particularly informative (several experiments where already mentioned in the previous section).

To further dissect if *Wdr4*/*Mettl1* function is related to its tRNA modifying activity co-electroporation of miRNAs knocking down *METTL1* and co-injection of tRNAs, miRNAs or

mRNAs with m⁷G modification (synthesized *in vitro*) could reveal which substrates are most implicated in its neuronal function. In the particular case of tRNAs it would be interesting to overexpress tRNAs ValTAC, ValAAC, ValCAC, ProCGG, ProAGG, and IleAAT as they were more decreased than other WDR4/METTL1 substrates upon *METTL1* KO in mESCs (Lin et al., 2018).

Similar experiments, however, have not been performed yet and it is not clear if modified tRNAs, miRNAs or mRNAs would be successfully be incorporated into cells. Similar experiments could be performed with plasmids to overexpress these molecules, nevertheless, one of the major drawbacks of these experiments is that they would not be modified in a Wdr4/Mettl1 depleted context. Similar experiments for Adat3, Adat2 with tRNAs could also confirm that the phenotype is associated directly to tRNAs.

To further assess if some of the functions of ADAT3, ADAT2 or WDR4 and METTL1 are independent on the other subunit, rescue experiments with a variant of the protein which cannot interact with the other subunit (while not affecting protein stability) could be particularly informative.

Finally, another way to confirm indirectly implication of tRNAs would be get a spatial resolution of defects in protein translation. For that, formation of nascent polypeptide chain by fluorescence (O-propargylpuromycin)(Blanco et al., 2014) in organotypic brain slice culture (WT versus cKO or KI at different developmental stages) could be performed.

4. Other brain related functions?

Many patients with *ADAT3*, *WDR4* or *METTL1* mutations present ID, microcephaly, spasticity, epilepsy, brain anomalies, attention deficit/hyperactivity, aggressiveness, seizures, agenesis of corpus callosum, myelination defects or atrophy of the cerebellum. All these brain-related clinical features support further functions of these genes in addition to their role in cortical radial migration and neurogenesis.

Some patients have been reported to have atrophy of the cerebellum. Consistent with these observations, many patients have been reported to have motor developmental delay, including difficulties for processes such as walking or crawling, functions which are mainly regulated by the cerebellum. Therefore, investigating the potential function of these genes in other brain structures apart from the cerebral cortex, such as the cerebellum (for example by the use of cKO animal models) would contribute to further understand how impairment of these genes lead to disease in human patients.

Furthermore, observing spasticity (disrupted communication between the brain and muscles) and defects in myelination and corpus callosum suggest that defects in these genes could lead to cell death, demyelination or axonal/dendrites extension defects, in addition to playing important functions in synapses and dendrites. Axonal or dendrite extension defects are particularly likely, since these structures are dependent on local translation (Holt et al., 2019). Having an alteration of local translation in dendrites and axon would imply that these structures would depend more on soma protein synthesis and their transport. Such an impairment would probably cause that axons and dendrites are not supplied efficiently with the proteins that they need for their biological functions. Altogether, such problems in protein translation and axon/dendrite extension could lead to defective neuronal connectivity and result in impairments in neuronal activity thus explaining the epilepsy in many patients. further studies of these neuronal compartments in a context of dysfunction of these genes should contribute to better understand the pathologies.

The presence of seizures in many patients suggest that there is an abnormal electric activity in the brain, this could be due to neuronal connectivity or impairment in synapses. In accordance, KO brains for the tRNA modifier *Nsun2* (m^5C) showed impaired synapses formation (Blanco et al., 2014). Altogether these clinical symptoms suggest that *ADAT3*, *WDR4* or *METTL1* could be important for neuronal local translation. Thus, it would be particularly relevant to study in detail the impact of impairment of these genes in connectivity and neuronal synapses.

To gain insights into other functions of these complexes in the brain I propose several experiments. I suggest to further assess cell death defects in different models of these genes. To determine if these complexes are involved in corpus callosum and axonal or dendritic function I propose: 1) To determine if the number of layer II/III neurons (layers where callosal axons originate) in animal models; 2) To stain brains from animal models for these genes with axonal and commissural markers; 3) To transfect *in vitro* cortical neurons with miRNAs targeting these genes and analyze the effect in dendrites and axons; by labeling with markers such as MAP2; which would allow to measure for example the area of the cell body, axonal length and growth cone area. To analyze synapses, I suggest analyzing the number of synaptic puncta, for example by labeling with pre- and post-synaptic markers (such as *Synapsin* and *PSD95*) in cultured cortical neurons (derived from cKO models for example). Finally, if some defects in dendrites and axons are found, I would study the roles of these genes in local protein synthesis. That could be achieved for example by transfection of neurons with a GFP reporter containing the 3'UTR from *Camk2a* for dendritic targeting (Holt et al., 2019).

5. Effect of ADAT3 and WDR4 variants in cortical development

5.1 Variants in ADAT3, WDR4 and METTL1 and human disease

There exist several variants of ADAT3, WDR4 and METTL1 associated to human disease, leading in all cases to neurodevelopmental disorders. By the time I started my PhD thesis only ADAT3 p.Val144Met and WDR4 p.Arg170Leu were described (Alazami et al., 2013; X. Chen et al., 2018; Shaheen et al., 2016). As described in Article1, in collaboration with clinicians, we identified more variants in human patients for ADAT3 and WDR4. Furthermore, we described for the first-time patient mutations in METTL1. Interestingly, patients with METTL1 variant display similar phenotypes to those with mutations in *WDR4* (Shaheen et al., 2016; Trimouille et al., 2018) leading to neurodevelopmental disorders.

Several facts suggest that ADAT3, WDR4 and METTL1 mutations are loss of functions mutations: 1) All mutations in human patients described so far were recessive or compound heterozygous (Alazami et al., 2013; Braun et al., 2018; X. Chen et al., 2018; El-Hattab et al., 2016; Hengel et al., 2020; Salehi Chaleshtori et al., 2018; Shaheen et al., 2016; Sharkia et al., 2018; Thomas et al., 2019; Trimouille et al., 2018); 2) Patients with ADAT3 p.Val144Met and p.Arg128Leu mutations exhibit lower ADAT3 protein levels 3) Lack of tRNA modification activity in patient derived cells with p.Val144Met ADAT3 and p.Arg170Leu WDR4 variants (J. Ramos et al., 2019; Shaheen et al., 2015); 4) Lack of rescue for all variants in migration rescue experiments (with the exception of ADAT3 A180V).

In the following sections I will discuss about the mentioned facts and the structural, molecular and cellular consequences of variants in these genes.

5.1.1 Structural consequences

It was unknown whether variants in these genes could impair their interaction with the other subunits. Towards this aim we performed recombinant overproduction and purification of mouse full-length Adat3-wt or Adat3-V128M (recapitulating human p.Val144Met variant) fused to an affinity tag co-expressed with untagged full-length Adat2 in *E.coli* and showed that although p.V128M ADAT3 impacts protein stability it still interacts with ADAT2 (data not shown). In line with our results, Ramos and colleagues (J. Ramos et al., 2019) showed that p.Val144Met has a higher tendency to self-associate, and interact with cytoplasmic chaperonin complexes than the WT form if not properly assembled with ADAT2. Authors showed that co-expression of ADAT2 with this variant also induced a greater nuclear accumulation of ADAT3 suggesting that p.Val144Met can still interact with ADAT2. They further co-expressed GFP-

tagged ADAT3 WT or p.Val144Met together with Strep-tagged ADAT2 in HEK293T cells and showed after affinity purification that comparable levels of WT and p.Val144Met ADAT3 interact with ADAT2 (J. Ramos et al., 2019).

We carried out similar experiments to those performed for Adat3 with Wdr4 p.Arg170Leu variant. In publication 1, we performed recombinant overproduction and purification of mouse Wdr4-wt or Wdr4-R215L (recapitulating human p.Arg170Leu variant) fused to an affinity tag co-expressed with untagged full-length Mettl1 in *E.coli* and showed that R215L Wdr4 variant does not impair its interaction with Mettl1.

It remains to be determined how and to which extent other variants in ADAT3, WDR4 and METTL1 affect the complex. Towards this aim, we established a collaboration with C.Romier (IGBMC, Strasbourg). We plan to purify different Adat2-Adat3 or Wdr4-Mettl1 complexes, with different variants to see if interaction between the subunits is kept in all cases. In addition, we will assess binding to tRNAs for the different complexes.

Our preliminary results for the Adat2/3 complex (data not shown), have revealed that V128M, R112L, A180L and A180V still interact with Adat2 and bind tRNAs, with a similar affinity to the WT complex. This further supports that mutations in *ADAT3* which completely impair the catalytically activity of the complex might be lethal in humans. Interestingly, there is no binding of Adat2 alone or Adat3 alone to tRNAs and the N-terminal domain of Adat3 seems to be an important determinant for binding to tRNAs.

Interestingly, modelling of mutations described in *METTL1* using the structure of the complex in yeast (Leulliot et al., 2008) showed that p.Arg174Gln (R174Q in yeast) might affect the interaction with WDR4 and/or RNA binding, while p.Ile120Met (I139M in yeast) might affect METTL1 binding to SAM. In addition, variants p.Arg170Gln (K223 in yeast) (Trimouille et al., 2018) and p.Asp164Ala (D219 in yeast) (X. Chen et al., 2018) in WDR4 would be particularly interesting to study, since K223 (p.Arg170) and D219 (p.Asp164) Trm82 residues was shown to form salt bridges with E204 and K164 residues in Trm8. Considering that 3 out of 7 variants in *WDR4* and 1 out of 2 in *METTL1* are located in regions that are crucial for the formation of salt bridges between the subunits, it is reasonable to speculate that the WDR4/METTL1 complex might be particularly sensitive to mutations affecting the interaction between both subunits or the catalytic activity of the complex. It remains to be confirmed how all the variants in *WDR4* and *METTL1* affect their stability, the complex and their activity and binding for tRNAs. Such experiments will be carried out soon with Christophe Romier team (IGBMC, Strasbourg).

In our modeling, the side chain of METTL1 Arg174 interacts with Glu183, in addition, this glutamate corresponds to E204 in yeast, which forms a salt bridge with Trm82 K223. Given the fact that METTL1 Glu183 appears to be a very important residue for the WDR4/METTL1 complex, it would be particularly interesting to test for the function of METTL1 Glu183 mutants *in vivo*, checking for example, if their overexpression in cortices could lead to a neuronal or proliferation defect or if they would be able to rescue the neuronal migration phenotype in a context of malfunctioning of the Wdr4/Mettl1 complex. It would be also valuable to correlate the *in vivo* effect with any defects in binding of the complex and/or tRNAs.

5.1.2 Molecular consequences

In Article 1, I performed Western Blot analysis (using our homemade Adat3 and Adat2 antibodies, which detect also human ADAT3 and ADAT2 respectively) and showed that ADAT3 protein levels are reduced whereas ADAT2 protein levels are unmodified in p.Val144Met and p.Arg128Leu patient LCLs in comparison to the controls (WT and heterozygous). Ramos and colleagues also checked ADAT3 levels in human LCL extracts comparing p.Val144Met patient LCLs to controls by immunoblot but observed no differences between both genotypes (J. Ramos et al., 2019). Interestingly, the LCLs that Ramos and colleagues used I used are coming from the same patients as they were obtained from the same collaborator (Fowzan Alkuraya Team, Alfaisal University). I think this discrepancy could be due to a better detection of ADAT3 levels by our homemade antibody (Ramos and colleagues argued problems to detect endogenous ADAT3 and ADAT2 levels). My results are further supported by the observation of reduced ADAT3 levels in the *Adat3* KI line. Further experiments with other antibodies might help clarifying these differences between my results and Ramos and colleagues. Overall, my Western-Blot results with the cell line and the KI model provide further evidence into the critical role of this residue for protein stability. Similar experiments will soon be performed for patient LCLs with p.Ala196Val and p.Ala196Leu variants ADAT3 variants.

In publication 1, I did not observe any reduction in ADAT2 levels in *ADAT3* V144M LCLs, nevertheless, in preliminary results¹, I observed a reduction in Adat2 levels in the KI line. It is thus unclear if a reduction of ADAT3 levels might lead to a reduction of ADAT2 levels, although it could be a plausible hypothesis, considering how dependent ADAT2 and ADAT3 appear to be on the levels of the other subunit (discussed in 2). Such differences between both experiments could be due to the use of animal tissue or *in vitro* cultures or to the different origin of the samples (nervous system vs LCLs), or differences between species. I thus suggest checking for Adat2 levels in different human and mice samples with reduced ADAT3 levels to further clarify this. We plan to determine also WDR4 and METTL1 protein levels in cells

derived from patients with p.Arg170Leu WDR4 variant and p.Ile120Met and p.Arg174Gln METTL1 variant. Assessment of *ADAT3*, *WDR4* and *METTL1* transcript levels by RT-qPCR is also planned in patient derived cell lines. Such experiments should provide important insights into whether reduced protein levels are due to protein degradation or instability rather than transcriptional effects. To evaluate further protein stability defects protein levels could be assessed after transfecting *in vitro* cell cultures with equal amounts of plasmids overexpressing each of the variants, and treating the cells with cycloheximide (protein synthesis inhibitor) and/or MG132 (proteasome inhibitor).

Regarding ADAT3 p.Ala196Leu and p.Ala196Val, based on my migration rescue experiments, p.Ala196Leu seems to be more deleterious for the protein than p.Ala196Val. Leucine side chain is larger than Valine side chain (which is more similar to Alanine side chain), probably this closer similarity of Valine side chain to Alanine side chain and its minor steric effect account for why A180V rescues the migration phenotype while A180L does not fully rescue the phenotype. The presence of the disease in p.Ala196Leu;p.Ala196Val compound heterozygous patients and not in p.Ala196Leu heterozygous individuals suggests that even if the effect of p.Ala196Val is not highly deleterious for ADAT3, the variant could still affect protein stability, activity or its interaction with other proteins even in a weak manner. This together with the presence of the other variant might lead to a low threshold of activity of *Adat3* below the optimal dosage and have a deleterious effect in the organism leading to the disease. Modelling of all Adat3 mutations in the Adat3/Adat2 structure, RT-qPCR, Cycloheximide/MG132, Western Blot on patient LCLs and biochemical experiments with Christophe Romier's (IGBMC, Strasbourg) are expected to determine further the effect of each variant.

Interestingly, some of the variants in *ADAT3* and *WDR4* have already been reported to lead to decrease in I_{34} and m^7G_{46} modifications respectively: Ramos and colleagues determined that human patient LCLs with *ADAT3* Val144Met mutation exhibited reduced I_{34} levels in tRNA-Val-AAC, tRNA-Ile-AAU and tRNA-Leu-AAG (J. Ramos et al., 2019). In accordance with these experiments, we showed by a different method, that I_{34} levels are decreased for tRNA-Val-AAC and tRNA-Thr-AGT (Article1). For *WDR4* Arg170Leu Shaheen and colleagues reported an abrupt decrease in m^7G_{46} levels (they determined it in tRNA-Phe) in homozygous patient fibroblasts. My results and these two publications (J. Ramos et al., 2019; Shaheen et al., 2015) are in accordance with a loss of function effect for these variants.

It remains to be determined how and to which extent other variants in *ADAT3*, *WDR4* and *METTL1* affect tRNA modification levels. Towards this aim, for *ADAT3*, we established a collaboration with D. Nedialkova (MPIB; Munich). We will carry out tRNA-sequencing

experiments, using a new unpublished method that they developed for unbiased and quantitative tRNA sequencing. By taking advantage of the fact that I₃₄ is read as a G upon sequencing we will quantify I₃₄ modification level in tRNAs. This method is particularly suitable for our purpose, since it will allow us to analyze of all ANN anticodon tRNAs in a single-experiment. Some tRNA modifications act as positive or negative determinants for other tRNA modifications, for example s²U serves as negative determinant for C to U editing (Wohlgamuth-Benedum et al., 2009). These experiments will allow us to determine a possible putative effect of I₃₄ over other tRNA modifications (only for those tRNA modifications that impair the sequencing). Altogether, such analysis should allow us to obtain a clear idea about the effect of each *ADAT3* variant in tRNA I₃₄ modification profiles and determine if some other modifications might be impaired as well upon lack of I₃₄.

Given the results from Ramos and co-workers about p.Val144Met (J. Ramos et al., 2019) and the decreased in protein levels for p.Val144Met and p.Arg128Leu, and tRNA modification (p.Val144Met, Article1), we expect major tRNA modification impairment with these variants, probably in all ANN anticodon containing tRNAs.

tRNA seq does not allow to analyze methylation. Towards the aim of dissecting how variants in *WDR4* and *METTL1* impair m⁷G₄₆ tRNA modification levels, as a first approach we planned NorthWesternBlot experiments in RNA extracts from patient derived cells (Method established by Lin and co-workers (Lin et al., 2018)). Like for *ADAT3*, considering the deleterious effect of each of the variants in both *WDR4* and *METTL1* proteins (already discussed in 5.1.1) we expect also major impairments of m⁷G₄₆ tRNA modification levels in patient derived cells. As METTL1 was also shown to methylate mRNAs and miRNAs (Pandolfini et al., 2019) we plan, by using the same approach, to determine also if miRNA and mRNAs also show lower m⁷G levels. If we find reduction of m⁷G₄₆ tRNA modification levels, we plan to perform m⁷G MeRIP-Seq or m⁷G TRAC-Seq to dissect the extent of impairment of the modification and the species affected(Lin et al., 2018).

Finally, the different variants might alter the interaction of the proteins with other proteins, this was shown to be the case already of *ADAT3* p.Val144Met, which is interacting more with cellular chaperonins than WT ADAT3 (J. Ramos et al., 2019). Assessment of protein interactome in cells derived from WT and mutated patients would determine if this also occurs for other *ADAT3* variants and variants in *WDR4* and *METTL1*. Such experiments would be particularly relevant for *WDR4* variants, as it is a protein composed of 7 WD domains, which are known to participate in protein-protein interactions (Smith, 2008).

5.1.3 Cellular consequences

Variants in *ADAT3*, *WDR4* and *METTL1* are expected to have important repercussions in cells. In article 1 I already showed that most of the *ADAT3* and *WDR4* variants failed to rescue the radial migration defects in mice. In addition, in preliminary results 1, I showed how *Adat3* V128M impairs cortical progenitor's proliferation.

Variants in *ADAT3* and *WDR4* are thought to be loss of function variants (discussed in 5.1). We showed that all *Adat3* and *Wdr4* patient variants tested (with the exception of *Adat3* A180V) affect neuronal migration. Briefly, *Adat3* V128M variant was shown to be particularly deleterious for *Adat3* function in migration showing similar results to the miRNA (no rescue). p.R112L and p.A180L variants partially attenuated the phenotype (partial rescue). On the other hand, WT and p.A180V *Adat3* forms fully restored the phenotype (full rescue). For *Wdr4*, R215L and M1T (modelled with lower dose of *Wdr4* in the rescue experiments) variants did not rescue the migration phenotype neither. Altogether, my results further suggest that *Adat3* V128M, R112L, A180L and *Wdr4* R215L and M1T are loss of function variants and support that *Adat3* A180L substitution is more deleterious than A180V which rescued the migration phenotype (discussed in 2.2).

I showed that *Adat3* V128M impairs cortical proliferation (discussed in 1.2) by decreasing their cell cycle exit at E14.5. It remains to be determined if other variants in *ADAT3*, *WDR4* or *METTL1* also lead to cell cycle impairments. However, considering the variants are thought to be loss of function and the evidences pointing at implication of these genes in progenitor's biology (See 1.2) we expect that other variants in these genes also lead to proliferation/specification defects.

In addition to their involvement in cellular migration and proliferation, other effects could occur in cells with variants in these genes. Due to the fact that most variants lead to microcephaly in patients and that lack of tRNA modifications in the cortex have already been associated to apoptosis (Blanco et al., 2014) we expect that they could be associated to cell death (further discussed in 3.2). In the *Adat3* KI mouse model I checked for Caspase 3 staining at E18.5 and observed no differences in the number of Caspase3-positive cells with the WT littermates (data not shown). As microcephaly is not recapitulated in the model, it could be that there is apoptosis in humans but not in mice. This could be due to the different level of complexity between humans and mice and a possible different sensitiveness of human and mice cells to ADAT2/3 and I₃₄ modification levels (discussed in 5.2.3). Assessment of apoptosis, also by looking for other apoptosis markers (such as Cytochrome C), in further developmental stages in the KI model and *in vitro* cultures of cells derived from patients could provide answers to these open questions.

Furthermore, as described in section 4, variants in *ADAT3*, *WDR4* and *METTL1* are expected to lead to neuronal connectivity impairment and possible alterations in neuronal axons and dendrites, possibly through local translation defects.

In addition, variant *ADAT3* p.Val144Met was reported to exhibit abnormal cellular compartmentalization between the cytoplasm and the nucleus (J. Ramos et al., 2019), I thus propose to determine if other variants identified in these genes may also exhibit an abnormal cellular compartmentalization and increased interaction with cellular chaperonins.

5.1.4 No variants for *ADAT2* in patients: Impossibility or lack of screening?

To date, although the number of variants identified for *ADAT3* keeps increasing there are no variants identified for *ADAT2* in human patients. I hypothesize that this could be due to the following reasons: 1) Severe mutations in *ADAT2* might be incompatible for life in homozygosity; 2) Lack of screening for recessive mutations and in fetuses. Considering that *ADAT2* bears the catalytic activity of the complex, it is likely that mutations in *ADAT2* could be even more devastating for the complex activity than mutations in *ADAT3* probably mutations having a strong effect might not be compatible with life and might lead to abortion without being diagnosed in most of the cases. Although *METTL1* also bears the catalytic activity of the complex, mutations in the complex have been identified, this might be because, unlike *ADAT2* (A. P. Gerber et al., 1999), *METTL1* is not an essential gene in human cells (Lin et al., 2018). To note, *ADAT2* is smaller in size than *ADAT3* which could explain why *ADAT3* is more prone to mutations than *ADAT2*. Interestingly, the Genome Aggregation Database (gnomAD) (<https://gnomad.broadinstitute.org>) (Karczewski et al., 2020) reports a probability of being loss of function intolerant (pLI) for *ADAT2* equal to 0. This value indicates that there exist several loss of function variants in the general population, but not in homozygosity. This data from gnomAD further supports the importance of *ADAT3*/*ADAT2* dosage (discussed in 2.1) supporting that having one WT allele in the population might be sufficient for life. I strongly believe that if an exome sequencing was performed routinely in human embryos undergoing abortion some mutations in *ADAT2* would potentially be identified in some cases.

5.2 The Adat3 V128M Knock-in model

In order to generate a model to study *Adat3* function in disease, we tried to generate an *Adat3* Knockout mouse line with the idea of studying heterozygous mice, as homozygous knock-out animals were expected to be lethal (A. P. Gerber et al., 1999). Nevertheless, *Adat3* knockout animals were lethal even in heterozygosity. We therefore decided to generate a knock-in

model. Based on our results and Ramos and colleagues (J. Ramos et al., 2019) ADAT3 p.Val144Met (recapitulated in mice by A128M) impairs tRNA activity and ADAT3 protein levels (discussed in 5.1.2), we therefore generated and studied an *Adat3* p.V128M KI line with the initial purpose of creating a perfect model to study the human disease and analyze the consequences of the loss of *Adat3* (and I_{34}) during cortical development.

5.2.1 A good model for disease?

My work in this model, which is still preliminary, has shown that this model in line with our results in human ADAT3 p.Val144Met LCLs also bear lower *Adat3* levels, at least in three nervous system related tissues (cortex, hippocampus and GE). ADAT3 p.V144M was shown to have an aberrant cellular localization by Ramos and colleagues (J. Ramos et al., 2019), we plan to further characterize this line by assessing cellular localization of *Adat3* p.V128M in the cortex. Despite the lower *Adat3* levels, these mice do not present microcephaly or other defects in cortical size (neither in males or females) nor major neuroanatomical defects (analysis done in males). It remains to be determined if females do show major neuroanatomical defects (unlike males), nevertheless, to date, no reason indicates that there should be a difference between sexes since ADAT3 mutations affect both males and females to similar extents.

Additionally, no differences were detected between $+/+$ and KI/KI cortices when I look at radial migration from E14.5 to E18.5. There exist several options which could explain not observing a migration defect in the KI model but observing it when an acute depletion of *Adat3* levels is carried out with miRNAs. It should be kept in mind that the nature of both experiments is different, whereas in the KI line all the cells carry *Adat3* p.V128M variant, in the IUE experiments only a small percentage of cells (the electroporated ones) will have an acute depletion of *Adat3* levels. One possibility could be that there exist compensatory mechanisms which are able to compensate for *Adat3* reduced activity which might not have enough time to compensate upon an acute depletion (discussed in 5.2.4). The KI line might express enough *Adat3* activity not to observe any migration defect (at least in the studied time window). However, different phases of cortical development could be differentially sensitive to *Adat3* levels, since proliferation defects are detected in the KI line (For a discussion of KI progenitor's defects see 1.2). As this KI model does not present microcephaly or any neuroanatomical features it does not appear to be an ideal model to study the disease.

5.2.2 Which could be the alternatives to this model?

As previously mentioned in 2.1 one of the alternatives could be the use of a cKO *Adat3* line, nevertheless, there exist also some alternatives which are discussed in the following lines. Several other mouse models that were expected to recapitulate the phenotypes observed in

patients and did not exhibit the expected cortical phenotypes are known to exist. For example *Flna* KO mice do not develop periventricular heterotopia unlike the patients, on the other hand, its knockdown in rats leads to ectopic neurons (Carabalona et al., 2012). Likewise, *TUBA1A* mutations are associated with subcortical band heterotopia, lissencephaly, microcephaly and abnormal gyration in human patients (Hebebrand et al., 2019), nonetheless, *Tub1a* KI mutant mice show no cortical defects (J. S. Liu, 2011). Similarly, *FAT4* mutations lead to cortical heterotopia in patients (Badouel et al., 2015), however, its acute knockdown leads to over-proliferation and reduced neuronal differentiation (Cappello et al., 2013). Finally, several rodent lines have been generated to model *DCX*-related heterotopias, nevertheless, while *Dcx* KO mice for example show no obvious lamination defects in the cortex, its acute depletion in rat mimics the human phenotype (Nosten-Bertrand et al., 2008) (R. L. Ramos et al., 2006). The fact that many phenotypes found in human are missing in the mouse brain suggests an additional level of regulation in humans.

Gyrencephalic and lissencephalic species display several differences including the balance between direct and indirect neurogenesis and the importance of some cell types, such as bIPs and bRGCs. This *Adat3* KI line does not recapitulate some of the major phenotypes in human patients, such as microcephaly, this could be due to the differences in cell types and level or regulation between human and mice brain development. Nevertheless, my results support that its further study could provide more insights into *Adat3* function, particularly in its role in cortical progenitors and during neurogenesis.

To overcome such differences between mouse and human, other models could be used, for example ferret animal models (gyrencephalic species). As discussed before, another possibility could be the use of *in vitro* models, such as human cortical organoids derived from hESCs (Cakir et al., 2019). One of the main advantages for such models, particularly for studying proliferation or migration is that they form an accessible 3d structure which resembles the early steps for human brain development. Bershteyn and colleagues (Bershteyn et al., 2017) generated cerebral organoids from induced pluripotent stem cells derived from patients with a heterozygous deletion of 17p13.3, which results in lissencephaly. In addition to recapitulating many of the defects identified in mouse models, such as migration defects, the organoids exhibited additional human-specific features, such as increased horizontal divisions of aRGCs and apoptosis, which could not be recapitulated in mice. Another possibility, would be the use of transplantation of *in vitro* generated tissues and cells. Espuny-Camacho and colleagues (Espuny-Camacho et al., 2017) transplanted glial progenitor cells derived from induced pluripotent stem cells from a schizophrenia patient into mouse brains. This chimeric mouse model showed even patient-like phenotypes in behavioural experiments such as increased

anxiety or disturbed social interaction (Espuny-Camacho et al., 2017). The use of one of the mentioned models could help to recapitulate some of the patient phenotypes that were not observed in this KI line.

5.2.3 Different sensitivity to *ADAT3* or *I₃₄* impairment in human and mice?

Due to the high homology between ADAT3 in human and mice from a structural point of view, human and mouse ADAT3/ADAT2 complexes are expected to be equally sensitive to p.Val144Met and p.V128M mutations respectively (Collaboration with Christophe Romier, IBGMC, data not shown). However, it is currently unknown if human and mice cells are differentially sensitive to impairments in ADAT3. Gene profiling in human and mouse cortices have revealed specie-specific molecular signatures, revealing that a 21% of genes exhibit differential expression between both species (Zeng et al., 2012). Such differences in gene expression between species could account for the possible differential sensitivity as well. Knockdown experiment with similar efficiencies among both species (for example mESCs and hESCs) and assessment of cell death and cellular fitness could provide and answer to this question. If human cells were more sensitive to ADAT3 impairment than mouse cells it could be due to the protein itself, its substrates, interacting partners or effect on translation on each specie. Assessment of ADAT3 interactome, *I₃₄* tRNA modification profiles or ribosome profiling and their comparison in both cases could be particularly relevant to answer these questions. If human cells are more sensitive to depletion of ADAT3 levels this could easily explain for example the lack neuroanatomical features or microcephaly in the KI model.

5.2.4 Which compensatory effects?

The discrepancies observed in the radial migration results upon an acute knockdown and in the *Adat3* KI line suggest there might exist compensatory mechanisms. Such cellular mechanisms or pathways could account for observing a phenotype with an acute depletion but not a sustained *Adat3* function impairment in mice.

These compensatory mechanisms might include several types of cellular signaling mechanisms. For example, Lack of Nsun2 catalyzed tRNA m⁵C methylation in the anticodon loop was shown to induce generation of 5'tRNA fragments by activation of angiogenin triggering cellular stress responses (Blanco et al., 2014). Similarly, lack of tRNA methylation by Dnmt2, was shown to increase-stress induced cleavage of tRNAs and sensitivity to oxidative stress in flies (Schaefer et al., 2010). Reduction of *Adat3* and *I₃₄* levels might produce unidentified tRNA fragments which might activate cellular pathways that can compensate at least partially the effect of their reduction. Heat shock response pathway, for example, is known to be activated in response to many stimuli, such as misfolded proteins, oxidative stress and

heavy metals to compensate such stresses and promote cellular survival (Samali et al., 1998). ADAT3 p.V144M shows a higher interaction with members of the heat shock response pathway, including HSP60 the TCP1 and CCT7 subunits of the TriC complex (all members of the chaperonin protein family) (J. Ramos et al., 2019). Another cellular response that could be particularly involved in this case is the ribosome-associated quality control (RQC) pathway, which is induced by stalled ribosomes, and promotes a cellular response to truncated polypeptides (Brandman et al., 2016).

Finally, CPC-1 (homolog of ATF4 in mammals) was recently shown to mediate the response upon *adat2* silencing in *Neurospora crassa* (Lyu et al., 2020). CPC-1/GATF4 are major factors mediating transcriptional response upon amino acid starvation (Luo et al., 1995). ATF4 (Activating transcription factor 4) is an ubiquitously expressed transcription factor which plays multiple roles in cellular physiology and pathology (Harding et al., 2000; D. C. Singleton et al., 2012). It plays a role in the response to unfolded proteins and/or amino acid deprivation (Ameri et al., 2008; Kilberg et al., 2009; Rutkowski et al., 2003) by regulating transcription of several genes which altogether will allow cells to compensate this effects or lead to cell death if compensation does not occur. Interestingly, ATF4 has been shown to promote cell migration and anchorage independent cell growth in human gliomas (D. Chen et al., 2017). Thus, activation of ATF4 and its downstream effectors might explain why there is not migration defects in the *Adat3* KI line.

Based on everything mentioned above I suggest assessing if different cellular signaling pathways Heat shock proteins, RQC or ATF4 response to amino acid starvation signaling might be activated in the *Adat3* KI line. I therefore propose assessing the expression of several markers belonging to each of the signaling pathways, such as the E3 ubiquitin ligase Ltn1 for the RQC pathway. by RT-qPCR or Western Blot as a first approach to look for possible cellular compensatory mechanisms of the cell to *Adat3* function impairment.

6. Sensitivity of the cortex to ADAT2/3-WDR4/METTL1 and tRNA impairment

As discussed during the introduction the brain and the cerebral cortex are particularly sensitive to tRNA impairment and defects in protein translation. The mechanisms that could be behind this high sensitivity are still not fully understood. Nevertheless, the high protein demand during brain development (M.Lowe, 2017), the specialized and complex cellular compartmentalization of neurons, local protein translation in neurons (Hafner et al., 2019) and the lower half-life of some neuronal proteins (ex: synapses and axonal growth cones proteins) (Cohen et al., 2013)

(Deglincerti et al., 2015; Fornasiero et al., 2018) could all account for the high sensitivity of the brain to translation defects.

This sensitivity is not specific not ADAT2/3 or WDR4/METTL1, as discussed in the introduction, many factors related to tRNA synthesis or function lead to impairment in the brain. In the particular case of ADAT2/3 and WDR4/METTL1 I hypothesize neurons and progenitors are particularly dependent on proteins whose translation could be impaired upon miss-function of these complexes. As discussed previously, performing ribosome profiling or RNA-seq in animal models, or organoids could help providing an answer to these questions.

Regarding the particular case of tRNA impairment, several facts could account to the high sensitivity of the brain and the cortex. As mentioned during the introduction, tRNA level changes have been reported between different developmental stages in the brain, including embryonic and post-natal conditions (Schmitt et al., 2014). In addition, the brain expresses high levels of tRNAs compared to other organs (Dittmar et al., 2006), being some of them specific to the brain (Ishimura et al., 2014). Moreover, Gingold and colleagues demonstrated the existence of different tRNA expression patterns between differentiating or proliferative cellular states in human samples by comparing cancer and normal cells. They reported that tRNAs that are repressed in differentiating cells typically contained anticodons that were associated to a “proliferation-related” codon usage whereas those that were repressed in proliferating cells typically contained anticodons associated to “differentiation” codon usage (Gingold et al., 2014). Based on these findings and the high sensitivity of the brain to tRNA impairment I hypothesize that in the brain and particularly the cortex there is a differential expression of tRNAs to favor that different changes in the proteome that encompass different stages of brain development. Based on the findings from Gingold and colleagues, and the complex differentiation of brain structures such as the cortex, which encompasses a huge process of proliferation and differentiation, it is tempting to speculate that tRNAs could be differentially expressed in different brain populations, such as cortical progenitors and neurons. Those differences in tRNA expression might interfere in their proteome by modulating codon usage. Such changes would have consequences in cellular state and determine, for example, whether cells are found in a more proliferative or differentiative stage. For long, tRNAs were just considered as adaptor molecules participating in protein translation, however, I strongly think they might have many important regulatory roles in living organisms.

BIBLIOGRAPHY

Abraham, H., Toth, Z., Bari, F., Domoki, F., & Seress, L. (2005). Novel calretinin and reelin expressing neuronal population includes Cajal-Retzius-type cells in the neocortex of adult pigs. *Neuroscience*, 136(1), 217-230. doi:10.1016/j.neuroscience.2005.07.039

Agris, P. F., Sierzputowska-Gracz, H., & Smith, C. (1986). Transfer RNA contains sites of localized positive charge: carbon NMR studies of [¹³C]methyl-enriched Escherichia coli and yeast tRNAPhe. *Biochemistry*, 25(18), 5126-5131. doi:10.1021/bi00366a022

Aillaud, C., Bosc, C., Peris, L., Bosson, A., Heemeryck, P., Van Dijk, J., . . . Moutin, M. J. (2017). Vasohibins/SVBP are tubulin carboxypeptidases (TCPs) that regulate neuron differentiation. *Science*, 358(6369), 1448-1453. doi:10.1126/science.aoa4165

Alazami, A. M., Hijazi, H., Al-Dosari, M. S., Shaheen, R., Hashem, A., Aldahmesh, M. A., . . . Alkuraya, F. S. (2013). Mutation in ADAT3, encoding adenosine deaminase acting on transfer RNA, causes intellectual disability and strabismus. *J Med Genet*, 50(7), 425-430. doi:10.1136/jmedgenet-2012-101378

Alexandrov, A., Chernyakov, I., Gu, W., Hiley, S. L., Hughes, T. R., Grayhack, E. J., & Phizicky, E. M. (2006). Rapid tRNA decay can result from lack of nonessential modifications. *Mol Cell*, 21(1), 87-96. doi:10.1016/j.molcel.2005.10.036

Alexandrov, A., Grayhack, E. J., & Phizicky, E. M. (2005). tRNA m7G methyltransferase Trm8p/Trm82p: evidence linking activity to a growth phenotype and implicating Trm82p in maintaining levels of active Trm8p. *RNA*, 11(5), 821-830. doi:10.1261/rna.2030705

Alexandrov, A., Martzen, M. R., & Phizicky, E. M. (2002). Two proteins that form a complex are required for 7-methylguanosine modification of yeast tRNA. *RNA*, 8(10), 1253-1266.

Allen, N. J., & Lyons, D. A. (2018). Glia as architects of central nervous system formation and function. *Science*, 362(6411), 181-185. doi:10.1126/science.aat0473

Ambrozkiewicz, M. C., Schwark, M., Kishimoto-Suga, M., Borisova, E., Hori, K., Salazar-Lazaro, A., . . . Kawabe, H. (2018). Polarity Acquisition in Cortical Neurons Is Driven by Synergistic Action of Sox9-Regulated Wwp1 and Wwp2 E3 Ubiquitin Ligases and Intrinsic miR-140. *Neuron*, 100(5), 1097-1115 e1015. doi:10.1016/j.neuron.2018.10.008

Ameri, K., & Harris, A. L. (2008). Activating transcription factor 4. *Int J Biochem Cell Biol*, 40(1), 14-21. doi:10.1016/j.biocel.2007.01.020

Amy Rosenfeld, P. D. (2017). Zika virus blocks the neuron road. Retrieved from <https://www.virology.ws/2017/11/09/zika-virus-blocks-the-neuron-road-2/>

Andachi, Y., Yamao, F., Iwami, M., Muto, A., & Osawa, S. (1987). Occurrence of unmodified adenine and uracil at the first position of anticodon in threonine tRNAs in Mycoplasma

capricolum. *Proc Natl Acad Sci U S A*, 84(21), 7398-7402. doi:10.1073/pnas.84.21.7398

Anderson, C. T., & Stearns, T. (2009). Centriole age underlies asynchronous primary cilium growth in mammalian cells. *Curr Biol*, 19(17), 1498-1502. doi:10.1016/j.cub.2009.07.034

Anderson, S. A., Kaznowski, C. E., Horn, C., Rubenstein, J. L., & McConnell, S. K. (2002). Distinct origins of neocortical projection neurons and interneurons in vivo. *Cereb Cortex*, 12(7), 702-709. doi:10.1093/cercor/12.7.702

Anelli, T., & Sitia, R. (2008). Protein quality control in the early secretory pathway. *EMBO J*, 27(2), 315-327. doi:10.1038/sj.emboj.7601974

Arrondel, C., Missouri, S., Snoek, R., Patat, J., Menara, G., Collinet, B., . . . Mollet, G. (2019). Defects in t(6)A tRNA modification due to GON7 and YRDC mutations lead to Galloway-Mowat syndrome. *Nat Commun*, 10(1), 3967. doi:10.1038/s41467-019-11951-x

Auxilien, S., Crain, P. F., Trewyn, R. W., & Grosjean, H. (1996). Mechanism, specificity and general properties of the yeast enzyme catalysing the formation of inosine 34 in the anticodon of transfer RNA. *J Mol Biol*, 262(4), 437-458. doi:10.1006/jmbi.1996.0527

Ayala, R., Shu, T., & Tsai, L. H. (2007). Trekking across the brain: the journey of neuronal migration. *Cell*, 128(1), 29-43. doi:10.1016/j.cell.2006.12.021

Azevedo, F. A., Carvalho, L. R., Grinberg, L. T., Farfel, J. M., Ferretti, R. E., Leite, R. E., . . . Herculano-Houzel, S. (2009). Equal numbers of neuronal and nonneuronal cells make the human brain an isometrically scaled-up primate brain. *J Comp Neurol*, 513(5), 532-541. doi:10.1002/cne.21974

Azzarelli, R., Guillemot, F., & Pacary, E. (2015). Function and regulation of Rnd proteins in cortical projection neuron migration. *Front Neurosci*, 9, 19. doi:10.3389/fnins.2015.00019

Azzarelli, R., Pacary, E., Garg, R., Garcez, P., van den Berg, D., Riou, P., . . . Guillemot, F. (2014). An antagonistic interaction between PlexinB2 and Rnd3 controls RhoA activity and cortical neuron migration. *Nat Commun*, 5, 3405. doi:10.1038/ncomms4405

Badouel, C., Zander, M. A., Liscio, N., Bagherie-Lachidan, M., Sopko, R., Coyaud, E., . . . McNeill, H. (2015). Fat1 interacts with Fat4 to regulate neural tube closure, neural progenitor proliferation and apical constriction during mouse brain development. *Development*, 142(16), 2781-2791. doi:10.1242/dev.123539

Bahr, A., Hankeln, T., Fiedler, T., Hegemann, J., & Schmidt, E. R. (1999). Molecular analysis of METTL1, a novel human methyltransferase-like gene with a high degree of phylogenetic conservation. *Genomics*, 57(3), 424-428. doi:10.1006/geno.1999.5780

Barnes, A. P., & Polleux, F. (2009). Establishment of axon-dendrite polarity in developing neurons. *Annu Rev Neurosci*, 32, 347-381. doi:10.1146/annurev.neuro.31.060407.125536

Battini, R., D'Arrigo, S., Cassandrini, D., Guzzetta, A., Fiorillo, C., Pantaleoni, C., . . . Santorelli, F. M. (2014). Novel mutations in TSEN54 in pontocerebellar hypoplasia type 2. *J Child Neurol*, 29(4), 520-525. doi:10.1177/0883073812470002

Beattie, R., & Hippenmeyer, S. (2017). Mechanisms of radial glia progenitor cell lineage progression. *FEBS Lett*, 591(24), 3993-4008. doi:10.1002/1873-3468.12906

Bellion, A., Baudoin, J. P., Alvarez, C., Bornens, M., & Metin, C. (2005). Nucleokinesis in tangentially migrating neurons comprises two alternating phases: forward migration of the Golgi/centrosome associated with centrosome splitting and myosin contraction at the rear. *J Neurosci*, 25(24), 5691-5699. doi:10.1523/JNEUROSCI.1030-05.2005

Bershteyn, M., Nowakowski, T. J., Pollen, A. A., Di Lullo, E., Nene, A., Wynshaw-Boris, A., & Kriegstein, A. R. (2017). Human iPSC-Derived Cerebral Organoids Model Cellular Features of Lissencephaly and Reveal Prolonged Mitosis of Outer Radial Glia. *Cell Stem Cell*, 20(4), 435-449 e434. doi:10.1016/j.stem.2016.12.007

Besson, A., Gurian-West, M., Schmidt, A., Hall, A., & Roberts, J. M. (2004). p27Kip1 modulates cell migration through the regulation of RhoA activation. *Genes Dev*, 18(8), 862-876. doi:10.1101/gad.1185504

Bian, S., Hong, J., Li, Q., Schebelle, L., Pollock, A., Knauss, J. L., . . . Sun, T. (2013). MicroRNA cluster miR-17-92 regulates neural stem cell expansion and transition to intermediate progenitors in the developing mouse neocortex. *Cell Rep*, 3(5), 1398-1406. doi:10.1016/j.celrep.2013.03.037

Bielle, F., Griveau, A., Narboux-Neme, N., Vigneau, S., Sigrist, M., Arber, S., . . . Pierani, A. (2005). Multiple origins of Cajal-Retzius cells at the borders of the developing pallium. *Nat Neurosci*, 8(8), 1002-1012. doi:10.1038/nn1511

Blanco, S., Dietmann, S., Flores, J. V., Hussain, S., Kutter, C., Humphreys, P., . . . Frye, M. (2014). Aberrant methylation of tRNAs links cellular stress to neuro-developmental disorders. *EMBO J*, 33(18), 2020-2039. doi:10.1525/embj.201489282

Boccaletto, P., Machnicka, M. A., Purta, E., Piatkowski, P., Baginski, B., Wirecki, T. K., . . . Bujnicki, J. M. (2018). MODOMICS: a database of RNA modification pathways. 2017 update. *Nucleic Acids Res*, 46(D1), D303-D307. doi:10.1093/nar/gkx1030

Bock, H. H., & May, P. (2016). Canonical and Non-canonical Reelin Signaling. *Front Cell Neurosci*, 10, 166. doi:10.3389/fncel.2016.00166

Boitard, M., Bocchi, R., Egervari, K., Petrenko, V., Viale, B., Gremaud, S., . . . Kiss, J. Z. (2015). Wnt signaling regulates multipolar-to-bipolar transition of migrating neurons in the cerebral cortex. *Cell Rep*, 10(8), 1349-1361. doi:10.1016/j.celrep.2015.01.061

Bornelov, S., Selmi, T., Flad, S., Dietmann, S., & Frye, M. (2019). Codon usage optimization in pluripotent embryonic stem cells. *Genome Biol*, 20(1), 119. doi:10.1186/s13059-019-1726-z

Brandman, O., & Hegde, R. S. (2016). Ribosome-associated protein quality control. *Nat Struct Mol Biol*, 23(1), 7-15. doi:10.1038/nsmb.3147

Braun, D. A., Rao, J., Mollet, G., Schapiro, D., Daugeron, M. C., Tan, W., . . . Hildebrandt, F. (2017). Mutations in KEOPS-complex genes cause nephrotic syndrome with primary microcephaly. *Nat Genet*, 49(10), 1529-1538. doi:10.1038/ng.3933

Braun, D. A., Shril, S., Sinha, A., Schneider, R., Tan, W., Ashraf, S., . . . Hildebrandt, F. (2018). Mutations in WDR4 as a new cause of Galloway-Mowat syndrome. *Am J Med Genet A*, 176(11), 2460-2465. doi:10.1002/ajmg.a.40489

Brooks, S. S., Wall, A. L., Golzio, C., Reid, D. W., Kondyles, A., Willer, J. R., . . . Davis, E. E. (2014). A novel ribosomopathy caused by dysfunction of RPL10 disrupts neurodevelopment and causes X-linked microcephaly in humans. *Genetics*, 198(2), 723-733. doi:10.1534/genetics.114.168211

Bryan Kolb, B. D. F. (2009). *Handbook of Clinical Child Neuropsychology* (E. F.-J. C.R Reynolds Ed.): Springer Science

Bultje, R. S., Castaneda-Castellanos, D. R., Jan, L. Y., Jan, Y. N., Kriegstein, A. R., & Shi, S. H. (2009). Mammalian Par3 regulates progenitor cell asymmetric division via notch signaling in the developing neocortex. *Neuron*, 63(2), 189-202. doi:10.1016/j.neuron.2009.07.004

Butt, S. J., Fuccillo, M., Nery, S., Noctor, S., Kriegstein, A., Corbin, J. G., & Fishell, G. (2005). The temporal and spatial origins of cortical interneurons predict their physiological subtype. *Neuron*, 48(4), 591-604. doi:10.1016/j.neuron.2005.09.034

Bykhovskaya, Y., Casas, K., Mengesha, E., Inbal, A., & Fischel-Ghodsian, N. (2004). Missense mutation in pseudouridine synthase 1 (PUS1) causes mitochondrial myopathy and sideroblastic anemia (MLASA). *Am J Hum Genet*, 74(6), 1303-1308. doi:10.1086/421530

Cakir, B., Xiang, Y., Tanaka, Y., Kural, M. H., Parent, M., Kang, Y. J., . . . Park, I. H. (2019). Engineering of human brain organoids with a functional vascular-like system. *Nat Methods*, 16(11), 1169-1175. doi:10.1038/s41592-019-0586-5

Calarco, J. A., Zhen, M., & Blencowe, B. J. (2011). Networking in a global world: establishing functional connections between neural splicing regulators and their target transcripts. *RNA*, 17(5), 775-791. doi:10.1261/rna.2603911

Calegari, F., & Huttner, W. B. (2003). An inhibition of cyclin-dependent kinases that lengthens, but does not arrest, neuroepithelial cell cycle induces premature neurogenesis. *J Cell Sci*, 116(Pt 24), 4947-4955. doi:10.1242/jcs.00825

Cantara, W. A., Crain, P. F., Rozenski, J., McCloskey, J. A., Harris, K. A., Zhang, X., . . . Agris, P. F. (2011). The RNA Modification Database, RNAMDB: 2011 update. *Nucleic Acids Res*, 39(Database issue), D195-201. doi:10.1093/nar/gkq1028

Cappello, S., Gray, M. J., Badouel, C., Lange, S., Einsiedler, M., Srour, M., . . . Robertson, S. P. (2013). Mutations in genes encoding the cadherin receptor-ligand pair DCHS1 and FAT4 disrupt cerebral cortical development. *Nat Genet*, 45(11), 1300-1308. doi:10.1038/ng.2765

Carabalona, A., Beguin, S., Pallesi-Pocachard, E., Buhler, E., Pellegrino, C., Arnaud, K., . . . Cardoso, C. (2012). A glial origin for periventricular nodular heterotopia caused by

impaired expression of Filamin-A. *Hum Mol Genet*, 21(5), 1004-1017. doi:10.1093/hmg/ddr531

Cartlidge, R. A., Knebel, A., Peggie, M., Alexandrov, A., Phizicky, E. M., & Cohen, P. (2005). The tRNA methylase METTL1 is phosphorylated and inactivated by PKB and RSK in vitro and in cells. *EMBO J*, 24(9), 1696-1705. doi:10.1038/sj.emboj.7600648

Chai, X., Zhao, S., Fan, L., Zhang, W., Lu, X., Shao, H., . . . Frotscher, M. (2016). Reelin and cofilin cooperate during the migration of cortical neurons: a quantitative morphological analysis. *Development*, 143(6), 1029-1040. doi:10.1242/dev.134163

Chan, P. P., & Lowe, T. M. (2009). GtRNAdb: a database of transfer RNA genes detected in genomic sequence. *Nucleic Acids Res*, 37(Database issue), D93-97. doi:10.1093/nar/gkn787

Chan, P. P., & Lowe, T. M. (2016). GtRNAdb 2.0: an expanded database of transfer RNA genes identified in complete and draft genomes. *Nucleic Acids Res*, 44(D1), D184-189. doi:10.1093/nar/gkv1309

Chen, D., Fan, Z., Rauh, M., Buchfelder, M., Eyupoglu, I. Y., & Savaskan, N. (2017). ATF4 promotes angiogenesis and neuronal cell death and confers ferroptosis in a xCT-dependent manner. *Oncogene*, 36(40), 5593-5608. doi:10.1038/onc.2017.146

Chen, X., Gao, Y., Yang, L., Wu, B., Dong, X., Liu, B., . . . Wang, H. (2018). Speech and language delay in a patient with WDR4 mutations. *Eur J Med Genet*, 61(8), 468-472. doi:10.1016/j.ejmg.2018.03.007

Cheng, I. C., Chen, B. C., Shuai, H. H., Chien, F. C., Chen, P., & Hsieh, T. S. (2016). Wuho Is a New Member in Maintaining Genome Stability through its Interaction with Flap Endonuclease 1. *PLoS Biol*, 14(1), e1002349. doi:10.1371/journal.pbio.1002349

Chenn, A., & Walsh, C. A. (2002). Regulation of cerebral cortical size by control of cell cycle exit in neural precursors. *Science*, 297(5580), 365-369. doi:10.1126/science.1074192

Choi, M., Scholl, U. I., Ji, W., Liu, T., Tikhonova, I. R., Zumbo, P., . . . Lifton, R. P. (2009). Genetic diagnosis by whole exome capture and massively parallel DNA sequencing. *Proc Natl Acad Sci U S A*, 106(45), 19096-19101. doi:10.1073/pnas.0910672106

Chou, H. J., Donnard, E., Gustafsson, H. T., Garber, M., & Rando, O. J. (2017). Transcriptome-wide Analysis of Roles for tRNA Modifications in Translational Regulation. *Mol Cell*, 68(5), 978-992 e974. doi:10.1016/j.molcel.2017.11.002

Clark, W. C., Evans, M. E., Dominissini, D., Zheng, G., & Pan, T. (2016). tRNA base methylation identification and quantification via high-throughput sequencing. *RNA*, 22(11), 1771-1784. doi:10.1261/rna.056531.116

Clovis, Y. M., Enard, W., Marinaro, F., Huttner, W. B., & De Pietri Tonelli, D. (2012). Convergent repression of Foxp2 3'UTR by miR-9 and miR-132 in embryonic mouse neocortex: implications for radial migration of neurons. *Development*, 139(18), 3332-3342. doi:10.1242/dev.078063

Cohen, L. D., Zuchman, R., Sorokina, O., Muller, A., Dieterich, D. C., Armstrong, J. D., . . . Ziv, N. E. (2013). Metabolic turnover of synaptic proteins: kinetics, interdependencies and

implications for synaptic maintenance. *PLoS One*, 8(5), e63191. doi:10.1371/journal.pone.0063191

Costa, C., Harding, B., & Copp, A. J. (2001). Neuronal migration defects in the Dreher (Lmx1a) mutant mouse: role of disorders of the glial limiting membrane. *Cereb Cortex*, 11(6), 498-505. doi:10.1093/cercor/11.6.498

Cozen, A. E., Quartley, E., Holmes, A. D., Hrabetá-Robinson, E., Phizicky, E. M., & Lowe, T. M. (2015). ARM-seq: AlkB-facilitated RNA methylation sequencing reveals a complex landscape of modified tRNA fragments. *Nat Methods*, 12(9), 879-884. doi:10.1038/nmeth.3508

Creppe, C., Malinouskaya, L., Volvert, M. L., Gillard, M., Close, P., Malaise, O., . . . Nguyen, L. (2009). Elongator controls the migration and differentiation of cortical neurons through acetylation of alpha-tubulin. *Cell*, 136(3), 551-564. doi:10.1016/j.cell.2008.11.043

D'Arcangelo, G., Miao, G. G., Chen, S. C., Soares, H. D., Morgan, J. I., & Curran, T. (1995). A protein related to extracellular matrix proteins deleted in the mouse mutant reeler. *Nature*, 374(6524), 719-723. doi:10.1038/374719a0

Daugeron, M. C., Lenstra, T. L., Frizzarin, M., El Yacoubi, B., Liu, X., Baudin-Baillieu, A., . . . Libri, D. (2011). Gcn4 misregulation reveals a direct role for the evolutionary conserved EKC/KEOPS in the t6A modification of tRNAs. *Nucleic Acids Res*, 39(14), 6148-6160. doi:10.1093/nar/gkr178

Dave, R. K., Ellis, T., Toumpas, M. C., Robson, J. P., Julian, E., Adolphe, C., . . . Wainwright, B. J. (2011). Sonic hedgehog and notch signaling can cooperate to regulate neurogenic divisions of neocortical progenitors. *PLoS One*, 6(2), e14680. doi:10.1371/journal.pone.0014680

Davis, T. H., Cuellar, T. L., Koch, S. M., Barker, A. J., Harfe, B. D., McManus, M. T., & Ullian, E. M. (2008). Conditional loss of Dicer disrupts cellular and tissue morphogenesis in the cortex and hippocampus. *J Neurosci*, 28(17), 4322-4330. doi:10.1523/JNEUROSCI.4815-07.2008

de Anda, F. C., Meletis, K., Ge, X., Rei, D., & Tsai, L. H. (2010). Centrosome motility is essential for initial axon formation in the neocortex. *J Neurosci*, 30(31), 10391-10406. doi:10.1523/JNEUROSCI.0381-10.2010

de Brouwer, A. P. M., Abou Jamra, R., Kortel, N., Soyris, C., Polla, D. L., Safra, M., . . . Schwartz, S. (2018). Variants in PUS7 Cause Intellectual Disability with Speech Delay, Microcephaly, Short Stature, and Aggressive Behavior. *Am J Hum Genet*, 103(6), 1045-1052. doi:10.1016/j.ajhg.2018.10.026

de Crecy-Lagard, V., Boccaletto, P., Mangleburg, C. G., Sharma, P., Lowe, T. M., Leidel, S. A., & Bujnicki, J. M. (2019). Matching tRNA modifications in humans to their known and predicted enzymes. *Nucleic Acids Res*, 47(5), 2143-2159. doi:10.1093/nar/gkz011

de Ligt, J., Willemsen, M. H., van Bon, B. W., Kleefstra, T., Yntema, H. G., Kroes, T., . . . Vissers, L. E. (2012). Diagnostic exome sequencing in persons with severe intellectual disability. *N Engl J Med*, 367(20), 1921-1929. doi:10.1056/NEJMoa1206524

Deglincerti, A., Liu, Y., Colak, D., Hengst, U., Xu, G., & Jaffrey, S. R. (2015). Coupled local translation and degradation regulate growth cone collapse. *Nat Commun*, 6, 6888. doi:10.1038/ncomms7888

Dehay, C., & Kennedy, H. (2007). Cell-cycle control and cortical development. *Nat Rev Neurosci*, 8(6), 438-450. doi:10.1038/nrn2097

Del Toro, D., Ruff, T., Cederfjall, E., Villalba, A., Seyit-Bremer, G., Borrell, V., & Klein, R. (2017). Regulation of Cerebral Cortex Folding by Controlling Neuronal Migration via FLRT Adhesion Molecules. *Cell*, 169(4), 621-635 e616. doi:10.1016/j.cell.2017.04.012

Delker, R. K., Zhou, Y., Strikoudis, A., Stebbins, C. E., & Papavasiliou, F. N. (2013). Solubility-based genetic screen identifies RING finger protein 126 as an E3 ligase for activation-induced cytidine deaminase. *Proc Natl Acad Sci U S A*, 110(3), 1029-1034. doi:10.1073/pnas.1214538110

Demeule, B., Gurny, R., & Arvinte, T. (2007). Detection and characterization of protein aggregates by fluorescence microscopy. *Int J Pharm*, 329(1-2), 37-45. doi:10.1016/j.ijpharm.2006.08.024

Deng, W., Babu, I. R., Su, D., Yin, S., Begley, T. J., & Dedon, P. C. (2015). Trm9-Catalyzed tRNA Modifications Regulate Global Protein Expression by Codon-Biased Translation. *PLoS Genet*, 11(12), e1005706. doi:10.1371/journal.pgen.1005706

Deng, Y., Zhou, Z., Ji, W., Lin, S., & Wang, M. (2020). METTL1-mediated m(7)G methylation maintains pluripotency in human stem cells and limits mesoderm differentiation and vascular development. *Stem Cell Res Ther*, 11(1), 306. doi:10.1186/s13287-020-01814-4

Deng, Y., Zhou, Z., Lin, S., & Yu, B. (2020). METTL1 limits differentiation and functioning of EPCs derived from human-induced pluripotent stem cells through a MAPK/ERK pathway. *Biochem Biophys Res Commun*, 527(3), 791-798. doi:10.1016/j.bbrc.2020.04.115

Derer, P., & Derer, M. (1990). Cajal-Retzius cell ontogenesis and death in mouse brain visualized with horseradish peroxidase and electron microscopy. *Neuroscience*, 36(3), 839-856. doi:10.1016/0306-4522(90)90027-2

Dever, T. E., & Green, R. (2012). The elongation, termination, and recycling phases of translation in eukaryotes. *Cold Spring Harb Perspect Biol*, 4(7), a013706. doi:10.1101/cshperspect.a013706

Devi, M., & Lyngdoh, R. H. D. (2018). Favored and less favored codon-anticodon duplexes arising from the GC codon family box encoding for alanine: some computational perspectives. *J Biomol Struct Dyn*, 36(4), 1029-1049. doi:10.1080/07391102.2017.1308886

Dewe, J. M., Fuller, B. L., Lentini, J. M., Kellner, S. M., & Fu, D. (2017). TRMT1-Catalyzed tRNA Modifications Are Required for Redox Homeostasis To Ensure Proper Cellular Proliferation and Oxidative Stress Survival. *Mol Cell Biol*, 37(21). doi:10.1128/MCB.00214-17

Dhahbi, J. M., Spindler, S. R., Atamna, H., Yamakawa, A., Boffelli, D., Mote, P., & Martin, D. I. (2013). 5' tRNA halves are present as abundant complexes in serum, concentrated in

blood cells, and modulated by aging and calorie restriction. *BMC Genomics*, 14, 298. doi:10.1186/1471-2164-14-298

Dittmar, K. A., Goodenbour, J. M., & Pan, T. (2006). Tissue-specific differences in human transfer RNA expression. *PLoS Genet*, 2(12), e221. doi:10.1371/journal.pgen.0020221

Dong, J., Qiu, H., Garcia-Barrio, M., Anderson, J., & Hinnebusch, A. G. (2000). Uncharged tRNA activates GCN2 by displacing the protein kinase moiety from a bipartite tRNA-binding domain. *Mol Cell*, 6(2), 269-279. doi:10.1016/s1097-2765(00)00028-9

Drees, F., & Gertler, F. B. (2008). Ena/VASP: proteins at the tip of the nervous system. *Curr Opin Neurobiol*, 18(1), 53-59. doi:10.1016/j.conb.2008.05.007

Dulabon, L., Olson, E. C., Taglienti, M. G., Eisenhuth, S., McGrath, B., Walsh, C. A., . . . Anton, E. S. (2000). Reelin binds alpha3beta1 integrin and inhibits neuronal migration. *Neuron*, 27(1), 33-44. doi:10.1016/s0896-6273(00)00007-6

Dyubankova, N., Sochacka, E., Kraszewska, K., Nawrot, B., Herdewijn, P., & Lescrinier, E. (2015). Contribution of dihydrouridine in folding of the D-arm in tRNA. *Org Biomol Chem*, 13(17), 4960-4966. doi:10.1039/c5ob00164a

Edvardson, S., Prunetti, L., Arraf, A., Haas, D., Bacusmo, J. M., Hu, J. F., . . . Elpeleg, O. (2017). tRNA N6-adenosine threonylcarbamoyltransferase defect due to KAE1/TCS3 (OSGE) mutation manifest by neurodegeneration and renal tubulopathy. *Eur J Hum Genet*, 25(5), 545-551. doi:10.1038/ejhg.2017.30

El-Hattab, A. W., Saleh, M. A., Hashem, A., Al-Owain, M., Asmari, A. A., Rabei, H., . . . Alkuraya, F. S. (2016). ADAT3-related intellectual disability: Further delineation of the phenotype. *Am J Med Genet A*. doi:10.1002/ajmg.a.37578

El Yacoubi, B., Bailly, M., & de Crecy-Lagard, V. (2012). Biosynthesis and function of posttranscriptional modifications of transfer RNAs. *Annu Rev Genet*, 46, 69-95. doi:10.1146/annurev-genet-110711-155641

Elias, L. A., Wang, D. D., & Kriegstein, A. R. (2007). Gap junction adhesion is necessary for radial migration in the neocortex. *Nature*, 448(7156), 901-907. doi:10.1038/nature06063

Elias, Y., & Huang, R. H. (2005). Biochemical and structural studies of A-to-I editing by tRNA:A34 deaminases at the wobble position of transfer RNA. *Biochemistry*, 44(36), 12057-12065. doi:10.1021/bi050499f

Eom, D. S., Amarnath, S., & Agarwala, S. (2013). Apicobasal polarity and neural tube closure. *Dev Growth Differ*, 55(1), 164-172. doi:10.1111/dgd.12030

Espuny-Camacho, I., Arranz, A. M., Fiers, M., Snellinx, A., Ando, K., Munck, S., . . . De Strooper, B. (2017). Hallmarks of Alzheimer's Disease in Stem-Cell-Derived Human Neurons Transplanted into Mouse Brain. *Neuron*, 93(5), 1066-1081 e1068. doi:10.1016/j.neuron.2017.02.001

Fahiminiya, S., Almuriekhi, M., Nawaz, Z., Staffa, A., Lepage, P., Ali, R., . . . Ben-Omran, T. (2014). Whole exome sequencing unravels disease-causing genes in consanguineous families in Qatar. *Clin Genet*, 86(2), 134-141. doi:10.1111/cge.12280

Falconer, D. S. (1951). Two new mutants, 'trembler' and 'reeler', with neurological actions in the house mouse (*Mus musculus* L.). *J Genet*, 50(2), 192-201. doi:10.1007/BF02996215

Fan, G., Martinowich, K., Chin, M. H., He, F., Fouse, S. D., Hutnick, L., . . . Sun, Y. E. (2005). DNA methylation controls the timing of astrogliogenesis through regulation of JAK-STAT signaling. *Development*, 132(15), 3345-3356. doi:10.1242/dev.01912

Fatica, A., & Bozzoni, I. (2014). Long non-coding RNAs: new players in cell differentiation and development. *Nat Rev Genet*, 15(1), 7-21. doi:10.1038/nrg3606

Flores, J. V., Cordero-Espinoza, L., Oeztuerk-Winder, F., Andersson-Rolf, A., Selmi, T., Blanco, S., . . . Frye, M. (2017). Cytosine-5 RNA Methylation Regulates Neural Stem Cell Differentiation and Motility. *Stem Cell Reports*, 8(1), 112-124. doi:10.1016/j.stemcr.2016.11.014

Fornasiero, E. F., Mandad, S., Wildhagen, H., Alevra, M., Rammner, B., Keihani, S., . . . Rizzoli, S. O. (2018). Precisely measured protein lifetimes in the mouse brain reveal differences across tissues and subcellular fractions. *Nat Commun*, 9(1), 4230. doi:10.1038/s41467-018-06519-0

Franco, S. J., Martinez-Garay, I., Gil-Sanz, C., Harkins-Perry, S. R., & Muller, U. (2011). Reelin regulates cadherin function via Dab1/Rap1 to control neuronal migration and lamination in the neocortex. *Neuron*, 69(3), 482-497. doi:10.1016/j.neuron.2011.01.003

Frantz, G. D., & McConnell, S. K. (1996). Restriction of late cerebral cortical progenitors to an upper-layer fate. *Neuron*, 17(1), 55-61. doi:10.1016/s0896-6273(00)80280-9

Fredrick, K., & Ibba, M. (2010). How the sequence of a gene can tune its translation. *Cell*, 141(2), 227-229. doi:10.1016/j.cell.2010.03.033

Freude, K., Hoffmann, K., Jensen, L. R., Delatycki, M. B., des Portes, V., Moser, B., . . . Ropers, H. H. (2004). Mutations in the FTSJ1 gene coding for a novel S-adenosylmethionine-binding protein cause nonsyndromic X-linked mental retardation. *Am J Hum Genet*, 75(2), 305-309. doi:10.1086/422507

Gal, J. S., Morozov, Y. M., Ayoub, A. E., Chatterjee, M., Rakic, P., & Haydar, T. F. (2006). Molecular and morphological heterogeneity of neural precursors in the mouse neocortical proliferative zones. *J Neurosci*, 26(3), 1045-1056. doi:10.1523/JNEUROSCI.4499-05.2006

Gaspard, N., Bouschet, T., Hourez, R., Dimidschstein, J., Naeije, G., van den Ameele, J., . . . Vanderhaeghen, P. (2008). An intrinsic mechanism of corticogenesis from embryonic stem cells. *Nature*, 455(7211), 351-357. doi:10.1038/nature07287

Gaughwin, P., Ciesla, M., Yang, H., Lim, B., & Brundin, P. (2011). Stage-specific modulation of cortical neuronal development by Mmu-miR-134. *Cereb Cortex*, 21(8), 1857-1869. doi:10.1093/cercor/bhq262

Gebetsberger, J., & Polacek, N. (2013). Slicing tRNAs to boost functional ncRNA diversity. *RNA Biol*, 10(12), 1798-1806. doi:10.4161/rna.27177

Gerber, A., Ito, K., Chu, C. S., & Roeder, R. G. (2020). Gene-Specific Control of tRNA Expression by RNA Polymerase II. *Mol Cell*. doi:10.1016/j.molcel.2020.03.023

Gerber, A. P., & Keller, W. (1999). An adenosine deaminase that generates inosine at the wobble position of tRNAs. *Science*, 286(5442), 1146-1149.

Gertz, C. C., & Kriegstein, A. R. (2015). Neuronal Migration Dynamics in the Developing Ferret Cortex. *J Neurosci*, 35(42), 14307-14315. doi:10.1523/JNEUROSCI.2198-15.2015

Geslain, R., & Pan, T. (2010). Functional analysis of human tRNA isodecoders. *J Mol Biol*, 396(3), 821-831. doi:10.1016/j.jmb.2009.12.018

Ghezzi, D., Baruffini, E., Haack, T. B., Invernizzi, F., Melchionda, L., Dallabona, C., . . . Zeviani, M. (2012). Mutations of the mitochondrial-tRNA modifier MTO1 cause hypertrophic cardiomyopathy and lactic acidosis. *Am J Hum Genet*, 90(6), 1079-1087. doi:10.1016/j.ajhg.2012.04.011

Giege, R. (2008). Toward a more complete view of tRNA biology. *Nat Struct Mol Biol*, 15(10), 1007-1014. doi:10.1038/nsmb.1498

Gil-Sanz, C., Franco, S. J., Martinez-Garay, I., Espinosa, A., Harkins-Perry, S., & Muller, U. (2013). Cajal-Retzius cells instruct neuronal migration by coincidence signaling between secreted and contact-dependent guidance cues. *Neuron*, 79(3), 461-477. doi:10.1016/j.neuron.2013.06.040

Gilmore, E. C., & Walsh, C. A. (2013). Genetic causes of microcephaly and lessons for neuronal development. *Wiley Interdiscip Rev Dev Biol*, 2(4), 461-478. doi:10.1002/wdev.89

Gingold, H., Tehler, D., Christoffersen, N. R., Nielsen, M. M., Asmar, F., Kooistra, S. M., . . . Pilpel, Y. (2014). A dual program for translation regulation in cellular proliferation and differentiation. *Cell*, 158(6), 1281-1292. doi:10.1016/j.cell.2014.08.011

Godin, J. D., Creppe, C., Lagusse, S., & Nguyen, L. (2016). Emerging Roles for the Unfolded Protein Response in the Developing Nervous System. *Trends Neurosci*, 39(6), 394-404. doi:10.1016/j.tins.2016.04.002

Godin, J. D., & Nguyen, L. (2014). Novel functions of core cell cycle regulators in neuronal migration. *Adv Exp Med Biol*, 800, 59-74. doi:10.1007/978-94-007-7687-6_4

Godin, J. D., Thomas, N., Lagusse, S., Malinouskaya, L., Close, P., Malaise, O., . . . Nguyen, L. (2012). p27(Kip1) is a microtubule-associated protein that promotes microtubule polymerization during neuron migration. *Dev Cell*, 23(4), 729-744. doi:10.1016/j.devcel.2012.08.006

Gongidi, V., Ring, C., Moody, M., Brekken, R., Sage, E. H., Rakic, P., & Anton, E. S. (2004). SPARC-like 1 regulates the terminal phase of radial glia-guided migration in the cerebral cortex. *Neuron*, 41(1), 57-69. doi:10.1016/s0896-6273(03)00818-3

Goodarzi, H., Nguyen, Hoang C. B., Zhang, S., Dill, Brian D., Molina, H., & Tavazoie, Sohail F. (2016). Modulated Expression of Specific tRNAs Drives Gene Expression and Cancer Progression. *Cell*, 165(6), 1416-1427. doi:10.1016/j.cell.2016.05.046

Goodliffe, J. W., Olmos-Serrano, J. L., Aziz, N. M., Pennings, J. L., Guedj, F., Bianchi, D. W., & Haydar, T. F. (2016). Absence of Prenatal Forebrain Defects in the Dp(16)1Yey/+ Mouse Model of Down Syndrome. *J Neurosci*, 36(10), 2926-2944. doi:10.1523/JNEUROSCI.2513-15.2016

Gotz, M., & Huttner, W. B. (2005). The cell biology of neurogenesis. *Nat Rev Mol Cell Biol*, 6(10), 777-788. doi:10.1038/nrm1739

Greer, C. L. (1986). Assembly of a tRNA splicing complex: evidence for concerted excision and joining steps in splicing in vitro. *Mol Cell Biol*, 6(2), 635-644. doi:10.1128/mcb.6.2.635

Greig, L. C., Woodworth, M. B., Galazo, M. J., Padmanabhan, H., & Macklis, J. D. (2013). Molecular logic of neocortical projection neuron specification, development and diversity. *Nat Rev Neurosci*, 14(11), 755-769. doi:10.1038/nrn3586

Grosjean, H., de Crecy-Lagard, V., & Marck, C. (2010). Deciphering synonymous codons in the three domains of life: co-evolution with specific tRNA modification enzymes. *FEBS Lett*, 584(2), 252-264. doi:10.1016/j.febslet.2009.11.052

Guerrini, R., & Dobyns, W. B. (2014). Malformations of cortical development: clinical features and genetic causes. *The Lancet Neurology*, 13(7), 710-726. doi:10.1016/s1474-4422(14)70040-7

Hafner, A. S., Donlin-Asp, P. G., Leitch, B., Herzog, E., & Schuman, E. M. (2019). Local protein synthesis is a ubiquitous feature of neuronal pre- and postsynaptic compartments. *Science*, 364(6441). doi:10.1126/science.aau3644

Hanganu, I. L., Kilb, W., & Luhmann, H. J. (2002). Functional synaptic projections onto subplate neurons in neonatal rat somatosensory cortex. *J Neurosci*, 22(16), 7165-7176. doi:20026716

Hansen, D. V., Lui, J. H., Parker, P. R., & Kriegstein, A. R. (2010). Neurogenic radial glia in the outer subventricular zone of human neocortex. *Nature*, 464(7288), 554-561. doi:10.1038/nature08845

Harding, H. P., Novoa, I., Zhang, Y., Zeng, H., Wek, R., Schapira, M., & Ron, D. (2000). Regulated translation initiation controls stress-induced gene expression in mammalian cells. *Mol Cell*, 6(5), 1099-1108. doi:10.1016/s1097-2765(00)00108-8

Haslam, R. J., & Krebs, H. A. (1963). The Metabolism of Glutamate in Homogenates and Slices of Brain Cortex. *Biochem J*, 88, 566-578. doi:10.1042/bj0880566

Hatakeyama, J., Bessho, Y., Katoh, K., Ookawara, S., Fujioka, M., Guillemot, F., & Kageyama, R. (2004). Hes genes regulate size, shape and histogenesis of the nervous system by control of the timing of neural stem cell differentiation. *Development*, 131(22), 5539-5550. doi:10.1242/dev.01436

Hatanaka, Y., Hisanaga, S., Heizmann, C. W., & Murakami, F. (2004). Distinct migratory behavior of early- and late-born neurons derived from the cortical ventricular zone. *J Comp Neurol*, 479(1), 1-14. doi:10.1002/cne.20256

Hebebrand, M., Huffmeier, U., Trollmann, R., Hehr, U., Uebe, S., Ekici, A. B., . . . Popp, B. (2019). The mutational and phenotypic spectrum of TUBA1A-associated tubulinopathy. *Orphanet J Rare Dis*, 14(1), 38. doi:10.1186/s13023-019-1020-x

Hecht, J. H., Siegenthaler, J. A., Patterson, K. P., & Pleasure, S. J. (2010). Primary cellular meningeal defects cause neocortical dysplasia and dyslamination. *Ann Neurol*, 68(4), 454-464. doi:10.1002/ana.22103

Heins, N., Malatesta, P., Cecconi, F., Nakafuku, M., Tucker, K. L., Hack, M. A., . . . Gotz, M. (2002). Glial cells generate neurons: the role of the transcription factor Pax6. *Nat Neurosci*, 5(4), 308-315. doi:10.1038/nn828

Hekman, K. E., Yu, G. Y., Brown, C. D., Zhu, H., Du, X., Gervin, K., . . . Gomez, C. M. (2012). A conserved eEF2 coding variant in SCA26 leads to loss of translational fidelity and increased susceptibility to proteostatic insult. *Hum Mol Genet*, 21(26), 5472-5483. doi:10.1093/hmg/ddz392

Hengel, H., Buchert, R., Sturm, M., Haack, T. B., Schelling, Y., Mahajnah, M., . . . Schols, L. (2020). First-line exome sequencing in Palestinian and Israeli Arabs with neurological disorders is efficient and facilitates disease gene discovery. *Eur J Hum Genet*. doi:10.1038/s41431-020-0609-9

Hershey, J. W. B., Sonenberg, N., & Mathews, M. B. (2019). Principles of Translational Control. *Cold Spring Harb Perspect Biol*, 11(9). doi:10.1101/csdperspect.a032607

Hiesberger, T., Trommsdorff, M., Howell, B. W., Goffinet, A., Mumby, M. C., Cooper, J. A., & Herz, J. (1999). Direct binding of Reelin to VLDL receptor and ApoE receptor 2 induces tyrosine phosphorylation of disabled-1 and modulates tau phosphorylation. *Neuron*, 24(2), 481-489. doi:10.1016/s0896-6273(00)80861-2

Higher Functions of the Nervous System. (2016). Retrieved from <https://basicmedicalkey.com/higher-functions-of-the-nervous-system/>

Hinnebusch, A. G. (2014). The scanning mechanism of eukaryotic translation initiation. *Annu Rev Biochem*, 83, 779-812. doi:10.1146/annurev-biochem-060713-035802

Hirabayashi, Y., Itoh, Y., Tabata, H., Nakajima, K., Akiyama, T., Masuyama, N., & Gotoh, Y. (2004). The Wnt/beta-catenin pathway directs neuronal differentiation of cortical neural precursor cells. *Development*, 131(12), 2791-2801. doi:10.1242/dev.01165

Holt, C. E., Martin, K. C., & Schuman, E. M. (2019). Local translation in neurons: visualization and function. *Nat Struct Mol Biol*, 26(7), 557-566. doi:10.1038/s41594-019-0263-5

Horesh, D., Sapir, T., Francis, F., Wolf, S. G., Caspi, M., Elbaum, M., . . . Reiner, O. (1999). Doublecortin, a stabilizer of microtubules. *Hum Mol Genet*, 8(9), 1599-1610. doi:10.1093/hmg/8.9.1599

Hyun, H. S., Kim, S. H., Park, E., Cho, M. H., Kang, H. G., Lee, H. S., . . . Cheong, H. I. (2018). A familial case of Galloway-Mowat syndrome due to a novel TP53RK mutation: a case report. *BMC Med Genet*, 19(1), 131. doi:10.1186/s12881-018-0649-y

Ibba, M., & Soll, D. (2000). Aminoacyl-tRNA synthesis. *Annu Rev Biochem*, 69, 617-650. doi:10.1146/annurev.biochem.69.1.617

Iben, J. R., & Maraia, R. J. (2014). tRNA gene copy number variation in humans. *Gene*, 536(2), 376-384. doi:10.1016/j.gene.2013.11.049

Igoillo-Esteve, M., Genin, A., Lambert, N., Desir, J., Pirson, I., Abdulkarim, B., . . . Cnop, M. (2013). tRNA methyltransferase homolog gene TRMT10A mutation in young onset diabetes and primary microcephaly in humans. *PLoS Genet*, 9(10), e1003888. doi:10.1371/journal.pgen.1003888

Ingolia, N. T. (2014). Ribosome profiling: new views of translation, from single codons to genome scale. *Nat Rev Genet*, 15(3), 205-213. doi:10.1038/nrg3645

Ingolia, N. T., Brar, G. A., Rouskin, S., McGeechey, A. M., & Weissman, J. S. (2012). The ribosome profiling strategy for monitoring translation in vivo by deep sequencing of ribosome-protected mRNA fragments. *Nat Protoc*, 7(8), 1534-1550. doi:10.1038/nprot.2012.086

Inoue, M., Iwai, R., Tabata, H., Konno, D., Komabayashi-Suzuki, M., Watanabe, C., . . . Mizutani, K. I. (2017). Prdm16 is crucial for progression of the multipolar phase during neural differentiation of the developing neocortex. *Development*, 144(3), 385-399. doi:10.1242/dev.136382

Inoue, M., Kuroda, T., Honda, A., Komabayashi-Suzuki, M., Komai, T., Shinkai, Y., & Mizutani, K. (2014). Prdm8 regulates the morphological transition at multipolar phase during neocortical development. *PLoS One*, 9(1), e86356. doi:10.1371/journal.pone.0086356

Inoue, S., Hayashi, K., Fujita, K., Tagawa, K., Okazawa, H., Kubo, K. I., & Nakajima, K. (2019). Drebrin-like (Dbnl) Controls Neuronal Migration via Regulating N-Cadherin Expression in the Developing Cerebral Cortex. *J Neurosci*, 39(4), 678-691. doi:10.1523/JNEUROSCI.1634-18.2018

Inoue, T., Ogawa, M., Mikoshiba, K., & Aruga, J. (2008). Zic deficiency in the cortical marginal zone and meninges results in cortical lamination defects resembling those in type II lissencephaly. *J Neurosci*, 28(18), 4712-4725. doi:10.1523/JNEUROSCI.5735-07.2008

Inui, T., Kobayashi, S., Ashikari, Y., Sato, R., Endo, W., Uematsu, M., . . . Hagiwara, K. (2016). Two cases of early-onset myoclonic seizures with continuous parietal delta activity caused by EEF1A2 mutations. *Brain Dev*, 38(5), 520-524. doi:10.1016/j.braindev.2015.11.003

Ishii, K., Kubo, K. I., & Nakajima, K. (2016). Reelin and Neuropsychiatric Disorders. *Front Cell Neurosci*, 10, 229. doi:10.3389/fncel.2016.00229

Ishimura, R., Nagy, G., Dotu, I., Zhou, H., Yang, X. L., Schimmel, P., . . . Ackerman, S. L. (2014). RNA function. Ribosome stalling induced by mutation of a CNS-specific tRNA causes neurodegeneration. *Science*, 345(6195), 455-459. doi:10.1126/science.1249749

Itoh, Y., Moriyama, Y., Hasegawa, T., Endo, T. A., Toyoda, T., & Gotoh, Y. (2013). Scratch regulates neuronal migration onset via an epithelial-mesenchymal transition-like mechanism. *Nat Neurosci*, 16(4), 416-425. doi:10.1038/nn.3336

Ivanova, E. L., Gilet, J. G., Sulimenko, V., Duchon, A., Rudolf, G., Runge, K., . . . Hinckelmann, M. V. (2019). TUBG1 missense variants underlying cortical malformations disrupt neuronal locomotion and microtubule dynamics but not neurogenesis. *Nat Commun*, 10(1), 2129. doi:10.1038/s41467-019-10081-8

Jabaudon, D. (2017). Fate and freedom in developing neocortical circuits. *Nat Commun*, 8, 16042. doi:10.1038/ncomms16042

Jaglin, X. H., & Chelly, J. (2009). Tubulin-related cortical dysgenesis: microtubule dysfunction underlying neuronal migration defects. *Trends Genet*, 25(12), 555-566. doi:10.1016/j.tig.2009.10.003

Jakkamsetti, V., Marin-Valencia, I., Ma, Q., Good, L. B., Terrill, T., Rajasekaran, K., . . . Pascual, J. M. (2019). Brain metabolism modulates neuronal excitability in a mouse model of pyruvate dehydrogenase deficiency. *Sci Transl Med*, 11(480). doi:10.1126/scitranslmed.aan0457

Jamuar, S. S., & Walsh, C. A. (2015). Genomic variants and variations in malformations of cortical development. *Pediatr Clin North Am*, 62(3), 571-585. doi:10.1016/j.pcl.2015.03.002

Jeong, S. J., Luo, R., Singer, K., Giera, S., Kreidberg, J., Kiyozumi, D., . . . Piao, X. (2013). GPR56 functions together with alpha3beta1 integrin in regulating cerebral cortical development. *PLoS One*, 8(7), e68781. doi:10.1371/journal.pone.0068781

Judas, M., Sedmak, G., & Pletikos, M. (2010). Early history of subplate and interstitial neurons: from Theodor Meynert (1867) to the discovery of the subplate zone (1974). *J Anat*, 217(4), 344-367. doi:10.1111/j.1469-7580.2010.01283.x

Kanold, P. O., Kara, P., Reid, R. C., & Shatz, C. J. (2003). Role of subplate neurons in functional maturation of visual cortical columns. *Science*, 301(5632), 521-525. doi:10.1126/science.1084152

Kapur, M., & Ackerman, S. L. (2018). mRNA Translation Gone Awry: Translation Fidelity and Neurological Disease. *Trends Genet*. doi:10.1016/j.tig.2017.12.007

Kapur, M., Monaghan, C. E., & Ackerman, S. L. (2017). Regulation of mRNA Translation in Neurons-A Matter of Life and Death. *Neuron*, 96(3), 616-637. doi:10.1016/j.neuron.2017.09.057

Karaca, E., Weitzer, S., Pehlivan, D., Shiraishi, H., Gogakos, T., Hanada, T., . . . Lupski, J. R. (2014). Human CLP1 mutations alter tRNA biogenesis, affecting both peripheral and central nervous system function. *Cell*, 157(3), 636-650. doi:10.1016/j.cell.2014.02.058

Karczewski, K. J., Francioli, L. C., Tiao, G., Cummings, B. B., Alfoldi, J., Wang, Q., . . . MacArthur, D. G. (2020). The mutational constraint spectrum quantified from variation in 141,456 humans. *Nature*, 581(7809), 434-443. doi:10.1038/s41586-020-2308-7

Kawase-Koga, Y., Otaegi, G., & Sun, T. (2009). Different timings of Dicer deletion affect neurogenesis and gliogenesis in the developing mouse central nervous system. *Dev Dyn*, 238(11), 2800-2812. doi:10.1002/dvdy.22109

Kawauchi, T., Chihama, K., Nabeshima, Y., & Hoshino, M. (2006). Cdk5 phosphorylates and stabilizes p27kip1 contributing to actin organization and cortical neuronal migration. *Nat Cell Biol*, 8(1), 17-26. doi:10.1038/ncb1338

Kawauchi, T., Sekine, K., Shikanai, M., Chihama, K., Tomita, K., Kubo, K., . . . Hoshino, M. (2010). Rab GTPases-dependent endocytic pathways regulate neuronal migration and maturation through N-cadherin trafficking. *Neuron*, 67(4), 588-602. doi:10.1016/j.neuron.2010.07.007

Kawaue, T., Shitamukai, A., Nagasaka, A., Tsunekawa, Y., Shinoda, T., Saito, K., . . . Kawaguchi, A. (2019). Lzts1 controls both neuronal delamination and outer radial glial-like cell generation during mammalian cerebral development. *Nat Commun*, 10(1), 2780. doi:10.1038/s41467-019-10730-y

Kearse, M. G., & Wilusz, J. E. (2017). Non-AUG translation: a new start for protein synthesis in eukaryotes. *Genes Dev*, 31(17), 1717-1731. doi:10.1101/gad.305250.117

Keays, D. A., Tian, G., Poirier, K., Huang, G. J., Siebold, C., Cleak, J., . . . Flint, J. (2007). Mutations in alpha-tubulin cause abnormal neuronal migration in mice and lissencephaly in humans. *Cell*, 128(1), 45-57. doi:10.1016/j.cell.2006.12.017

Khade, P. K., & Joseph, S. (2011). Messenger RNA interactions in the decoding center control the rate of translocation. *Nat Struct Mol Biol*, 18(11), 1300-1302. doi:10.1038/nsmb.2140

Kilberg, M. S., Shan, J., & Su, N. (2009). ATF4-dependent transcription mediates signaling of amino acid limitation. *Trends Endocrinol Metab*, 20(9), 436-443. doi:10.1016/j.tem.2009.05.008

Kirchner, S., & Ignatova, Z. (2015). Emerging roles of tRNA in adaptive translation, signalling dynamics and disease. *Nat Rev Genet*, 16(2), 98-112. doi:10.1038/nrg3861

Kishi, Y., Fujii, Y., Hirabayashi, Y., & Gotoh, Y. (2012). HMGA regulates the global chromatin state and neurogenic potential in neocortical precursor cells. *Nat Neurosci*, 15(8), 1127-1133. doi:10.1038/nn.3165

Klauck, S. M., Felder, B., Kolb-Kokocinski, A., Schuster, C., Chiocchetti, A., Schupp, I., . . . Poustka, A. (2006). Mutations in the ribosomal protein gene RPL10 suggest a novel modulating disease mechanism for autism. *Mol Psychiatry*, 11(12), 1073-1084. doi:10.1038/sj.mp.4001883

Klingler, E., & Jabaudon, D. (2020). Do progenitors play dice? *eLife*, 9. doi:10.7554/eLife.54042

Knight, J. R. P., Garland, G., Poyry, T., Mead, E., Vlahov, N., Sfakianos, A., . . . Willis, A. E. (2020). Control of translation elongation in health and disease. *Dis Model Mech*, 13(3). doi:10.1242/dmm.043208

Kodera, H., Osaka, H., Iai, M., Aida, N., Yamashita, A., Tsurusaki, Y., . . . Matsumoto, N. (2015). Mutations in the glutaminyl-tRNA synthetase gene cause early-onset epileptic encephalopathy. *J Hum Genet*, 60(2), 97-101. doi:10.1038/jhg.2014.103

Kon, E., Calvo-Jimenez, E., Cossard, A., Na, Y., Cooper, J. A., & Jossin, Y. (2019). N-cadherin-regulated FGFR ubiquitination and degradation control mammalian neocortical projection neuron migration. *eLife*, 8. doi:10.7554/eLife.47673

Konno, D., Shioi, G., Shitamukai, A., Mori, A., Kiyonari, H., Miyata, T., & Matsuzaki, F. (2008). Neuroepithelial progenitors undergo LGN-dependent planar divisions to maintain self-renewability during mammalian neurogenesis. *Nat Cell Biol*, 10(1), 93-101. doi:10.1038/ncb1673

Kopajtich, R., Murayama, K., Janecke, A. R., Haack, T. B., Breuer, M., Knisely, A. S., . . . Staufner, C. (2016). Biallelic IARS Mutations Cause Growth Retardation with Prenatal

Onset, Intellectual Disability, Muscular Hypotonia, and Infantile Hepatopathy. *Am J Hum Genet*, 99(2), 414-422. doi:10.1016/j.ajhg.2016.05.027

Kosodo, Y., Roper, K., Haubensak, W., Marzesco, A. M., Corbeil, D., & Huttner, W. B. (2004). Asymmetric distribution of the apical plasma membrane during neurogenic divisions of mammalian neuroepithelial cells. *EMBO J*, 23(11), 2314-2324. doi:10.1038/sj.emboj.7600223

Kriegstein, A., & Alvarez-Buylla, A. (2009). The glial nature of embryonic and adult neural stem cells. *Annu Rev Neurosci*, 32, 149-184. doi:10.1146/annurev.neuro.051508.135600

Kutter, C., Brown, G. D., Goncalves, A., Wilson, M. D., Watt, S., Brazma, A., . . . Odom, D. T. (2011). Pol III binding in six mammals shows conservation among amino acid isotypes despite divergence among tRNA genes. *Nat Genet*, 43(10), 948-955. doi:10.1038/ng.906

Lacerda, R., Menezes, J., & Romao, L. (2017). More than just scanning: the importance of cap-independent mRNA translation initiation for cellular stress response and cancer. *Cell Mol Life Sci*, 74(9), 1659-1680. doi:10.1007/s00018-016-2428-2

Laguisse, S., Creppe, C., Nedialkova, D. D., Prevot, P. P., Borgs, L., Huysseune, S., . . . Nguyen, L. (2015). A Dynamic Unfolded Protein Response Contributes to the Control of Cortical Neurogenesis. *Dev Cell*, 35(5), 553-567. doi:10.1016/j.devcel.2015.11.005

Laguisse, S., Peyre, E., & Nguyen, L. (2015). Progenitor genealogy in the developing cerebral cortex. *Cell Tissue Res*, 359(1), 17-32. doi:10.1007/s00441-014-1979-5

Lam, W. W., Millichap, J. J., Soares, D. C., Chin, R., McLellan, A., FitzPatrick, D. R., . . . Abbott, C. M. (2016). Novel de novo EEF1A2 missense mutations causing epilepsy and intellectual disability. *Mol Genet Genomic Med*, 4(4), 465-474. doi:10.1002/mgg3.219

Lancaster, M. A., & Knoblich, J. A. (2012). Spindle orientation in mammalian cerebral cortical development. *Curr Opin Neurobiol*, 22(5), 737-746. doi:10.1016/j.conb.2012.04.003

Lange, C., Huttner, W. B., & Calegari, F. (2009). Cdk4/cyclinD1 overexpression in neural stem cells shortens G1, delays neurogenesis, and promotes the generation and expansion of basal progenitors. *Cell Stem Cell*, 5(3), 320-331. doi:10.1016/j.stem.2009.05.026

Lavdas, A. A., Grigoriou, M., Pachnis, V., & Parnavelas, J. G. (1999). The medial ganglionic eminence gives rise to a population of early neurons in the developing cerebral cortex. *J Neurosci*, 19(18), 7881-7888.

Lee, C. C., & Hsieh, T. S. (2018). Wuhu/WDR4 deficiency inhibits cell proliferation and induces apoptosis via DNA damage in mouse embryonic fibroblasts. *Cell Signal*, 47, 16-26. doi:10.1016/j.cellsig.2018.03.007

Lee, S., Wolfrain, L. A., & Wang, E. (1993). Differential expression of S1 and elongation factor-1 alpha during rat development. *J Biol Chem*, 268(32), 24453-24459.

Lentini, J. M., Alsaif, H. S., Faqeih, E., Alkuraya, F. S., & Fu, D. (2020). DALRD3 encodes a protein mutated in epileptic encephalopathy that targets arginine tRNAs for 3-methylcytosine modification. *Nat Commun*, 11(1), 2510. doi:10.1038/s41467-020-16321-6

Leulliot, N., Chaillet, M., Durand, D., Ulryck, N., Blondeau, K., & van Tilbeurgh, H. (2008). Structure of the yeast tRNA m7G methylation complex. *Structure*, 16(1), 52-61. doi:10.1016/j.str.2007.10.025

Li, J., Wang, Y. N., Xu, B. S., Liu, Y. P., Zhou, M., Long, T., . . . Liu, R. J. (2020). Intellectual disability-associated gene *ftsj1* is responsible for 2'-O-methylation of specific tRNAs. *EMBO Rep*, e50095. doi:10.15252/embr.202050095

Li, L., Wei, D., Wang, Q., Pan, J., Liu, R., Zhang, X., & Bao, L. (2012). MEC-17 deficiency leads to reduced alpha-tubulin acetylation and impaired migration of cortical neurons. *J Neurosci*, 32(37), 12673-12683. doi:10.1523/JNEUROSCI.0016-12.2012

Lim, V. I. (1995). Analysis of action of the wobble adenine on codon reading within the ribosome. *J Mol Biol*, 252(3), 277-282. doi:10.1006/jmbi.1995.0494

Lim, V. I., & Curran, J. F. (2001). Analysis of codon:anticodon interactions within the ribosome provides new insights into codon reading and the genetic code structure. *RNA*, 7(7), 942-957. doi:10.1017/s135583820100214x

Lin, S., Liu, Q., Lelyveld, V. S., Choe, J., Szostak, J. W., & Gregory, R. I. (2018). Mettl1/Wdr4-Mediated m(7)G tRNA Methylome Is Required for Normal mRNA Translation and Embryonic Stem Cell Self-Renewal and Differentiation. *Mol Cell*, 71(2), 244-255 e245. doi:10.1016/j.molcel.2018.06.001

Liu, J. S. (2011). Molecular genetics of neuronal migration disorders. *Curr Neurol Neurosci Rep*, 11(2), 171-178. doi:10.1007/s11910-010-0176-5

Liu, Y., Zhang, Y., Chi, Q., Wang, Z., & Sun, B. (2020). Methyltransferase-like 1 (METTL1) served as a tumor suppressor in colon cancer by activating 7-methyguanosine (m7G) regulated let-7e miRNA/HMGA2 axis. *Life Sci*, 249, 117480. doi:10.1016/j.lfs.2020.117480

Livingstone, M., Atas, E., Meller, A., & Sonenberg, N. (2010). Mechanisms governing the control of mRNA translation. *Phys Biol*, 7(2), 021001. doi:10.1088/1478-3975/7/2/021001

Llorca, A., Ciceri, G., Beattie, R., Wong, F. K., Diana, G., Serafeimidou-Pouliou, E., . . . Marin, O. (2019). A stochastic framework of neurogenesis underlies the assembly of neocortical cytoarchitecture. *eLife*, 8. doi:10.7554/eLife.51381

Loenarz, C., Sekirnik, R., Thalhammer, A., Ge, W., Spivakovskiy, E., Mackeen, M. M., . . . Schofield, C. J. (2014). Hydroxylation of the eukaryotic ribosomal decoding center affects translational accuracy. *Proc Natl Acad Sci U S A*, 111(11), 4019-4024. doi:10.1073/pnas.1311750111

Long, K. R., & Huttner, W. B. (2019). How the extracellular matrix shapes neural development. *Open Biol*, 9(1), 180216. doi:10.1098/rsob.180216

Lorenz, C., Lunse, C. E., & Morl, M. (2017). tRNA Modifications: Impact on Structure and Thermal Adaptation. *Biomolecules*, 7(2). doi:10.3390/biom7020035

LoTurco, J., Manent, J. B., & Sidiqi, F. (2009). New and improved tools for in utero electroporation studies of developing cerebral cortex. *Cereb Cortex*, 19 Suppl 1, i120-125. doi:10.1093/cercor/bhp033

LoTurco, J. J., & Bai, J. (2006). The multipolar stage and disruptions in neuronal migration. *Trends Neurosci*, 29(7), 407-413. doi:10.1016/j.tins.2006.05.006

Lowe, T. M., & Eddy, S. R. (1997). tRNAscan-SE: a program for improved detection of transfer RNA genes in genomic sequence. *Nucleic Acids Res*, 25(5), 955-964. doi:10.1093/nar/25.5.955

Lund, E., & Dahlberg, J. E. (1998). Proofreading and aminoacylation of tRNAs before export from the nucleus. *Science*, 282(5396), 2082-2085. doi:10.1126/science.282.5396.2082

Luo, Z., Freitag, M., & Sachs, M. S. (1995). Translational regulation in response to changes in amino acid availability in *Neurospora crassa*. *Mol Cell Biol*, 15(10), 5235-5245. doi:10.1128/mcb.15.10.5235

Lyu, X., Yang, Q., Li, L., Dang, Y., Zhou, Z., Chen, S., & Liu, Y. (2020). Adaptation of codon usage to tRNA I34 modification controls translation kinetics and proteome landscape. *PLoS Genet*, 16(6), e1008836. doi:10.1371/journal.pgen.1008836

M.Lowe, V. H. M. N. (2017). *Nutrition and the developing brain* (Taylor & Francis ed.): CRC Press.

Marck, C., & Grosjean, H. (2002). tRNomics: analysis of tRNA genes from 50 genomes of Eukarya, Archaea, and Bacteria reveals anticodon-sparing strategies and domain-specific features. *RNA*, 8(10), 1189-1232.

Marin, O. (2013). Cellular and molecular mechanisms controlling the migration of neocortical interneurons. *Eur J Neurosci*, 38(1), 2019-2029. doi:10.1111/ejn.12225

Marin, O., & Rubenstein, J. L. (2001). A long, remarkable journey: tangential migration in the telencephalon. *Nat Rev Neurosci*, 2(11), 780-790. doi:10.1038/35097509

Martinez-Cerdeno, V., & Noctor, S. C. (2014). Cajal, Retzius, and Cajal-Retzius cells. *Front Neuroanat*, 8, 48. doi:10.3389/fnana.2014.00048

Martinez-Martinez, M. A., Ciceri, G., Espinos, A., Fernandez, V., Marin, O., & Borrell, V. (2019). Extensive branching of radially-migrating neurons in the mammalian cerebral cortex. *J Comp Neurol*, 527(10), 1558-1576. doi:10.1002/cne.24597

Martynoga, B., Drechsel, D., & Guillemot, F. (2012). Molecular control of neurogenesis: a view from the mammalian cerebral cortex. *Cold Spring Harb Perspect Biol*, 4(10). doi:10.1101/cshperspect.a008359

Mateyak, M. K., & Kinzy, T. G. (2010). eEF1A: thinking outside the ribosome. *J Biol Chem*, 285(28), 21209-21213. doi:10.1074/jbc.R110.113795

Matsuki, T., Matthews, R. T., Cooper, J. A., van der Brug, M. P., Cookson, M. R., Hardy, J. A., ... Howell, B. W. (2010). Reelin and stk25 have opposing roles in neuronal polarization and dendritic Golgi deployment. *Cell*, 143(5), 826-836. doi:10.1016/j.cell.2010.10.029

Matsumoto, K., Tomikawa, C., Toyooka, T., Ochi, A., Takano, Y., Takayanagi, N., ... Hori, H. (2008). Production of yeast tRNA (m(7)G46) methyltransferase (Trm8-Trm82 complex) in a wheat germ cell-free translation system. *J Biotechnol*, 133(4), 453-460. doi:10.1016/j.jbiotec.2007.11.009

Matsumoto, K., Toyooka, T., Tomikawa, C., Ochi, A., Takano, Y., Takayanagi, N., . . . Hori, H. (2007). RNA recognition mechanism of eukaryote tRNA (m7G46) methyltransferase (Trm8-Trm82 complex). *FEBS Lett.*, *581*(8), 1599-1604. doi:10.1016/j.febslet.2007.03.023

McConnell, S. K., Ghosh, A., & Shatz, C. J. (1989). Subplate neurons pioneer the first axon pathway from the cerebral cortex. *Science*, *245*(4921), 978-982. doi:10.1126/science.2475909

McConnell, S. K., & Kaznowski, C. E. (1991). Cell cycle dependence of laminar determination in developing neocortex. *Science*, *254*(5029), 282-285. doi:10.1126/science.1925583

Megel, C., Morelle, G., Lalande, S., Duchene, A. M., Small, I., & Marechal-Drouard, L. (2015). Surveillance and cleavage of eukaryotic tRNAs. *Int J Mol Sci*, *16*(1), 1873-1893. doi:10.3390/ijms16011873

Mei, Y., Yong, J., Liu, H., Shi, Y., Meinkoth, J., Dreyfuss, G., & Yang, X. (2010). tRNA binds to cytochrome c and inhibits caspase activation. *Mol Cell*, *37*(5), 668-678. doi:10.1016/j.molcel.2010.01.023

Michaud, J., Kudoh, J., Berry, A., Bonne-Tamir, B., Lalioti, M. D., Rossier, C., . . . Scott, H. S. (2000). Isolation and characterization of a human chromosome 21q22.3 gene (WDR4) and its mouse homologue that code for a WD-repeat protein. *Genomics*, *68*(1), 71-79. doi:10.1006/geno.2000.6258

Mishima, E., Inoue, C., Saigusa, D., Inoue, R., Ito, K., Suzuki, Y., . . . Abe, T. (2014). Conformational change in transfer RNA is an early indicator of acute cellular damage. *J Am Soc Nephrol*, *25*(10), 2316-2326. doi:10.1681/ASN.2013091001

Miyata, T., Kawaguchi, A., Okano, H., & Ogawa, M. (2001). Asymmetric inheritance of radial glial fibers by cortical neurons. *Neuron*, *31*(5), 727-741. doi:10.1016/s0896-6273(01)00420-2

Miyata, T., Kawaguchi, A., Saito, K., Kawano, M., Muto, T., & Ogawa, M. (2004). Asymmetric production of surface-dividing and non-surface-dividing cortical progenitor cells. *Development*, *131*(13), 3133-3145. doi:10.1242/dev.01173

Miyoshi, G., & Fishell, G. (2012). Dynamic FoxG1 expression coordinates the integration of multipolar pyramidal neuron precursors into the cortical plate. *Neuron*, *74*(6), 1045-1058. doi:10.1016/j.neuron.2012.04.025

Molyneaux, B. J., Arlotta, P., & Macklis, J. D. (2007). Molecular development of corticospinal motor neuron circuitry. *Novartis Found Symp*, *288*, 3-15; discussion 15-20, 96-18.

Molyneaux, B. J., Arlotta, P., Menezes, J. R., & Macklis, J. D. (2007). Neuronal subtype specification in the cerebral cortex. *Nat Rev Neurosci*, *8*(6), 427-437. doi:10.1038/nrn2151

Morris, R. C., Brown, K. G., & Elliott, M. S. (1999). The effect of queuosine on tRNA structure and function. *J Biomol Struct Dyn*, *16*(4), 757-774. doi:10.1080/07391102.1999.10508291

Motorin, Y., & Grosjean, H. (2005). Transfer RNA Modification. In *Encyclopedia of life sciences*: Wiley Online.

Motorin, Y., & Helm, M. (2010). tRNA Stabilization by Modified Nucleotides. *Biochemistry*, 49(24), 4934-4944. doi:10.1021/bi100408z

MuhChyi, C., Juliandi, B., Matsuda, T., & Nakashima, K. (2013). Epigenetic regulation of neural stem cell fate during corticogenesis. *Int J Dev Neurosci*, 31(6), 424-433. doi:10.1016/j.ijdevneu.2013.02.006

Mukhtar, T., & Taylor, V. (2018). Untangling Cortical Complexity During Development. *J Exp Neurosci*, 12, 1179069518759332. doi:10.1177/1179069518759332

Murphy, F. V. t., & Ramakrishnan, V. (2004). Structure of a purine-purine wobble base pair in the decoding center of the ribosome. *Nat Struct Mol Biol*, 11(12), 1251-1252. doi:10.1038/nsmb866

Mysh rall, T. D., Moore, S. A., Ostendorf, A. P., Satz, J. S., Kowalczyk, T., Nguyen, H., . . . Hevner, R. F. (2012). Dystroglycan on radial glia end feet is required for pial basement membrane integrity and columnar organization of the developing cerebral cortex. *J Neuropathol Exp Neurol*, 71(12), 1047-1063. doi:10.1097/NEN.0b013e318274a128

Na, W., Fu, L., Luu, N., & Shi, Y. B. (2020). Direct activation of tRNA methyltransferase-like 1 (Mettl1) gene by thyroid hormone receptor implicates a role in adult intestinal stem cell development and proliferation during *Xenopus tropicalis* metamorphosis. *Cell Biosci*, 10, 60. doi:10.1186/s13578-020-00423-1

Nadarajah, B. (2003). Radial glia and somal translocation of radial neurons in the developing cerebral cortex. *Glia*, 43(1), 33-36. doi:10.1002/glia.10245

Nadarajah, B., Brunstrom, J. E., Grutzendler, J., Wong, R. O., & Pearlman, A. L. (2001). Two modes of radial migration in early development of the cerebral cortex. *Nat Neurosci*, 4(2), 143-150. doi:10.1038/83967

Nadarajah, B., & Parnavelas, J. G. (2002). Modes of neuronal migration in the developing cerebral cortex. *Nat Rev Neurosci*, 3(6), 423-432. doi:10.1038/nrn845

Nakajima, J., Okamoto, N., Tohyama, J., Kato, M., Arai, H., Funahashi, O., . . . Miyake, N. (2015). De novo EEF1A2 mutations in patients with characteristic facial features, intellectual disability, autistic behaviors and epilepsy. *Clin Genet*, 87(4), 356-361. doi:10.1111/cge.12394

Nakashima, K., Takizawa, T., Ochiai, W., Yanagisawa, M., Hisatsune, T., Nakafuku, M., . . . Taga, T. (2001). BMP2-mediated alteration in the developmental pathway of fetal mouse brain cells from neurogenesis to astrocytogenesis. *Proc Natl Acad Sci U S A*, 98(10), 5868-5873. doi:10.1073/pnas.101109698

Namba, T., & Huttner, W. B. (2017). Neural progenitor cells and their role in the development and evolutionary expansion of the neocortex. *Wiley Interdiscip Rev Dev Biol*, 6(1). doi:10.1002/wdev.256

Nedialkova, D. D., & Leidel, S. A. (2015). Optimization of Codon Translation Rates via tRNA Modifications Maintains Proteome Integrity. *Cell*, 161(7), 1606-1618. doi:10.1016/j.cell.2015.05.022

Ng, S. Y., Bogu, G. K., Soh, B. S., & Stanton, L. W. (2013). The long noncoding RNA RMST interacts with SOX2 to regulate neurogenesis. *Mol Cell*, 51(3), 349-359. doi:10.1016/j.molcel.2013.07.017

Nguyen, L., Besson, A., Heng, J. I., Schuurmans, C., Teboul, L., Parras, C., . . . Guillemot, F. (2006). p27kip1 independently promotes neuronal differentiation and migration in the cerebral cortex. *Genes Dev*, 20(11), 1511-1524. doi:10.1101/gad.377106

Nicole, O., Bell, D. M., Leste-Lasserre, T., Doat, H., Guillemot, F., & Pacary, E. (2018). A novel role for CAMKIIbeta in the regulation of cortical neuron migration: implications for neurodevelopmental disorders. *Mol Psychiatry*, 23(11), 2209-2226. doi:10.1038/s41380-018-0046-0

Nieoullon, V., Belvindrah, R., Rougon, G., & Chazal, G. (2005). mCD24 regulates proliferation of neuronal committed precursors in the subventricular zone. *Mol Cell Neurosci*, 28(3), 462-474. doi:10.1016/j.mcn.2004.10.007

Nishimura, T., Kato, K., Yamaguchi, T., Fukata, Y., Ohno, S., & Kaibuchi, K. (2004). Role of the PAR-3-KIF3 complex in the establishment of neuronal polarity. *Nat Cell Biol*, 6(4), 328-334. doi:10.1038/ncb1118

Nishimura, Y. V., Nabeshima, Y. I., & Kawauchi, T. (2017). Morphological and Molecular Basis of Cytoplasmic Dilation and Swelling in Cortical Migrating Neurons. *Brain Sci*, 7(7). doi:10.3390/brainsci7070087

Nishimura, Y. V., Sekine, K., Chihama, K., Nakajima, K., Hoshino, M., Nabeshima, Y., & Kawauchi, T. (2010). Dissecting the factors involved in the locomotion mode of neuronal migration in the developing cerebral cortex. *J Biol Chem*, 285(8), 5878-5887. doi:10.1074/jbc.M109.033761

Nishimura, Y. V., Shikanai, M., Hoshino, M., Ohshima, T., Nabeshima, Y., Mizutani, K., . . . Kawauchi, T. (2014). Cdk5 and its substrates, Dcx and p27kip1, regulate cytoplasmic dilation formation and nuclear elongation in migrating neurons. *Development*, 141(18), 3540-3550. doi:10.1242/dev.111294

Nishri, D., Goldberg-Stern, H., Noyman, I., Blumkin, L., Kivity, S., Saitsu, H., . . . Lev, D. (2016). RARS2 mutations cause early onset epileptic encephalopathy without ponto-cerebellar hypoplasia. *Eur J Paediatr Neurol*, 20(3), 412-417. doi:10.1016/j.ejpn.2016.02.012

Noctor, S. C., Martinez-Cerdeno, V., Ivic, L., & Kriegstein, A. R. (2004). Cortical neurons arise in symmetric and asymmetric division zones and migrate through specific phases. *Nat Neurosci*, 7(2), 136-144. doi:10.1038/nn1172

Norden, C., Young, S., Link, B. A., & Harris, W. A. (2009). Actomyosin is the main driver of interkinetic nuclear migration in the retina. *Cell*, 138(6), 1195-1208. doi:10.1016/j.cell.2009.06.032

Norris, A. D., & Calarco, J. A. (2012). Emerging Roles of Alternative Pre-mRNA Splicing Regulation in Neuronal Development and Function. *Front Neurosci*, 6, 122. doi:10.3389/fnins.2012.00122

Nosten-Bertrand, M., Kappeler, C., Dinocourt, C., Denis, C., Germain, J., Phan Dinh Tuy, F., . . . Francis, F. (2008). Epilepsy in Dcx knockout mice associated with discrete lamination

defects and enhanced excitability in the hippocampus. *PLoS One*, 3(6), e2473. doi:10.1371/journal.pone.0002473

Novoa, E. M., Pavon-Eternod, M., Pan, T., & Ribas de Pouplana, L. (2012). A role for tRNA modifications in genome structure and codon usage. *Cell*, 149(1), 202-213. doi:10.1016/j.cell.2012.01.050

Novoa, E. M., & Ribas de Pouplana, L. (2012). Speeding with control: codon usage, tRNAs, and ribosomes. *Trends Genet*, 28(11), 574-581. doi:10.1016/j.tig.2012.07.006

Oberst, P., Fievre, S., Baumann, N., Concetti, C., Bartolini, G., & Jabaudon, D. (2019). Temporal plasticity of apical progenitors in the developing mouse neocortex. *Nature*, 573(7774), 370-374. doi:10.1038/s41586-019-1515-6

Ognjenovic, J., & Simonovic, M. (2018). Human aminoacyl-tRNA synthetases in diseases of the nervous system. *RNA Biol*, 15(4-5), 623-634. doi:10.1080/15476286.2017.1330245

Ohtaka-Maruyama, C., & Okado, H. (2015). Molecular Pathways Underlying Projection Neuron Production and Migration during Cerebral Cortical Development. *Front Neurosci*, 9, 447. doi:10.3389/fnins.2015.00447

Ohtaka-Maruyama, C., Okamoto, M., Endo, K., Oshima, M., Kaneko, N., Yura, K., . . . Maeda, N. (2018). Synaptic transmission from subplate neurons controls radial migration of neocortical neurons. *Science*, 360(6386), 313-317. doi:10.1126/science.aar2866

Okamoto, H., Watanabe, K., Ikeuchi, Y., Suzuki, T., Endo, Y., & Hori, H. (2004). Substrate tRNA recognition mechanism of tRNA (m7G46) methyltransferase from *Aquifex aeolicus*. *J Biol Chem*, 279(47), 49151-49159. doi:10.1074/jbc.M408209200

Okamoto, M., Miyata, T., Konno, D., Ueda, H. R., Kasukawa, T., Hashimoto, M., . . . Kawaguchi, A. (2016). Cell-cycle-independent transitions in temporal identity of mammalian neural progenitor cells. *Nat Commun*, 7, 11349. doi:10.1038/ncomms11349

Onishi, K., Uyeda, A., Shida, M., Hirayama, T., Yagi, T., Yamamoto, N., & Sugo, N. (2017). Genome Stability by DNA Polymerase beta in Neural Progenitors Contributes to Neuronal Differentiation in Cortical Development. *J Neurosci*, 37(35), 8444-8458. doi:10.1523/JNEUROSCI.0665-17.2017

Overview of translation. (2016). Retrieved from <https://www.khanacademy.org/science/biology/gene-expression-central-dogma/translation-polypeptides/a/translation-overview>

Pacary, E., & Guillemot, F. (2020). In Utero Electroporation to Study Mouse Brain Development. *Methods Mol Biol*, 2047, 513-523. doi:10.1007/978-1-4939-9732-9_29

Pacary, E., Haas, M. A., Wildner, H., Azzarelli, R., Bell, D. M., Abrous, D. N., & Guillemot, F. (2012). Visualization and genetic manipulation of dendrites and spines in the mouse cerebral cortex and hippocampus using in utero electroporation. *J Vis Exp*(65). doi:10.3791/4163

Pandey, S., Agarwala, P., Jayaraj, G. G., Gargallo, R., & Maiti, S. (2015). The RNA Stem-Loop to G-Quadruplex Equilibrium Controls Mature MicroRNA Production inside the Cell. *Biochemistry*, 54(48), 7067-7078. doi:10.1021/acs.biochem.5b00574

Pandolfini, L., Barbieri, I., Bannister, A. J., Hendrick, A., Andrews, B., Webster, N., . . . Kouzarides, T. (2019). METTL1 Promotes let-7 MicroRNA Processing via m7G Methylation. *Mol Cell*, 74(6), 1278-1290 e1279. doi:10.1016/j.molcel.2019.03.040

Pang, Y. L., Poruri, K., & Martinis, S. A. (2014). tRNA synthetase: tRNA aminoacylation and beyond. *Wiley Interdiscip Rev RNA*, 5(4), 461-480. doi:10.1002/wrna.1224

Paolini, N. A., Attwood, M., Sondalle, S. B., Vieira, C., van Adrichem, A. M., di Summa, F. M., . . . MacInnes, A. W. (2017). A Ribosomopathy Reveals Decoding Defective Ribosomes Driving Human Dysmorphism. *Am J Hum Genet*, 100(3), 506-522. doi:10.1016/j.ajhg.2017.01.034

Paridaen, J. T., & Huttner, W. B. (2014). Neurogenesis during development of the vertebrate central nervous system. *EMBO Rep*, 15(4), 351-364. doi:10.1002/embr.201438447

Paridaen, J. T., Wilsch-Brauninger, M., & Huttner, W. B. (2013). Asymmetric inheritance of centrosome-associated primary cilium membrane directs ciliogenesis after cell division. *Cell*, 155(2), 333-344. doi:10.1016/j.cell.2013.08.060

Parisien, M., Wang, X., & Pan, T. (2013). Diversity of human tRNA genes from the 1000-genomes project. *RNA Biol*, 10(12), 1853-1867. doi:10.4161/rna.27361

Penisson, M., Ladewig, J., Belvindrah, R., & Francis, F. (2019). Genes and Mechanisms Involved in the Generation and Amplification of Basal Radial Glial Cells. *Front Cell Neurosci*, 13, 381. doi:10.3389/fncel.2019.00381

Pereira, M., Francisco, S., Varanda, A. S., Santos, M., Santos, M. A. S., & Soares, A. R. (2018). Impact of tRNA Modifications and tRNA-Modifying Enzymes on Proteostasis and Human Disease. *Int J Mol Sci*, 19(12). doi:10.3390/ijms19123738

Peyre, E., Jaouen, F., Saadaoui, M., Haren, L., Merdes, A., Durbec, P., & Morin, X. (2011). A lateral belt of cortical LGN and NuMA guides mitotic spindle movements and planar division in neuroepithelial cells. *J Cell Biol*, 193(1), 141-154. doi:10.1083/jcb.201101039

Phizicky, E. M., & Hopper, A. K. (2010). tRNA biology charges to the front. *Genes Dev*, 24(17), 1832-1860. doi:10.1101/gad.1956510

Pinheiro, E. M., Xie, Z., Norovich, A. L., Vidaki, M., Tsai, L. H., & Gertler, F. B. (2011). Lpd depletion reveals that SRF specifies radial versus tangential migration of pyramidal neurons. *Nat Cell Biol*, 13(8), 989-995. doi:10.1038/ncb2292

Poirier, K., Saillour, Y., Bahi-Buisson, N., Jaglin, X. H., Fallet-Bianco, C., Nabbout, R., . . . Chelly, J. (2010). Mutations in the neuronal ss-tubulin subunit TUBB3 result in malformation of cortical development and neuronal migration defects. *Hum Mol Genet*, 19(22), 4462-4473. doi:10.1093/hmg/ddq377

Popow, J., Englert, M., Weitzer, S., Schleiffer, A., Mierzwa, B., Mechtler, K., . . . Martinez, J. (2011). HSPC117 is the essential subunit of a human tRNA splicing ligase complex. *Science*, 331(6018), 760-764. doi:10.1126/science.1197847

Postiglione, M. P., Juschke, C., Xie, Y., Haas, G. A., Charalambous, C., & Knoblich, J. A. (2011). Mouse inscuteable induces apical-basal spindle orientation to facilitate intermediate progenitor generation in the developing neocortex. *Neuron*, 72(2), 269-284. doi:10.1016/j.neuron.2011.09.022

Powell, C. A., Kopajtich, R., D'Souza, A. R., Rorbach, J., Kremer, L. S., Husain, R. A., . . . Minczuk, M. (2015). TRMT5 Mutations Cause a Defect in Post-transcriptional Modification of Mitochondrial tRNA Associated with Multiple Respiratory-Chain Deficiencies. *Am J Hum Genet*, 97(2), 319-328. doi:10.1016/j.ajhg.2015.06.011

Price, D. J., Aslam, S., Tasker, L., & Gillies, K. (1997). Fates of the earliest generated cells in the developing murine neocortex. *J Comp Neurol*, 377(3), 414-422.

Price, D. J., Kennedy, H., Dehay, C., Zhou, L., Mercier, M., Jossin, Y., . . . Molnar, Z. (2006). The development of cortical connections. *Eur J Neurosci*, 23(4), 910-920. doi:10.1111/j.1460-9568.2006.04620.x

Pütz, J., Florentz, C., Benseler, F., & Giegé, R. (1994). A single methyl group prevents the mischarging of a tRNA. *Nature structural biology*, 1, 580-582. doi:10.1038/nsb0994-580

Qian, X., Shen, Q., Goderie, S. K., He, W., Capela, A., Davis, A. A., & Temple, S. (2000). Timing of CNS cell generation: a programmed sequence of neuron and glial cell production from isolated murine cortical stem cells. *Neuron*, 28(1), 69-80. doi:10.1016/s0896-6273(00)00086-6

Quax, T. E., Claassens, N. J., Soll, D., & van der Oost, J. (2015). Codon Bias as a Means to Fine-Tune Gene Expression. *Mol Cell*, 59(2), 149-161. doi:10.1016/j.molcel.2015.05.035

Rafels-Ybern, A., Attolini, C. S., & Ribas de Pouplana, L. (2015). Distribution of ADAT-Dependent Codons in the Human Transcriptome. *Int J Mol Sci*, 16(8), 17303-17314. doi:10.3390/ijms160817303

Rafels-Ybern, A., Torres, A. G., Grau-Bove, X., Ruiz-Trillo, I., & Ribas de Pouplana, L. (2018). Codon adaptation to tRNAs with Inosine modification at position 34 is widespread among Eukaryotes and present in two Bacterial phyla. *RNA Biol*, 15(4-5), 500-507. doi:10.1080/15476286.2017.1358348

Rago, L., Beattie, R., Taylor, V., & Winter, J. (2014). miR379-410 cluster miRNAs regulate neurogenesis and neuronal migration by fine-tuning N-cadherin. *EMBO J*, 33(8), 906-920. doi:10.1002/embj.201386591

Ragone, F. L., Spears, J. L., Wohlgamuth-Benedum, J. M., Kreel, N., Papavasiliou, F. N., & Alfonzo, J. D. (2011). The C-terminal end of the Trypanosoma brucei editing deaminase plays a critical role in tRNA binding. *RNA*, 17(7), 1296-1306. doi:10.1261/rna.2748211

Raina, M., & Ibba, M. (2014). tRNAs as regulators of biological processes. *Front Genet*, 5, 171. doi:10.3389/fgene.2014.00171

Ramakrishnan, V. (2002). Ribosome structure and the mechanism of translation. *Cell*, 108(4), 557-572. doi:10.1016/s0092-8674(02)00619-0

Ramirez, A., Shuman, S., & Schwer, B. (2008). Human RNA 5'-kinase (hClp1) can function as a tRNA splicing enzyme in vivo. *RNA*, 14(9), 1737-1745. doi:10.1261/rna.1142908

Ramos, J., & Fu, D. (2019). The emerging impact of tRNA modifications in the brain and nervous system. *Biochim Biophys Acta Gene Regul Mech*, 1862(3), 412-428. doi:10.1016/j.bbagr.2018.11.007

Ramos, J., Han, L., Li, Y., Hagelskamp, F., Kellner, S. M., Alkuraya, F. S., . . . Fu, D. (2019). Formation of tRNA Wobble Inosine in Humans Is Disrupted by a Millennia-Old Mutation Causing Intellectual Disability. *Mol Cell Biol*, 39(19). doi:10.1128/MCB.00203-19

Ramos, R. L., Bai, J., & LoTurco, J. J. (2006). Heterotopia formation in rat but not mouse neocortex after RNA interference knockdown of DCX. *Cereb Cortex*, 16(9), 1323-1331. doi:10.1093/cercor/bhj074

Ranjan, N., & Rodnina, M. V. (2016). tRNA wobble modifications and protein homeostasis. *Translation (Austin)*, 4(1), e1143076. doi:10.1080/21690731.2016.1143076

Rapino, F., Delaunay, S., Rambow, F., Zhou, Z., Tharun, L., De Tullio, P., . . . Close, P. (2018). Codon-specific translation reprogramming promotes resistance to targeted therapy. *Nature*, 558(7711), 605-609. doi:10.1038/s41586-018-0243-7

Rastegari, E., Kajal, K., Tan, B. S., Huang, F., Chen, R. H., Hsieh, T. S., & Hsu, H. J. (2020). WD40 protein Wuho controls germline homeostasis via TRIM-NHL tumor suppressor Mei-p26 in Drosophila. *Development*, 147(2). doi:10.1242/dev.182063

Reiner, O. (2013). LIS1 and DCX: Implications for Brain Development and Human Disease in Relation to Microtubules. *Scientifica (Cairo)*, 2013, 393975. doi:10.1155/2013/393975

Rezgui, V. A., Tyagi, K., Ranjan, N., Konevega, A. L., Mittelstaet, J., Rodnina, M. V., . . . Pedrioli, P. G. (2013). tRNA tKUUU, tQUUG, and tEUUC wobble position modifications fine-tune protein translation by promoting ribosome A-site binding. *Proc Natl Acad Sci U S A*, 110(30), 12289-12294. doi:10.1073/pnas.1300781110

Rice, D. S., & Curran, T. (2001). Role of the reelin signaling pathway in central nervous system development. *Annu Rev Neurosci*, 24, 1005-1039. doi:10.1146/annurev.neuro.24.1.1005

Rodriguez, M., Choi, J., Park, S., & Sockanathan, S. (2012). Gde2 regulates cortical neuronal identity by controlling the timing of cortical progenitor differentiation. *Development*, 139(20), 3870-3879. doi:10.1242/dev.081083

Romero, D. M., Bahi-Buisson, N., & Francis, F. (2018). Genetics and mechanisms leading to human cortical malformations. *Semin Cell Dev Biol*, 76, 33-75. doi:10.1016/j.semcdb.2017.09.031

Ross, S. E., Greenberg, M. E., & Stiles, C. D. (2003). Basic helix-loop-helix factors in cortical development. *Neuron*, 39(1), 13-25. doi:10.1016/s0896-6273(03)00365-9

Roura Frigole, H., Camacho, N., Castellvi Coma, M., Fernandez-Lozano, C., Garcia-Lema, J., Rafels-Ybern, A., . . . Ribas de Pouplana, L. (2019). tRNA deamination by ADAT requires substrate-specific recognition mechanisms and can be inhibited by tRFs. *RNA*, 25(5), 607-619. doi:10.1261/rna.068189.118

Rubin, B. Y., & Anderson, S. L. (2017). IKBKAP/ELP1 gene mutations: mechanisms of familial dysautonomia and gene-targeting therapies. *Appl Clin Genet*, 10, 95-103. doi:10.2147/TACG.S129638

Rubio, M. A., Gaston, K. W., McKenney, K. M., Fleming, I. M., Paris, Z., Limbach, P. A., & Alfonzo, J. D. (2017). Editing and methylation at a single site by functionally interdependent activities. *Nature*, 542(7642), 494-497. doi:10.1038/nature21396

Rubio, M. A., Pastar, I., Gaston, K. W., Ragone, F. L., Janzen, C. J., Cross, G. A., . . . Alfonzo, J. D. (2007). An adenosine-to-inosine tRNA-editing enzyme that can perform C-to-U deamination of DNA. *Proc Natl Acad Sci U S A*, 104(19), 7821-7826. doi:10.1073/pnas.0702394104

Russell, P. (2010). iGenetics 3rd Ed. .

Rutkowski, D. T., & Kaufman, R. J. (2003). All roads lead to ATF4. *Dev Cell*, 4(4), 442-444. doi:10.1016/s1534-5807(03)00100-x

Saade, M., Gutierrez-Vallejo, I., Le Dreau, G., Rabadan, M. A., Miguez, D. G., Buceta, J., & Marti, E. (2013). Sonic hedgehog signaling switches the mode of division in the developing nervous system. *Cell Rep*, 4(3), 492-503. doi:10.1016/j.celrep.2013.06.038

Saikia, M., Fu, Y., Pavon-Eternod, M., He, C., & Pan, T. (2010). Genome-wide analysis of N1-methyl-adenosine modification in human tRNAs. *RNA*, 16(7), 1317-1327. doi:10.1261/rna.2057810

Sailhour, Y., Broix, L., Bruel-Jungerman, E., Lebrun, N., Muraca, G., Rucci, J., . . . Chelly, J. (2014). Beta tubulin isoforms are not interchangeable for rescuing impaired radial migration due to Tubb3 knockdown. *Hum Mol Genet*, 23(6), 1516-1526. doi:10.1093/hmg/ddt538

Saint-Leger, A., Bello, C., Dans, P. D., Torres, A. G., Novoa, E. M., Camacho, N., . . . Ribas de Pouplana, L. (2016). Saturation of recognition elements blocks evolution of new tRNA identities. *Sci Adv*, 2(4), e1501860. doi:10.1126/sciadv.1501860

Salehi Chaleshtori, A. R., Miyake, N., Ahmadvand, M., Bashti, O., Matsumoto, N., & Noruzinia, M. (2018). A novel 8-bp duplication in ADAT3 causes mild intellectual disability. *Hum Genome Var*, 5, 7. doi:10.1038/s41439-018-0007-9

Salmi, M., Bruneau, N., Cillario, J., Lozovaya, N., Massacrier, A., Buhler, E., . . . Szepetowski, P. (2013). Tubacin prevents neuronal migration defects and epileptic activity caused by rat SrpX2 silencing in utero. *Brain*, 136(Pt 8), 2457-2473. doi:10.1093/brain/awt161

Samali, A., & Orrenius, S. (1998). Heat shock proteins: regulators of stress response and apoptosis. *Cell Stress Chaperones*, 3(4), 228-236. doi:10.1379/1466-1268(1998)003<0228:hspros>2.3.co;2

Sandbaken, M. G., & Culbertson, M. R. (1988). Mutations in elongation factor EF-1 alpha affect the frequency of frameshifting and amino acid misincorporation in *Saccharomyces cerevisiae*. *Genetics*, 120(4), 923-934.

Sasaki, S., Mori, D., Toyo-oka, K., Chen, A., Garrett-Beal, L., Muramatsu, M., . . . Hirotsune, S. (2005). Complete loss of Ndel1 results in neuronal migration defects and early

embryonic lethality. *Mol Cell Biol*, 25(17), 7812-7827. doi:10.1128/MCB.25.17.7812-7827.2005

Scardigli, R., Baumer, N., Gruss, P., Guillemot, F., & Le Roux, I. (2003). Direct and concentration-dependent regulation of the proneural gene Neurogenin2 by Pax6. *Development*, 130(14), 3269-3281. doi:10.1242/dev.00539

Schaar, B. T., & McConnell, S. K. (2005). Cytoskeletal coordination during neuronal migration. *Proc Natl Acad Sci U S A*, 102(38), 13652-13657. doi:10.1073/pnas.0506008102

Schaefer, M., & Lyko, F. (2010). Lack of evidence for DNA methylation of Invader4 retroelements in *Drosophila* and implications for Dnmt2-mediated epigenetic regulation. *Nat Genet*, 42(11), 920-921; author reply 921. doi:10.1038/ng1110-920

Schaffer, A. E., Eggens, V. R., Caglayan, A. O., Reuter, M. S., Scott, E., Coufal, N. G., . . . Gleeson, J. G. (2014). CLP1 founder mutation links tRNA splicing and maturation to cerebellar development and neurodegeneration. *Cell*, 157(3), 651-663. doi:10.1016/j.cell.2014.03.049

Schaffer, A. E., Pinkard, O., & Coller, J. M. (2019). tRNA Metabolism and Neurodevelopmental Disorders. *Annu Rev Genomics Hum Genet*, 20, 359-387. doi:10.1146/annurev-genom-083118-015334

Schimmel, P. (2017). The emerging complexity of the tRNA world: mammalian tRNAs beyond protein synthesis. *Nat Rev Mol Cell Biol*. doi:10.1038/nrm.2017.77

Schimmel, P. (2018). The emerging complexity of the tRNA world: mammalian tRNAs beyond protein synthesis. *Nat Rev Mol Cell Biol*, 19(1), 45-58. doi:10.1038/nrm.2017.77

Schmid, R. S., McGrath, B., Berechid, B. E., Boyles, B., Marchionni, M., Sestan, N., & Anton, E. S. (2003). Neuregulin 1-erbB2 signaling is required for the establishment of radial glia and their transformation into astrocytes in cerebral cortex. *Proc Natl Acad Sci U S A*, 100(7), 4251-4256. doi:10.1073/pnas.0630496100

Schmitt, B. M., Rudolph, K. L., Karagianni, P., Fonseca, N. A., White, R. J., Talianidis, I., . . . Kutter, C. (2014). High-resolution mapping of transcriptional dynamics across tissue development reveals a stable mRNA-tRNA interface. *Genome Res*, 24(11), 1797-1807. doi:10.1101/gr.176784.114

Schneider, A. (2011). Mitochondrial tRNA import and its consequences for mitochondrial translation. *Annu Rev Biochem*, 80, 1033-1053. doi:10.1146/annurev-biochem-060109-092838

Schwamborn, J. C., Berezikov, E., & Knoblich, J. A. (2009). The TRIM-NHL protein TRIM32 activates microRNAs and prevents self-renewal in mouse neural progenitors. *Cell*, 136(5), 913-925. doi:10.1016/j.cell.2008.12.024

Sekine, K., Honda, T., Kawauchi, T., Kubo, K., & Nakajima, K. (2011). The outermost region of the developing cortical plate is crucial for both the switch of the radial migration mode and the Dab1-dependent "inside-out" lamination in the neocortex. *J Neurosci*, 31(25), 9426-9439. doi:10.1523/JNEUROSCI.0650-11.2011

Senger, B., Auxilien, S., Englisch, U., Cramer, F., & Fasiolo, F. (1997). The modified wobble base inosine in yeast tRNA^{Alle} is a positive determinant for aminoacylation by isoleucyl-tRNA synthetase. *Biochemistry*, 36(27), 8269-8275. doi:10.1021/bi970206l

Senger, B., Auxilien, S., Englisch, U., Cramer, F., & Fasiolo, F. (1997). The Modified Wobble Base Inosine in Yeast tRNA^{Alle} Is a Positive Determinant for Aminoacylation by Isoleucyl-tRNA Synthetase. *Biochemistry*, 36(27), 8269-8275. doi:10.1021/bi970206l

Shah, P., Ding, Y., Niemczyk, M., Kudla, G., & Plotkin, J. B. (2013). Rate-limiting steps in yeast protein translation. *Cell*, 153(7), 1589-1601. doi:10.1016/j.cell.2013.05.049

Shaheen, R., Abdel-Salam, G. M., Guy, M. P., Alomar, R., Abdel-Hamid, M. S., Afifi, H. H., . . . Alkuraya, F. S. (2015). Mutation in WDR4 impairs tRNA m(7)G46 methylation and causes a distinct form of microcephalic primordial dwarfism. *Genome Biol*, 16, 210. doi:10.1186/s13059-015-0779-x

Shaheen, R., Han, L., Faqeih, E., Ewida, N., Alobeid, E., Phizicky, E. M., & Alkuraya, F. S. (2016). A homozygous truncating mutation in PUS3 expands the role of tRNA modification in normal cognition. *Hum Genet*, 135(7), 707-713. doi:10.1007/s00439-016-1665-7

Shao, S., Murray, J., Brown, A., Taunton, J., Ramakrishnan, V., & Hegde, R. S. (2016). Decoding Mammalian Ribosome-mRNA States by Translational GTPase Complexes. *Cell*, 167(5), 1229-1240 e1215. doi:10.1016/j.cell.2016.10.046

Sharkia, R., Zalan, A., Jabareen-Masri, A., Zahalka, H., & Mahajnah, M. (2018). A new case confirming and expanding the phenotype spectrum of ADAT3-related intellectual disability syndrome. *Eur J Med Genet*. doi:10.1016/j.ejmg.2018.10.001

Shen, Q., Wang, Y., Dimos, J. T., Fasano, C. A., Phoenix, T. N., Lemischka, I. R., . . . Temple, S. (2006). The timing of cortical neurogenesis is encoded within lineages of individual progenitor cells. *Nat Neurosci*, 9(6), 743-751. doi:10.1038/nn1694

Shimogori, T., & Ogawa, M. (2008). Gene application with in utero electroporation in mouse embryonic brain. *Dev Growth Differ*, 50(6), 499-506. doi:10.1111/j.1440-169X.2008.01045.x

Shitamukai, A., Konno, D., & Matsuzaki, F. (2011). Oblique radial glial divisions in the developing mouse neocortex induce self-renewing progenitors outside the germinal zone that resemble primate outer subventricular zone progenitors. *J Neurosci*, 31(10), 3683-3695. doi:10.1523/JNEUROSCI.4773-10.2011

Shu, T., Ayala, R., Nguyen, M. D., Xie, Z., Gleeson, J. G., & Tsai, L. H. (2004). Ndel1 operates in a common pathway with LIS1 and cytoplasmic dynein to regulate cortical neuronal positioning. *Neuron*, 44(2), 263-277. doi:10.1016/j.neuron.2004.09.030

Sibler, A. P., Dirheimer, G., & Martin, R. P. (1986). Codon reading patterns in *Saccharomyces cerevisiae* mitochondria based on sequences of mitochondrial tRNAs. *FEBS Lett*, 194(1), 131-138. doi:10.1016/0014-5793(86)80064-3

Simo, S., & Cooper, J. A. (2013). Rbx2 regulates neuronal migration through different cullin 5-RING ligase adaptors. *Dev Cell*, 27(4), 399-411. doi:10.1016/j.devcel.2013.09.022

Simo, S., Jossin, Y., & Cooper, J. A. (2010). Cullin 5 regulates cortical layering by modulating the speed and duration of Dab1-dependent neuronal migration. *J Neurosci*, 30(16), 5668-5676. doi:10.1523/JNEUROSCI.0035-10.2010

Singleton, D. C., & Harris, A. L. (2012). Targeting the ATF4 pathway in cancer therapy. *Expert Opin Ther Targets*, 16(12), 1189-1202. doi:10.1517/14728222.2012.728207

Singleton, R. S., Liu-Yi, P., Formenti, F., Ge, W., Sekirnik, R., Fischer, R., . . . Cockman, M. E. (2014). OGFOD1 catalyzes prolyl hydroxylation of RPS23 and is involved in translation control and stress granule formation. *Proc Natl Acad Sci U S A*, 111(11), 4031-4036. doi:10.1073/pnas.1314482111

Smith, T. F. (2008). Diversity of WD-repeat proteins. *Subcell Biochem*, 48, 20-30. doi:10.1007/978-0-387-09595-0_3

Smits, P., Smeitink, J., & van den Heuvel, L. (2010). Mitochondrial translation and beyond: processes implicated in combined oxidative phosphorylation deficiencies. *J Biomed Biotechnol*, 2010, 737385. doi:10.1155/2010/737385

Solecki, D. J., Trivedi, N., Govek, E. E., Kerekes, R. A., Gleason, S. S., & Hatten, M. E. (2009). Myosin II motors and F-actin dynamics drive the coordinated movement of the centrosome and soma during CNS glial-guided neuronal migration. *Neuron*, 63(1), 63-80. doi:10.1016/j.neuron.2009.05.028

Sonawane, K. D., Bavi, R. S., Sambhare, S. B., & Fandilolu, P. M. (2016). Comparative Structural Dynamics of tRNA(Phe) with Respect to Hinge Region Methylated Guanosine: A Computational Approach. *Cell Biochem Biophys*, 74(2), 157-173. doi:10.1007/s12013-016-0731-z

Sonenberg, N., & Hinnebusch, A. G. (2009). Regulation of translation initiation in eukaryotes: mechanisms and biological targets. *Cell*, 136(4), 731-745. doi:10.1016/j.cell.2009.01.042

Spears, J. L., Rubio, M. A., Gaston, K. W., Wywial, E., Strikoudis, A., Bujnicki, J. M., . . . Alfonzo, J. D. (2011). A single zinc ion is sufficient for an active Trypanosoma brucei tRNA editing deaminase. *J Biol Chem*, 286(23), 20366-20374. doi:10.1074/jbc.M111.243568

Spencer, P. S., & Barral, J. M. (2012). Genetic code redundancy and its influence on the encoded polypeptides. *Comput Struct Biotechnol J*, 1, e201204006. doi:10.5936/csbj.201204006

Sulima, S. O., Gulay, S. P., Anjos, M., Patchett, S., Meskauskas, A., Johnson, A. W., & Dinman, J. D. (2014). Eukaryotic rpL10 drives ribosomal rotation. *Nucleic Acids Res*, 42(3), 2049-2063. doi:10.1093/nar/gkt1107

Sultan, K. T., & Shi, S. H. (2018). Generation of diverse cortical inhibitory interneurons. *Wiley Interdiscip Rev Dev Biol*, 7(2). doi:10.1002/wdev.306

Sultan, M., Piccini, I., Balzereit, D., Herwig, R., Saran, N. G., Lehrach, H., . . . Yaspo, M. L. (2007). Gene expression variation in Down's syndrome mice allows prioritization of candidate genes. *Genome Biol*, 8(5), R91. doi:10.1186/gb-2007-8-5-r91

Suter, T., Blagburn, S. V., Fisher, S. E., Anderson-Keightly, H. M., D'Elia, K. P., & Jaworski, A. (2020). TAG-1 Multifunctionality Coordinates Neuronal Migration, Axon Guidance, and Fasciculation. *Cell Rep*, 30(4), 1164-1177 e1167. doi:10.1016/j.celrep.2019.12.085

Sutton, M. A., & Schuman, E. M. (2006). Dendritic protein synthesis, synaptic plasticity, and memory. *Cell*, 127(1), 49-58. doi:10.1016/j.cell.2006.09.014

Suzuki, T., Nagao, A., & Suzuki, T. (2011). Human mitochondrial tRNAs: biogenesis, function, structural aspects, and diseases. *Annu Rev Genet*, 45, 299-329. doi:10.1146/annurev-genet-110410-132531

Tabata, H., & Nagata, K. (2016). Decoding the molecular mechanisms of neuronal migration using in utero electroporation. *Med Mol Morphol*, 49(2), 63-75. doi:10.1007/s00795-015-0127-y

Tabata, H., & Nakajima, K. (2001). Efficient in utero gene transfer system to the developing mouse brain using electroporation: visualization of neuronal migration in the developing cortex. *Neuroscience*, 103(4), 865-872. doi:10.1016/s0306-4522(01)00016-1

Tahmasebi, S., Khoutorsky, A., Mathews, M. B., & Sonenberg, N. (2018). Translation deregulation in human disease. *Nat Rev Mol Cell Biol*, 19(12), 791-807. doi:10.1038/s41580-018-0034-x

Takahashi, T., Nowakowski, R. S., & Caviness, V. S., Jr. (1995). The cell cycle of the pseudostratified ventricular epithelium of the embryonic murine cerebral wall. *J Neurosci*, 15(9), 6046-6057.

Takano, K., Nakagawa, E., Inoue, K., Kamada, F., Kure, S., Goto, Y., & Japanese Mental Retardation, C. (2008). A loss-of-function mutation in the FTSJ1 gene causes nonsyndromic X-linked mental retardation in a Japanese family. *Am J Med Genet B Neuropsychiatr Genet*, 147B(4), 479-484. doi:10.1002/ajmg.b.30638

Tanaka, T., Serneo, F. F., Higgins, C., Gambello, M. J., Wynshaw-Boris, A., & Gleeson, J. G. (2004). Lis1 and doublecortin function with dynein to mediate coupling of the nucleus to the centrosome in neuronal migration. *J Cell Biol*, 165(5), 709-721. doi:10.1083/jcb.200309025

Tang, J., Ip, J. P., Ye, T., Ng, Y. P., Yung, W. H., Wu, Z., . . . Ip, N. Y. (2014). Cdk5-dependent Mst3 phosphorylation and activity regulate neuronal migration through RhoA inhibition. *J Neurosci*, 34(22), 7425-7436. doi:10.1523/JNEUROSCI.5449-13.2014

Tararuk, T., Ostman, N., Li, W., Bjorkblom, B., Padzik, A., Zdrojewska, J., . . . Coffey, E. T. (2006). JNK1 phosphorylation of SCG10 determines microtubule dynamics and axodendritic length. *J Cell Biol*, 173(2), 265-277. doi:10.1083/jcb.200511055

Tasic, B., Yao, Z., Graybuck, L. T., Smith, K. A., Nguyen, T. N., Bertagnolli, D., . . . Zeng, H. (2018). Shared and distinct transcriptomic cell types across neocortical areas. *Nature*, 563(7729), 72-78. doi:10.1038/s41586-018-0654-5

Taverna, E., & Huttner, W. B. (2010). Neural progenitor nuclei IN motion. *Neuron*, 67(6), 906-914. doi:10.1016/j.neuron.2010.08.027

Telley, L., Agirman, G., Prados, J., Amberg, N., Fievre, S., Oberst, P., . . . Jabaudon, D. (2019). Temporal patterning of apical progenitors and their daughter neurons in the developing neocortex. *Science*, 364(6440). doi:10.1126/science.aav2522

Telley, L., Govindan, S., Prados, J., Stevant, I., Nef, S., Dermitzakis, E., . . . Jabaudon, D. (2016). Sequential transcriptional waves direct the differentiation of newborn neurons in the mouse neocortex. *Science*, 351(6280), 1443-1446. doi:10.1126/science.aad8361

Tessier-Lavigne, M., & Goodman, C. S. (1996). The molecular biology of axon guidance. *Science*, 274(5290), 1123-1133. doi:10.1126/science.274.5290.1123

Thevenon, J., Michot, C., Bole, C., Nitschke, P., Nizon, M., Faivre, L., . . . Amiel, J. (2015). RPL10 mutation segregating in a family with X-linked syndromic Intellectual Disability. *Am J Med Genet A*, 167A(8), 1908-1912. doi:10.1002/ajmg.a.37094

Thomas, E., Lewis, A. M., Yang, Y., Chanprasert, S., Potocki, L., & Scott, D. A. (2019). Novel Missense Variants in ADAT3 as a Cause of Syndromic Intellectual Disability. *J Pediatr Genet*, 8(4), 244-251. doi:10.1055/s-0039-1693151

Thompson, M., Haeusler, R. A., Good, P. D., & Engelke, D. R. (2003). Nucleolar clustering of dispersed tRNA genes. *Science*, 302(5649), 1399-1401. doi:10.1126/science.1089814

Tian, Q. H., Zhang, M. F., Zeng, J. S., Luo, R. G., Wen, Y., Chen, J., . . . Xiong, J. P. (2019). METTL1 overexpression is correlated with poor prognosis and promotes hepatocellular carcinoma via PTEN. *J Mol Med (Berl)*, 97(11), 1535-1545. doi:10.1007/s00109-019-01830-9

Tomikawa, C. (2018). 7-Methylguanosine Modifications in Transfer RNA (tRNA). *Int J Mol Sci*, 19(12). doi:10.3390/ijms19124080

Torabi, N., & Kruglyak, L. (2011). Variants in SUP45 and TRM10 underlie natural variation in translation termination efficiency in *Saccharomyces cerevisiae*. *PLoS Genet*, 7(7), e1002211. doi:10.1371/journal.pgen.1002211

Torres, A. G., Batlle, E., & Ribas de Pouplana, L. (2014). Role of tRNA modifications in human diseases. *Trends Mol Med*, 20(6), 306-314. doi:10.1016/j.molmed.2014.01.008

Torres, A. G., Pineyro, D., Rodriguez-Escriba, M., Camacho, N., Reina, O., Saint-Leger, A., . . . Ribas de Pouplana, L. (2015). Inosine modifications in human tRNAs are incorporated at the precursor tRNA level. *Nucleic Acids Res*, 43(10), 5145-5157. doi:10.1093/nar/gkv277

Torres, A. G., Reina, O., Stephan-Otto Attolini, C., & Ribas de Pouplana, L. (2019). Differential expression of human tRNA genes drives the abundance of tRNA-derived fragments. *Proc Natl Acad Sci U S A*, 116(17), 8451-8456. doi:10.1073/pnas.1821120116

Toyo-Oka, K., Sasaki, S., Yano, Y., Mori, D., Kobayashi, T., Toyoshima, Y. Y., . . . Hirotsune, S. (2005). Recruitment of katanin p60 by phosphorylated NDEL1, an LIS1 interacting protein, is essential for mitotic cell division and neuronal migration. *Hum Mol Genet*, 14(21), 3113-3128. doi:10.1093/hmg/ddi339

Trimouille, A., Lasseaux, E., Barat, P., Deiller, C., Drunat, S., Rooryck, C., . . . Lacombe, D. (2018). Further delineation of the phenotype caused by biallelic variants in the WDR4 gene. *Clin Genet*, 93(2), 374-377. doi:10.1111/cge.13074

Trotta, C. R., Miao, F., Arn, E. A., Stevens, S. W., Ho, C. K., Rauhut, R., & Abelson, J. N. (1997). The yeast tRNA splicing endonuclease: a tetrameric enzyme with two active site subunits homologous to the archaeal tRNA endonucleases. *Cell*, 89(6), 849-858. doi:10.1016/s0092-8674(00)80270-6

Tsai, J. W., Chen, Y., Kriegstein, A. R., & Vallee, R. B. (2005). LIS1 RNA interference blocks neural stem cell division, morphogenesis, and motility at multiple stages. *J Cell Biol*, 170(6), 935-945. doi:10.1083/jcb.200505166

Tsai, L. H., & Gleeson, J. G. (2005). Nucleokinesis in neuronal migration. *Neuron*, 46(3), 383-388. doi:10.1016/j.neuron.2005.04.013

Tsutsumi, S., Sugiura, R., Ma, Y., Tokuoka, H., Ohta, K., Ohte, R., . . . Kuno, T. (2007). Wobble inosine tRNA modification is essential to cell cycle progression in G(1)/S and G(2)/M transitions in fission yeast. *J Biol Chem*, 282(46), 33459-33465. doi:10.1074/jbc.M706869200

Tuoc, T. C., & Stoykova, A. (2008). Trim11 modulates the function of neurogenic transcription factor Pax6 through ubiquitin-proteosome system. *Genes Dev*, 22(14), 1972-1986. doi:10.1101/gad.471708

Tuorto, F., Herbst, F., Alerasool, N., Bender, S., Popp, O., Federico, G., . . . Lyko, F. (2015). The tRNA methyltransferase Dnmt2 is required for accurate polypeptide synthesis during hematopoiesis. *EMBO J*, 34(18), 2350-2362. doi:10.15252/embj.201591382

Tuorto, F., Liebers, R., Musch, T., Schaefer, M., Hofmann, S., Kellner, S., . . . Lyko, F. (2012). RNA cytosine methylation by Dnmt2 and NSun2 promotes tRNA stability and protein synthesis. *Nat Struct Mol Biol*, 19(9), 900-905. doi:10.1038/nsmb.2357

Tuorto, F., & Lyko, F. (2016). Genome recoding by tRNA modifications. *Open Biol*, 6(12). doi:10.1098/rsob.160287

Turrero Garcia, M., Chang, Y., Arai, Y., & Huttner, W. B. (2016). S-phase duration is the main target of cell cycle regulation in neural progenitors of developing ferret neocortex. *J Comp Neurol*, 524(3), 456-470. doi:10.1002/cne.23801

Valverde, F., De Carlos, J. A., & Lopez-Mascaraque, L. (1995). Time of origin and early fate of preplate cells in the cerebral cortex of the rat. *Cereb Cortex*, 5(6), 483-493. doi:10.1093/cercor/5.6.483

Vare, V. Y., Eruysal, E. R., Narendran, A., Sarachan, K. L., & Agris, P. F. (2017). Chemical and Conformational Diversity of Modified Nucleosides Affects tRNA Structure and Function. *Biomolecules*, 7(1). doi:10.3390/biom7010029

Volvert, M. L., Prevot, P. P., Close, P., Lagusse, S., Pirotte, S., Hemphill, J., . . . Nguyen, L. (2014). MicroRNA targeting of CoREST controls polarization of migrating cortical neurons. *Cell Rep*, 7(4), 1168-1183. doi:10.1016/j.celrep.2014.03.075

Wang, H., Ge, G., Uchida, Y., Luu, B., & Ahn, S. (2011). Gli3 is required for maintenance and fate specification of cortical progenitors. *J Neurosci*, 31(17), 6440-6448. doi:10.1523/JNEUROSCI.4892-10.2011

Wang, M., & Kaufman, R. J. (2014). The impact of the endoplasmic reticulum protein-folding environment on cancer development. *Nat Rev Cancer*, 14(9), 581-597. doi:10.1038/nrc3800

Wang, X., Tsai, J. W., Imai, J. H., Lian, W. N., Vallee, R. B., & Shi, S. H. (2009). Asymmetric centrosome inheritance maintains neural progenitors in the neocortex. *Nature*, 461(7266), 947-955. doi:10.1038/nature08435

Weiss, B., & Landrigan, P. J. (2000). The developing brain and the environment: an introduction. *Environ Health Perspect*, 108 Suppl 3, 373-374. doi:10.1289/ehp.00108s3373

Weitzer, S., & Martinez, J. (2007). The human RNA kinase hClp1 is active on 3' transfer RNA exons and short interfering RNAs. *Nature*, 447(7141), 222-226. doi:10.1038/nature05777

Whipple, J. M., Lane, E. A., Chernyakov, I., D'Silva, S., & Phizicky, E. M. (2011). The yeast rapid tRNA decay pathway primarily monitors the structural integrity of the acceptor and T-stems of mature tRNA. *Genes Dev*, 25(11), 1173-1184. doi:10.1101/gad.2050711.

10.1101/gad.2050711

William, J. (2020). *Neuroscience: Canadian 1st Edition*.

Wilusz, J. E., Whipple, J. M., Phizicky, E. M., & Sharp, P. A. (2011). tRNAs marked with CCACCA are targeted for degradation. *Science*, 334(6057), 817-821. doi:10.1126/science.1213671

Wohlgamuth-Benedum, J. M., Rubio, M. A., Paris, Z., Long, S., Poliak, P., Lukes, J., & Alfonzo, J. D. (2009). Thiolation controls cytoplasmic tRNA stability and acts as a negative determinant for tRNA editing in mitochondria. *J Biol Chem*, 284(36), 23947-23953. doi:10.1074/jbc.M109.029421

Wu, J., Hou, J. H., & Hsieh, T. S. (2006). A new Drosophila gene wh (wuho) with WD40 repeats is essential for spermatogenesis and has maximal expression in hub cells. *Dev Biol*, 296(1), 219-230. doi:10.1016/j.ydbio.2006.04.459

Xing, L., Larsen, R. S., Bjorklund, G. R., Li, X., Wu, Y., Philpot, B. D., . . . Newbern, J. M. (2016). Layer specific and general requirements for ERK/MAPK signaling in the developing neocortex. *eLife*, 5. doi:10.7554/eLife.11123

Yang, G. Y., & Luo, Z. G. (2011). Implication of Wnt signaling in neuronal polarization. *Dev Neurobiol*, 71(6), 495-507. doi:10.1002/dneu.20851

Yang, T., Sun, Y., Zhang, F., Zhu, Y., Shi, L., Li, H., & Xu, Z. (2012). POSH localizes activated Rac1 to control the formation of cytoplasmic dilation of the leading process and neuronal migration. *Cell Rep*, 2(3), 640-651. doi:10.1016/j.celrep.2012.08.007

Yarham, J. W., Lamichhane, T. N., Pyle, A., Mattijssen, S., Baruffini, E., Bruni, F., . . . Taylor, R. W. (2014). Defective i6A37 modification of mitochondrial and cytosolic tRNAs results from pathogenic mutations in TRIT1 and its substrate tRNA. *PLoS Genet*, 10(6), e1004424. doi:10.1371/journal.pgen.1004424

Yee, K. T., Simon, H. H., Tessier-Lavigne, M., & O'Leary, D. M. (1999). Extension of long leading processes and neuronal migration in the mammalian brain directed by the chemoattractant netrin-1. *Neuron*, 24(3), 607-622. doi:10.1016/s0896-6273(00)81116-2

Zaborske, J. M., DuMont, V. L., Wallace, E. W., Pan, T., Aquadro, C. F., & Drummond, D. A. (2014). A nutrient-driven tRNA modification alters translational fidelity and genome-wide protein coding across an animal genus. *PLoS Biol*, 12(12), e1002015. doi:10.1371/journal.pbio.1002015

Zanni, G., Kalscheuer, V. M., Friedrich, A., Barresi, S., Alfieri, P., Di Capua, M., . . . Breitenbach-Koller, L. (2015). A Novel Mutation in RPL10 (Ribosomal Protein L10) Causes X-Linked Intellectual Disability, Cerebellar Hypoplasia, and Spondylo-Epiphyseal Dysplasia. *Hum Mutat*, 36(12), 1155-1158. doi:10.1002/humu.22860

Zeng, H., Shen, E. H., Hohmann, J. G., Oh, S. W., Bernard, A., Royall, J. J., . . . Jones, A. R. (2012). Large-scale cellular-resolution gene profiling in human neocortex reveals species-specific molecular signatures. *Cell*, 149(2), 483-496. doi:10.1016/j.cell.2012.02.052

Zhang, A., Sun, H., Wang, P., Han, Y., & Wang, X. (2012). Modern analytical techniques in metabolomics analysis. *Analyst*, 137(2), 293-300. doi:10.1039/c1an15605e

Zhang, K., Lentini, J. M., Prevost, C. T., Hashem, M. O., Alkuraya, F. S., & Fu, D. (2020). An intellectual disability-associated missense variant in TRMT1 impairs tRNA modification and reconstitution of enzymatic activity. *Hum Mutat*, 41(3), 600-607. doi:10.1002/humu.23976

Zhang, L. S., Liu, C., Ma, H., Dai, Q., Sun, H. L., Luo, G., . . . He, C. (2019). Transcriptome-wide Mapping of Internal N(7)-Methylguanosine Methylome in Mammalian mRNA. *Mol Cell*, 74(6), 1304-1316 e1308. doi:10.1016/j.molcel.2019.03.036

Zhang, Y., Zhang, Y., Shi, J., Zhang, H., Cao, Z., Gao, X., . . . Duan, E. (2014). Identification and characterization of an ancient class of small RNAs enriched in serum associating with active infection. *J Mol Cell Biol*, 6(2), 172-174. doi:10.1093/jmcb/mjt052

Zhao, C., Sun, G., Ye, P., Li, S., & Shi, Y. (2013). MicroRNA let-7d regulates the TLX/microRNA-9 cascade to control neural cell fate and neurogenesis. *Sci Rep*, 3, 1329. doi:10.1038/srep01329

Zhao, X., D, D. A., Lim, W. K., Brahmachary, M., Carro, M. S., Ludwig, T., . . . Lasorella, A. (2009). The N-Myc-DLL3 cascade is suppressed by the ubiquitin ligase Huwe1 to inhibit proliferation and promote neurogenesis in the developing brain. *Dev Cell*, 17(2), 210-221. doi:10.1016/j.devcel.2009.07.009

Zheng, G., Qin, Y., Clark, W. C., Dai, Q., Yi, C., He, C., . . . Pan, T. (2015). Efficient and quantitative high-throughput tRNA sequencing. *Nat Methods*, 12(9), 835-837. doi:10.1038/nmeth.3478

Zhou, W., Karcher, D., & Bock, R. (2014). Identification of enzymes for adenosine-to-inosine editing and discovery of cytidine-to-uridine editing in nucleus-encoded transfer RNAs of *Arabidopsis*. *Plant Physiol*, 166(4), 1985-1997. doi:10.1104/pp.114.250498

Résumé du projet en français

Le développement du cortex cérébral résulte de processus finement régulés tels que la prolifération, l'immigration et la maturation. La perturbation d'une ou plusieurs de ces étapes conduit à des malformations du développement cortical (MDC). Des mutations affectant des gènes codant pour des enzymes de modification des ARN de transfert (ARNt), molécules clés dans la machinerie de traduction des protéines, ont été associées à de telles MDC, ce qui suggère qu'une régulation fine de la traduction assure le bon développement du cortex cérébral. Bien que les modifications des ARNt soient cruciales pour leur structure, fonction et stabilité, les rôles cellulaires des ARNt modifiés ne sont pas bien compris. Ici, j'ai étudié deux hétérodimères modificateurs des ARNts avec des variants associés à ces maladies : ADAT2/3, qui modifie l'adénosine en inosine à la position 34 (I₃₄), et METTL1/WDR4 qui catalyse la formation de N(7)-methylguanosine à la position 46 (m⁷G₄₆).

Mon travail de thèse identifie ces deux complexes comme régulateurs des processus clés pour le développement du cortex cérébral, tels que la migration radiale et la neurogenèse, chez la souris et l'humain. J'ai montré qu'ADAT2/3 et METTL1/WDR4 montrent une expression dynamique dans l'espace et le temps au cours du développement cortical murin. Par électroporation *in utero*, j'ai démontré qu'une réduction des niveaux de protéines ADAT3 ou WDR4 WT était associée à un retard de la migration radiale des neurones corticaux. En utilisant la même technique, j'ai également démontré un rôle de ADAT3 dans la sortie du cycle cellulaire des progéniteurs corticaux. En plus, j'ai identifié des nouvelles variants dans ADAT3, WDR4 et METTL1, en utilisant une combinaison de techniques biochimiques, ainsi que des travaux sur des souris et des cellules de patients j'ai montré que principalement les mutations dans ces gènes provoquent une diminution des niveaux de ces protéines ainsi que les modifications d'ARNt associées, expliquant ainsi comment de telles mutations peuvent conduire à des troubles neurodéveloppementaux.

J'ai également caractérisé un modèle de souris knock-in ADAT3 V128M. En utilisant ce modèle, nous avons étudié comment une mutation dans Adat3 et les défauts qui en résultent dans la modification des ARNt contribuent à la malformation cérébrale. Les résultats obtenus lors de la caractérisation de cette lignée montrent que cette lignée de souris ne récapitule pas la plupart des défauts observés chez les patients, bien que présentant des niveaux de protéine ADAT3 inférieurs. Cependant, il a montré une diminution de la sortie du cycle cellulaire dans les cortex ainsi que l'augmentation du nombre de progéniteurs corticaux, ce qui fournit des informations importantes sur les pathomécanismes possibles à l'origine de la maladie humaine. Dans l'ensemble, ces résultats indiquent que cette lignée de souris n'est probablement pas la meilleure pour modéliser la maladie humaine, cependant, elle peut fournir

des informations pertinentes sur la manière dont la mutation Adat3 p.V128M peut affecter la prolifération et la spécification des progéniteurs corticaux et les mécanismes moléculaires à l'origine de la maladie humaine.

Je crois fermement que les travaux que j'ai réalisés sur les complexes ADAT2/ 3 et METTL1 / WDR4 au cours de ma thèse éclaireront non seulement dans la compréhension des modifications de l'ARNt fonctionnent sur le développement cortical mais aussi dans le rôle de ces complexes pour la biologie humaine et contribueront fournissent des recherches précieuses sur la manière dont les mutations de ces gènes peuvent conduire à des maladies humaines.

Résumé du projet en français

Le développement du cortex cérébral résulte de processus finement régulés tels que la prolifération, la migration et la maturation. La perturbation d'une ou plusieurs de ces étapes conduit à des malformations du développement cortical (MDC). Des mutations affectant des gènes codant pour des enzymes de modification des ARN de transfert (ARNt), molécules clés dans la machinerie de traduction des protéines, ont été associées à de telles MDC, ce qui suggère qu'une régulation fine de la traduction assure le bon développement du cortex cérébral. Bien que les modifications des ARNt soient cruciales pour leur structure, fonction et stabilité, les rôles cellulaires des ARNt modifiés ne sont pas bien compris. Au cours de ma thèse, j'ai étudié deux hétérodimères modificateurs des ARNt avec des variants associés à ces maladies : ADAT2/3, qui modifie l'adénosine en inosine à la position 34 (I₃₄), et METTL1/WDR4 qui catalyse la formation de N(7)-methylguanosine à la position 46 (m⁷G₄₆).

Mon travail de thèse identifie ces deux complexes comme régulateurs des processus clés pour le développement du cortex cérébral, telles que la migration radiale et la neurogenèse, chez la souris et l'humain. J'ai montré qu'ADAT2/3 et METTL1/WDR4 montrent une expression dynamique dans l'espace et le temps au cours du développement cortical murin. Grâce à des expériences d'électroporation in utero, j'ai démontré qu'une réduction des niveaux de protéines ADAT3 ou WDR4 était associée à un retard de la migration radiale des neurones corticaux. En utilisant la même technique, j'ai également démontré un rôle de ADAT3 dans la sortie du cycle cellulaire des progéniteurs corticaux. Par ailleurs, j'ai identifié des variants nouvellement identifiés dans ADAT3, WDR4 et METTL1. En combinant des analyses biochimiques, ainsi que des *in vivo* sur les cortex de souris ou dans des cellules de patients j'ai montré que ces variants entraînent une diminution des niveaux de ces protéines ainsi que des modifications d'ARNt associées, expliquant ainsi comment de telles mutations peuvent conduire à des troubles neurodéveloppementaux.

J'ai également caractérisé un modèle de souris knock-in ADAT3 V128M. En utilisant ce modèle, nous avons étudié comment une mutation dans Adat3 et les défauts de modification des ARNt qui en résultent contribuent aux malformations cérébrales. Les résultats obtenus lors de la caractérisation de cette lignée montrent que cette lignée de souris ne récapitule pas la plupart des défauts observés chez les patients, bien que présentant des niveaux de protéine ADAT3 inférieurs. Cependant, nous avons observé une diminution de la sortie du cycle cellulaire dans les cortex ainsi que l'augmentation du nombre de progéniteurs corticaux. Dans l'ensemble, ces résultats indiquent que cette lignée de souris n'est probablement pas la meilleure pour modéliser la maladie humaine, cependant, elle peut fournir des informations pertinentes sur la manière dont la mutation Adat3 p.V128M peut affecter la prolifération et la

spécification des progéniteurs corticaux et les mécanismes moléculaires à l'origine de la maladie humaine.

Je crois fermement que les travaux que j'ai réalisés sur les complexes ADAT2/ 3 et METTL1/WDR4 au cours de ma thèse apporteront une meilleure compréhension du rôle des modifications de l'ARNt au cours du développement cortical et de la manière dont les mutations de ces gènes peuvent conduire à des maladies humaines.

Understanding the role of the tRNA modifiers ADAT3-ADAT2 & WDR4-METTL1 in the development of the cerebral cortex

Résumé

Des mutations dans des gènes codants pour ces enzymes de modification des ARNts ont été récemment associées à des maladies neurodéveloppementales, telles que la déficience intellectuelle ou l'épilepsie. Cependant, les mécanismes fonctionnels par lesquels ils conduisent à ce type de maladies demeurent encore méconnus. Au cours de ma thèse, j'ai étudié deux hétérodimères modificateurs des ARNts avec des variants associés à ces maladies : ADAT2/3, qui modifie l'adénosine en inosine à la position 34 (I₃₄), et METTL1/WDR4 qui catalyse la formation de N(7)-methylguanosine à la position 46 (m⁷G₄₆). Mon travail de thèse identifie ces deux complexes comme régulateurs des processus clés pour le développement du cortex cérébral, tels que la migration radiale et la neurogenèse, chez la souris et l'humain. En plus, j'ai identifié des nouvelles variants dans *ADAT3*, *WDR4* et *METTL1* et j'ai montré comment ces mutations peuvent conduire à des troubles neurodéveloppementaux.

Mots-clés : ADAT2, ADAT3, WDR4, METTL1, ARNt, développement cortical, migration neuronale, neurogenèse

Résumé en anglais

Mutations in genes encoding these tRNA modifying enzymes have recently been linked to neurodevelopmental diseases, such as intellectual disability or epilepsy. However, the functional mechanisms by which they lead to such diseases are still poorly understood. During my thesis, I studied two tRNA modifying heterodimers with variants associated with these types of diseases: ADAT2/3, which modifies adenosine to inosine at position 34 (I₃₄), and METTL1/WDR4 which catalyzes the formation of N (7) -methylguanosine at position 46 (m⁷G₄₆). My thesis work identifies these two complexes as regulators of key processes for the development of the cerebral cortex, such as radial migration and neurogenesis, in mice and humans. In addition, I have identified new variants in *ADAT3*, *WDR4* and *METTL1* and I have shown how these mutations can lead to neurodevelopmental disorders.

Keywords: ADAT2, ADAT3, WDR4, METTL1, tRNA, cortical development, neuronal migration, neurogenesis